SYNTHESIS AND CHARACTERISATION OF NOVEL Ru(II) COMPLEXES WITH SELECTIVE DEUTERIATION

By

Christine.M. O'Connor, B.Sc. (Hons)

A Thesis presented to Dublin City University for the degree of Doctor of Philosophy.

Supervisor Prof. J.G. Vos,
School of Chemical Sciences,
Dublin City University.

December 1999

To my parents William and Deirdre.

I hereby certify that this material, which I now submit for assessment on the programme of study leading to the award of Doctor of Philosophy and thesis is entirely my own work and has not been taken from the work of others save and to the extent that such work has been cited and acknowledged within the text of my work.

Signed: Christine O Connor

Christine O'Connor

I.D. No.: 95970690

Date: 18.02.2000

Acknowledgements

Firstly I would like to thank my supervisor Prof. Han Vos for giving me the opportunity to carry out postgraduate studies at DCU. I would like to thank him for his guidance, encouragement and support during my project. I would like to also thank Hans wife Mary and the kids for entertaining the 'Vos group' at their home over the years.

Secondly, I would like to express my sincere gratitude to Dr. Helen Hughes for the encouragement and friendship since my days in Waterford RTC. It is thanks to Helen and Peter that I had the courage to go on and do my postgraduate studies.

I would like to thank the technical staff especially 'The Bruv's- Mick and Morris and also Damien and Ambrose for all the help and the craic that went along with it!

After that where do I start....for once in my life I am lost for words!! I will start with members of my research group, past (Tia, Rachel (sure we'll have another one?) Kierse, Miriam, Karen, Una, Nick, Tim, Benedicte, Johanne, Egbert, Pepe, Sven & Astrid (the nicest German couple in the world)) and present (Luke (Kerry for the all-Ireland) O'Brien, Scott (Hoochymama) Killeen, Anthea (gingerspice) Lees, Frances (sportyspice) Weldon, Marco (crazy salsa-mad Italian) Duati , Stefano (redbreast) Fanni, Declan, Adrian, Helen and Wesley (good luck to you)) thanks for delaying me in my work by talking to me so much and helping me with everything and making me go to the pub....how could you!! I have to say you were the best bunch of people I have ever known. I would like to thank Tia, Marco, Karen, and Denis for helping me with my laser measurements and also to Richard and Jenny. I would also like to thank Helen H and Frances for giving me my 'kick start' into ruthenium chemistry.

Next my technical support advisers or the 'Foster group' who have taught me what computers can really do and helped me immensely in my electrochemistry, thanks goes to Conor, Joe, Dr. Foster, Aoife and especially Dominic. Thank you for all the help lads I finally get to say it properly!

Thanks to all of the postgrads Bronagh, Rachel, Ben, Colm, Conor, Luke, Marco, Frank, Scott, Ollie, Dominic, Shane, Cormac, James D., Peter, Dec, Cathal, Darren Carol, Mairead, Davnat, Andrea, Deidre, Donal, Mike Sheehy, Ger, Jenny, Richard, Ger, Fran, Dara and Keith, the postdocs: Frances, Anthea, Siobhain, Theresa, Stefano, Paddy K, Mary, Kieran, Jean-Luc and Sharon, Paul K, Jacintha, P.J, Orla, Collette, Marie and Michaela. It has been a pleasure knowing you.

Being a veteran of colleges at this stage I have a few more people to thank from around the country. My friends from Dundalk RTC Trish (& the infamous Banty!), Amanda (de Cadenet) D, Suzann & Roddy, Amanda S, Maeve K, Maeve O (you always told me I could do it!), Phil & Marie(Osnabruck), Sgt. Garda Kevin and all the lovely Meath men I know! My friends from Sligo RTC Rachel T, Margaret, Sinead (the T's), Ritchie, Conor, Gavin, all the Ballina gang (the G's) and Denis (up the banner!). Also my friends from Waterford RTC Dave, Ambrose, Helen, Peter and John Griffith. I must also thank Seamus and Tara for being good friends to me over the years. To all my relations in Limerick ....I have finally finished school! The girls in 46, Dalcassian Downs, Bronagh, Anna and Grainne thanks for putting up with me. I would also like to thank my very close friends Trish and all the Mc Garrys and Rachel T thanks for all the love, support and friendship you have giving me in the last few years.

Some things you cannot do alone, and I must say, because of my family I didn't have to. I want to express my sincere gratitude and love for the encouragement, love and support my family have given me especially my Mum and Dad. It was always nice to know that you are always there for me and I dedicate this thesis to you both for being such remarkable parents and friends to me. Thanks to my brothers Diarmuid, John-Paul and Brian who also expressed their love and support to me over the years in a brotherly kind of way!! Thanks to my Granny Chrissie (grannyspice) for her love and support and not forgetting my Nana Etta who I know would be so proud.

Abstract

The aim of my research was to investigate Ru(II) mixed ligand complexes through synthesis and characterisation and through the use of deuteriation. The location of the excited state in the dinuclear species was to be determined through use of selective deuteriation of ligands. Acid/ base dependency of these 1,2,4-triazole-containing complexes may be applied in the area of supramolecular chemistry due to its switch on/off effect. However to arrive at this stage a series of studies were necessary.

In chapter 3, reveals the description of the synthesis of the starting material $[Ru(L)_2Cl_2].2H_2O$, where L is bipyridyl, phenanthroline and biquinoline. This is followed by the deuteriation of these ligands (bpy, phen and biq) and the Hpytr and Hpztr ligands. The starting materials with the deuteriated ligands d_8-bpy, d_8-phen and d_{12}-biq where consequently prepared .The synthesis and characterisation of the ligands 3-(pyridin-2-yl)-1,2,4-triazole, Hpytr and 3-(pyrazin-2-yl)-1,2,4-triazole, Hpztr and their complexes are shown in chapter 3. The use of deuteriation in the location of the excited state of the $pztr^-$ complexes was not as facile as first thought as the complex was found to have dual emitting properties due to close-lying excited states. New developments arose in the isolation of the stereoisomers of the $pytr^-$ and $pztr^-$ complexes in collaboration with Dr. C. Villani, University of Rome, also a new concept of ^{99}Ru NMR was investigated of the $pytr^-$ and $pztr^-$ isomers in collaboration with Prof. C. Elsevier, University of Amsterdam.

Chapter 4 is the investigation of complexes containing the ligand 3-(pyrazin-2-yl)-5-(pyridin-2-yl)-1,2,4-triazole, Hppt. This ligand was synthesised and also deuteriated to prepare selectively deuteriated complexes as in chapter 3 with the same starting materials. The synthesis and characterisation was described in this chapter for these complexes and ^{99}Ru NMR was obtained.

Also a crystal structure of the N2 of the triazole ring to the pyrazine isomer of the ppt$^-$ complex was achieved. Chapter 5 is the conclusive chapter of this text, which describes the synthesis of the dinuclear complexes of the ppt$^-$ ligand, and this is prepared via two routes the indirect and the direct route. The indirect route is prepared using the isolated isomers of the monomers. The characterisation and selective deuteriation is discussed. From the redox and photophysical behaviour of the dinuclear complexes some theories were derived. Chapter 6 is conclusions and future work, which sums up the results of this thesis and the consequential studies, which have evolved.

TABLE OF CONTENTS PAGE NO.

Chapter 1

INTRODUCTION

1 INTRODUCTION

1.1 Supramolecular Chemistry -A "switch" for the future?

Miniaturisation of components for the construction of useful devices is currently pursued by a "large-downward" approach. This approach, which leads physicists to deal with progressively smaller molecular aggregates, becomes difficult or even impossible when the size of the miniaturised component has to be in dimension of nanometers. A chemical solution has been put forward to overcome this "size" dilemma. Through chemical strategies nanometer sized species may be produced via a "small-upward" approach[1] starting with molecular components. This approach is very appealing since it allows the assembly of functionally integrated molecular building blocks.[2]

Assembly of molecular components into large and functional arrays[3] (supramolecular species) can be based on a variety of intermolecular forces such as hydrogen bonds, donor-acceptor interactions, stacking interactions, or on coordination and covalent bonds[4,5]. When the molecular building blocks contain transition metals, a strategy called "complexes as metals/ complexes as ligands" [6,7] can allow the construction of large polynuclear metal complexes via metal-ligand coordination bonds.

Of particular interest are the dendrimers that incorporate some specific properties in their building blocks such as the capability to absorb visible light, to give luminescence, and to undergo reversible multielectron redox processes. Such species, in fact, could find applications as components in molecular electronics and as photochemical molecular devices for solar energy conversion and information storage [4,8]. Transition-metal complexes of polypyridine- type ligands [4] are ideal components to build up dendrimers of this type. Species containing up to 22 metal-based units have been obtained [9].

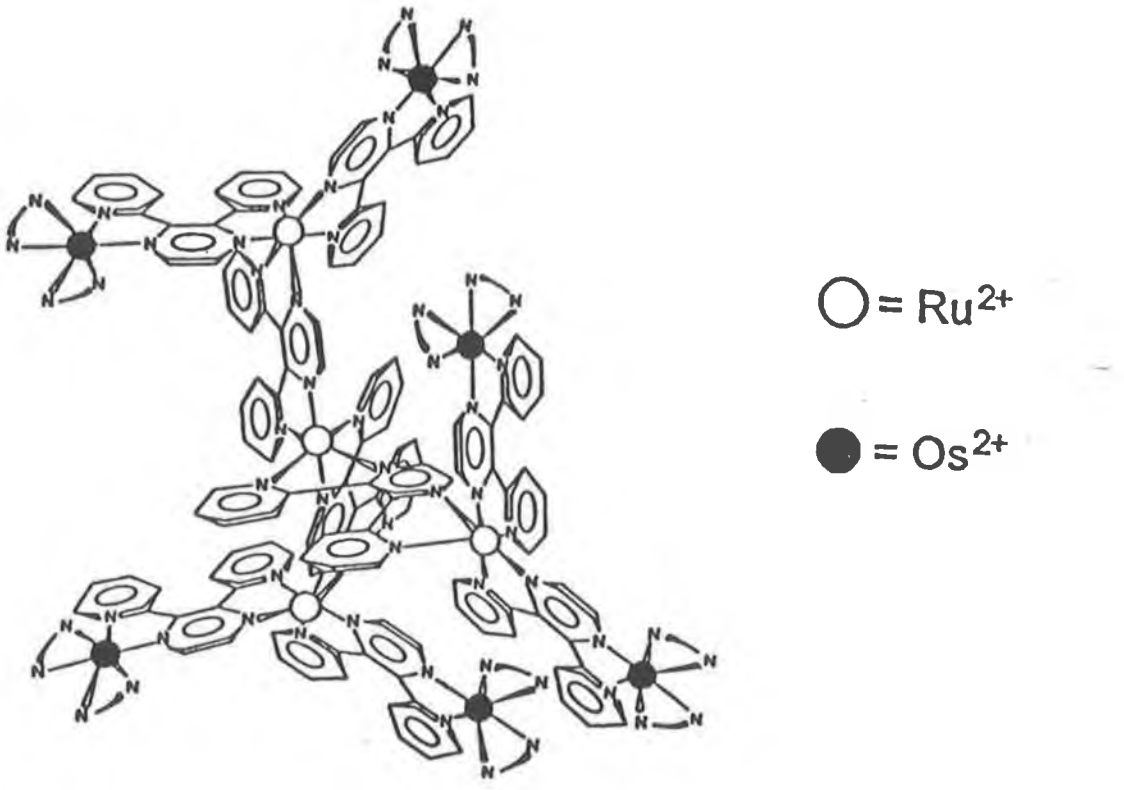

Figure 1 Example of a decanuclear supramolecular species [3].

The interest in these dendrimers is related not only to their size but also to the presence of chemically different units, since each unit introduces into the supramolecular structure its own "pieces of information"(in the form of specific properties such as absorption spectra, luminescence, and redox levels etc.)[10,11]. One of the most interesting aspects of the chemistry of supramolecular systems is their interaction with light and the great variety of processes that may ensue. In molecular photochemistry, a single molecule performs simple intramolecular and/or intermolecular photoinduced acts such as bond breaking, light emission, electron transfer etc. These simple acts may find useful applications in the field of photochemical synthesis, photodecomposition, photochromism, photoluminescence etc. But, more complex light induced functions such as vectorial electron transfer, migration of electronic energy, and switch on/off of receptor ability, cannot be performed by single molecules but need the cooperation of several components. [4]

In the area of coordination chemistry, there are three types of Supramolecular systems:

I. Second sphere coordination compounds, i.e. complexes associated to other species by electrostatic interactions, hydrogen bonds, or other intramolecular forces.[5]

II. Cage type coordination compounds i.e. complexes in which the metal ion is encapsulated in a single, polydentate ligand.

III. Molecular building blocks linked via bridging units by means of covalent or coordination bonds.[6]

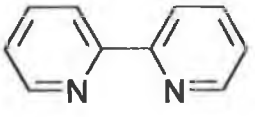

Bipyridine (Bpy)

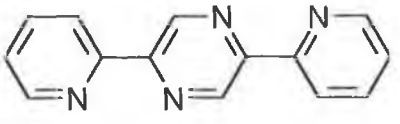

2,5-bis(2-pyridyl)pyrazine (2,5-dpp)

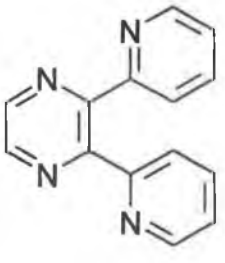

2,3-Bis(2-pyridyl)pyrazine
(2,3-dpp)

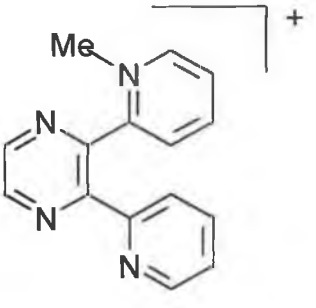

2-[2-(1-methylpyridiumyl]-3-(pyridyl)pyrazine
(2,3-Medpp)

Figure 2 Examples of ligands employed in the synthesis of polynuclear assemblies.

The design of effective synthetic procedures to prepare systems of particular compositions and topologies represents a major target in the area of supramolecular assemblies.

One route taken by Serroni et al[12, 13] was by taking a general step-by-step approach to the synthesis, which is based on the so-called "complexes-as-ligands/complexes as metals" strategy and consists of reacting "metals" or "complex-metals" with ligands or "complex-ligands", which enables the formation of up to tridecanuclear species. Another route would be to select a suitable bridging ligand (spacer) which would give you the desired profile i.e. the bridging ligands based on terpyridine (Tpy) will form linear complexes[13,76]. Other large molecular assemblies have been prepared using 1,4,5,8,9,12-hexaazatriphenylene (Hat) as a tris-chelating ligand, which is complexed to a metal and then used as a "metal- complex" to add to other ligands such as 1,10-phenanthroline[14].

Further approaches taken by Serroni et al were the "divergent" and "convergent" approaches, the former being a stepwise method in which the peripheral ligands are selectively protected to limit the binding sites. The latter approach is just the direct route in which the ligand is added to the "metal-complex" in large excess.[15] More recently several studies have been published on the synthesis of these supramolecular complexes[16,17,18] with the use of a variety of ligands containing pyridine and pyrazine moieties. The most common of the ligands used as bridging ligands in these systems are shown in Figure 2. Pyridine and pyrazine rings are employed in such bridging ligands due to the variety and versatility of their binding sites, which is useful in the assembly of such macromolecules. Such structural control enables the pattern of energy migration to be synthetically controlled.[19,20,21]

Knowledge of the fact that the absorbance and electrochemical properties of dendretic complexes are based on the actual properties of each building block of the assembly has been established thus far[15,18] but, a newer concept is that of creating and investigating stereochemically pure dendrimers[22]. The idea of enantiomerically pure complexes has been investigated previously but not on supramolecular systems[23] and is desirable for the clear interpretation of photophysical results.

1.1.1 Supramolecular Photochemical Assemblies

As an introduction to photochemistry the concepts of photoinduced processes should be discussed, which are illustrated in *Figure 3*. Photochemical reactions have been depicted in two different reaction pathways, that of Energy transfer (a) and of Electron transfer (b).

Bimolecular processes:

(a) $A^* + B \rightarrow A + B^*$ **Energy transfer**

(b) $A^* + B \rightarrow A^- + B^+$

$A^* + B \rightarrow A^+ + B^-$ **Electron transfer**

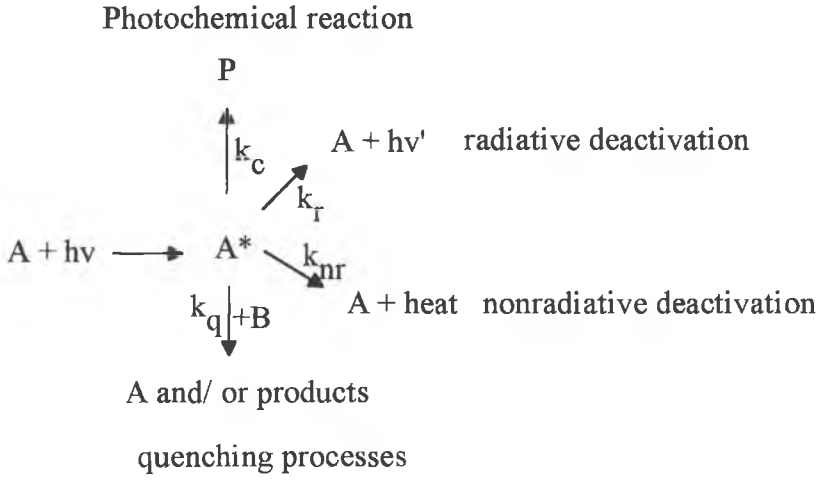

Figure 3 Unimolecular and bimolecular deactivation processes of an excited state[77].

This would be the case for bimolecular reactions however for intramolecular processes, reactions may be altered due to the linker molecule as it may alter the rate of the process.

Intramolecular processes:

$A^*\text{-L-B} \rightarrow A\text{-L-}B^*$ Energy transfer

(c) **$A^*\text{-L-B} \rightarrow A^-\text{-L-}B^+$**

$A^*\text{-L-B} \rightarrow A^+\text{-L-}B^-$ Electron transfer

In order to determine whether a photoinduced process is electron transfer or energy transfer several methods are used, as portrayed in Figure 3. Such methods would include;

(1) Luminescent lifetimes: the excited state energy, rate of decay and rate of formation (rise time),
(2) Absorption spectra of transient species (excited states and charge transfer intermediates): rate of decay and rate of formation,
(3) Electrochemistry: to collect thermodynamic data for electron transfer processes, and,
(4) Absorption spectra: to find wavelength of excitation. These methods may be useful in the interpretation of the photochemical reactions.

Other measurements such as resonance raman spectroscopy may also be incorporated.

The most common metal ions used in photochemistry are Ru^{2+}, Os^{2+}, Re^{2+}, Rh^{2+}, Ir^{2+} and Cu^+ etc. as they are good metal ions for energy transfer. Ru(II) complexes are mainly prepared with bipyridine type ligands as in Figure 4. Such complexes have been prepared as potential photocatalysts due to their characteristics i.e.

(i) good stability towards photo- and chemical decomposition,
(ii) strong absorption in the visible region,

the lowest excited state, a ^{3}MLCT level, is luminescent and long lived,

(iii) they have interesting electrochemical properties,
(iv) capable of photoinduced energy and electron transfer reactions.

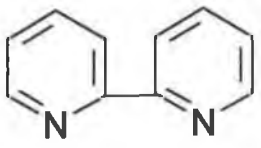

Bipyridine (Bpy)

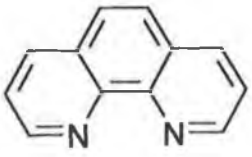

Phenanthroline (Phen)

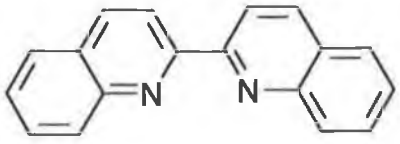

Biquinoline (Biq)

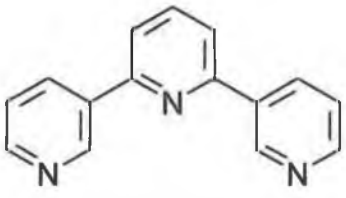

Terpyridine (Tpy)

Figure 4 Bipyridine type ligands

In supramolecular complexes the energy levels of the component building blocks are essentially maintained.[24] Light excitation in the near UV-Visible region populates ^{1}MLCT excited states of the various metal-based units. Investigations carried out on $[Ru(bpy)_3]^{2+}$ with fast techniques indicate that the originally populated ^{1}MLCT excited states undergo relaxation to the lowest energy ^{3}MLCT level in subpicosecond time scale.[25] If each unit were isolated, as it happens in mononuclear complexes, competition between radiative (luminescence) and radiationless decay to the ground state would account for the deactivation of the ^{3}MLCT level, with an overall rate constant, measured from the luminescence decay, in the range 10^6-10^8 s^{-1} [19]. Each isolated mononuclear $[M(L)_n(BL)_{3-n}]^{2+}$ component displays a characteristic luminescence, both in rigid matrix at 77 K and in fluid solution at room temperature. When the components are linked together in a supramolecular array, electronic energy can be transferred from an excited component to an unexcited one. In some dendrimetic complexes, the exoergonic energy transfer between contiguous units is so fast that the luminescence of the unit whose ^{3}MLCT level lies at higher energy can no longer be observed, with concomitant sensitisation of the luminescence of the unit possessing a lower ^{3}MLCT level.

The energy of the ^{3}MLCT level excited state of each unit depends on metal and ligands in a predictable way.[26] Following certain synthetic pathways a high degree of synthetic control in terms of the nature and position of metal centres, bridging ligands, and terminal ligands may be achieved. Thus, the synthetic approach translates into a high degree of control, on the direction of energy flow within these supramolecular arrays. The design of systems where a photoinduced energy flow can be either interrupted or initiated by a self-photosensitised reaction has been investigated. Systems of the first type are referred to as "self-poisoning" and of the second type are "self-educating". In principle, an artificial "self-educating" system can be designed by using the same donor and acceptor units of the "self-poisoning" device which is hoped to produce a photoswitchable supramolecular species.[27]

For Ru(II) supramolecular complexes of high nuclearity, the molar absorption coefficient is huge throughout the entire UV-Visible spectral region. The bands in the UV region are ligand centred. The bands observed in the visible region are due to metal-to-ligand charge-transfer (MLCT) transitions. The energies of these transitions depend on the nature of the donor metal ion and the acceptor ligand and, to a minor extent, on the remaining coordination environment.[19] Therefore, even in the case of homonuclear dendrimers, different types of MLCT transitions are present because there are two types of ligands (bridging and terminal ones) and topologically different positions for the metal ions (central, intermediate, peripheral).

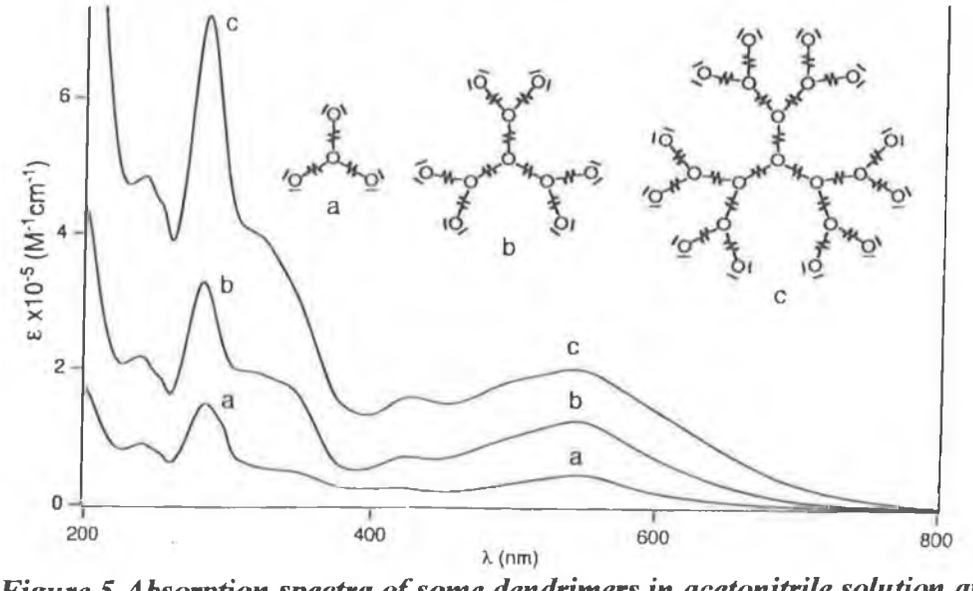

Figure 5 Absorption spectra of some dendrimers in acetonitrile solution at room temperature[28].

1.1.2 Concepts in supramolecular chemistry.

The term 'supramolecular assemblies' has grown in several directions and due to the large interest in these systems several sophisticated functionalised nanosystems have been created with basic principles based on common terminology such as acid/base dependency or photoinduced reactions.

Jean-Marie Lehn and co-workers[29] are currently working on intricate cylindrical nanoarchitectures based on polytopic linear oligobipyridine and circular hexaazatriphenylene (hat) ligands. These ligands undergo self-assembly with Cu (I) and Ag (I) ions to generate the large inorganic entities shown in Figure 6. The present results demonstrate that it is possible to access supramolecular architectures of nanometric size presenting a high level of structural complexity by metal ion-mediated self-assembly. Of particular interest is the simultaneous occurrence of two processes: self-assembly of a multitopic receptor and the selection of substrate entities possessing features compatible with inclusion in the internal cavities.

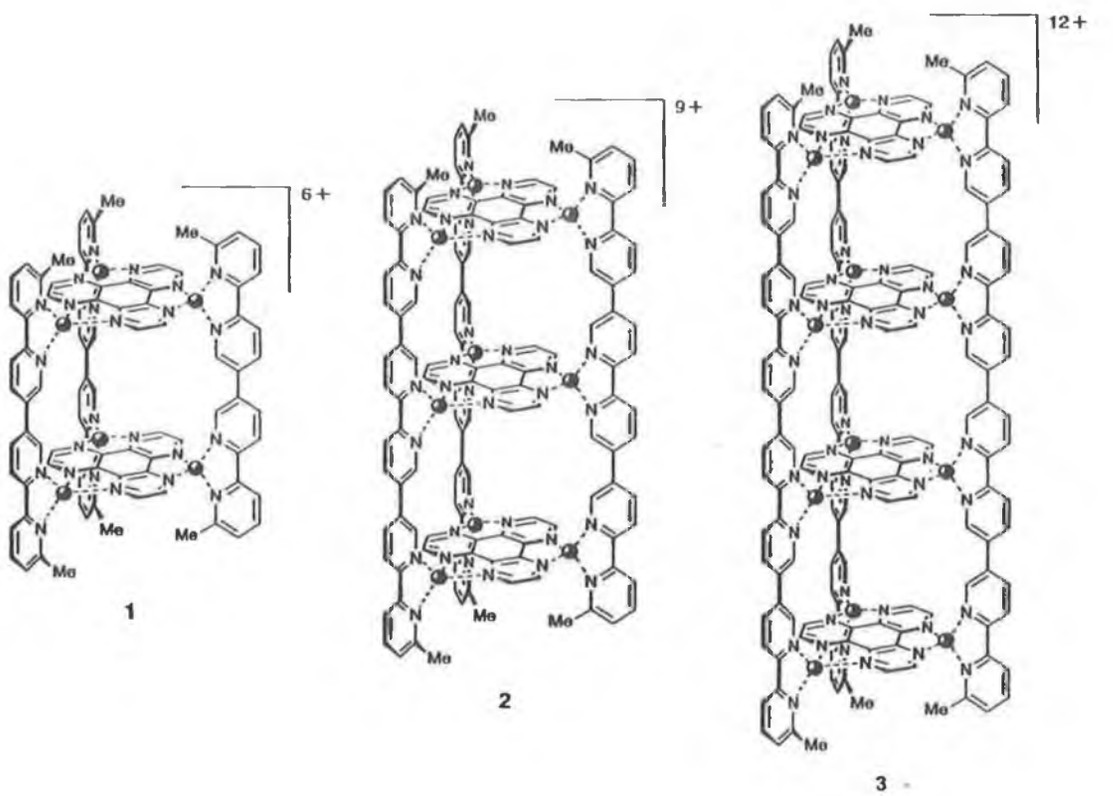

Figure 6 Schematic representation of the structures of the cylindrical inorganic architectures 1, 2, and 3 containing one, two and three internal cavities, respectively; their heights are 18 nm, 26 nm and 35 nm , respectively[29].

Vögtle et al. are currently investigating the photoswitchable-functionalised azobenzene dendrimers[30]. It is well known that azobenzene-type compounds undergo an efficient and fully reversible photoisomerisation reaction, hence their applications in the construction of photoswitchable devices. It has been found that the thermodynamically stable E isomers of the azobenzene groups contained in the periphery of the dendrimers are reversibly switched to the Z form by 313 nm light and can then be converted back to the E form by irradiation with 254 nm light or by heating Figure 7. In this study the dendrimer has been used as a potential host for eosin Y (2', 4', 5', 7'-tetrabromofluorescein dianion) and the resulting quenching studies were monitored.

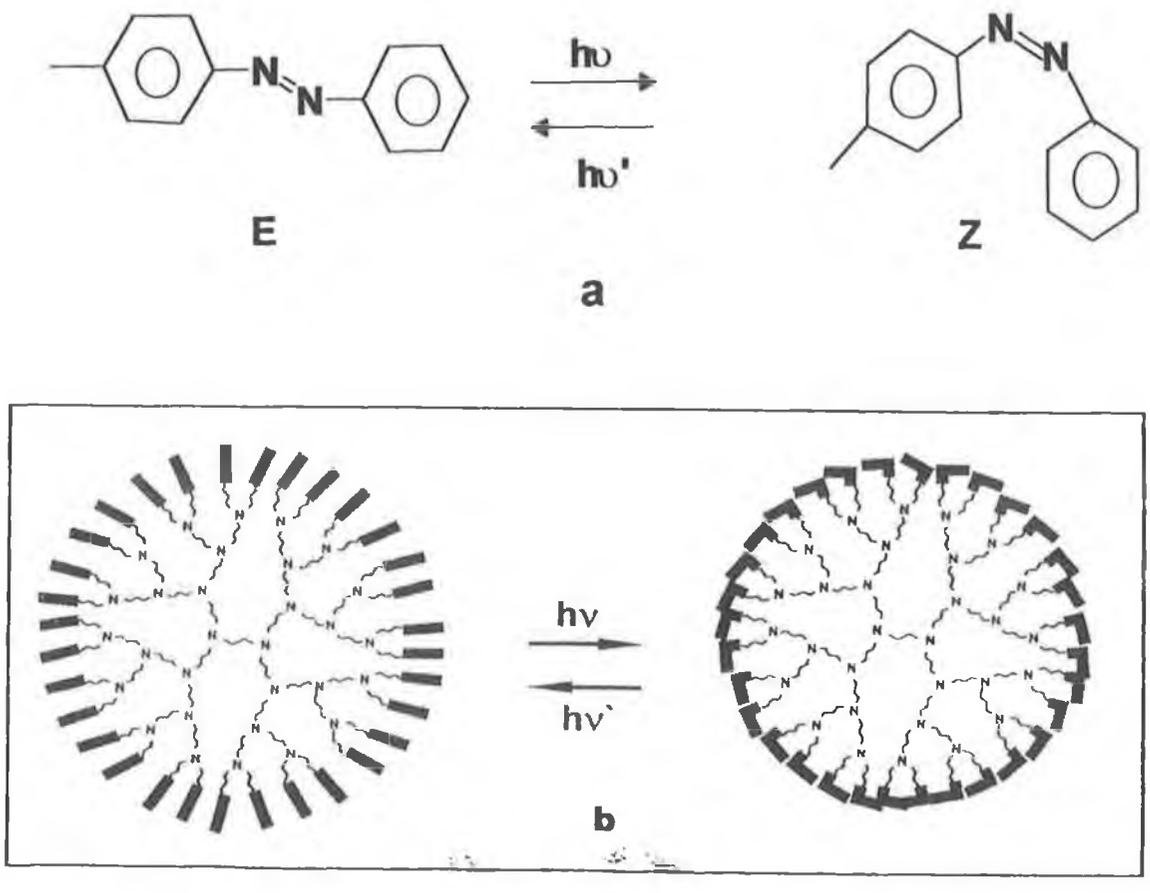

Figure 7 E and Z isomers of the azobenzene periphery groups (top) and photoisomerisation of azobenzene and of the fourth generation dendrimers bearing 32 photoisomerisable azobenzene groups in the periphery (bottom)[30].

It was found that in these systems (i) the lowest singlet, fluorescent excited state of eosin is quenched by the amine units contained in the branches of the dendrimers and (ii) the E→Z and Z→E photoisomerisation reactions of the peripheral azobenzene units are sensitised by triplet eosin. The fluorescence quenching experiments revealed that the Z form of the fourth generation dendrimers are better hosts than that of the E form.

Another area currently under investigation is the 'Molecular Shuttles' by Stoddart et al.[31] These large and impressive complexes have potential application in molecular information processing. Appealing examples of chemical species that have mechanically movable component parts are suitably designed catenanes, rotaxanes and pseudorotaxanes.

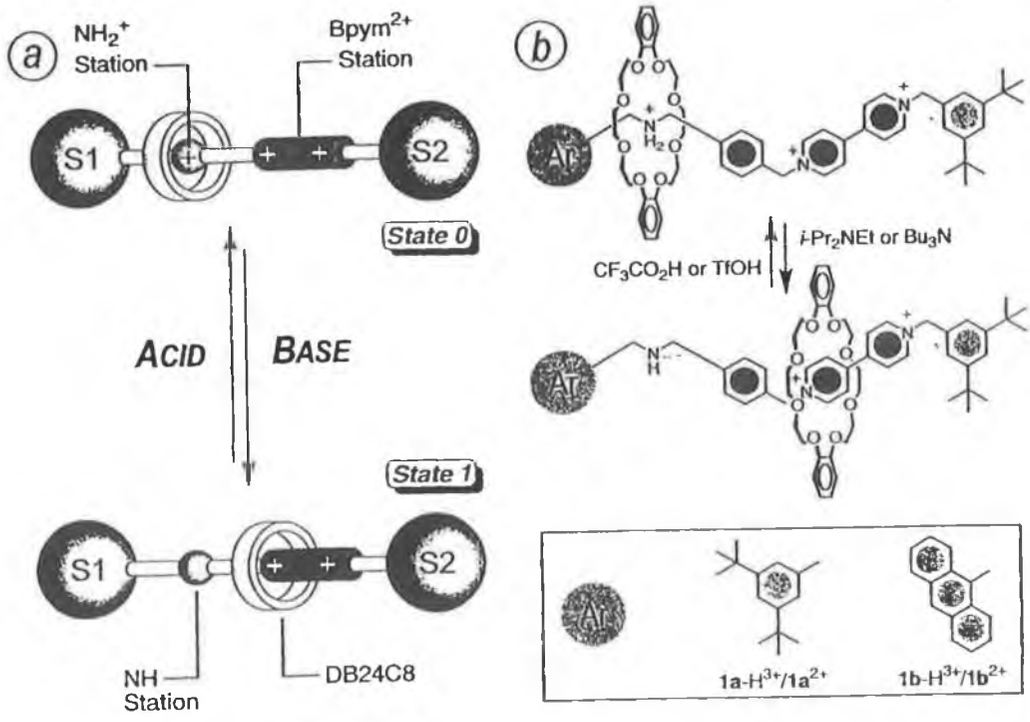

Figure 8 (a) Acid-base controllable molecular shuttle. Initially (state 0), the macrocyclic component resides solely on the NH_2^+ station. After treatment with a nonnucleophilic base, deprotonation coerces the macroring to move to the $Bpym^{2+}$ station (state 1). Addition of acid regenerates the NH_2^+ centre, moving the macrocyclic component back to bind its original station and rendering the switching cycle reversible. (b) Structural formulas of the switchable rotaxanes described here[31].

The relative displacements of these parts can be induced by chemical or electrical energies, as well as by light, and can be monitored by a variety of techniques, such as NMR, absorption and emission spectroscopies, along with electrochemistry. It has been reported that two novel rotaxanes composed of a DB24C8 macroring bound mechanically to a dumbbell-shaped component endowed with an NH_2^+ centre and a $Bypm^{2+}$ unit have been achieved by using the principles of synthetic supramolecular chemistry. Acid-base switching experiments, monitored by ^1H NMR spectroscopy, demonstrated that, upon addition of an appropriate base to a solution of either of the rotaxanes, the crown ether switches from the NH_2^+ to the $Bpym_2^+$ station as shown in Figure 8. Other examples of acid-base controlled supramolecular systems are 'Molecular Plugs' which incorporate racemic crown ethers and binaphthyl units[32]. This is the state of the art in nanotechnological design and may be the future in computer components shown in Figure 9.

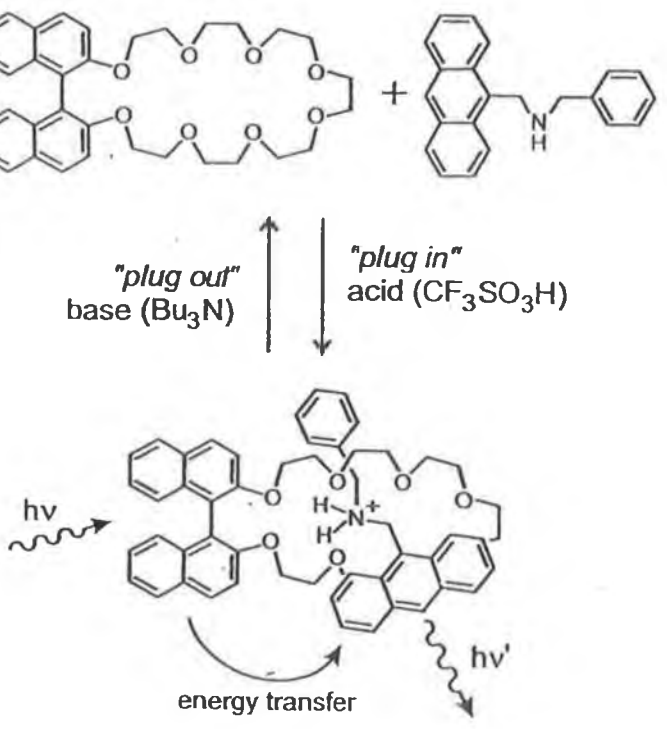

Figure 9 Reversible acid/base-controlled plug in/ plug out between BN26C8and ABH^+, and photoinduced energy transfer from the binaphthyl to the anthracenyl unit in the plug in state[32].

1.1.3 The Role of Artificial Photosynthesis

Photosynthesis represents the most efficient method of solar energy conversion known to date. Chlorophyll molecules act as light absorbers in such systems, and use the energy of the absorbed light, to effect a charge separation, thus converting light to electrochemical energy. This energy is then used to drive the conversion of carbon dioxide and water to glucose and oxygen, through a complicated cycle of events, not relevant to this discussion.

$$\mathbf{6CO_2 + 6H_2O + chlorophyll + light \rightarrow Glucose + 6O_2} \quad \textbf{eqn. 1}$$

Suffice to say that, photosynthesis can be defined as eqn. 1 and represents the origin of the food chain for all living matter. This clearly illustrates the power available from solar energy, if it can be harnessed efficiently.

Based on the capabilities of the photosynthetic model, it is hardly surprising that molecular approaches to solar energy conversion have attempted to mimic the functions of the system. One such effort has focussed on creating molecular assemblies, which function in a manner similar to the chlorophyll units in green plants. In essence a chromophoric centre for light collection, capable of transferring the energy collected to a suitable acceptor, thus creating a charge separated species, with electrochemical potential, analogous to the chlorophyll unit is desired. Such species can, therefore substitute for the chlorophyll unit, as photosensitisers in inorganic solar energy conversion schemes.

Currently porphyrins and ruthenium (II) complexes have been employed as components of supramolecular arrays both for the mimicry of processes taking place in nature and for the development of devices at the molecular level. It has been found that the occurrence of energy-transfer processes, which are formally forbidden on the basis of the spin multiplicity (i.e., from the free porphyrin based excited singlet to the ^{3}MLCT excited state localised on the ruthenium complex), is made possible by the heavy Ru atom perturbing effect[33]. Efficient systems are under investigation with the use of bis(terpyridine)ruthenium(II) complexes[34].

Natural photosynthetic processes convert sunlight into chemical energy by means of a very specific supramolecular organisation formed as the result of evolution.[35] Part of the natural photosynthetic system is devoted to optimise light absorption i.e., to convert the incident sunlight into electronic energy of molecular components.[36]Such an electronic energy is then channelled, thanks to an appropriate energy gradient, [37] toward a "reaction centre" [37] where the electronic energy is used to create charge separation, i.e., redox chemical energy. In subsequent thermal steps, the redox energy is used to transform low-energy chemical species such as water and carbon dioxide into high-energy chemical species such as carbohydrates and dioxygen.

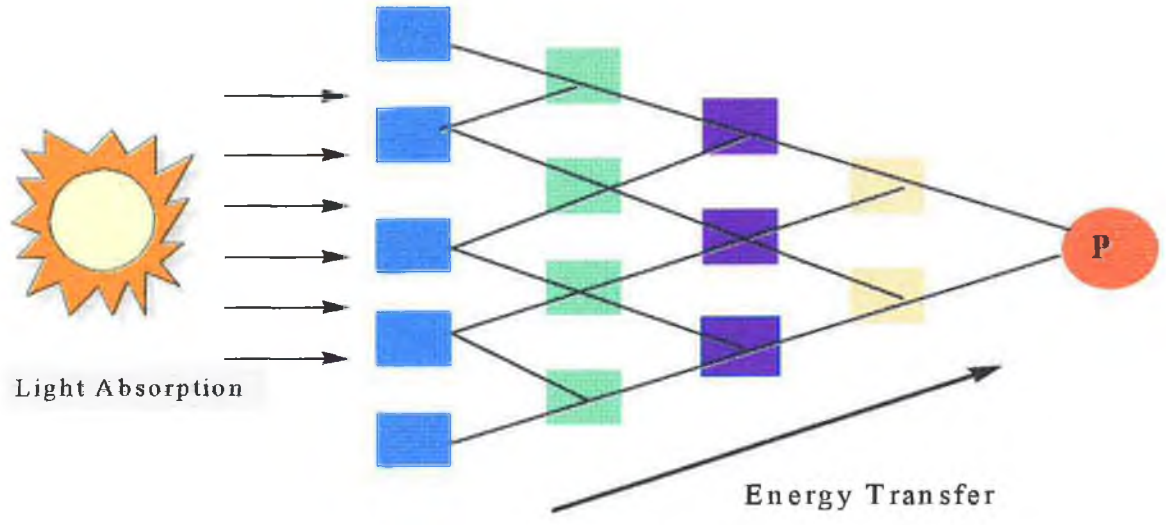

Figure 10 Schematic representation of a light harvesting system. Light is absorbed by an array of chromophores, and the electronic energy is then channelled to a reaction centre (P).

An intelligent approach toward the design of artificial systems for solar energy conversion is to take the natural energy conversion sequence as a model and see whether the natural devices can be replaced by artificial ones. The strive to produce enhanced photosensitisers for the conversion of solar energy has been given a lot of attention in recent years. Current solar panels have an efficiency of about 13%[2] but in order for solar energy to become a source of household and industrial energy the efficiency of their cells must be increased.

As previously stated, the discovery of $[Ru(bpy)_3]^{2+}$ put ruthenium polypyridyl complexes into the mainstream of suitable photocatalysts for solar cells. However due to the photophysical properties of $[Ru(bpy)_3]^{2+}$, extensive research has gone into ligand substitution in order for photostability to be enhanced.

1.1.4 Photomolecular Devices (PMD's) and photosensitisers.

An assembly of molecular components capable of performing light induced functions can be called a photochemical molecular device (PMD). The increasing interest in developing a means of artificially replicating photosynthesis or creating other optically electronic materials for example; photosensitive receptor molecules which may be used for substrate selective optical signal generation [15], has resulted in a large growth in the area of "Supramolecular photochemistry".[16,17,18,19]

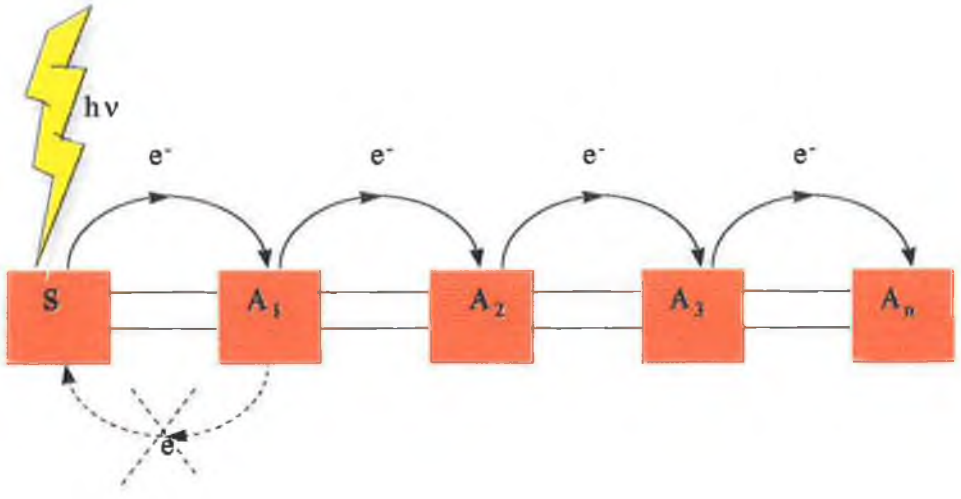

Figure 11 Model of vectorial electron transfer in photochemical molecular devices.

Light absorption by a component of a PMD generates "localised" electronic energy. For several practical purposes an important function is represented by the possibility of transmitting the electronic energy to another component of the PMD over a more or less long distance, where the energy will be used for chemical purposes or reconverted into light.

Figure 11 shows a model for light energy conversion, this consists of a sensitiser species S, possessing suitable redox, ground and excited state properties, linked to a series of relay species, i.e. a series of electron acceptors A_n along a redox gradient. Following sensitisation via light absorption, an electron is transferred from the excited sensitiser to the relays until charge separation has been accomplished via oxidation of the sensitiser and reduction of the final acceptor. There are some interesting applications of PMD's based on energy transfer, which deal with:

1) spectral sensitisation
2) antenna effect
3) remote photosensitization
4) light energy up conversion.

PMD's performing such functions must have energy transfer photosensitiser (Pen) at the interface toward light, i.e.; the "Pen" should be a molecular species capable of absorbing light and donating electronic energy to another component of the device.

There are potential photochemical reactions, which do not occur because the reactants are not able to absorb light. Such reactions can be photosensitised using suitable chemical species that have been called L.A.S (light absorption sensitisers). During the photochemical reaction light must be absorbed yielding an excited state. This excited state must be able to oxidise or reduce one of the reactants. The resulting reduced (or oxidised) form of the photosensitiser must be capable of reducing or oxidising the other reactant in order to complete the redox process and regenerate the light absorption sensitiser. The dicarboxybipyridine type ligands have been used extensively as sensitisers in these PMD systems. More recent studies have gone in the direction of the metal cyanide dicarboxy complexes i.e. cis-[(4,4'-$(CO_2H)_2$bpy)$_2$M$(CN)_2$], where M = Ru or Os.[20] Other examples of sensitisers are [Ru(dcbH)($dcbH_2$)(L)], where L is diethyldithiocarbamate, dibenzyldithiocarbamate or pyrrolidinedithiocarbamate and dcbH is 4-(COOH)-4'-(COO^-)-2,2'-bipyridine, and $dcbH_2$ is 4,4'-$(COOH)_2$-2,2'-bipyridine,[38] but the most efficient sensitiser to date is cis-Ru($dcbH_2$)$_2$$(NCS)_2$[39]which the above examples were compared and contrasted against.

Simple molecules like water and carbon dioxide may be converted into fuels (H_2,CH_4) by means of non-biological photosynthetic processes through the use of photosensitisers. The sensitisers must contain the following properties:

1) reversible redox behaviour,
2) suitable ground and excited state potentials,
3) stability towards thermal and photochemical decomposition,
4) intense absorption at a suitable spectral region,
5) small energy gap between the reactive excited states,
6) high efficiency of population of the reactive excited state,
7) suitable lifetime of the reactive excited state,
8) high energy content of the reactive excited state,
9) adequate kinetic factors for outer sphere electron transfer reactions,
10) long excited state lifetime.[40]

Generally photosensitisers exhibit intense charge transfer bands in the visible region. Their lowest excited states are undistorted because they involve promotion of the electron to a delocalised π^* orbital[24]. They can be populated very efficiently due to the spin-orbit induced by the heavy metal atom, and may be sufficiently long lived to be involved in biomolecular processes. Even though the lifetimes are shorter than the lowest triplet of the free ligand, this is due to enhancement of intersystem crossing to the ground state. Redox sites must be present on both the metal and the ligands, which lead to additional redox possibilities not available to simple metal ions or organic molecules.

Photosensitisers should be intensely coloured, cheap, stable and readily available. Ligand photodissociation is a hindrance when dealing with Ru(II) bipyridyl complexes as thermally activated formation of a ^{3}MC excited state leads to the cleavage of a Ru-N bond forming a 5 coordinate square pyramidal species.

The population of the ^{3}MC state may be prevented by:

(a) adding enough quencher to capture the ^{3}MLCT state before crossing to ^{3}MC can occur,
(b) working at lower temperatures,
(c) increasing the energy gap between the ^{3}MLCT and the ^{3}MC,
(d) avoiding coordinating anions in solvents of low dielectric constants,
(e) increasing the pressure,
(f) linking together the three bpy ligands so as to form a single caging ligand which encapsulates the metal ion.[11]

If photodissociation is prevented Ruthenium polypyridyl complexes may be used as suitable photosensitisers for an artificial photosynthetic system, as it satisfies the kinetic, thermodynamic, spectroscopic and excited state requirements. Much study has gone into the creation of PMD's [41,42,43,44,45,46] and the optimisation of the photosensitisers. [47,48,49,50,51] In order to optimise the efficiency of photosensitisers and to form photostable and regenerative Ru(II) polypyridyl complexes more knowledge is required into the properties of these systems.

Early models of solar energy conversion were based on the water splitting reaction to generate O_2 and H_2. In simplistic terms, the Ru(II) polypyridyl complex photosensitisers harnessed the sun's energy, to yield its excited state, which in turn is quenched by a suitable electron relay, which in the presence of an appropriate catalyst, could perform oxidation and reduction steps. The excited state redox potentials of the $[Ru(bpy)_3]^{2+}$ are highly suited to this application, and electron relay is only required because the kinetics of the reduction of H^+ is slow, and not obtainable within the range of the excited state lifetime of $[Ru(bpy)_3]^{2+}$. Methylviologen has been successfully incorporated as a quencher in this scheme and the mechanism is shown in *Figure 12*.

This basic scheme has been expanded and developed by Gratzel and co-workers[52], who devised the first successful model for cyclic water photolysis in 1992, but the model has never achieved adequate efficiencies, to complete a viable and cost effective method of solar energy conversion.

Nevertheless, such work paved the way for a second scheme, employing Ru(II) polpyridyl sensitisers in a photovoltaic cell [53,54], which exhibits a commercially realistic energy conversion efficiency. The device consists of a semiconductor film of TiO_2, of nanometer size, coated with a charge transfer dye to sensitise the film for light harvesting. Current is generated when absorption of a photon gives rise to electron injection into the conduction band of the semiconductor. Regeneration of the dye is accomplished by electron transfer from a redox species in solution, which is in turn reduced at a counter electrode.

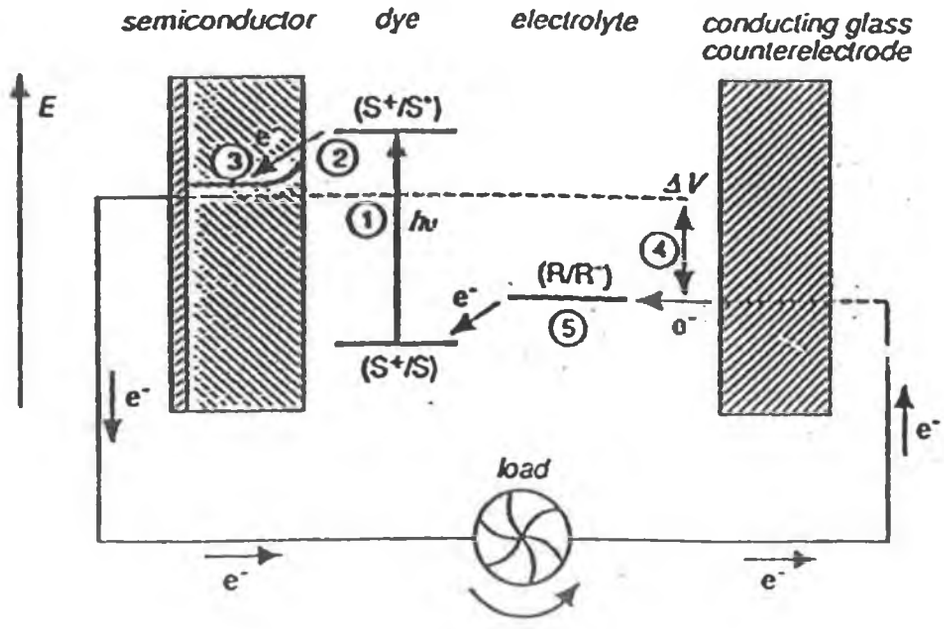

Figure 12 Dye sensitised photovoltaic cell for solar energy conversion [53].

Much attention has been given to the optimisation of the various parameters affecting the efficiency of these "solar cells".[55,56] Of particular interest was the chromophores of $Ru(bpy)_3^{2+}$ with TiO_2 or $SrTiO_2$ since this offers the possibility to shift the water cleavage activity of the oxides into the visible. High efficiencies in the sensitisation of colloidal anatase particles and polycrystalline electrodes were achieved using tris-(2,2'-bipyridyl-4,4'-dicarboxylate) ruthenium(II) dichloride as a sensitiser.[57]

Another such cell employed the trimeric ruthenium complex, $RuL_2(\mu(CN)Ru(CN)L_2')_2$, where L is 2,2'-bipyridine,4,4'-dicarboxylic acid and L' is 2,2'-bipyridine.[58] The absorption range of this dye extends to about 700 nm and is almost 100 % below 500 nm. The device was reported to harvest a high proportion of incident solar energy (46 %), and convert >80 % of this to electrical current. The overall solar conversion efficiency was 7.1-7.9 % in stimulated sunlight and 12% in diffuse daylight. On using different dyes, greater levels of efficiency may be reached. Cis-Ru(II)-(2,2'-bipyridyl,4,4'-dicarboxylate)X_2, (where X = Cl, Br, CN, I and SCN) have been used, again showing broad absorption over the visible spectrum, and suitable emission to promote electron injection into wide band gap semiconductors. [59] These cells displayed an efficiency of 10 % and demonstrated long term stability, another important consideration in the choice of dye, for such systems. The efficiency of these cells, is not solely dependent on the dye, and different semiconductors have been introduced such as ZnO_2. [60] However, the dye dictates many parameters, such as range of the solar spectrum captured and stability of the cell. Therefore it seems worthwhile to seek optimisation of the dyes properties, as an approach to improve efficiency and commercial viability.

1.2 Chemistry of Ruthenium

In 1884 Ruthenium[61] was first reported as a distinct metal by Karl K. Klaus at the University of Tartu in Estonia, and was named after the Latin name for Russia, Ruthenia. Ruthenium is a rare noble metal and a member of the six platinum group metals (Ru, Os, Rh, Ir, Pd and Pt). The natural abundance of Ruthenium in the earth's crust is very low (10^{-3} to 10^{-4} ppm), rhodium is the only element of the six platinum group metals, which is more rare. Ruthenium is extracted from the platinum sludges obtained during the electrolytical refinement of nickel.

Ruthenium is of great interest in the field of inorganic synthesis of metal complexes due to its rich coordination chemistry, and oxidation states from VIII (d^o valence electron configuration) to II (d^6 valence electron configuration) are obtained in complexes with nitrogen-, phosphorus- and some oxygen- containing ligands. The source of ruthenium in this thesis was $RuCl_3$ which was used for the synthesis of the starting dichloride's $[Ru(L)_2Cl_2]$.[62] The scope of this thesis is strictly confined to coordination compounds of Ru(II) with nitrogen donor ligands. To this day Ru(II) compounds are of great interest as they are intensely coloured complexes, which display interesting photophysical and photochemical behaviour.

1.2.1 Ruthenium tris-bipyridine – The "parent" complex

The complex Ruthenium tris(bipyridyl) $[Ru(bpy)_3]^{2+}$ in Figure 13 is the parent molecule of the complexes illustrated in this report. Ruthenium(II), binds 3 bidentate bipyridine ligands, in an octahedral configuration. $[Ru(bpy)_3]^{2+}$ has become of great interest since the 1950's when its luminescence was first reported [63] as it has potential use as a building block for photoactive studies of molecules. [64] Emission of light in the form of luminescence occurs from a metal-ligand charge transfer (^{3}MLCT) state with quantum efficiency at room temperature of about 4%.[65]

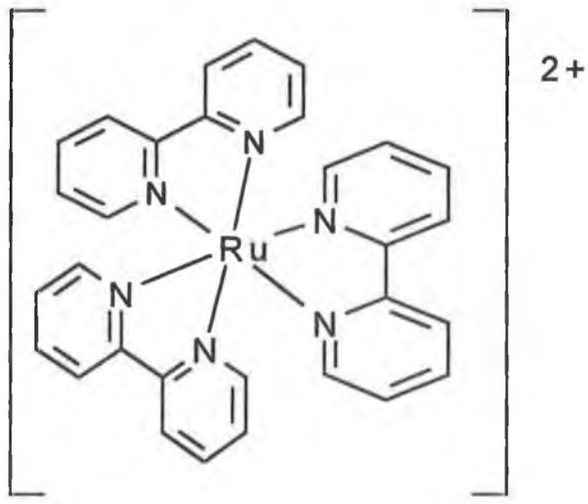

Figure 13 Ruthenium tris-bipyridine, $[Ru(bpy)_3]^{2+}$.

For $[Ru(bpy)_3]^{2+}$ the HOMO (highest occupied molecular orbital) is the t_{2g} and the LUMO (lowest unoccupied molecular orbital) is the ligand π^* orbital. Consequently the lowest energy transition in this complex is MLCT in nature and may be seen in the visible region of the absorption spectrum. This absorption band is observed at 450nm (ε_{max} = 13000 $M^{-1}cm^{-1}$) [66,67,68,63,69]. Weaker bands in the absorption spectra have been assigned to (Laporte forbidden) charge transfer transitions (322 and 344 nm)[36], to states having largely triplet character, providing evidence of the existence of such levels. This interpretation is supported by absorption spectra of the excited state species, whose spectral features displayed striking similarity to that of bpy^-, and further confirmation by resonance raman spectroscopy.[70] The intensity of the absorption can be justified on the basis of a spin allowed transition, whereby charge transfer is believed to take place for the singlet ground state, to a MLCT singlet state. [67] The luminescence excited state in the absence of a quencher, can then decay to ground state, with the emission of light.

For metal - ligand complexes the molecular orbital theory calculations of orbital interaction between a metal and ligand suggest the orbital arrangement shown in Figure 15 for metal ligand complexes. Various transitions are possible, MC: metal centred, LC: ligand centred, MLCT: metal to ligand charge transfer, LMCT: ligand to metal charge transfer. The relative energy of these levels may vary, depending on the nature of the ligands.

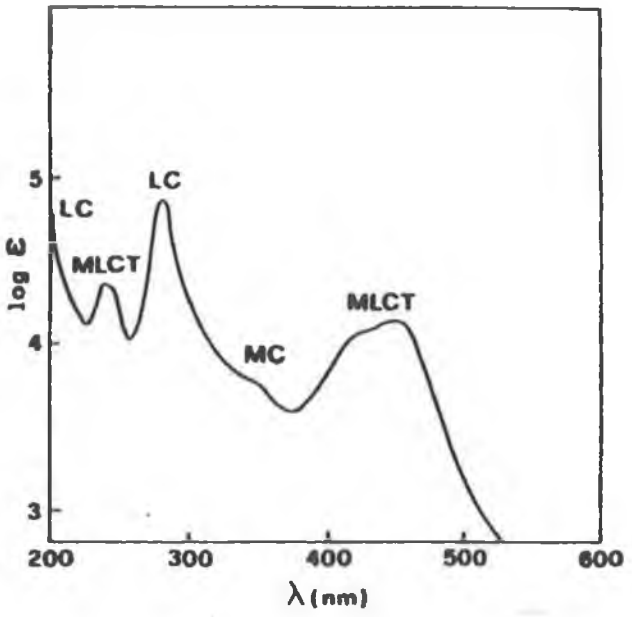

Figure 14 The electronic absorbance spectrum of $[Ru(bpy)_3]^{2+}$ [10].

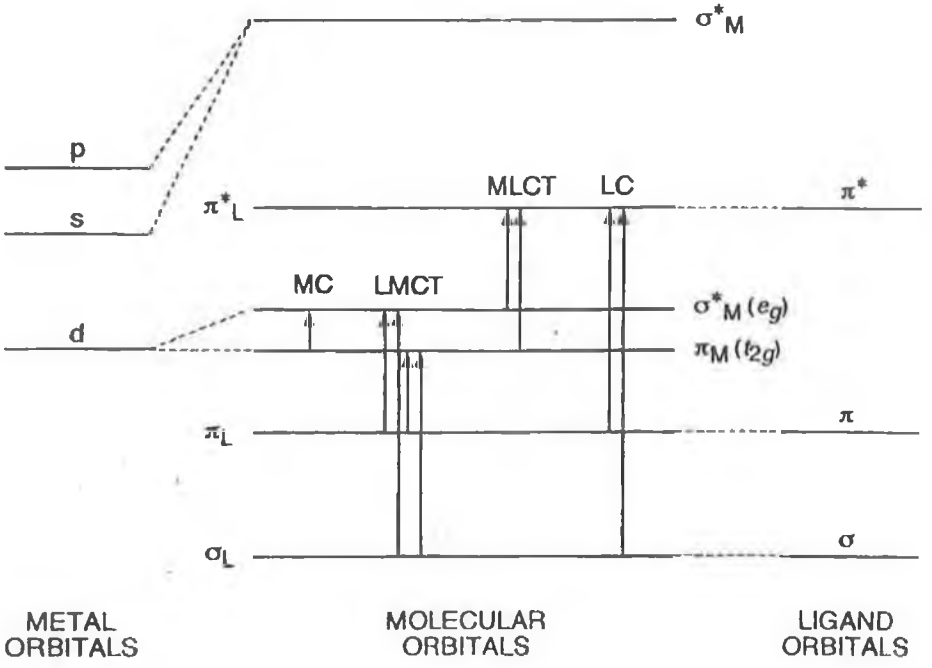

Figure 15 Molecular Orbital diagram for an octahedral transition metal Complex[10].

Much debate on the nature of the emissive state has concluded that emission is dominated by relaxation from lower triplet states illustrated in Figure 16, based on the magnitude of the excited state lifetimes (0.5-10 μs)[69], and longer wavelength emission (582nm). Intersystem crossing (ISC) between the singlet and triplet states occurs as a result of spin-orbit coupling, which is relatively strong because of the presence of a second row transition metal, and allows effective mixing of the two states, which would normally be dipole forbidden. In fact the efficiency of ISC in this compound has been shown to be 100%[71]. The lowest lying states however remain largely triplet in character, and emission, to the singlet ground state, is now believed to be mainly phosphorescence. Phosphorescent decay, because dipole forbidden, displays longer excited state lifetimes than that of fluorescence, this is desirable for photosensitisers, since relatively long lifetimes are required, to allow charge or energy transfer to take place.

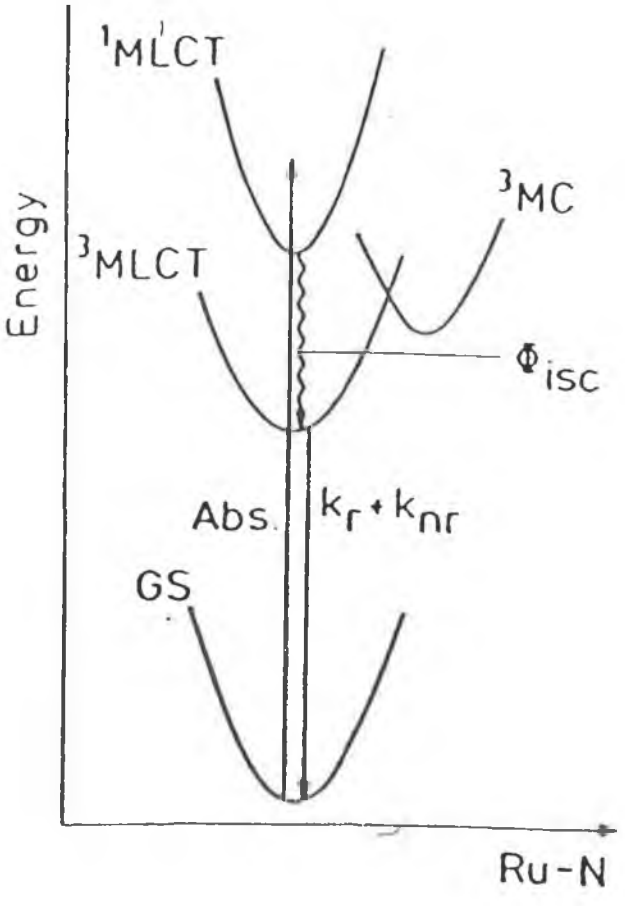

Figure 16 Photophysical processes in $[Ru(bpy)_3]^{2+}$ [10]

Emission is not the only decay pathway for the excited state of $[Ru(bpy)_3]^{2+}$. In addition to the radiative and direct non-radiative pathways, two other thermally accessible pathways have been found for Ru(II) polypyridine systems[72], one a ligand field d-d and the second a 4th MLCT state as shown in Figure 16.

Temperature dependent studies have shown increased photochemical activity for $[Ru(bpy)_3]^{2+}$ at elevated temperatures [73,74]. Although relatively photoinert in aqueous solution at room temperature [73,74,75], photolysis of $[Ru(bpy)_3]^{2+}$ in aqueous solution has been observed at higher temperatures [74] and substantial photochemical deactivation is observed at 95°C [73]. It is this photochemical deactivation, that precludes $[Ru(bpy)_3]^{2+}$ from being a suitable photosensitiser, and has spurred interest in alternative Ru(II) complexes.

1.3 Characteristics of Ruthenium(II) polpyridyl complexes

Several contributions have been published [63,64] on the ground- and excited- state properties of $[Ru(bpy)_3]^{2+}$ as a source of theoretical and experimental reference for the model Ru(II) complexes to be compared with. These citations describe the available techniques and methods of study, which included; absorption spectroscopy, emission spectroscopy, photo-oxidation, temperature dependence of the emitting excited state lifetime (τ) and quantum yield emission (Φem), photosubstitution, ground and excited state reduction potentials, and electron transfer quenching studies.

Several important topics arise when describing the photophysics of the parent molecule $[Ru(bpy)_3]^{2+}$:

- the nature of the lowest excited state (^{3}MLCT),
- localisation of the excitation energy,
- the relative importance of low-lying metal-centred dd states (^{3}MC; important pathways for photodeactivation to occur at higher temperatures),
- the correlation between the emission energy and the lifetime of the emitting state (the "energy gap law" suggests that the higher the energy, the more long-lived the emitting state),
- solvent and medium effects (solvation of the more polar excited state).

1.3.1 The nature of the ground state

Absorption of a photon of energy in the visible or ultraviolet region by a metal complex S leads to its transformation to an electronically excited state S*. At upper excited state levels, molecules are also usually vibrationally excited in a way that depends upon the relationship of the geometry of the upper electronic state to the ground state i.e. Franck - Condon principle. Relaxation of the complex in the upper electronically excited state to the lowest excited state S* often occurs rapidly (picoseconds or less).

S* can undergo radiationless transition to a nearby excited state S** of the same or different spin multiplicity. Non- radiative relaxation between two states of the same multiplicity is called an internal conversion, while those of different multiplicity are known as intersystem crossing (ISC). The molecule in the excited state S* can return to the ground state S dissipating the excess electronic energy in the form of heat to the surrounding medium (non-radiative decay) or by emission of a photon (radiative decay as shown in S* → S + hν'(luminescence) eqn. 3),

S + hν → S* eqn. 2

S* → S + hν'(luminescence) eqn. 3

Radiative processes between states of same multiplicity are called fluorescence and those between states of different multiplicity phosphorescence. Transition metal complex excited states involve the promotion of d electrons rather than s or p, as partially filled, essentially non-bonding molecular orbitals in d can function in either a donor or acceptor capacity.

Absorption spectra of Ru polypyridyl complexes contain various bands corresponding to transitions between several well-defined electronic configurations. Excited states in the case of organic molecules are described as electronic transitions involving electrons of σ and π bonds and lone pairs (n): σ-σ*, π-π* and n-π*. It is convenient to describe transitions of transition metal complexes in three categories (Figure 18);

1. LC: those centred primarily on the ligand orbitals,
2. MC: those centred primarily on the metal,
3. CT: charge transfer types involving the electrons of the central metal and the ligands.

Crystal field theory provides a general framework to analyse the bonding interactions between the electrons on the metal ion and those on the ligands during the formation of the metal complex.

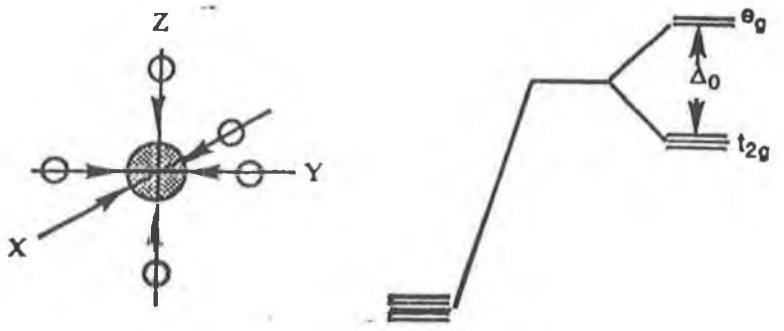

Figure 17 Schematic presentation of splitting of metal d orbitals in an octahedral ligand field [10].

Ligand field theory is a molecular orbital extension of crystal field theory. In general the majority of coordination complexes are assumed to be octahedral. Figure 17 presents schematically the splitting of metal d orbitals in an octahedral field. Not all d electrons of the central metal ion are destabilised equally by the ligand cage. Those d electrons residing in the d orbitals that point toward the ligands (e_g set) are repelled more by the negative ligands than those residing in the d orbitals that are directed between the ligands (t_{2g} set). The difference Δ_0 in destabilisation energy leads to the splitting of the d orbital energies. The magnitude of the crystal field splitting parameter Δ_0 is determined by several factors;

(i) the radius of the metal ion,
(ii) the charge of the central ion,
(iii) the nature of the ligands.

The metal orbital diagram is combined with the ligand orbital diagram in order to arrive at a composite model for the entire system. Since the relative disposition of the two sets of orbitals can vary, and indeed is determined by the very nature of a specific complex, several different possibilities for orbital arrangements arise.

Figure 18 presents possible electronic transitions in an octahedral complex: ligand centred (π_L-π_L*)(IL or LC), metal centred or ligand field (LF, MC or d-d) and charge transfer (CT). The charge transfer process may be further subdivided into charge transfer from metal to ligand (d-π_L*) (MLCT) and ligand to metal (σ_L or π_L- d) (LMCT). A charge transfer transition (CT) is defined as the addition or removal of an electron from a partly filled shell of a metal and a change in the oxidation state by +1 or -1.

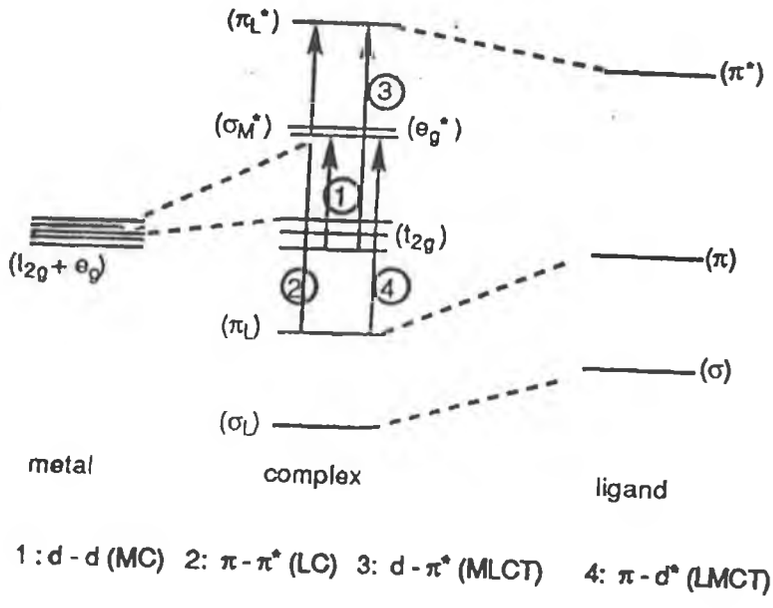

Figure 18 Relative disposition of metal and ligand orbitals and possible electronic transitions in an octahedral ligand field of a transition metal complex [10].

Most common are the intramolecular type involving the metal ion and the ligand system. Charge transfer from the ligands to the coordinated metal leads to transitions that are known as ligand to metal charge transfer (LMCT). Ligand to metal charge transfer bands are found in the UV and visible light region. Metal to ligand charge transfer (MLCT) transitions involve promotion of an electron from an orbital largely localised on the metal to an orbital, which is essentially ligand localised.

1.3.2 Properties of electronically excited states

The decay dynamics and photochemical reaction pathways depend to a large extent on some of the physical properties of the excited state $[Ru(bpy)_3]^{2+}*$, e.g. the efficiency of population of the emitting excited state (ϕ), usually [64,71] taken to be unity; the lifetime of the emitting excited state (τ), and the quantum yield of this emission (ϕem) in relation to competing, non-radiative decay pathways. By investigation of these fundamental photophysical properties an estimate of the practicality of using such photochemical properties as part of a photosensitiser can be made.

Design of stable sensitisers requires knowledge of the relative rates of these processes. The energy distribution of the emitted light (emission spectrum), lifetime and quantum yields together quantitatively describe the relaxation of the excited state. Emission spectra provide two important pieces of information on the excited state: the electronic origin (v=0 level) of the lowest excited state and the extent of distortion of the excited state relative to the ground state. The latter is known as the " Stokes shift". Excited electronic states in metal complexes relax by a combination of radiative and non-radiative processes with rate constants k_r and k_{nr} respectively. Relaxation of electronically excited states of transition metal complexes can be investigated by luminescence spectroscopic techniques i.e. pulsed excitation. The relative magnitude of these two processes can be deduced from the emission quantum yield ϕ and lifetime data τ:

$$\mathbf{1/\tau = k_r + k_{nr}} \quad \textbf{eqn. 4}$$

$$\mathbf{\phi_{em} = k_r/ (k_r + k_{nr})} \quad \textbf{eqn. 5}$$

Non- radiative relaxation processes can occur in one of the following ways:

(1) vibrational relaxation of an excited state species within one electronic state by collisional interaction with the surrounding medium,
(2) internal conversion from one electronic state to another state of same multiplicity; and
(3) intersystem crossing between states of different multiplicity.

The mechanisms by which electronically excited states transfer excess vibrational energy during radiationless transitions have been of much theoretical interest. In general C-C and C-H stretching modes are considered as principal "accepting" modes, the vibrational modes into which the majority of the excited state energy is disposed. The role this concept plays in deuteriation effect will be discussed later.

1.3.3 Acid - base properties

An excited state molecule is a new chemical entity with physical and chemical properties quite different from those of the ground state. One such chemical property that can change in the overall acidity/ basicity of the complex is its pK_a (pK_a (S)≠ pK_a (S*)), then the excited state molecule during its short lifetime can accept or release a proton from one of its ligands. In some cases, distinct emission can occur from both the protonated (SH*) and unprotonated (S^-*) species. Thus occurrence of such acid-base reactions can be detected and analysed by the pH dependence of luminescence.

Due to the negative triazole ring contained in the complexes cited in this text the pH dependencies of the compounds must be closely monitored as on protonation of this triazole a large shift in the photophysical properties of the complex will arise i.e. reducing the σ-donor capacity of the ligand. Also with compounds containing pyrazine rings over-protonation may arise where the triazole ring and the pyrazine ring is protonated so for this reason the pK_a of the complexes is of utmost importance.

For polypyridyl complexes, the protonation constant pK_{BH+} is often used as a measure of ligand σ-donation to the central metal ion, which results in a higher formal charge of the metal ion and consequently stabilisation of the metal dπ orbitals. π-acceptor ability of the ligands can be estimated from the reduction potentials, and in fact they correlate with the calculated LUMO of the ligand π* orbitals. Thus acid-base properties of the coordinated ligands provide direct information of the interplay between the σ-donor strength and π- acceptor properties in influencing the metal to ligand charge transfer (dπ-π*) transitions.

Förster has provided a quantitative relationship between the frequency shift accompanying the protonation and the change in the equilibrium constant upon excitation ΔpK_a. At 298 K, the relationship is (in cm^{-1})

$$\mathbf{\Delta pK_a = 0.00209(\nu_S^- - \nu_{SH}) \quad eqn.\ 6}$$

where ν_S and ν_{SH+} are the frequencies of the lowest absorption bands of S^- and SH. The inflection point of the fluorescence intensity against acidity gives a first approximation of the pK_a^* of the excited state, but this involves the assumption that the protolytic equilibrium is established within the lifetime of the excited state and that the emission lifetimes of S and SH^+ are equal. When the rate of luminescence decay is considerably less than the protolytic rate constants, the system reaches equilibrium. In this case:

$$\mathbf{pH = pK_a^* - \log(\tau/\tau_0') \quad eqn.\ 7}$$

where pH is the acidity at which the relative emission intensity curves show the inflection and τ_0' and τ are the excited state lifetimes of S and SH^{+*} respectively.

1.3.4 Redox properties

The intense interest regarding the nature of the lowest lying excited state is quite understandable; the luminescence emission data are readily accessible experimentally, as well as electrochemical data. The properties of the ground and excited states of $[Ru(bpy)_3]^{2+}$ are often summarised in an illustration as in Figure 19. The excited state is a powerful reductant (-0.86V), and oxidative quenching of $[Ru(bpy)_3]^{2+*}$ has been extensively employed in electron transfer studies. $[Ru(bpy)_3]^{2+*}$ is also a quite good oxidant (+0.86V), and reductive quenching does sometimes compete. By convention it is always the redox couple which is defined for a given couple e.g. Ru(III)/Ru(II)*, for the sake of comparison with other redox couples.[76] The half cell reactions are written as reductions:

$$\mathbf{Ru(III) + e^- \rightarrow Ru(II)^*} \qquad \mathbf{E^o = -0.86V \quad eqn.\ 8}$$

$$\mathbf{Ru(III) + e^- \rightarrow Ru(II)} \qquad \mathbf{E^o = +1.26V \quad eqn.\ 9}$$

The significance of the much lower reduction potential for the couple Ru(III)/Ru(II)* is that any couple with lower standard reduction potential reduces any couple with higher standard reduction potential. Thus, if the reduction potential is lowered, by the change in properties on going to the excited state from +1.26V for the ground state couple Ru(III)/Ru(II)*, all couples between +1.26V and –0.86V can be reduced.

All molecular excited states are potential redox reagents since the absorption of light leads to excitation of an electron to a higher level where it is more weakly bound and at the same time to an electron hole in the lower level. Excited state species hence can be better oxidants as well as reductants than the corresponding ground state as previously mentioned. The ground and excited state inter- relationships are best illustrated in the form of a Latimer-type diagram, as shown in Figure 19 for the MLCT excited state of $[Ru(bpy)_3]^{2+}$.

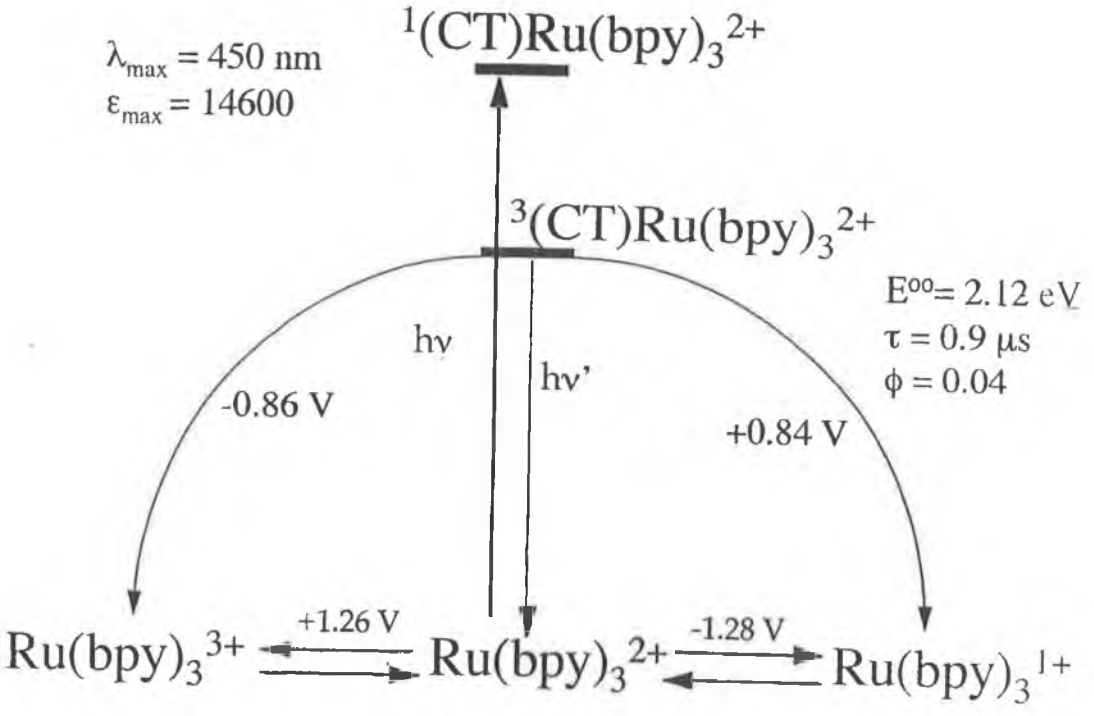

Figure 19 Latimer-type diagram illustrating the inter-relationships of ground state redox potentials with that of the excited state [77].

The correlations between spectroscopic and electrochemical quantities are based on the assumption that the spatially isolated π* acceptor orbital is the same for both the reduction process and the charge transfer transition. It turns out that, for most transition metal polypyridyl complexes, the redox and spectroscopic orbitals are the same. In this report the characterisation of several Ruthenium polypyridyl complexes are portrayed and the measurements achieved for each property as outlined in this chapter are tabulated and discussed.

1.4 Tuning of the excited states

1.4.1 Use of different metal centres

Polypyridine complexes with different metal centres have been investigated, the most obvious being those of the other group 8a metals, iron and osmium. Iron, being readily available and less expensive, would be a very attractive alternative, but the chemistry of its complexes are in stark contrast to those of their Ruthenium analogues. $[Fe(bpy)_3]^{2+}$ does not luminesce significantly in the visible region however it is deep red in colour and absorbs strongly in the visible region. Its lowest excited state is ligand field rather than charge transfer in nature [78]. Osmium analogues, on the other hand, exhibit a chemistry closely related to that of Ruthenium, but their charge transfer excited state lifetime has been reported to be 10-30 times shorter[78]. However, Osmium's MLCT state lies at lower energy than that of Ruthenium, and for this reason, Osmium complexes are, as expected, more stable toward photodissociation[79]. The following illustrates the difference in luminescent lifetimes on altering the metal centre:

Metal complex	Lowest excited state	Luminescent
$[Fe(bpy)_3]^{2+}$	MC	No
$[Ru(bpy)_3]^{2+}$	MLCT	Yes(610nm)
$[Os(bpy)_3]^{2+}$	MLCT	Weakly(720nm)
$[Ir(bpy)_3]^{2+}$	LC	Yes(450nm)

Interest in Osmium complexes to date has been small, relative to the vast research performed on Ruthenium polpyridine complexes, however the two families have been found to complement each other well in mixed metal complexes.

1.4.2 Ligand substitution

Since the number of suitable metals is very limited, the search for alternatives has thus far focussed mainly on the ligand system, with the maintenance of the Ru metal centre and the presence of three bidentate ligands allowing for fine-tuning of the properties.

A considerable amount of effort has been directed towards modification of the polypyridine ligand systems, with a view to obtaining more robust complexes with richer spectroscopic and electrochemical properties, essentially fine tuning excited state energies, lifetimes and modes of decay. Approaches have included attachment of electron mediating substituents to the pyridine rings, employing ligands with different electronic contributions to σ-donor and π-acceptor systems, in homoleptic and heteroleptic configurations, and the development of polynuclear complexes, presenting interesting and varied spectroscopic and electrochemical properties, unattainable with mononuclear complexes.

The ligands which may be encountered in such substitution may be grouped into 2 classes, according to their σ-donor and π-acceptor abilities. Strong π-acceptor ligands are referred to as Class A type ligands, the effect of which are expected to lower the energy of the π-bonding and anti-bonding levels. Pyridine, Pyrazine and Pyrimidine containing ligands have relatively low lying π* orbitals and therefore act as good π-acceptors [80,81,82,83,84,85]. Some coordinating ligands which are greater π-acceptors have been studied extensively i.e. bipyrazine[86,87,88,89,90,26,91], bipyrimidines [92], and biquinolines each of which have been studied in their mononuclear and dinuclear forms and with one or all of the bipyridyls replaced.

These complexes were found to have a λ_{max} which is red-shifted compared to that of $[Ru(bpy)_3]^{2+}$, hence the absorbance range is made more accessible to the solar spectrum [93]. As π-acceptance strength of these ligands is increased (estimated on the basis of reduction potentials), the absorbance and emission spectra shifted further into the red. Correlation between LUMO energy, reduction potential and absorption and emission energy have shown that they are linearly dependant on each other [94], so the red shift observed is indicative of lower LUMO's in these complexes. In the case of mixed ligand complexes, the MLCT excited state has been shown to be localised on the most easily reduced ligand and that emission occurs solely from this state, as seen for $[Ru(biq)(bpy)_2]^{2+}$ [95],$[Ru(bpz)(bpy)_2]^{2+}$ and $[Ru(bpm)(bpy)_2]^{2+}$ [93], where emission originated only from the Ru→biq, bpz and bpm MLCT state respectively.

Interestingly, absorption spectra of the above mentioned complexes showed MLCT bands characteristic of both ligands in the complex. Emission for these complexes occurs entirely from the lowest MLCT excited state [96].While the red-shifted absorption of the Class A type ligands, as a consequence of, lower lying LUMO's, is advantageous, these ligands are usually weaker σ-donors than bipyridine, and the ligand field splitting is reduced in their metal complexes. This effect renders them, in general, less photostable, as a result of easier accessibilty of the MC decay pathway. Homoleptic complexes, can be particularly problematic in this regard, the photodissociative MC state of $[Ru(biq)_3]^{2+}$ in *Figure 20* is shown to be easily populated at room temperature[95]. Mixed ligand complexes have circumvented this problem to some degree, as weak and stronger σ donors can be combined in the same complex, and the LUMO can be lowered with less effect on ligand field splitting.

Considerable improvement in photostability has been observed in going from $[Ru(biq)_3]^{2+}$ to $[Ru(biq)(bpy)_2]^{2+}$. Studies have predicted that the lowest MC excited state lies approximately 5500 cm^{-1} above the Ru→biq lowest excited state in $[Ru(biq)(bpy)_2]^{2+}$, in contrast to 2700 cm^{-1} in $[Ru(biq)_3]^{2+}$, suggesting that $[Ru(biq)(bpy)_2]^{2+}$ is less susceptible to photodecomposition.[95] Indeed, a report investigating the synthetic manipulation of decay pathways of the excited state in $[Ru(bpy)(bpz)_2]^{2+}$ heteroleptic complexes, illustrated the effect of increased donor strength of the spectator ligand, on the accessibility of the lowest MC state and concluded that complexes containing stronger donors, will be more photostable.[72] The donor strength of the bipyridine ring can be increased on attachment of methyl and phenyl derivatives, the latter giving a stronger effect. Luminescence and photochemical quantum yield data, as reported [97] for homo and heteroleptic complexes of these bipyridine derivatives, have shown that methyl and phenyl substitution to inhibit photodecomposition and enhance excited state lifetimes.

Such effects as mentioned above, brings about interest in a second class of ligands, the strong σ-donors. Strong σ-donation, increases ligand field splitting, and is also responsible for stabilisation of the t_{2g} d orbitals of the metal.

This is characteristic to class B type ligands such as triazoles [98,99,100,101,102,103,104], the imidazoles [105,106] and the pyrazoles [107,108,109]. These type of ligands posses π^* levels of much higher energy than bpy, due to their strong σ-donor abilities, and as a result, in mixed chelate complexes containing these ligands and bipyridyls the excited state is always on the bipyridyl [110]. Higher energy absorption would therefore be required for MLCT excitation in their homoleptic complexes, and this is reflected by a blue shift in absorption, as for Ruthenium tris-[1-(2-pyridyl)-3,5-dimethyl pyrazole], λ_{max}=382 nm [111]. Since such a shift is undesirable for solar energy absorption, mixed ligand complexes of these ligands, where they participate as spectator ligands, forms the basis of interest in class B ligands.

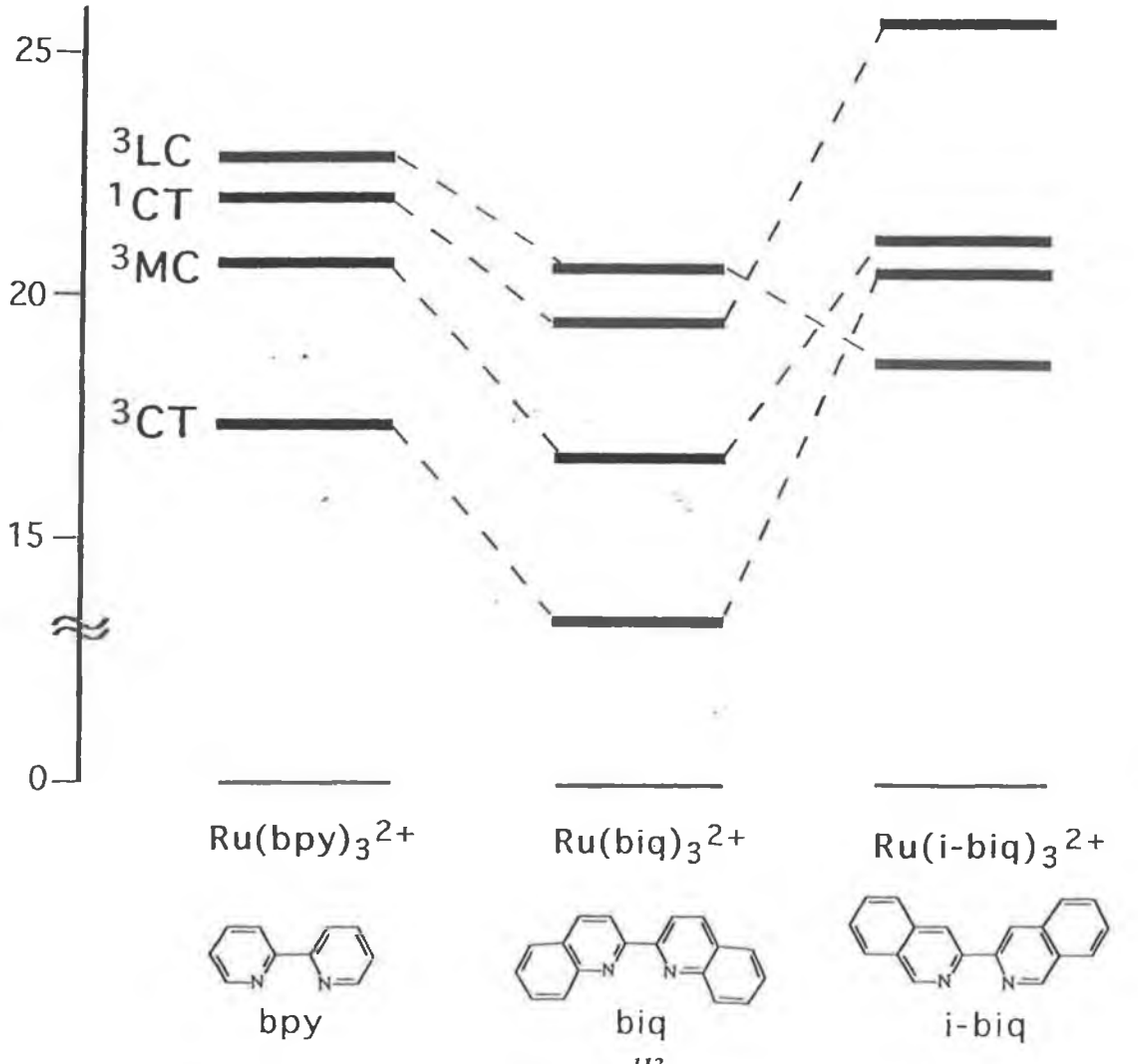

Figure 20 Tuning the excited state properties[112].

A spectator ligand does not actually get involved in the excited state, that is, it is not reduced. Mononuclear mixed ligand complexes containing these ligands, as for those cited in this text, have been studied for localisation of the excited state. Resonance Raman spectra and electrochemical data for $[Ru(bpy)_2bpt]^+$, has indicated that reduction is bipyridine based [113], as is consistent with the view the lowest excited state lies on the ligand with the lowest π^* level. Despite being redox inactive in many mixed ligand complexes, the role of these ligands in the manipulation of the excited state is twofold. Firstly a red shift in the MLCT absorption band is observed for heterocomplexes, containing class B ligands i.e. $[Ru(bpy)_2bpt]^+$, compared to that of the parent complex $[Ru(bpy)_3]^{2+}$ [66] and for $[Ru(bpz)_2(dmb)]^+$ [72] whose absorption is red shifted, compared with $[Ru(bpz)_3]^{2+}$ and $[Ru(bpy)_3]^{2+}$. This can be justified by the increased electronic charge on the metal centre, leading to easier reduction of the ligand. Secondly, as previously discussed, in the case of the methyl and phenyl derived bipyridine ligand, increased donor strength enhances ligand field splitting and inhibits photodecomposition. Thermal activation of the upper MC excited state in $[Ru(bpy)_2bpt]^+$ is found to be absent [66]. Proof that this can be attributed to the ligand donor strength is found in the reduced photostability of the dinuclear $[(Ru(bpy)_2)_2bpt]^+$, where the ligand donor strength is shared between the two metal centres, and so ligand field splitting is smaller.

The asymmetry of the coordination sites of the triazoles is a very useful property whereby the specific sites chosen by the coordinating ligand effects the magnitude of σ-donation experienced by the metal [114]. The acid/base chemistry of the triazoles is very important as the uncoordinated nitrogen can undergo protonation and deprotonation, which profoundly effects the π-acceptor and σ-donor properties of the ligand.

Therefore the combination of the two classes of ligands, in mixed ligand complexes, has provided photostable complexes with most desirable spectroscopic properties. Thus ligand nature can be instrumental in manipulation of excited state properties, and following the above classification, predictions of ligand effects can be employed in the design of complexes of a given application.

1.4.3 Bridging ligands

The bridging and non-bridging ligands incorporated in these studies are aromatic, nitrogen-heterocyclic ligands that form chelate complexes with many transition metal species. The ligands below which are cited in this text, all possess low-lying π^* orbitals, are thermally robust, and are stable when reduced in either their free or metal coordinated forms.

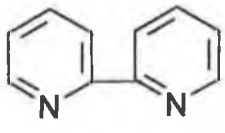

Bipyridine (Bpy)

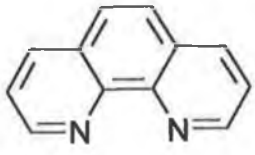

Phenanthroline (Phen)

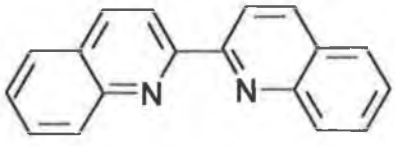

Biquinoline (Biq)

Other examples of such ligands are:

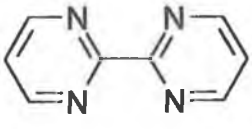

Bipyrimidine (Bpm)

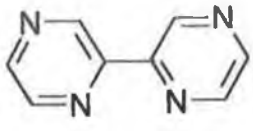

Bipyrazine (Bpz)

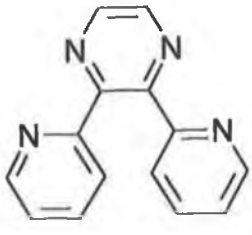

Dipyridylpyrazine (Dpp)

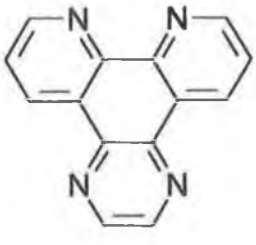

Phenanthrolinepyrazine (Ppz)

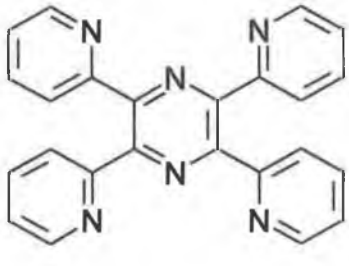

Tetrapyridylpyrazine(Tpp)

Figure 21 Examples of nitrogen containing ligands that form chelate complexes with transition metals.

The ligands Bipyridine (bpy), phenanthroline (phen) and biquinoline (biq) will only bind one metal centre, whereas ligands such as bipyrimidine (bpm), dipyridylpyrazine (dpp) and tetrapyridylpyrazine (Tpp) can bridge two metal centres.[115,116] Where bpy, phen, bpm and dpp are bidentate ligands, tpp is a tridentate ligand. For bpm, both six membered rings interact with the two metal centres in an equivalent fashion, while for dpp and tpp there are some rings bound to both metal centres and others that are only bound to one metal centre.

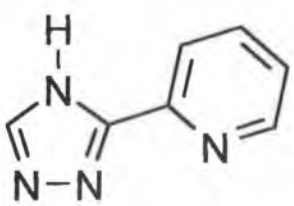

3-(pyridin-2-yl)-1,2,4-triazole, (Hpytr)

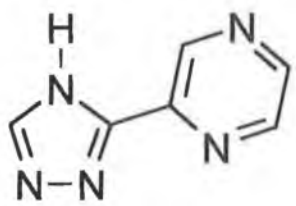

3-(pyrazin-2-yl)-1,2,4-triazole, (Hpztr)

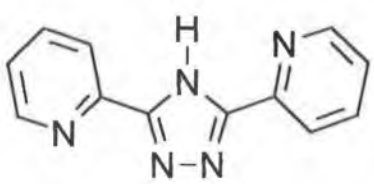

3,5-Bis-(pyridin-2-yl)-1,2,4-triazole,(Hbpt)

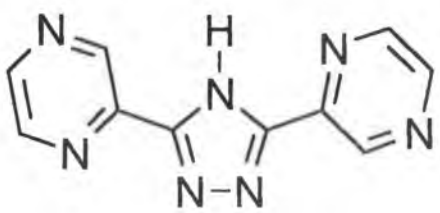

3,5-Bis-(pyrazin-2-yl)-1,2,4-triazole,(Hbpzt)

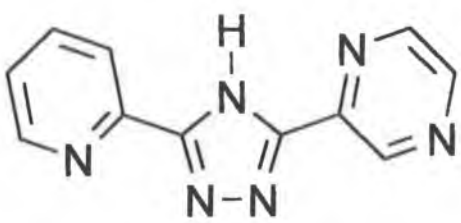

3- (pyridin-2-yl)-5-(pyrazin-2-yl)-1,2,4-triazole, (Hppt)

Figure 22 Assymetric and symmetric Ligands containing 1,2,4-triazole

The ligands of interest in this study all contain a triazole ring, which possess π^* levels much higher in energy than bipyridine. It has been observed for all the asymmetric ligands cited, on synthesis, coordination isomers are formed.

The ligands Hbpt, Hbpzt and Hppt all form mononuclear and dinuclear complexes. Also the design of the ligands incorporates the pyridine and pyrazine class A type ligands and the triazole of class B type ligands which should give interesting results in the photophysics of their ruthenium(II) complexes. The combination of the two classes of ligands is hoped to perturb the excited state energy levels enough to enhance photostability. This will be referred to further in the experimental chapters of this text.

1.5 Applications of deuteriation in inorganic chemistry

Deuteriation has been incorporated into the characterisation of excited states of organic compounds for many years, prior to its potential for use in coordination chemistry was revealed. Several uses were discovered for deuterium exchange in the investigations of organic molecules[117,118,119,120]. As deuteriation became more practical further studies were carried out on deuteriation techniques[121,122,123]. As the uses of deuteriation grew in the organic field, one of its first reports of its application in inorganic chemistry was by Van Houten and Watts in 1975[124]. The investigation of the effect of ligand and solvent deuteriation on the excited state properties of $[Ru(bpy)_3]^{2+}$ were studied, which revealed that deuteriation of the free ligand caused the measured luminescent lifetime, τ_m, to more than double. The effect of ligand deuteriation was, however, mitigated in the complex, but a large isotope effect was then observed for the solvent. Deuteriation of the solvent caused the radiationless lifetime to almost double, while the deuteriation of the ligand caused only a 20% increase.

Sample	*Solvent*	*Temperature*	τ_m
$[Ru(bpy)_3]Cl_2$	H_20	25°C	0.58μsec
$[Ru(d_8\text{-}bpy)_3]Cl_2$	H_20	25°C	0.69μsec
$[Ru(bpy)_3]Cl_2$	D_20	25°C	1.02μsec
$[Ru(d_8\text{-}bpy)_3]Cl_2$	D_20	25°C	1.25μsec
$[Ru(bpy)_3]Cl_2$	EtOH/ MeOH 4:1(v/v)	77K	5.10μsec
$[Ru(d_8\text{-}bpy)_3]Cl_2$	EtOH/ MeOH 4:1(v/v)	77K	6.10μsec
H_8-bpy	EtOH/ MeOH 4:1(v/v)	77K	0.97sec
D_8-bpy	EtOH/ MeOH 4:1(v/v)	77K	2.20sec

Table 1 Lifetimes of $[Ru(bpy)_3]^{2+}$ complex ion in aqueous solutions[124].

The results for this investigation are listed in *Table 1*, effect of solvent deuteriation was explained in terms of an excited state model involving partial charge transfer to solvent (CTTS).

In mixed ligand systems such as $[Ru(bpy)_2L][PF_6]_n$, the excited state may lie on either the bipyridine or the ligand(L). Methods of determining its location are required for the correct assignment of spectroscopic bands and LUMO energies. Current methods incorporated to locate the excited state are electrochemical data and Resonance Raman spectroscopy, but a more recent approach has investigated the deuteriation of ligands [125] in order to achieve this purpose. It was found that upon deuteriation the emission lifetimes will increase which is in agreement with Siebrands theory of non-radiative transitions, which states that, high energy, anharmonic C-H stretching vibrations are important promotional modes in non-radiative decay.[126] To describe this phenomenon, the word "overlap" must be used in terms of; the greater the overlap of the vibrational modes of the C-H and C-D stretches the greater the non-radiative decay (k_{nr}). However, there is an increase in amplitude of the vibrational stretches on going from C-H to C-D due to the heavier Deuterium atom, the "overlap" decreases causing k_{nr} to decrease and consequently increasing the lifetime.

In homoleptic $[Ru(bpy)_3]^{2+}$, deuteriation of the bipyridyl ligand has been shown to dramatically increase the lifetime of the excited state, and this can be explained, as already stated, in terms of the reduced vibrational energy of the C-D stretching modes compared with those of C-H, which are involved in the non-radiative relaxation modes of the excited state. The location of where the excited state lies in $[Ru(bpy)_3]^{2+}$ is under investigation by Kincaid[127,128,129] , Krausz[130,131,132] and Yersin[133,134,135] in order to determine if the excited electron is localised on one of the three bpy ligands, or delocalised over all three (identical) bpy units. Specific deuteriation experiments are being used to investigate this question and Yersin et al[134] suggest that the excited state electron is delocalised over all three bpy units in $[Ru(bpy)_3]^{2+}$.

This is based on a comparative study of the emission spectra of $[Ru(bpy)_2(bpz)]^{2+}$ (where bpz is 2,2'-bipyrazine), which has a localised excited state from Ru $d\pi \rightarrow$ bpz π^* as the energy of the bpz π^* is considerably lower than that of bpy and this was compared to the emission of $[Ru(h_8\text{-bpy})_2(d_8\text{-bpy})]^{2+}$. In the emission spectra of $[Ru(bpy)_2(bpz)]^{2+}$, only ligand centred modes of bpz could be found, whereas, in contrast, for $[Ru(h_8\text{-bpy})_2(d_8\text{-bpy})]^{2+}$ the ligand centred vibrations of h_8-bpy and d_8-bpy accompany the same electronic origin.

Riesen et al[132] portrayed that the presence or absence of vibrational sidelines cannot be used, as evidence for localisation/ delocalisation of ^{3}MLCT excitations. In the excitation spectra of the series $[Ru(bpy)_{3-x}(d_8\text{-bpy})_x]^{2+}$ (x= 0-3), in $[Zn(bpy)_3](ClO_4)_2$, they observed two sets of electronic ^{3}MLCT origins for the x = 1 and x = 2 systems. These were assigned as independent ^{3}MLCT transitions involving either the h_8-bpy or the d_8-bpy ligands. In order to confirm their assertion that the excited state electron is localised on a single bpy ligand, they extended their study of deuteriation effects to $[Ru(d_x\text{-bpy})_3]^{2+}$ (x = 0,2,6,8). One set of origins was observed and the origins gradually shifted to higher energy with increasing deuteriation degree. Transitions involving the d_2-bpy and the d_6-bpy ligand shifted to higher and lower energy respectively, whereas transitions involving the d_8-bpy or the h_8-bpy ligand remained at the same energy as in the $[Ru(bpy)(d_8\text{-bpy})_2]^{2+}$ complex. Hence it may be suggested that the lowest ^{3}MLCT levels in $[Ru(bpy)_3]^{2+}$ systems are invariably localised. Results published by Kincaid et al[127,128,129] also concur that the excited state electron is localised on one bpy ligand i.e. the excited state formulated as $[Ru^{(III)}(bpy)_2(bpy^-)]^{2+}$.

It was then proposed that such a phenomenon could be useful in simple determination of excited state location in heteroleptic complexes. This is based on the fact that lifetime is only affected, if the ligand deuteriated is responsible for excited state emission. However in the case of deuteriation of a spectator ligand, no effect on lifetime would be observed. This effect has been portrayed by Keyes et al [125], in the case of deuteriation of a bpy ligand in $[Ru(bpy)_2L][PF_6]_n$, where L= 3-phenyl–5-(pyridin-2-yl)-1,2,4-triazole or 5,6-diphenyl-3-(pyridin-2-yl)-1,2,4-triazine.

For the former, the excited state lifetime increased from 225 ns to 410 ns upon deuteriation, whereas the latter showed no such increase, 740 ns to 780 ns [125]. This can be explained, as in case one of the 3-phenyl –5-(pyridin-2-yl)-1,2,4-triazole, that the LUMO is located on the bpy, as the triazoles are electron rich and have higher lying π* levels than the bpy. Whereas in case two of 5,6-diphenyl-3-(pyridin-2-yl)-1,2,4-triazine, the LUMO would be situated on this ligand as the triazines are electron poor, so the π* levels of the bpy would be higher.[125,136]

Kincaid et al.[137], studied the excited state of the complex $[Ru(bpy)_2(pypz)]^{2+}$ by deuteriating the pyridine half of the asymmetric ligand 2-(2-pyridyl)pyrazine (pypz) Figure 23, which demonstrated that the excited state electron is localised on the pyrazine half of the pypz ligand.

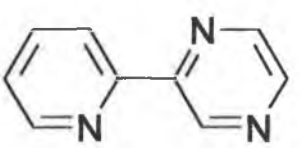

Figure 23 2-(2-pyridyl)pyrazine (pypz)[137]

Apart from the advantages of photophysical characterisation, which deuteriation facilitates another important motive is the simplification of their ^1H NMR spectra. In Ru(II) complexes an asymmetric mononuclear complex will have up to sixteen non-equivalent protons from the bipyridyl moieties, and in the case of dinuclear up to thirty two protons may arise, making complete unambiguous structural assignment extremely difficult.

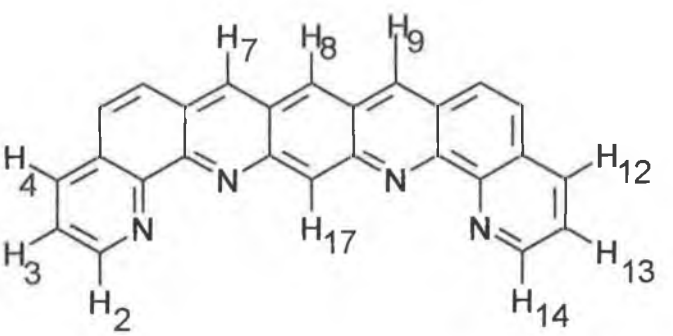

Figure 24 5,6,10,11-tetra-hydro-16, 18-diazadipyrido[2,3-.a:3',2'-n]pentacene (L1)[138].

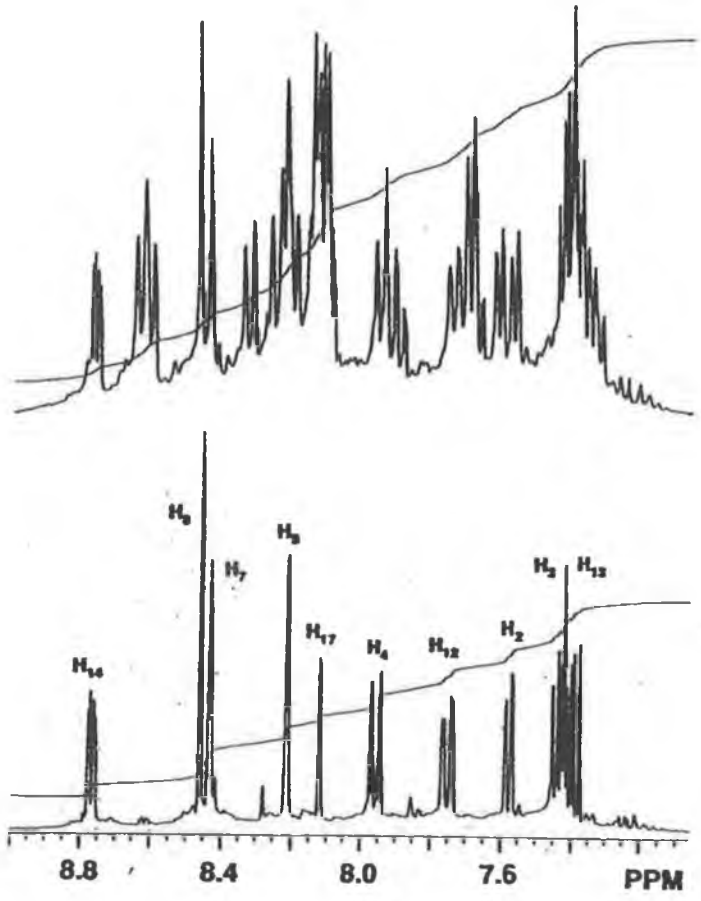

Figure 25 ^1H NMR spectra of $[Ru(bpy)_2(L1)]$ $[PF_6]_2$ (top) and $[Ru(d_8\text{-}bpy)_2(L1)][PF_6]_2$ (bottom) recorded at 300 MHz in CD_3CN[138].

One of the first examples of this was reported by Thummel et al[138] in which $Ru(d_8\text{-}bpy)_2Cl_2.2H_20$ was used to prepare a mononuclear complex from a ligand with two equivalent bidentate sites: 5,6,10,11-tetra-hydro-16, 18-diazadipyrido[2,3-.a:3',2'-n]pentacene **(L1)**.

When the 16 proton signals due to the bpy were eliminated, the spectrum of the coordinated **(L1)** Figure 25, is easily interpreted, by comparison with previously established chemical shifts values for ruthenium (II) complexes. Thummel et al. have continued to use deuteriation as a characterisation tool for large polyaza cavity-shaped ligands similar to that of **(L1)**[139].

It is envisaged that systematic deuteriation of the individual ligands, and observation of the effects on the lifetime, could provide a simple approach to the elucidation of the excited state location.

Up to recently, synthesis of the deuteriated ligands has proved cumbersome, but a novel method has been published [125] for the deuteriation of bpy, and may be applied to other ligands as will be seen in later chapters. If this method proved applicable to a wide range of ligands, then the ligand deuteriation would be easier than conventional approaches of electrochemical correlation and transient absorption spectra of the excited state complexes, in location of the excited state, particularly when extended to the area of polynuclear systems. Also, as will be illustrated in further chapters, the deuteriation of ligands aids in the elucidation of ^{1}H NMR as all of the deuteriated ligand hydrogen signals are suppressed which is useful in $[Ru(LL')_2L]$ systems where all LL'(LL' = bpy, phen and biq) signals are suppressed and ligand shifts on complexation may be clearly assigned. On the whole, the deuteriation of ligands has become a very attractive method to facilitate the characterisation of inorganic complexes.

Another enticing advantage of the deuteriation method is that the deuteriation also effects the C^{13} spectrum. Exchange of C-H to C-D brings about a substantial diminution in the height of the carbon signal and also effects a decrease in the height of the adjacent carbon signals. This was observed in 1974 for organic molecules by Echols and Levy[140] and was noted again in 1984[141]. Similarly, deuteriation of exchangeable functional groups (OH, NH) diminishes the height of the signal of the attached carbon atom. These signal changes may be attributed to various causes such as loss of heteronuclear nuclear Overhauser effect (NOE) effects, the fact that C-D coupling constants are smaller than C-H coupling constants, and signal 'splitting' owing to the presence of partially and fully deuteriated species, in a molecule where deuteriation takes place at different sites, different factors are obviously involved. In each case, however, the effect of deuteriation is made evident by an obvious decrease in the height of the signals of the relevant carbons. O'Brien et al give examples of complexes polyheterocyclic compounds and again we see deuteriation facilitating the assignment of NMR, but in this case it is C^{13} [142]. This phenomenon was also observed for the partially deuteriated complexes in this text and will concur that the same principles arise for the partially deuteriated inorganic complexes as for the organic molecules.

1.6 Scope of Thesis

The contents of this thesis describes the synthesis and characterisation of mononuclear and dinuclear ruthenium complexes with different ligands containing 1,2,4-triazole. The deuteriation of various ligands plays an important role both synthetically and theoretically, and will be incorporated into all aspects of this study. The ligands chosen for this study all contain 1,2,4-triazole moieties which have been chosen for their applications in redox and photo -chemistry. Chapter 1 gives the background of the Ru(II) complexes and outlines their applications in photochemical processes.

In Chapter 2 the instrumentation and techniques used to characterise the compounds are listed and the use of each will be described in the course of the work. The experimental chapters describe the deuteriation of all ligands involved in the chapters and the synthesis of the corresponding starting materials $[Ru(LL')_2Cl_2]$ (where LL' is d_8-bpy, d_8-phen or d_{12}-biq). Chapter 3 contains the synthesis of the ligands 3-(pyridin-2-yl)-1,2,4-triazole (Hpytr) and 3-(pyrazin-2-yl)-1,2,4-triazole (Hpztr) and the complexes $[Ru(LL')_2(X)]^{2+}$ (where LL' is bpy, phen or biq or their deuteriated analogues and X is either Hpytr or Hpztr). This chapter concentrates on the photophysics of the pyrazine-triazole containing complex and will be discussed further in the text.

The emphasis of this thesis is placed on chapters 4 and 5 as they deal with the ligand 3-(pyrazin-2-yl)-5-(pyridin-2-yl)-1,2,4-triazole (Hppt). Chapter 4 illustrates the synthesis of the ligand (Hppt) and its relevant mononuclear complexes $[Ru(LL')_2(ppt)]^{2+}$ (where LL' is bpy, phen or biq or their deuteriated analogues). Particular attention will be paid to the photophysics of the complexes with the use of partial deuteriation as a probe into the location of the excited state electron. Chapter 5 is the conclusive experimental chapter where the dinuclear complexes of the RuRu type for the Hppt ligand are made taking two different synthetic pathways. The characterisation of the dinuclear complexes both obtained 'directly' and 'indirectly' will be described. Chapter 6 depicts any future work, which may be relevant to this thesis.

Finally four appendices are supplemented to this thesis. The first consists of poster presentations and contributions made to publications during the course of my research. The second consists of ^{99}Ru NMR data obtained from the University of Amsterdam. The third appendix contains hplc and circular dichromism data obtained from the University of Rome. The final appendix relates to X-Ray crystal structure data for (i) N2-bound coordination isomer of $[Ru(bpy)_2pztr]^{2+}$ and (ii) pyridine-bound coordination isomer of $[Ru(bpy)_2ppt]^{2+}$.

1.7 References

1 V. Balzani, S. Campagna, G. Denti, A. Juris and M. Ventura, Coord. Chem. Rev., **1994**, *132*, 1.

2 S. Licht, "High efficiency solar cells", Electrochem. Soc. Interface, **1997**, 34.

3 V. Balzani, R. Ballardini, F. Bolletta, M.T. Gandolfi, A. Juris, M. Maestri, M.F. Manfrin, L. Moggi and N. Sabbatini, Coord. Chem. Rev., **1993**, *125*, 75.

4 V. Balzani and F. Scandola, Supramolecular Photochemistry, **1991**, Ellis Horwood Ltd..

5 H. Colquhoun, J. Stoddart and D.J. Williams, Angew. Chem. Int. Ed. Engl., **1986**, *25*, 6, 487.

6 V. Balzani, Pure and Appl. Chem., **1990**, *62*, 6, 1099.

7 J.P. Konopelski, F. Kotzyba-Hibert, J.M Lehn, J.P Desveeergne, F. Fages, A. Castellan, H.J Bouas-Laurant, J. Chem. Soc., Chem. Comm., **1985**, 433.

8 V. Balzani, Pure and Appl. Chem., **1990**, *62*, 6, 1099.

9 J.V. Caspar and T.J. Meyer, Inorg. Chem., **1983**, *22*, 2444.

10 A. Juris, V. Balzani, F. Barigelletti, S. Campagna, P. Belser and A. von Zelewsky, Coord. Chem. Rev., **1988**, *84*, 85.

11 I. Bedja, S. Hotchandani and P.V Kamat, J. Electrochem.,**1996**, *401*, 237.

12 S. Serroni and G. Denti, J. Am. Chem. Soc., **1992**, *31*, 21.

13 V. Balzani, F. Barigelletti, P. Belser, S. Bernhard, L. De Cola and L. Flamigni, J. Phys. Chem., **1996**, *100*, 16786.

14 C. Moucheron, A. Kirsch-De Mesmaeker, A. Dupont-Gervais, E. Leize and A. van Dorrselaer, J. Am. Chem. Soc., **1996**, *118*, 12834.

15 S. Serroni, A. Juris, M. Venturi, S. Campagna, I. Resino, G. Denti, A. Credi and V. Balzani, J. Mater. Chem., **1997**, *7*(7), 1227.

16 P. Ceroni, F. Paolucci, S. Roffia, S. Serroni and S. Campagna, Inorg. Chem., **1998**, *37*, 2829.

17 E. Ishow, A. Gourdon, J.P. Launay, P. Lecante, M. Verelst, C. Chiorboli, F. Scandola and C.A. Bignozzi, Inorg. Chem., **1998**, *37*, 3603.

18 P. Ceroni, F. Paolucci, C. Paradisi, A. Juris, S. Roffia, S. Serroni, S. Campagna and A. Bard, J. Am. Chem. Soc., **1998**, *120*, 5480.

19 A. Juris, V. Balzani, S. Campagna, G. Denti, S. Serroni, G. Frei and H. Güdel, Inorg. Chem., **1994**, *33*, 1491.

20 G. Giuffrida and S. Campagna, Coord. Chem. Rev., **1994**, *135*, 517.

21 A. Mamo, A. Juris, G. Calogero and S. Campagna, J. Chem. Soc., Chem. Comm., **1996**, 1225.

22 S. Campagna, S. Serroni, S. Bodige and F. Mac Donnell, Inorg. Chem., **1999**, *38*, 692.

23 P. Belser, S. Bernhard, E. Jandrasics, A. Von Zelewsky, L. De Cola and V. Balzani, Coord. Chem. Rev., **1997**, *159*, 1.

24 A. Juris, V. Balzani, F. Barigelletti, S. Campagna, P. Belser and A. von Zelewsky, Coord. Chem. Rev., **1988**, *84*, 85.

25 C.H. Braunstein, A. D. Baker, T. C. Strekas, H. D. Gafney, Inorg. Chem., **1984**, *23*, 857.

26 H. E. Toma, P. S. Santos, A. B. P. Lever, Inorg. Chem., **1988**, *27*, 3850

27 L. De Cola, V. Balzani, P. Belser, R. Dux and M. Baak, Supramol. Chem., **1995**, *5*, 297.

28 V. Balzani, S. Campagna, G. Denti, A. Juris, S. Serroni and M. Venturi, Acc. Chem. Res., **1998**, *31*, 26.

29 P. Baxter, J.M. Lehn, B. Kneisel, G. Baum and D. Fenske, Chem. Eur. J., **1999**, *5*, 1, 113.

30 A. Archut, G. Azzellini, V. Balzani, L. De Cola and F. Vögtle, J. Amer. Chem. Soc., **1998**, *120*, 12187.

31 P. Ashton, R. Ballardini, V. Balzani, I. Baxter, A. Credi, M. Fyfe, M. Gandolfi, M. Gomez-Lopez, M. Martinez-Diaz, A. Piersanti, N. Spencer, J. Stoddart, M. Venturi, A. White and D. Williams, J. Am. Chem. Soc., **1998**, *120*, 11932.

32 E. Ishow, A. Credi, V. Balzani, F. Spadola and L. Mandolini, Chem. Eur. J., **1999**, *5*, 3, 984.

33 L. Flamigni, F. Barigelletti, N. Armaroli, J.P. Collin, J.P. Sauvage and J.A. Williams, Chem. Eur. J., **1998**, *4*, 9, 1744.

34 L. Flamigni, F. Barigelletti, N. Armaroli, B. Ventura, J.P. Collin, J.P. Sauvage and J.A. Williams, Inorg. Chem., **1999**, *38*, 661.

35 R.Hage, J.G. Haasnoot, J Reedijk and J.G Vos, Chemtracts, Inorg. Chem., **1992**, *4*, 75.

36 K Kalyanasundaram, Coord. Chem. Rev., **1982**, *46*, 159.

37 R. Hage, J. G. Haasnoot, H. A. Nieuwenhuis, J. Reedijk, R. Wang, J. G. Vos, J. Chem. Soc., Dalton Trans., **1991**, 3271.

38 R. Argazzi, C. Bignozzi, G. Hasselmann and G. J. Meyer, Inorg. Chem., **1998**, *37*, 4533.

39 T. Heimer, C.Bignozzi and G. J. Meyer, J. Phys. Chem., **1993**, *97*, 11987.

40 J.V. Caspar and T.J. Meyer, Inorg. Chem., **1983**, *22*, 2444.

41 A. Harriman, F. Odobel and J.P Sauvage, J. Am. Chem. Soc., **1995**, *117*, 9461.

42 M. Braun and H.D Gafney, J. Phys. Chem., **1994**, *98*, 8108.

43 G.M. Tsivgoulis and J.M Lehn, Angew. Chem. Int. Ed. Engl., **1995**, *34*, 1119.

44 M. Borja and P. Dutta, Nature, **1993**, *362*, 43.

45 F. Cao, G Oskam and P.C.Searson, J. Phys. Chem., **1995**, *99*, 17071.

46 O Kohle, S Ruile and M Grätzel, Inorg. Chem., **1996**, *35*, 4779.

47 S. Serroni, S Campagna, G Denti, T Keyes and J.G Vos, Inorg. Chem., **1996**, *35*, 4513.

48 M Kropf, E Joselevich, H Durr and I Willner, J. Am. Chem. Soc., **1996**, *118*, 655.

49 S.L Larson, C.M Elliott and D.F Kelley, Inorg. Chem., **1996**, *35*, 2070.

50 P.V Kamat, I Bedja, S Hotchandani and L.K Patterson, J. Phys. Chem., **1996**, *100*, 4900.

51 J.P Paris and W.W Brandt, J. Am. Chem. Soc., **1959**, *81*, 5001.

52 M. Gratzel andP. Liska, Photoelectrochemical cells and process for making same, U.S. Patent, **1992**, *5*, 084, 365.

53 K. Kalyanasundaram, M. Grätzel and M. Nazeeruddin, J. Chem. Soc., Dalton Trans., **1991**, 343.

54 O. Kohle, S. Ruile and M. Grätzel, Inorg. Chem., **1996**, *35*, 4779.

55 R. Hoyle, J. Sotomayor, G. Will and D. Fitzmaurice, J. Phys. Chem., B, **1997**, *101*, 10791.

56 S. Licht, Electrochem. Soc. Interface, **1997**, 34.

57 J. Desilvestro, M. Grätzel, L. Kavan, J. Moser and J. Augustynshi, J. Amer. Chem. Soc., **1985**, *107*, 2988.

58 P. Schouten, J. Warman, M. de Haas, M. Fox and H. Pan, Nature, **1991**, *353*, 737.

59 M. Nazeeruddin, A. Kay, I. Rodicio, R. Humphry-Baker, E. Muller, P. Liska, N. Vlachopoulos and M. Grätzel, J. Amer. Chem. Soc., **1993**, *115*, 6382.

60 H. Rensmo, K. Keis, H. Lindstrom, S. Sodergren, A. Solbrand, A. Hagfedlt and S. Lindquist, J. Phys. Chem., **1997**, *101*, 2598.

61 F.A. Cotton and G. Wilkinson, Advanced Inorganic Chemistry, Wiley, Chichester, **1988**, 5th ed..

62 B.P. Sullivan, D.J. Salmon and T.J. Meyer, Inorg. Chem., **1978**, *17*, 334.

63 R.J. Watts, J.Chem. Ed., **1983**, *60*, 834.

64 A. Juris, V. Balzani, F. Barigelletti, S. Campagna, P. Belser and A. von Zelewsky, A; Coord. Chem. Rev., **1988**, *84*, 85.

65 X. Xu, K. Shreder, B.L. Iverson and J.A. Bard, J. Am. Chem. Soc., **1996**, *118*,3656.

66 F. Barigelletti, L. De Cola, V. Balzani, R. Hage, J. Haasnoot, J. Reedijk and J.G. Vos, Inorg. Chem., **1989**, *28*, 4344.

67 F. Felix, J. Ferguson, H. Gudel and A. Ludi, J. Am. Chem. Soc., **1980**, *102*, 4096.

68 E. Kober and T.J. Meyer, Inorg. Chem., **1983**, *22*, 1614.

69 J. Demas and G. Crosby, J. Mol. Spec., **1968**, *26*, 72.

70 P. Mabrouk and M. Wrighton, Inorg. Chem., **1986**, *25*, 526.

71 J. Demas and G. Crosby, J. Am. Chem. Soc., **1971**, *93*, 2840.

72 M. Sykora and J. Kincaid, Inorg. Chem., **1995**, *34*, 5852.

73 J. van Houten and J. Watts, J. Am. Chem. Soc., **1976**, *98*, 4853.

74 J. van Houten and J. Watts, Inorg. Chem., **1978**, *17*, 3381.

75 B. Durham, J. Caspar, J. Nagle and T. J. Meyer, J. Am. Chem. Soc., **1982**, *104*, 4803.

76 P. W. Atkins, Physical Chemistry, Oxford University Press, **1986**, 3rd ed., Ch. 12.

77 V. Balzani and M. Maestri, "Photosensitisation and photocatalysis

using inorganic and organometallic compounds", **1993**, *14*, 26.

78 C. Creutz, M. Chou, T. Netzel, M. Okumura and W. Sutin, J. Am. Chem. Soc., **1980**, *102*, 1309.

79 F. Barigelletti, L. De Cola, V. Balzani, R. Hage, J. Haasnoot, J. Reedijk and J.G. Vos, Inorg. Chem., **1991**, *30*, 641.

80 R. Hage, J. G. Haasnoot, H. A. Nieuwenhuis, J. Reedijk, R. Wang, J. G. Vos, J. Chem. Soc., Dalton Trans., **1991**, 3271.

81 C.H. Braunstein, A. D. Baker, T. C. Strekas, H. D. Gafney, Inorg. Chem., **1984**, *23*, 857.

82 H. E. Toma, P. S. Santos, A. B. P. Lever, Inorg. Chem., **1988**, *27*, 3850.

83 G. H. Allen, R. P. White, D. P. Rillema, T. J. Meyer, J. Am. Chem. Soc., **1984**, *106*, 2613.

84 G. F. Strousse, P. A. Anderson, J. R. Schoonover, T. J. Meyer, F. R. Keene, Inorg. Chem., **1992**, *31*, 3004.

85 R. J. Crutchley, A. B. P. Lever, J. Am. Chem. Soc., **1980**, *102*, 7128.

86 M. Venturi, Q. G. Mulazzani, M. Ciano, M. Z. Hoffman, Inorg. Chem., **1986**, *25*, 4493.

87 G. D. Danzer, K.R. Kincaid, J. Phys. Chem., **1990**, *94*, 3976.

88 R. J. Crutchley, N. Kress, A. B. P. Lever, J. Am. Chem. Soc., **1983**, *105*, 1170.

89 G. H. Allen, R. P. White, D. P. Rillema, T. J. Meyer, J. Am. Chem. Soc., **1984**, *106*, 2613.

90 D. P. Rillema, G. Allen, T. J. Meyer, D. Conrad, Inorg. Chem., **1988**, *22*, 1617.

91 K. Maruszewski, D. P. Strommen, K. Handrich, J. R. Kincaid, Inorg. Chem., **1991**, *30*, 4579.

92 E.V. Dose, L.J. Wilson, Inorg. Chem., **1978**, *17*, 2660.

93 S. Ernst and W. Kaim, Inorg. Chem., **1989**, *28*, 1520.

94 F. Barigelletti, A. Juris, V. Balzani, P. Belser and A. von Zelewsky, Inorg. Chem., **1987**, *26*, 4115.

95 F. Barigelletti, A. Juris, V. Balzani, P. Belser and A. von Zelewsky, Inorg. Chem., **1983**, *22*, 3335.

96 A. Juris, S. Campagna, V. Balzani, G. Gremaud and A. von Zelewsky, Inorg.

Chem., **1988**, *27*, 3652.

97 W. Jones Jnr., R. Smith, M. Abramo, M. Williams and J van Houten, Inorg. Chem., **1989**, *28*, 2281.

98 B. D. J. R. Fennema, R. Hage, J. G. Haasnoot, J. Reedijk, J. G. Vos, Inorg. Chim. Acta, **1990**, *171*, 223.

99 R. Hage, J. G. Haasnoot, J. Reedijk, R. Wang, E. M. Ryan, J. G. Vos, A. L. Speck, A. J. M. Duisenberg, Inorg. Chim. Acta., **1990**, *174*, 77.

100 G. Giuffrida, G. Calogero, G. Guglielmo, V. Ricevuto, M. Ciano, S. Campagna, Inorg. Chem., **1993**, *23*, 1179.

101 R. Hage, R. Prins, J. G. Haasnoot, J. Reedijk, J. G. Vos, J. Chem. Soc., Dalton Trans., **1987**, 1389.

102 J. M. de Wolf, R. Hage, J. G. Haasnoot, J. Reedijk, J. G. Vos, New J. Chem., **1991**, *15*, 501.

103 B. E. Buchanan, J. G. Vos, M. Kaneko, W. J. M. van der Putten, J. M. Kelly, R. Hage, R. A. G. de Graff, R. Prins, J. G. Haasnoot, J. Reedijk, J. Chem. Soc., Dalton Trans., **1990**, 2425.

104 H. A. Nieuwenhuis, J. G. Haasnoot, R. Hage, J. Reedijk, T. L. Snoeck, D. J. Stufkens, J. G. Vos, Inorg. Chem., **1991**, *30*, 48.

105 C. R. Johnson, W. W. Henderson, R. E. Shepherd, Inorg. Chem., **1984**, *23*, 2745.

106 W. Tang, D. Chen, Z. Liu, A. Dai, Sci. China, B. Ser, **1991**, *34*, 8, 897.

107 P. J. Steel, F. Lahousse, D. Lerner, C. Marzin, Inorg. Chem., **1983**, *22*, 1488.

108 B. P. Sullivan, D. J. Salmon, T. J. Meyer, J. Peedin, Inorg. Chem., **1979**, *18*, 12, 3369.

109 A. J. Downard, G. E. Honey, P. J. Steel, Inorg. Chem., **1991**, *30*, 3733.

110 H. A. Nieuwenhuis, J. G. Haasnoot, R. Hage, J. Reedijk, T. L. Snoeck, D. J. Stufkens, J. G. Vos, Inorg. Chem., **1991**, *30*, 48.

111 P. J. Steel, F. Lahousse, D. Lerner, C. Marzin, Inorg. Chem., **1983**, *22*, 1488.

112 L. De Cola, EPA summer school presentation, Noordwijk, **1998**.

113 R. Hage, J. Haasnoot, D. Stufkens, T. Snoeck, J.G. Vos and J. Reedijk, Inorg. Chem., **1989**, *28*, 1413-1414.

114 R. Hage, J. G. Haasnoot, H.A. Nieuwenhuis, J. Reedijk, R. Wang, J. G. Vos, J. Chem. Soc., Dalton Trans., **1991**, 3271.

115 K. Kalyanasundaram, Photochemistry of polypyridine and porphyrin complexes, Academic, London, **1992**, Ch. 2.

116 S. Wilkinson, J. Chem. Ed., **1983**, *60*, 784.

117 R. Fraser and R. Renaud, J. Amer. Chem. Soc., **1966**, *88*, 19, 4365.

118 J. Schaefer and J. Bertram, J. Amer. Chem. Soc., **1967**, *89*, 16, 4121.

119 G. Kabalka, R. Pagni, P. Bridewell, E. Walsh and H. Hassaneen, J. Org. Chem., **1981**, *46*, 7, 1513.

120 W.J.S. Lockley, Tett. Lett.,**1982**, *23*, 37, 3819.

121 J. Garnett, M. Long, R. Vining and T. Mole, J. Amer. Chem. Soc., **1972**, *94*, 16, 5913.

122 J. Larsen and L. Chang, J. Org. Chem., **1978**, *43*, 18, 3602.

123 T. Junk and W. Catallo, Tett. Lett., **1996**, *37*, 20, 3445.

124 J. Van Houten and R.J. Watts, J. Amer. Chem. Soc., **1975**, *97*, 3843.

125 T. Keyes, F. Weldon, E. Muller, P. Pechy, M. Gratzel and J. G. Vos, J. Chem.Soc., Dalton trans., **1995**, *16*, 2705.

126 (a) W. Siebrand, J. Chem. Phys., **1967**, *46*, 440. (b) W. Siebrand, J. Chem. Phys., **1971**, *55*, 5843.

127 S. Mc Clanahan and J. Kincaid, J. Amer. Chem. Soc., **1986**, *108*, 3840.

128 P. Mallick, G. Danzer, D. Strommen and J. Kincaid, J. Phys. Chem., **1988**, *92*, 5628.

129 D. Strommen, P. Mallick, G. Danzer, R. Lumpkin and J. Kincaid, J. Phys. Chem., **1990**, *94*, 1357.

130 H. Riesen, L. Wallace and E. Krausz, J. Phys. Chem., **1995**, *99*, 46, 16, 16807.

131 H. Reisen, L. Wallace and E. Krausz, Inorg. Chem., **1996**, *35*, 6908.

132 H. Reisen, L. Wallace and E. Krausz, J. Phys. Chem., **1996**, *100*, 17138.

133 P. Huber and H. Yersin, J. Phys. Chem., **1993**, *97*, 12705.

134 D. Braun, P. Huber, J. Wudy, J. Schmidt and H. Yersin, J. Phys. Chem., **1994**, *98*, 8044.

135 W. Humbs and H. Yersin, Inorg. Chem., **1996**, *35*, 2220.

136 R. Hage, J. Haasnoot, J. Reedijk, R. Wang and J. G. Vos, Inorg. Chem., **1991**, *30*, 3263-3269.

137 G. Danzer, J. Golus and J. Kincaid, J. Amer. Chem. Soc., **1993**, *115*, 8643.

138 S. Chirayil and R. Thummel, Inorg. Chem., **1989**, *28*, 813.

139 R. Thummel, D. Williamson and C. Hery, Inorg. Chem., **1993**, *32*, 1587.

140 R. Echols and G. Levy, J. Org. Chem., **1974**, *39*, 9, 1321.

141 M. Shapiro, M. Kolpak and T. Lemke, J. Org. Chem., **1984**, *49*, 187.

142 J. O'Brien, T. McMurry and C. O'Callaghan, J. Chem. Research, (s), **1998**, 448.

Chapter 2

EXPERIMENTAL PROCEDURES

All synthetic reagents were of commercial grade and no other purification employed, unless otherwise stated. All solvents used for spectroscopic measurements, with the exception of ethanol, were HPLC grade.

2.1 Chromatographic Techniques

High performance liquid chromatography (hplc) was carried out on a Shimadzu liquid chromatography LC-10AD hplc pump, a Waters 990 photodiode array detector equipped with a NEC PAC III computer, a 20 µl injector loop and a partisil SCX radial PAK cartridge. The detection wavelength used was 280 nm. The chromatography was achieved using a mobile phase, which consisted of acetonitrile: water 80:20 (v/v) containing 0.12 M lithium perchlorate, unless otherwise stated. (It should be noted that care should be taken when using perchlorates, as they are potentially **explosive** when in contact with combustible material!). The flowrate used was 2 cm^3/min.

Semi-preparative hplc was carried out using a Waters 510 hplc pump a, UV/ Vis detector ACS model 353, a 1 cm^3 injector loop and a Waters partisil cation exchange column (10 mm/ 25 cm). The mobile phase in this system consisted of acetonitrile: water 80:20 (v/v) containing 0.12 M potassium nitrate. (It should be noted that care should be taken when evaporating mobile phase to dryness, as nitrates are potentially explosive!). The flowrate used varied between 1.5 - 2.5 cm^3/ min.

Stereoisomers of compounds in chapter 5 were separated on hplc coupled to a circular dichromism detector in collaboration with Dr. Claudio Villani, University of Rome, Italy.

Column chromatography was carried out on activated neutral alumina (Al_2O_3, 150 mesh). In general a mobile phase of 100% acetonitrile eluted the N2 bound isomer and 100% methanol eluted the N4 bound isomer, unless otherwise stated.

2.2 Absorption and Emission spectroscopy

UV/Vis spectra were carried out on a Waters 990 photodiode array spectrometer or on a Shimadzu UV-3100 spectrophotometer.

Emission spectra were obtained both at room temperature and at low temperature, (77 K, cooled with liquid nitrogen) using a Perkin- Elmer LS50B luminescence spectrometer equipped with an Elonex-466 PC. This utilises fluorescence data manager software. An emission slitwidth of 10 nm was used at room temperature and 2.5 nm at 77 K. An excitation slitwidth of 10 nm was used at both temperatures.

Titrations in the pH range from 1 to 10 were carried out in a Britton-Robson buffer solution (0.04 M H_3BO_3, 0.04 M H_3PO_4, 0.04 M H_3 (COOH)). The pH of the solutions was adjusted using concentrated sulphuric acid or concentrated sodium hydroxide solution. The appropriate isosbestic point from the absorption titration data was used as the excitation wavelength for emission titrations. Normalisation of the absorption spectra was carried out using the Shimadzu-3100 UV and the emission spectra were carried out in the normal manner.

2.3 Nuclear Magnetic Resonance Spectroscopy

Proton nuclear magnetic resonance (NMR) spectra were obtained using a Bruker AC 400 MHz spectrometer. Measurements were carried out in d_6- acetone or in d_3-acetonitrile for the complexes and d_6-DMSO for the ligands, unless otherwise stated. The peak positions are relative to TMS. The spectra were converted from their free induction decay (FID) profiles using Bruker WINNMR software package.

The 2-D COSY (correlated spectroscopy) experiments involved the accumulation of 128 FIDs of 16 scans. Digital Filtering was sine-bell squared and the FID was zero filled in the F1 dimension. Acquisition parameters were F1 = ± 500 Hz, F2 = 1000 Hz and $t_{1/2}$ = 0.001 s. The cycle time delay was 2 s.

^{99}Ru NMR was carried out in collaboration the Institute of Molecular Chemistry, Universiteit van Amsterdam, under the supervision of Dr. S. Gaemers, J. van Slageren and Prof. C.J. Elsevier.

2.4 Electrochemical Measurements

Cyclic voltammetric (CV) measurements were carried out using an Model 660 CH software controlled potentiostat (Memphis, TN). A saturated calomel electrode (SCE) was used as the reference electrode. Measurements were carried out in spectroscopic grade acetonitrile with 0.1 M TEAP as the supporting electrolyte.

Tetraethylammoniumperchlorate (TEAP) was prepared by dissolving a 1 M of TEAB (tetraethylammoniumbromide) in water. Perchloric acid was added dropwise until precipitation of the white perchlorate salt ceased. The product was collected by filtration and redissolved in hot water, neutralised with NaOH and then recrystallised five times from hot water.

Glassy carbon and platinum (gauze or wire) electrodes were used as the working and counter electrodes respectively. The electrochemical cell used was a conventional three-compartment cell with glass frits. Solutions for reduction measurements were deoxygenated by purging with $N_{2\,(g)}$ for 15 minutes prior to scanning. Measurements were taken in the range -2 to 2.0 V. The complexes were protonated by adding two drops of 0.1 M $HClO_4$ to the electrolyte solution. The scan rate used was 0.1 V/sec.

2.5 Elemental Analysis

Elemental analysis on C, H and N were carried out at the Microanalytical Laboratory of the University College Dublin (UCD). The CHN analyser used is an Exador analytical CE440.

2.6 Luminescent Lifetime Measurements

The lifetime measurements were carried out using a Q-switched Nd-YAG spectrum laser system using the third harmonic (355 nm). Emission was detected in a right-angled configuration to the laser using an Oriel model IS520 gated intensified CCD coupled to an Oriel model MS125 spectrograph. They were carried out in deoxygenated analytical grade acetonitrile at room temperature (degassed by bubbling with argon). The lifetime errors are estimated to be less than 10%.

2.7 Deuteriation of ligands

The deuteriation of ligands was carried out in a General Purpose Bomb P/N 4744, supplied by Scientific Medical Products, which included a Teflon cup and cover. Palladium (10% on charcoal powder) was the catalyst employed, supplied by Johnson Matthey. The solvent and source of deuterium was deuterium oxide, 99 atom % D supplied by Aldrich.

2.8 X-Ray Crystallography

Crystal structures shown in this text were obtained from two different sources. The structure of the $[Ru(bpy)_2Hpztr]^{2+}$ N2 bound coordination isomer, shown in chapter 3 was obtained by Dr. J. G. Gallagher, Dublin City University, Dublin, Ireland. The second structure $[Ru(bpy)_2ppt]^{+}$ pyrazine bound shown in chapter 4 was obtained in collaboration with Sven Rau and Dr Helmar Gurls, Jena University, Germany.

2.9 Isis Draw Structures

The structures cited in this text were carried out by the author with the use of Chemsketch and Isis Draw. The models are to aid in the visual recognition of the various coordination isomers and their ^1H NMR elucidation.

Chapter 3

THE SYNTHESIS AND CHARACTERISATION OF RU(II) COMPLEXES CONTAINING THE LIGANDS 3-(PYRIDINE-2-YL)-1,2,4-TRIAZOLE (HPYTR) AND 3-(PYRAZINE-2-YL)-1,2,4-TRIAZOLE (HPZTR).

3.1 INTRODUCTION

The ligands 3-(pyridin-2-yl)-1,2,4 - triazole, (Hpytr) and 3-(pyrazin-2-yl)-1,2,4-triazole (Hpztr) are model compounds for the work carried out on the ligand 3-(pyrazin-2-yl)-5-(pyridin-2-yl)-1,2,4-triazole (Hppt). The Hpytr and Hpztr ligands were previously studied [1,2] and can be used as model compounds. In this thesis knowledge of synthetic procedures, purification methods and characterisation techniques was gained through the use of the pyridine and pyrazine triazole ligands.

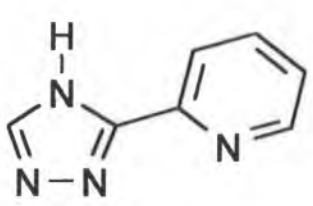

Hpytr

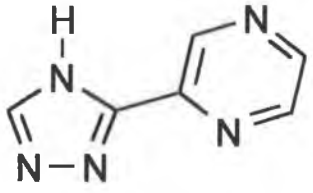

Hpztr

Figure 1: 3-(pyridin-2-yl) - 1,2,4 - triazole, (Hpytr) and 3-(pyrazin-2-yl) - 1,2,4 triazole, (Hpztr).

The ligands Hpytr and Hpztr were chosen for their σ-donor and π-acceptor properties and it is hoped that due to these properties the excited states of these Ru(II) complexes would be perturbed enough to enhance their photostability. The Hpytr ligand contains a pyridine ring which is a good π-acceptor and 1,2,4-triazole which is a good σ- donor and for the Hpztr ligand the pyrazine ring contains good π-acceptor properties and the 1,2,4-triazole has good σ- donor properties. In order to pinpoint the excited state in the Hppt ligand in further chapters it will be useful to have knowledge of the lifetimes of the pyridine and pyrazine triazole complexes. Due to their potential as building blocks in supramolecular systems it is necessary to be aware of their properties as individual units rather than containing both the pyridine and pyrazine rings as in the case of the Hppt ligand 3-(pyridin-2-yl)-5-(pyrazin-2-yl)-1,2,4-triazole.

Pyridine and Pyrazine have different properties and this will be seen in their acid/base properties. Also the binding sites of the ligands will possess different properties due to the difference of the pyridine/pyrazine rings. Initially $[Ru(bpy)_2pytr]^+$ and $[Ru(bpy)_2pztr]^+$ mononuclear complexes were prepared and characterised to determine the reproducibility of the synthesis and characterisation. This also proved useful in the synthesis of the partially and fully deuteriated complexes, $[Ru(d_8\text{-}bpy)_2pytr]^+$, $[Ru(d_8\text{-}bpy)d_5\text{-}pytr]^+$, $[Ru(d_8\text{-}bpy)_2pztr]^+$ and $[Ru(d_8\text{-}bpy)d_4\text{-}pztr]^+$. Some developments were made during this research as it was found that the isomers formed on preparation of the mononuclear complex were isolated through the use of neutral alumina columns. This turned out to be a more efficient method of separation compared to that of semi-preparative hplc. The semi-preparative hplc is a useful technique for the isolation of isomers [3,4] and a high percentage purity of the isolated isomers was achieved (95-100% purity), but it has its drawbacks.

Earlier studies of the $[Ru(bpy)_2(L)]^{2+}$ type complexes have been carried out on 3-(pyridyl-2-yl)-1,2,4-triazole compounds, which laid the path for future complexes to be investigated.[5,6,7,8,9] This pyridyl-triazole complex was the first example of a coordination isomers to be purified by semi-preparative hplc[4] It also had further uses as a probe into the characteristics of these novel heteroligand type complexes. The isolation and characterisation of the coordination isomers was just the beginning of a series of complexes containing the pyridine/pyrazine rings which would lead to a whole new chapter of N2/N4 bound coordination isomers. Introduction of a methyl group was introduced to the triazole ring as a steric hindering device to deter the formation of coordination isomers. Acid-base ground and excited state studies of the N2/N4 bound isomers showed large differences, which clearly portrayed the non-equivalence of the triazole coordination sites.[6] By varying the pyridyl-azole bond and introducing substituents, it was hoped that a more detailed understanding of the physical properties of the pyridyl-triazole complexes would arise. It was found that most pyridyl–1,2,4-triazole complexes are weaker π-acceptor ligands than bpy and that they all had comparable spectroscopic properties to $[Ru(bpy)_3]^{2+}$.[10] As further investigations progressed a new approach was taken to replace the pyridine ring of the pyridyl-1,2,4-triazole ligand with a pyrazine ring.[11]

It was found that the coordination mode of the isomers greatly effected the physical properties of the complexes. Due to the presence of the pyrazine ring the LUMO was lowered in the complexes and this was evident in the increased basicity of the excited state. Small shifts were observed in the absorption and emission maxima as a result of the acid-base behaviour of the triazole ring are unusual and in agreement with a shift from the pyrazine-triazole-based LUMO for the protonated compound to a bpy-based one in the deprotonated species. Also it had been suggested that the slightly increased pK_a* value of the triazole ring suggests strongly that in the excited state there is an appreciable interaction between the triazole and the pyrazine ring.

As the physical properties of these pyridyl/pyrazine-triazole complexes were further understood an investigation took place of their photochemical properties as they were proposed as future photosensitisers. For the complex 4-methyl-3-(pyridin-2-yl)-1,2,4-triazole in acetonitrile it was shown that the photochemically induced ligand dissociation can be reversed thermally.[7] A series of substituted pyridyl-triazole containing complexes were also studied and showed that they portrayed some unusual photochemical properties.[8] The photoinduced linkage isomerism and photoanation of pyridyl-triazole was studied in a controlled pH environment. This showed that by controlling protonation of the ground state of the complex the photolability of the complex could be controlled.[9] Dinuclear complexes of the ligand 1-methyl-3-(pyrazin-2-yl)-1,2,4-triazole have been prepared in mono- and bi-dentate fashions and their photochemical and spectroelectrochemical features have been investigated.[12] Efficient energy transfer in the excited state was reported for these RuOs dinuclear complexes leading to emission from one metal unit. More recent studies have unveiled the dual emission properties of the pyrazine-triazole complex over a temperature range of 75 K to 175 K, which will be looked at further in this text.[13]

In the following chapter the advances made in the study of the pyridine- and pyrazine-triazole containing complexes will be portrayed. A comparative view will be taken to demonstrate the progression from the prior studies carried out[1,2]. The studies will include a systematic approach in the uses of deuteriation and also in the general synthetic routes and characterisation.

The introduction of different Ru(II) moieties (2,2'-bipyridyl, 2,2'-biquinoline and 1,10-phenanthroline) was looked at with the Hpztr ligand, which may be compared to previous studies of the pyridyl-triazole species.[14] Tuning of the ligand properties generates more information in order to create further models for the interpretation of the excited state properties of mixed ligand complexes.

3.2 EXPERIMENTAL

The ligands were prepared according to literature methods [1,2].

3.2.1 Preparation of the Ligands

3-(pyridin-2-yl)-1,2,4-triazole, Hpytr

26 g (0.25 mol) 2-cyanopyridine was heated at 40°C with 50 cm^3 ethanol. An equimolar amount of hydrazine hydrate was added. The mixture was left to react overnight, after which the pale yellow intermediate 2-pyridylamidrazone was isolated in a 80 - 90 % yield. The amidrazone (125 mmol) was added slowly to 125 cm^3 formic acid at 0°C. After stirring for 3 hr, the excess of acid was evaporated and the remaining oil was heated approximately for 30 min at 130 - 150 ° C. ^{1}H NMR data [$(CD_3)_2(SO)$]: H^3, 8.09 ppm (d); H^4, 7.98 ppm (t); H^5, 7.51 ppm (t); H^6, 8.70 ppm (d); $H^{5'}$, 8.27 ppm (s).Yield: 50 %, M.P.:158-160 ^{0}C[1]

3-(pyrazin-2-yl)-1,2,4-triazole, Hpztr

20 cm^3 of ethanol was added to a mixture of (5.0 g; 0.048 mol) of molten 2-cyanopyrazine and an equimolar amount of 2.33 cm^3 hydrazine hydrate. The solution was stirred at room temperature for 1 hour. Yellow crystals of 2-pyrazylamidrazone were collected by filtration. The pyrazylamidrazone (14 g; 100 mmol) was dissolved in a 10 fold excess of cold formic acid at temperatures below 10 ^{0}C. The mixture was stirred for 3 hours at room temperature. After subsequent heating to dryness at 120 ^{0}C the ligand precipitated. The ligand was recrystalised from hot ethanol. Yield: 48 %, M.P: 213 ^{O}C[15]. ^{1}H NMR data [DMSO]: H3, 9.46 ppm (d); H5, 8.70 ppm (d); H6, 8.66 ppm (d) ; H5', 8.25 ppm (s). Yield:48 %, M.P.:213 ^{0}C[1]

3.2.2 Synthesis of $[Ru(L)_2Cl_2].2H_2O$

Cis-$[Ru(bpy)_2Cl_2].2H_2O$

This complex was prepared according to a modified method of the literature method [15] as follows:

(7.8 g, 29.83 mmol) of $RuCl_3$ was heated with 50 cm^3 of DMF and 1.5-2 g of LiCl, while being bubbled with $N_{2(g)}$. (9.307 g, 59.66 mmol) of 2,2'-bipyridine was added to the solution slowly and then heated under reflux for 8 hours. The solution was cooled and added to a large volume of acetone (400 cm^3), which was placed in the freezer (-4^{0}C) overnight. The product was collected by vacuum filtration and any traces of carbonyl removed by washing with water. Wash through the precipitate with ice cold water and then diethyl ether. Yield: 12 g, 80 %

Cis-$[Ru(phen)_2Cl_2].2H_2O$

This complex was prepared according to literature method [15]. (6.5 g; 31.23 mmol) of $RuCl_3$ and 2 g of LiCl were heated in 50 cm^3 of DMF with a gentle flow of N_2 (g) bubbling through the solution. (10.81 g; 60.00 mmol) of 1,10 - phenanthroline was added slowly in 3 to 4 batches and was heated under reflux for 8 hours. The solution was then cooled, added slowly to 300 cm^3 of Acetone and put in the freezer overnight at (-4^{0}C). The product was collected under vacuum filtration and washed with water and diethyl ether. Yield 12 g ; 70 %.

Cis-$[Ru(biq)_2Cl_2].2H_2O$

This complex was prepared according to literature method [14]. (2.5 g; 10 mmol) of $RuCl_3$, 2 g of LiCl and 3 g of ascorbic acid were heated in 40 cm^3 of DMF. (5 g; 20 mmol) of biquinoline was added to the solution slowly and heated under reflux for 40 min. The solution was left to cool, added slowly to 250 cm^3 of Acetone and placed in

the freezer at –4 ^{0}C overnight. The product was collected under vacuum filtration and washed with water and diethyl ether. Yield 5 g, 70 %

3.2.3 Deuteriation of Ligands

The following ligands were deuteriated according to literature method [16].

2,2'-Bipyridyl

3 g of 2,2'-bipyridyl was placed in a teflon bomb with 0.5 g palladium charcoal catalyst and 20 cm^3 of deuterium oxide. The bomb was placed in an oven at 200 ^{0}C for 3 days. The solution was vacuum filtered and the palladium charcoal collected, the deuteriated bpy was washed out of the bomb and the palladium charcoal with diethyl ether. The ether was allowed to evaporate and ^{1}H NMR determined the % deuterium exchange of the ligand. If deuteriation is not successful on first attempt, repeat the above procedure with fresh D_2O and palladium charcoal. ^{1}H NMR reveals a silent spectrum, infrared spectroscopy showed bands at 2250-2295 cm^{-1}, attributed to $\nu_{c\text{-}d}$ vibrations. Yield: 2.2 g, 73 %

1,10-Phenanthroline

3 g of 1,10-phenanthroline was placed in a teflon bomb with 0.5 g palladium charcoal catalyst and 20 cm^3 of deuterium oxide. The bomb was placed in an oven at 200 ^{0}C for 3 days. The solution was vacuum filtered and the palladium charcoal collected, the deuteriated phen was washed out of the bomb and the palladium charcoal with diethyl ether. The ether was allowed to evaporate and ^{1}H NMR determined the % deuterium exchange of the ligand. If deuteriation is not successful on first attempt, repeat the above procedure with fresh D_2O and palladium charcoal. ^{1}H NMR reveals a silent spectrum, infrared spectroscopy showed bands at 2250-2295 cm^{-1}, attributed to $\nu_{c\text{-}d}$ vibrations. Phenanthroline was found to be more difficult to deuteriate in comparison to other ligands i.e. bipyridyl. Yield: 1 g; 33 %

2,2'-Biquinoline

3 g of 2,2'-biquinoline was placed in a teflon bomb with 0.5 g palladium charcoal catalyst and 20 cm^3 of deuterium oxide. The bomb was placed in an oven at 200 ^0C for 3 days.

The solution was vacuum filtered and the palladium charcoal collected, the deuteriated biq was washed out of the bomb and the palladium charcoal with diethyl ether. The ether was allowed to evaporate and ^1H NMR determined the % deuterium exchange of the ligand. If deuteriation is not successful on first attempt, repeat the above procedure with fresh D_2O and palladium charcoal. ^1H NMR reveals a silent spectrum, infrared spectroscopy showed bands at 2250-2295 cm^{-1}, attributed to ν_{c-d} vibrations. Yield: 2 g; 66 %.

3-(pyridin-2-yl)-1,2,4-triazole, Hpytr

3 g of 3-(pyridin-2-yl)-1,2,4-triazole was placed in a teflon bomb with 0.5 g palladium charcoal catalyst and 20 cm^3 of deuterium oxide. The bomb was placed in an oven at 200 ^0C for 3 days. The solution was vacuum filtered and the palladium charcoal collected, the deuteriated Hpytr was washed out of the bomb and the palladium charcoal with hot ethanol. The ethanol was evaporated and a ^1H NMR determined the % deuterium exchange of the ligand. If deuteriation is not successful on first attempt, repeat the above procedure with fresh D_2O and palladium charcoal. ^1H NMR reveals a silent spectrum, infrared spectroscopy showed bands at 2250-2295 cm^{-1}, attributed to ν_{c-d} vibrations. Yield: 2.2 g, 73 %

3-(pyrazin-2-yl)-1,2,4-triazole, Hpztr

3 g of 3-(pyrazin-2-yl)-1,2,4-triazole was placed in a teflon bomb with 0.5 g palladium charcoal catalyst and 20 cm^3 of deuterium oxide. The bomb was placed in an oven at 200 ^0C for 3 days. The solution was vacuum filtered and the palladium charcoal collected, the deuteriated Hpztr was washed out of the bomb and the palladium charcoal with hot ethanol.

The ethanol was evaporated and a ^1H NMR determined the % deuterium exchange of the ligand. If deuteriation is not successful on first attempt, repeat the above procedure with fresh D_2O and palladium charcoal. ^1H NMR reveals a silent spectrum, infrared spectroscopy showed bands at 2250-2295 cm^{-1}, attributed to $\nu_{c\text{-}d}$ vibrations. Yield: 2.4 g; 80 %.

3.2.4 Synthesis of $[Ru(d_n\text{-}L)_2Cl_2].2H_2O$

Cis-$[Ru(d_8\text{-}bpy)_2Cl_2].2H_2O$

This complex was prepared according to a modified method of literature method[16] as follows:

(2.31 g, 8.84 mmol) of $RuCl_3$ was heated with 50 cm^3 of DMF and 1.0-1.5 g of LiCl, while being bubbled with $N_{2\,(g)}$. (2.9 g, 17.7 mmol) of deuteriated 2,2'-bipyridine was added to the solution slowly and then heated under reflux for 8 hours. The solution was cooled and added to a large volume of acetone (250 cm^3), which was placed in the freezer (-4 ^0C) overnight. The product was collected by vacuum filtration and any traces of carbonyl removed by washing with water. Wash through the precipitate with ice cold water and then diethyl ether. Yield: 2.8 g, 77 %.

Cis-$[Ru(d_8\text{-}phen)_2Cl_2].2H_2O$

This complex was prepared according to literature method[16]. (1.22 g, 5.88 mmol) of $RuCl_3$ and 1 g of LiCl were heated in 50 cm^3 of DMF with a gentle flow of $N_{2(g)}$ bubbling through the solution. (2.24 g ; 11.77 mmol) of deuteriated 1, 10 - phenanthroline was added slowly in 3 or 4 batches and was heated under reflux for 8 hours. The solution was then cooled, added slowly to 200 cm^3 of acetone and put in the freezer overnight at (-4 ^0C). The product was collected under vacuum filtration and washed with water and diethyl ether. Yield: 2 g ; 45 %.

Cis-[Ru(d_{12}-biq)$_2$Cl$_2$].2H$_2$O

This complex was prepared according to literature method [14].
(0.116 g ; 0.8 mmol) of $RuCl_3$, 1.5 g of LiCl and 2 g of ascorbic acid were heated in 40 cm^3 of DMF. (0.43 g; 1.6 mmol) of deuteriated biquinoline was added to the solution slowly and heated under reflux for 40 min. The solution was left to cool, added slowly to 250 cm^3 of acetone and placed in the freezer at –4 ^{0}C overnight. The product was collected under vacuum filtration and washed with water and diethyl ether. Yield: 5 g, 70 %.

3.2.5 Preparation of the Ruthenium complexes.

[Ru(bpy)$_2$Hpytr][PF$_6$]$_2$.H$_2$O

520 mg (1 mmol) of cis-[Ru(bpy)$_2$Cl$_2$].2H$_2$0 was heated under reflux with 0.3 g (2 mmol) of Hpytr for 4 hr in 50 cm^3 ethanol/water (1:1 v/v). The solvent was removed by rotary evaporation, and the remaining solid dissolved in 10 cm^3 water. The complex was precipitated with an aqueous solution of NH_4PF_6. The complex was collected under vacuum filtration and recrystallised in 30 cm^3 acetone: water 1:1 (v/v). Two isomers are formed. Separation of the isomers took place on a neutral alumina column under gravity. Isomer two (second isomer off analytical cation exchange hplc column) elutes first with 100% acetonitrile and isomer one elutes off with 100% methanol. Yield: 670 mg; 82%. CHN: Found: C, 37.26; H, 2.67; N, 12.77; $C_{27}H_{23}F_{12}N_8OP_2Ru$ requires C, 37.42; H, 2.67; N, 12.93 %. (N4-isomer)

[Ru(d_8-bpy)$_2$Hpytr][PF$_6$]$_2$.2H$_2$O

530 mg (1 mmol) of cis-[Ru(d_8-bpy)$_2$Cl$_2$].2H$_2$0 was heated under reflux with 0.3 g (2 mmol) of Hpytr for 4 hr in 50 cm^3 ethanol/water (1:1 v/v). The solvent was removed by rotary evaporation, and the remaining solid dissolved in 10 cm^3 water. The complex was precipitated with an aqueous solution of NH_4PF_6. The complex was collected under vacuum filtration and recrystallised in 30 cm^3 acetone:water 1:1 (v/v).

Two isomers are expected to form. Separation of the isomers took place on a neutral alumina column under gravity. Isomer two (second isomer off analytical cation exchange column) elutes first with 100% acetonitrile and isomer one elutes off with 100% methanol. Yield: 590 mg; 71 %. CHN: Found: C, 36.15; H, 2.41; N, 11.81; $C_{27}D_{16}H_{10}F_{12}N_8O_2P_2Ru$ requires C, 35.97; H, 2.91; N, 12.43 %. (N4-isomer)

$[Ru(bpy)_2d_5\text{-}Hpytr][PF_6]_{3/2}.1/2H_2O$

520 mg (1 mmol) of cis-$[Ru(bpy)_2Cl_2].2H_20$ was heated under reflux with 0.3 g (2 mmol) of d_5-pytr for 4 hr in 50 cm^3 ethanol/water (1:1 v/v). The solvent was removed by rotary evaporation, and the remaining solid dissolved in 10 cm^3 water. The complex was precipitated with an aqueous solution of NH_4PF_6. The complex was collected under vacuum filtration and recrystallised in 30 cm^3 acetone: water 1:1 (v/v). Two isomers are expected to form. Separation of the isomers took place on a neutral alumina column under gravity. Isomer two (the second isomer off analytical cation exchange column) elutes first with 100% acetonitrile and isomer one elutes off with 100% methanol. Yield: 620 mg; 76 %. CHN: Found: C, 41.42; H, 2.95; N, 14.34; $C_{27}D_5H_{18}F_9N_8O_{1/2}P_{1.5}Ru$ requires C, 41.00; H, 2.93; N, 14.17 % (N4-isomer)

$[Ru(d_8\text{-}bpy)_2d_5\text{-}Hpytr][PF_6]_2.4H_2O$

530 mg (1 mmol) of cis-$[Ru(d_8\text{-}bpy)_2Cl_2].2H_20$ was heated under reflux with 0.3 g (2 mmol) of d_5-pytr for 4 hr in 50 cm^3 ethanol/water (1:1 v/v). The solvent was removed by rotary evaporation, and the remaining solid dissolved in 10 cm^3 water. The complex was precipitated with an aqueous solution of NH_4PF_6. The complex was collected under vacuum filtration and recrystallised in 30 cm^3 acetone: water 1:1 (v/v). Two isomers are expected to form. Separation of the isomers took place on a neutral alumina column under gravity. Isomer two (second isomer off analytical cation exchange column) elutes first with 100 % acetonitrile and isomer one elutes off with 100% methanol. CHN: Found C, 35.43; H, 2.94; N, 10.31. $RuC_{27}D_{21}H_9F_{12}N_8O_4P_2$ requires C, 34.41; H, 3.21; N, 11.89.

$[Ru(bpy)_2pztr][PF_6]_{3/2}.\ H_2O$

(1 mmol; 0.5 g) of cis-$[Ru(bpy)_2Cl_2].2H_2O$ and an excess of ligand Hpztr (1.5-2 mmol; 0.2-0.3 g) were heated under reflux in 50 cm^3 of ethanol for 8 hours. The solvent was evaporated off and the residue was dissolved in 10 cm^3 of H_2O. The complex was precipitated with an aqueous solution of NH_4PF_6. The complex was collected under vacuum filtration and recrystallised in 30 cm^3 acetone: water 1:1 (v/v). Two isomers are expected to form. Separation of the isomers took place on a neutral alumina column under gravity. Isomer two (second isomer off analytical cation exchange column) elutes first with 100 % acetonitrile and isomer one elutes off with 100% methanol. Yield: 720 mg, 90 %. CHN: Found C, 39.30; H, 2.70; N, 15.48. $RuC_{26}H_{22}N_9O_1P_{3/2}F_9$ requires C, 39.28; H, 2.79; N, 15.86. (N2-isomer)

$[Ru(d_8\text{-}bpy)_2pztr][PF_6]_{3/2}.H_2O$

(1 mmol; 0.54 g) of cis-$[Ru(d_8\text{-}bpy)_2Cl_2].2H_2O$ and an excess of ligand Hpztr (1.5-2 mmol; 0.2-0.3 g) were heated under reflux in 50 cm^3 of ethanol for 8 hours. The solvent was evaporated off and the residue was dissolved in 10 cm^3 of H_2O. The complex was precipitated with an aqueous solution of NH_4PF_6. The complex was collected under vacuum filtration and recrystallised in 30 cm^3 acetone: water 1:1 (v/v). Two isomers are expected to form. Separation of the isomers took place on a neutral alumina column under gravity. Isomer two (second isomer off analytical cation exchange column) elutes first with 100% acetonitrile and isomer one elutes off with 100% methanol. Yield: 700 mg, 83 %. CHN: Found C, 38.88; H, 2.67; N, 15.50. $RuC_{26}D_{16}H_6N_9OP_{3/2}F_9$ requires C, 38.51; H, 2.73; N, 15.55.(N2-isomer)

$[Ru(bpy)_2d_4\text{-pztr}][PF_6]_{3/2}.\ 2H_2O$

(1 mmol; 0.52 g) of cis-$[Ru(bpy)_2Cl_2].2H_2O$ and an excess of ligand d_4-pztr (1.5-2 mmol; 0.2-0.3 g) were heated under reflux in 50 cm^3 of ethanol for 8 hours. The solvent was evaporated off and the residue was dissolved in 10 cm^3 of H_2O. The complex was precipitated with an aqueous solution of NH_4PF_6. The complex was collected under vacuum filtration and recrystallised in 30 cm^3 acetone: water 1:1 (v/v). Two isomers are expected to form. Separation of the isomers took place on a neutral alumina column under gravity. Isomer two (second isomer off analytical cation exchange column) elutes first with 100% acetonitrile and isomer one elutes off with 100% methanol. Yield: 750 mg, 91 %. CHN: Found C, 38.94; H, 2.76; N, 15.00. $RuC_{26}H_{20}D_4N_9O_2P_{3/2}F_9$ requires C, 38.22; H, 2.96; N, 15.43.(N2-isomer)

$[Ru(d_8\text{-bpy})_2d_4\text{-pztr}][PF_6]_{3/2}.H_2O$

(1 mmol; 0.54 g) of cis-$[Ru(d_8\text{-bpy})_2Cl_2].2H_2O$ and an excess of ligand d_4-pztr (1.5-2 mmol; 0.2-0.3 g) were heated under reflux in 50 cm^3 of ethanol for 8 hours. The solvent was evaporated off and the residue was dissolved in 10 cm^3 of H_2O. The complex was precipitated with an aqueous solution of NH_4PF_6. The complex was collected under vacuum filtration and recrystallised in 30 cm^3 acetone: water 1:1 (v/v). Two isomers are expected to form. Separation of the isomers took place on a neutral alumina column under gravity. Isomer two (second isomer off analytical cation exchange column) elutes first with 100 % acetonitrile and isomer one elutes off with 100 % methanol. Yield: 700 mg, 83 %. CHN: Found C, 38.50; H, 2.45; N, 15.13. $RuC_{26}D_{20}H_2N_9OP_{3/2}F_9$ requires C, 38.31; H, 2.72; N, 15.47. (N2-isomer)

$[Ru(phen)_2pztr]\ [PF_6]_{3/2}.H_2O$

(1 mmol; 0.53 g) of cis-$[Ru(phen)_2Cl_2].2H_2O$ and an excess of ligand pztr (1.5-2 mmol; 0.2-0.3 g) were heated under reflux in 50 cm^3 of ethanol for 8 hours. The solvent was evaporated off and the residue was dissolved in 10 cm^3 of H_2O. The complex was precipitated with an aqueous solution of NH_4PF_6. The complex was collected under vacuum filtration and recrystallised in 30 cm^3 acetone: water 1:1 (v/v).

Two isomers are expected to form. Separation of the isomers took place on a neutral alumina column under gravity. Isomer two (second isomer off analytical cation exchange column) elutes first with 100% acetonitrile and isomer one elutes off with 100% methanol. Yield: 600mg, 72 % CHN: Found C, 42.86; H, 2.65; N, 14.55. $RuC_{30}H_{22}N_9OP_{3/2}F_9$ requires C, 42.74; H, 2.63; N, 14.96 %. (N2-isomer)

$[Ru(d_8\text{-phen})_2Hpztr][PF_6]_2.2H_2O$

(1 mmol; 0.55 g) of cis-$[Ru(d_8\text{-phen})_2Cl_2].2H_2O$ and an excess of ligand pztr (1.5-2 mmol;0.2-0.3 g) were heated under reflux in 50 cm^3 of ethanol for 8 hours. The solvent was evaporated off and the residue was dissolved in 10 cm^3 of H_2O. The complex was precipitated with an aqueous solution of NH_4PF_6. The complex was collected under vacuum filtration and recrystallised in 30 cm^3 acetone: water 1:1 (v/v). Two isomers are expected to form. Separation of the isomers took place on a neutral alumina column under gravity. Isomer two (second isomer off analytical cation exchange column) elutes first with 100 % acetonitrile and isomer one elutes off with 100 % methanol. Yield: 650 mg, 76 %. CHN: Found C, 38.38; H, 2.48; N, 13.27. $RuC_{30}D_{16}H_9N_9O_2P_2F_{12}$ requires C, 37.91; H, 2.65; N, 13.27.

$[Ru(phen)_2d_4\text{-pztr}][PF_6]_2.2H_2O$

(1 mmol; 0.53 g) of cis-$[Ru(phen)_2Cl_2].2H_2O$ and an excess of ligand pztr (1.5-2 mmol; 0.2-0.3 g) were heated under reflux in 50 cm^3 of ethanol for 8 hours. The solvent was evaporated off and the residue was dissolved in 10 cm^3 of H_2O. The complex was precipitated with an aqueous solution of NH_4PF_6. The complex was collected under vacuum filtration and recrystallised in 30 cm^3 acetone: water 1:1 (v/v). Two isomers are expected to form. Separation of the isomers took place on a neutral alumina column under gravity. Isomer two (second isomer off analytical cation exchange column) elutes first with 100 % acetonitrile and isomer one elutes off with 100 % methanol. Yield: 670 mg, 80 %. CHN: Found C, 39.08; H, 2.55; N, 12.84. $RuC_{30}H_{20}D_4P_2F_{12}O_2N_9$ requires C, 38.43; H, 2.58; N, 13.45.

[Ru(d_8-phen)$_2$$d_4$-Hpztr][$PF_6$].2$H_2O$

(1 mmol; 0.55 g) of cis-[Ru(d_8-phen)$_2Cl_2$].2H_2O and an excess of ligand d_4-pztr (1.5-2 mmol; 0.2-0.3 g) were heated under reflux in 50 cm^3 of ethanol for 8 hours. The solvent was evaporated off and the residue was dissolved in 10 cm^3 of H_2O. The complex was precipitated with an aqueous solution of NH_4PF_6. The complex was collected under vacuum filtration and recrystallised in 30 cm^3 acetone: water 1:1 (v/v). Two isomers are expected to form. Separation of the isomers took place on a neutral alumina column under gravity. Isomer two (second isomer off analytical cation exchange column) elutes first with 100 % acetonitrile and isomer one elutes off with 100 % methanol. Yield: 720 mg, 85 %. CHN: Found C, 45.31; H, 3.01; N, 14.73. $RuC_{30}H_5N_9O_2D_{20}PF_6$ requires C, 44.51; H, 3.11; N, 15.56. (N2-isomer)

[Ru(biq)$_2$Hpztr][PF_6].H_2O

(1 mmol; 0.72 g) of cis-[Ru(biq)$_2Cl_2$].2H_2O and an excess of ligand pztr (1.2-1.5 mmol; 0.15-0.25 g) were heated under reflux in 50 cm^3 of ethanol for 8 hours. The solvent was evaporated off and the residue was dissolved in 10 cm^3 of H_2O. The complex was precipitated with an aqueous solution of NH_4PF_6. The complex was collected under vacuum filtration and recrystallised in 30 cm^3 acetone: water 1:1 (v/v). Two isomers are expected to form. Separation of the isomers took place on a neutral alumina column under gravity. Isomer two (the second isomer off analytical cation exchange column) elutes first with 100 % acetonitrile and isomer one elutes off with 100 % methanol. Yield: 900 mg, 90 %. CHN: Found C, 54.33; H, 3.26; N, 13.54. $RuC_{42}H_{31}N_9OPF_6$ requires C, 54.60; H, 3.38; N, 13.65. (N2-isomer)

[Ru(d_{12}-biq)$_2$Hpztr][PF_6]

(0.09 mmol; 0.067 g) of cis-[Ru(d_{12}-biq)$_2Cl_2$].$2H_2O$ and an excess of ligand pztr (0.1 mmol; 0.02 g) were heated under reflux in 50 cm^3 of ethanol for 8 hours. The solvent was evaporated off and the residue was dissolved in 10 cm^3 of H_2O. The complex was precipitated with an aqueous solution of NH_4PF_6. The complex was collected under vacuum filtration and recrystallised in 30 cm^3 acetone: water 1:1 (v/v). Two isomers are expected to form. Separation of the isomers took place on a neutral alumina column under gravity. Isomer two (second isomer off analytical cation exchange column) elutes first with 100 % acetonitrile and isomer one elutes off with 100 % methanol. Yield: 83 mg, 95 %. CHN: Found C, 54.35; H, 3.27; N, 13.50. $RuC_{42}D_{24}H_6N_9PF_6$ requires C, 54.20; H, 3.25; N, 13.55. (N2-isomer)

[Ru(biq)$_2$$d_4$-pztr] [$PF_6$]$_{3/2}$. H_2O

(0.09 mmol; 0.05 g) of cis-[Ru(biq)$_2Cl_2$].$2H_2O$ and an excess of ligand d_4-pztr (0.1 mmol; 0.02 g) were heated under reflux in 50 cm^3 of ethanol for 8 hours. The solvent was evaporated off and the residue was dissolved in 10 cm^3 of H_2O. The complex was precipitated with an aqueous solution of NH_4PF_6. The complex was collected under vacuum filtration and recrystallised in 30 cm^3 acetone: water 1:1 (v/v). Two isomers are expected to form. Separation of the isomers took place on a neutral alumina column under gravity. Isomer two (second isomer off analytical cation exchange column) elutes first with 100 % acetonitrile and isomer one elutes off with 100% methanol. Yield: 70 mg, 85 %. CHN: Found C, 50.63; H, 3.24; N, 8.59. $RuC_{42}D_4H_{26}N_9OP_{3/2}F_9$ requires C, 50.48; H, 3.03; N, 8.44. (N2-isomer)

[Ru(d_{12}-biq)$_2$$d_4$-pztr][$PF_6$].$H_2O$

(0.09 mmol; 0.06 g) of cis-[d_{12}-Ru(biq)$_2Cl_2$].$2H_2O$ and an excess of ligand d_4-pztr (0.1 mmol; 0.02 g) were heated under reflux in 50 cm^3 of ethanol for 8 hours. The solvent was evaporated off and the residue was dissolved in 10 cm^3 of H_2O. The complex was precipitated with an aqueous solution of NH_4PF_6. The complex was collected under vacuum filtration and recrystallised in 30 cm^3 acetone: water 1:1 (v/v).

Two isomers are expected to form. Separation of the isomers took place on a neutral alumina column under gravity. Isomer two (second isomer off analytical cation exchange column) elutes first with 100 % acetonitrile and isomer one elutes off with 100 % methanol. Yield: 74 mg, 92 %. CHN was not obtained for this complex , however, this complex was made in an identical manner to that of $[Ru(biq)_2pztr]^+$ and was found to be hplc pure and ^1H NMR pure.

3.3 RESULTS AND DISCUSSION

3.3.1 Synthetic analysis

The synthesis of the pytr$^-$ and pztr$^-$ containing complexes has previously been reported by Hage et al.[1] , which illustrated that the complexes resulting from the coordination of these ligands not only formed coordination isomers but also formed very pH sensitive complexes. The pytr$^-$ complexes in this study were reproduced as model compounds and the CHN analysis of the complexes show that the compounds were obtained with different amounts of counter ions (PF_6). This may be attributed to the fact that on recrystallisation of the complex Hage would have added a drop of basic solution in order to deprotonate the complex but however in this study acid or base was not added during recrystallisation. This does not effect any of the measurements as all measurements were carried out in acidic and basic media. The only difference that was noticed is during UV spectrum analysis of the complex, prior to addition of acid or base the spectrum obtained will give you a mixture of the two species. Also when obtaining a ^{1}H NMR of this complex the solution has to be pH controlled in order to obtain a clear spectrum.

The pztr$^-$ complexes are similar as the CHN results gave different results for the counter ions of various analogues of the pztr$^-$ compounds. The complexes were not recrystallised in acidic or basic media and therefore when the crystal structure was obtained we see a sharing of the counter ion resulting in the complexes having $[PF_6]_{3/2}$. The crystal structure of $[Ru(bpy)_2pztr]^+$N2-isomer is shown in Figure 3. The complexes containing the Hpztr ligand did not appear to be as pH sensitive as the Hpytr analogues as the ^{1}H NMR was obtained in d_3-acetonitrile for all the pztr$^-$ complexes. All characterisation measurements were obtained in a basic or protonated media. The CHN analysis was only obtained for one isomer of each complex, however all isomers were found to be hplc and ^{1}H NMR pure. As stated previously the ^{1}H NMR of the complexes illustrates their purity and the deuteriated analogues also confirm this.

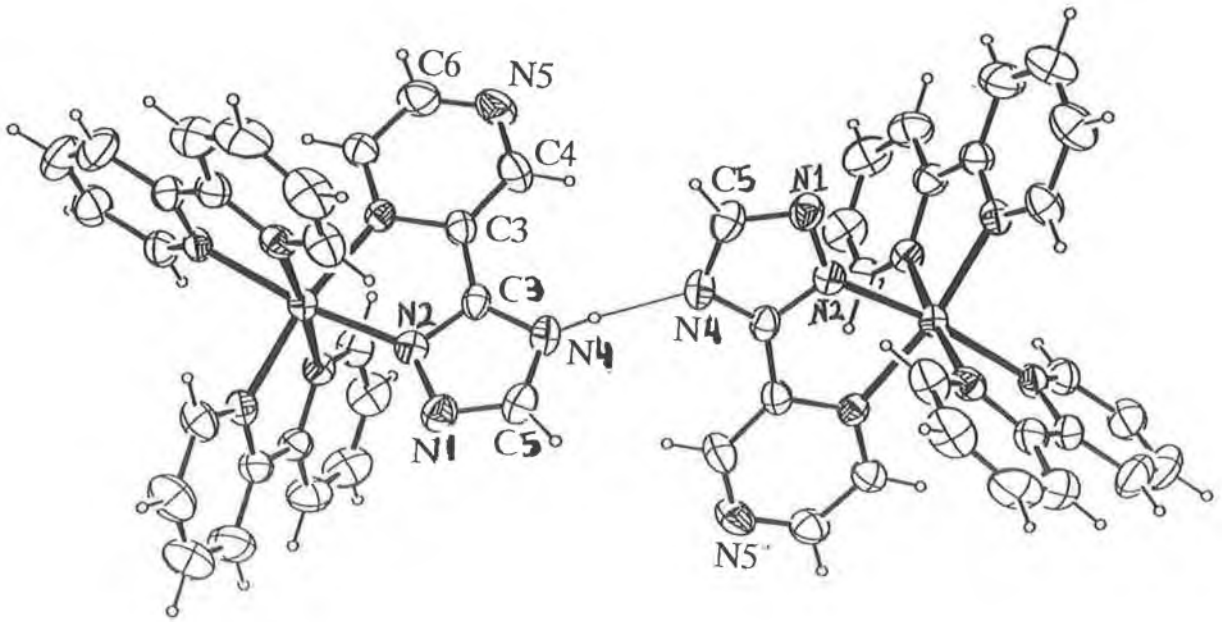

Figure 2 Crystal structure of $[Ru(bpy)_2Hpztr]^{2+}$ to illustrate sharing of proton.

3.3.2 Chromatographic interpretation

Initially the mononuclear complexes were run on an analytical hplc using a SCX cation exchange column and a mobile phase of 0.12 M $LiClO_4$, 80:20 acetonitrile: water, flowrate 2 cm^3/ min and a detector wavelength of 280 nm. The following is an example of (I) the mononuclear complex containing the two isomers and (II) after isolation on the alumina column the individual isomer traces.

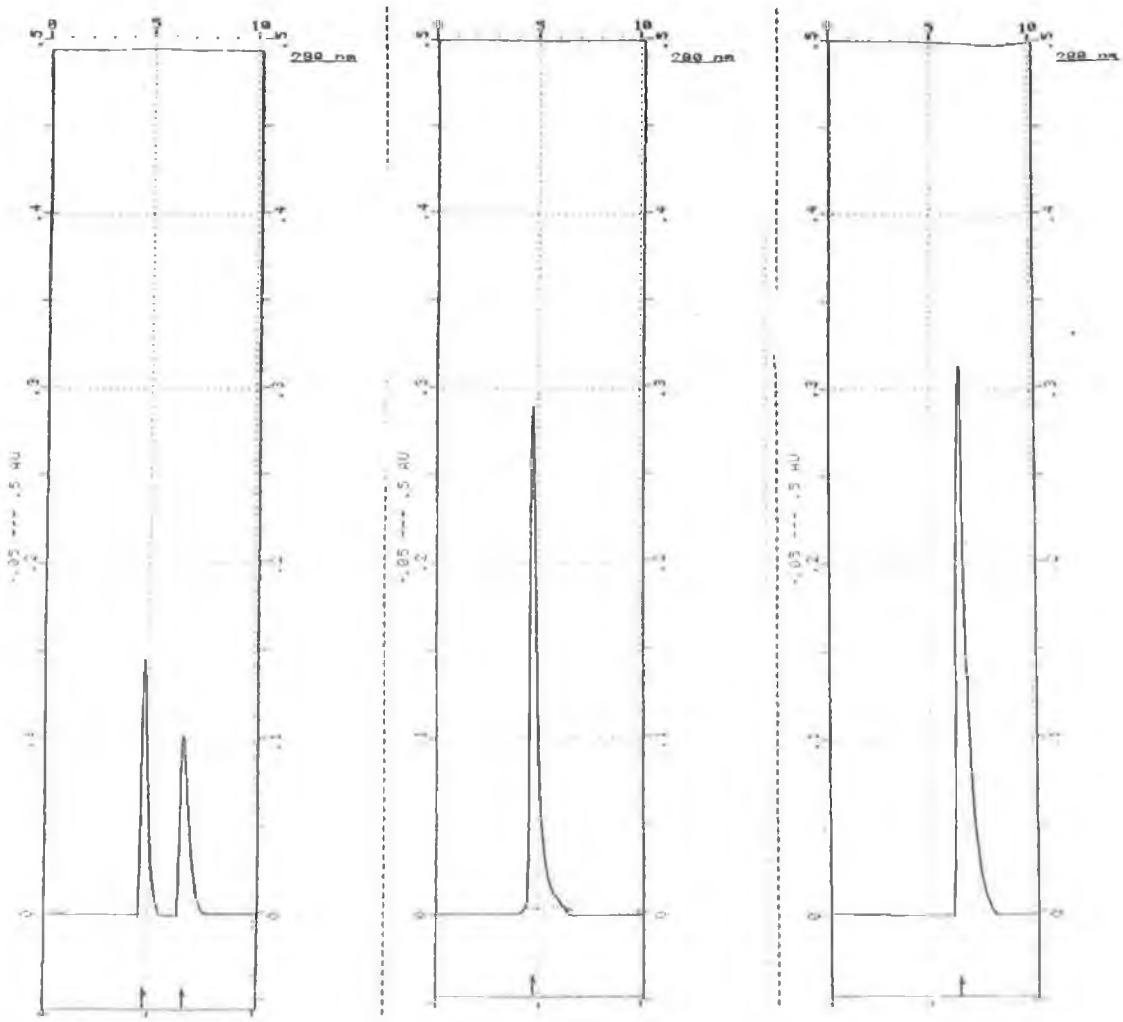

I II

Figure 3: Hplc traces of (I)[Ru(bpy)$_2$pztr]$^{2+}$ monomeric complex and (II) isolation of isomers.

The hplc trace of the monomer is presented in Figure 3, which portrays the two coordination isomers of the monomer at their different retention times but with similar UV spectra from the photodiode array detector. It is thought that the isomers are separated due to their difference in acid/base properties based on their binding sites as shown previously[6]. The separation was successfully achieved on neutral alumina columns using 100 % acetonitrile to isolate the first fraction and 100 % methanol to isolate the second fraction. The solvent is evaporated and isolated in an aqueous solution of PF_6. The precipitate is filtered, dried and the purity of the fraction is analysed by hplc. Deuteriation does not have any effect on retention times. Semi-preparative hplc was also used to isolate the isomers using a mobile phase of 0.12 M KNO_3 in 80:20 MeCN: H_2O, however on evaporation of the mobile phase to extract the pure isomers high concentrations of nitrate salts were also collected (**which are known to be potential explosives when heated to dryness!**). Hence this method of purification was not further pursued, as it was not drastically required for the purification of the compounds.

The pyridine-triazole (Hpytr) complexes were only synthesised in conjunction with bipyridyl and its deuteriated analogues. The isolation of the N2 and N4 isomers is straight forward as the retention time for each isomer is well separated. After recrystallisation, purification of the isomers took place on an alumina column 100 % MeCN followed by 100 % MeOH, to elute both isomers. The separation is facile and a crystalline product is collected after the solvent is removed.

A similar separation technique is included in the isolation of the pyrazine-triazole (Hpztr) containing complexes but due to the use of bipyridyl, phenanthroline or biquinoline in complexation the complexes will contain different properties and hence different retention times. Due to the well-separated retention times of the pyrazine-triazole containing isomers on the alumina columns the use of semi-preparative hplc was not required. For the phenanthroline containing compounds the retention times were 3 to 5 min which were similar as for the bipyridyl, however, in the case of the biquinoline containing complexes the retention time is very short (<2 min).

The biquinoline complex initially looked pure (1 peak, 100 %) when injected onto the analytical column. When this complex was eluted off an alumina column two fractions were isolated. This concurs with the previous complex, the only difference being that the N2: N4 isomers were collected in a yield of 90:10 respectfully. The argument for this ratio may be simply that the N2 coordination site is more sterically favourable than the N4 site and is revealed on using "peripheral" ligands bigger than that of the bipyridyl. In the case of the phenanthroline there was not an exact ratio of 60: 40 N2: N4 as there was for the bipyridyl complex. A ratio of 80: 20 N2: N4 is the estimated yield for the isolated isomers containing phenanthroline.

3.3.2.1 Stereoisomer separation

Current interest[17,18,19] lies in the isolation of the stereoisomers of Ru(II) complexes as it is suggested that in order to achieve accurate results for luminescent lifetimes of such complexes they would have to be enantiomerically pure. This has direct significance in the area of supramolecular chemistry[20,21], as it would have an amplified effect in such systems. Figure 4 and Figure 5 are examples of enantiomeric separation of the pytr$^-$ and pztr$^-$ complexes respectfully carried out by Villani et al[22].

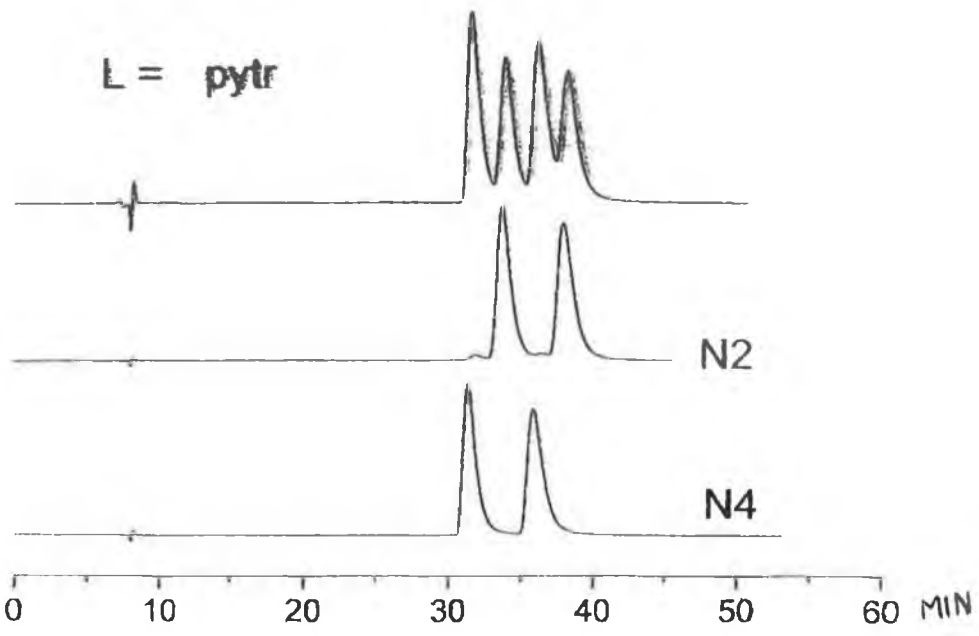

Figure 4 Chromatogram of enantiomeric separation of [Ru(bpy)$_2$pytr]$^{+}$[22]

The development of a hplc stationary phase[23,24] which is capable of separating enantiomers would be a great advantage in the synthesis and purification of Ru(II) complexes both for mononuclear and supramolecular studies. The study carried out revealed a new stationary phase (silica-bound Teicoplanin) which enables high efficient chromatographic resolution of chiral mono- and dinuclear Ru(II) complexes. A set of results were obtained for the mononuclear complexes of $[Ru(bpy)_2pytr]^+$, Figure 4 and $[Ru(bpy)_2pztr]^+$,Figure 5. The results obtained for both complexes revealed four peaks. On a cation exchange column two peaks are obtained for $pytr^-$ and $pztr^-$ mononuclear complexes.

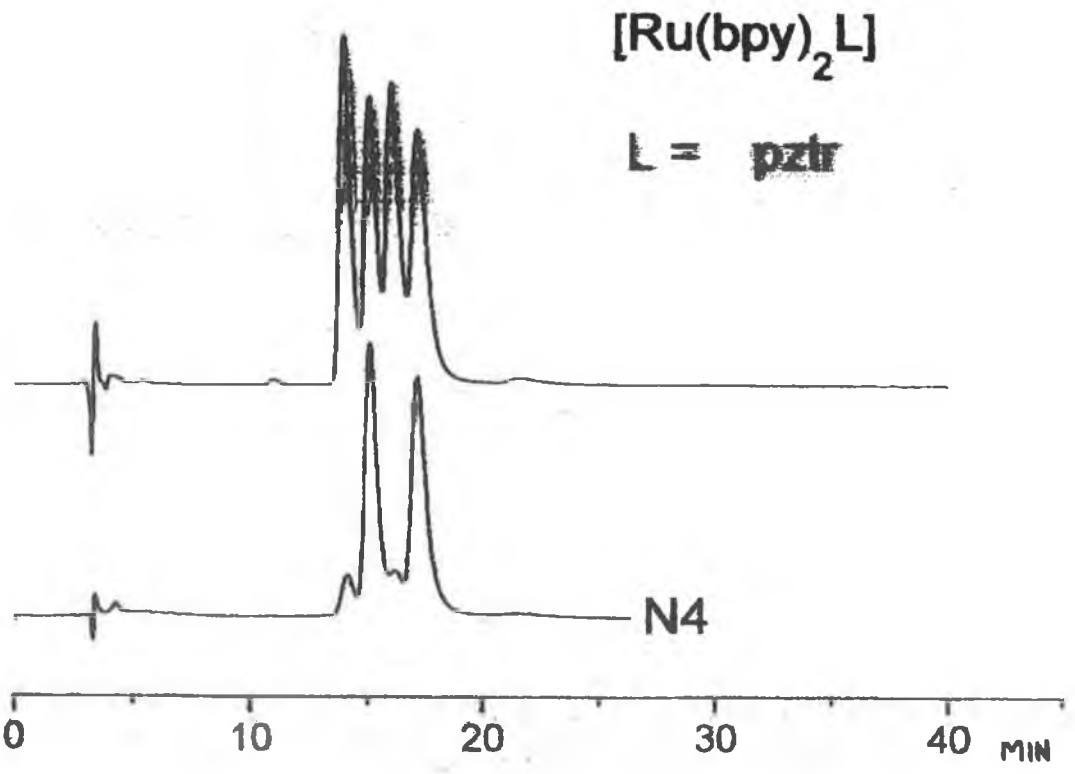

Figure 5 Chromatogram of enantiomeric separation of $[Ru(bpy)_2pztr]^{+}$[22]

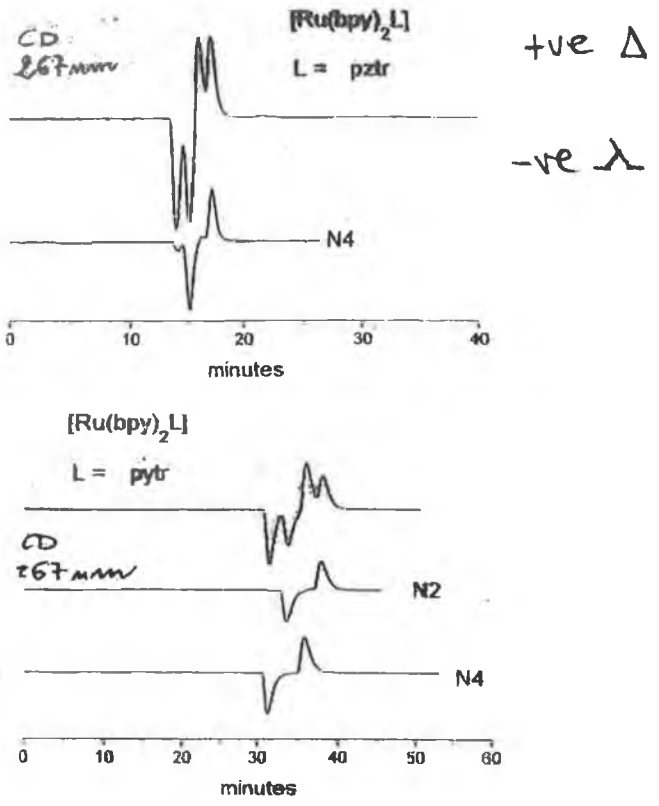

Figure 6 Circular dichromism of [Ru(bpy)$_2$pytr]$^+$ and [Ru(bpy)$_2$pztr]$^+$

Elution of the enantiomers was established by on-line circular dichromism detection and the data for the two complexes are shown in Figure 6, which highlights the orientation of the enantiomer (Δ or Λ). α is the observed angle of rotation and the angle may be left or right of the original value $\alpha = 0^0$. The Δ isomer, Dextrorotatory (Latin dexter, "right") are referred to as compounds which rotate the plane of polarisation to the right and are given a positive (+) value for α (observed angle of rotation). The Λ isomers, Levorotatory (Latin laevus, "left") and is given a negative (-) value for α. For these complexes the Δ enantiomers were retained on the column. A remarkable separation of regioisomers and enantiomers was achieved and this was extraordinary, as there is so little structural difference between the regioisomeric complexes. For further information refer to appendix 1, paper 4 and additional relevant data in appendix 3.

3.3.3 ^{1}H NMR Spectroscopy

In the elucidation of the structures of ruthenium polypyridyl complexes ^{1}H NMR [25,5,6,10] has proven to be a very powerful technique.[26,15,27,28,29] Interpretation of Ru(II) polypyridyl complexes in the past has sometimes proven to be difficult due to the large quantity of protons present on the peripheral ligands i.e. bipyridine. However, the idea of using deuteriated bipyridyl is to simplify the ^{1}H NMR spectra of ruthenium complexes[16]. ^{1}H NMR is used to determine the percentage deuteriation of the ligands as it is necessary to have the ligands >99 % deuteriated for accurate luminescent lifetime measurements to be determined.

3.3.3.1 ^{1}H NMR of deuteriated ligands

This procedure must be carried out in order to interpret the degree of deuterium exchange that takes place during the deuteriation of the ligands. The ligands should preferably be 99.99% deuteriated in order for accurate luminescent lifetimes to be measured on the complexes but for ^{1}H NMR > 95 % would be sufficient. The following is an example of how the % deuteriation was determined on a sample of bpy after 4 days at 200 ^{0}C using 3 g.

Calculation of % deuterium exchange e.g. 2,2'-bipyridyl:

Step 1: Ligand to solvent ratio of the undeuteriated ligand

6mg/1 cm^3

The ^{1}H NMR of the undeuteriated 2,2'- bipyridyl was obtained by dissolving 6 mg of bpy in 1 cm^3 of $CDCl_3$, and from this spectrum the ratio of the integration of the ligand peak (L) to the solvent peak (S) was determined. From this spectrum we get the ratio of the relative number of hydrogen's in the bpy sample compared to that in the deuteriated solvent. In order to calculate the overall % deuteriation of the ligand, an average of all four ligand peak integration values must be taken;

For undeuteriated bpy, L = (1.00+0.988+1.014+0.994) ÷ 4 = 0.999,

Hence, from the spectrum

Figure we can see the ligand to solvent ratio L/S =10, as the integration of the ligand averages at 0.999 and the solvent integration is 0.1.

RATIO of L/S = 1.0/0.1 = 10

Step 2: Ligand to solvent ratio of the deuteriated ligand

12mg/ 1 cm^3

The ^1H NMR spectrum of the deuteriated sample of bpy was obtained by dissolving 12 mg of deuteriated bpy in 1 cm^3. In this case the weight of the sample must be taken into account in order to compare it with the corresponding peaks of the undeuteriated sample.

For deuteriated bpy, L = (1.000+0.900+0.893+0.994) ÷ 4 = 0.947

Hence, from the spectrum in Figure we can see in this case that the ligand to solvent ratio L/S = 0.099, as the average ligand peak integrates as 0.947 and the solvent peak integrates as 9.557.

ratio of L/S = 0.947/9.557 = 0.099
This must be divided by the weight differences,

0.099 ÷ 12 mg/ 6mg = 0.0495

therefore,

$$\frac{\text{Deuteriated ratio L/S}}{\text{Undeuteriated ratio L/S}} = \frac{0.0495}{10} = 0.00495$$

Hence, the percentage of remaining hydrogen in the deuteriated sample, %H = 0.495 %, which means, therefore that the % deuterium exchange of the sample is 99.505 %. The experiment error, due to discrepancies in weight and volume measurements was estimated to be approximately 99 +/- 1 %.

Figure 12 to Figure 17 show examples of the ^1H NMR of the ligands and their respective deuteriated analogues, bpy, phen and biq.

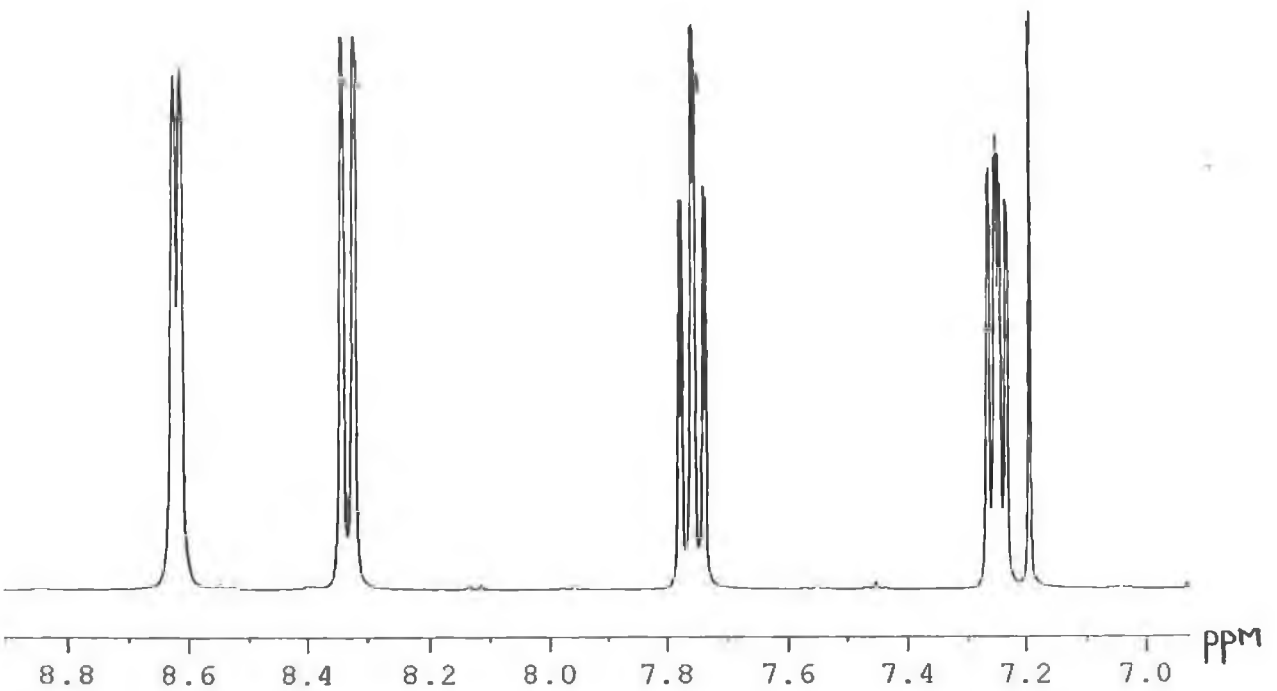

Figure 7: ^1H NMR of undeuteriated bpy in 1 cm^3 of $CDCl_3$.

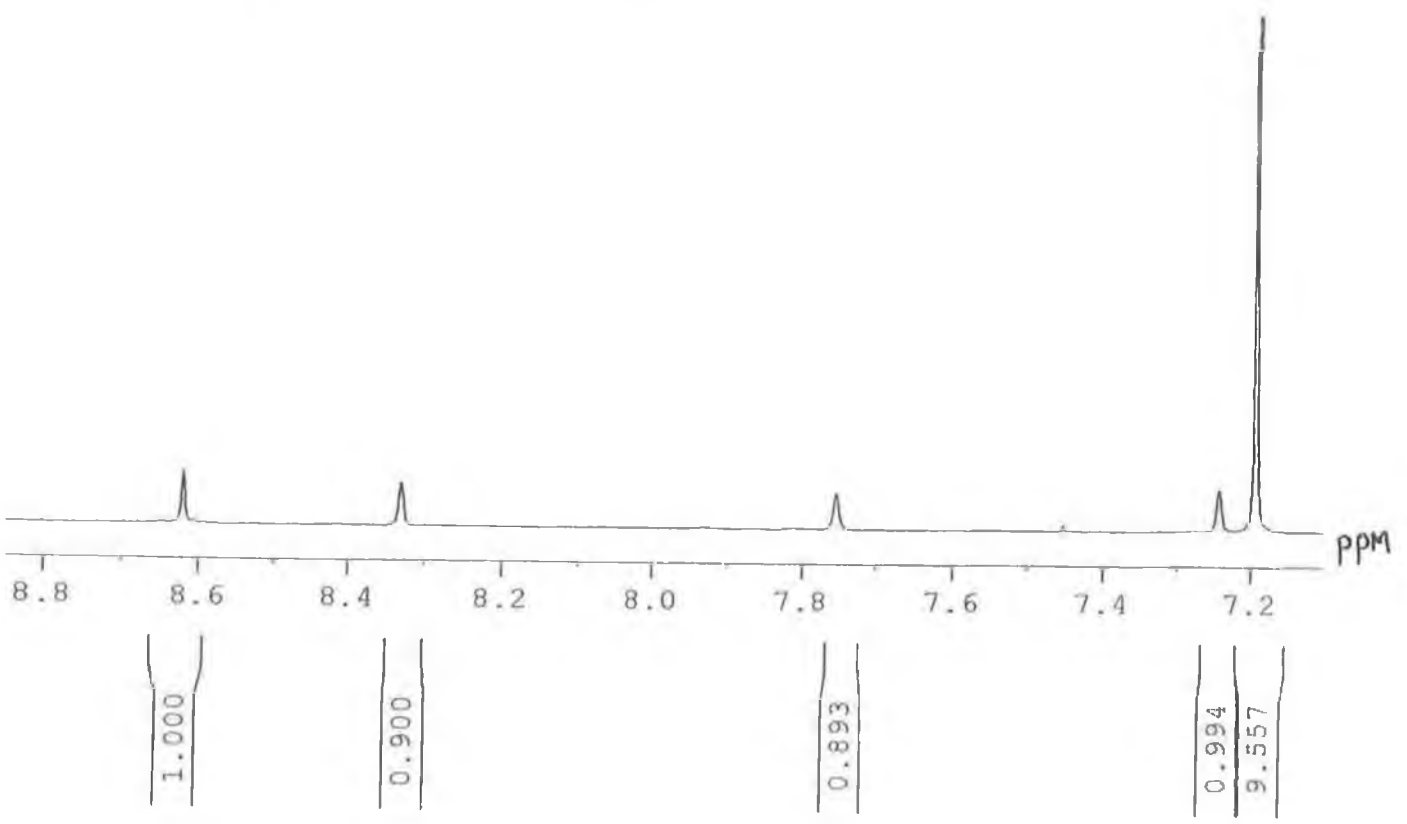

Figure 8: ^1H NMR of deuteriated bpy in 1 cm^3 of $CDCl_3$

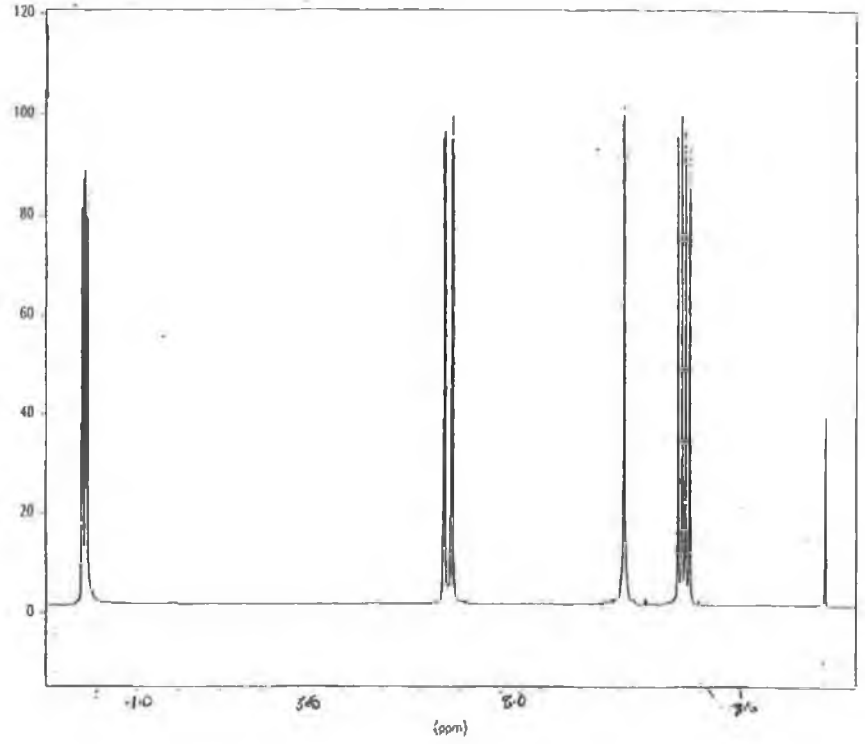

Figure 9 ^{1}H NMR of undeuteriated phen in 1 cm^3 of $CDCl_3$.

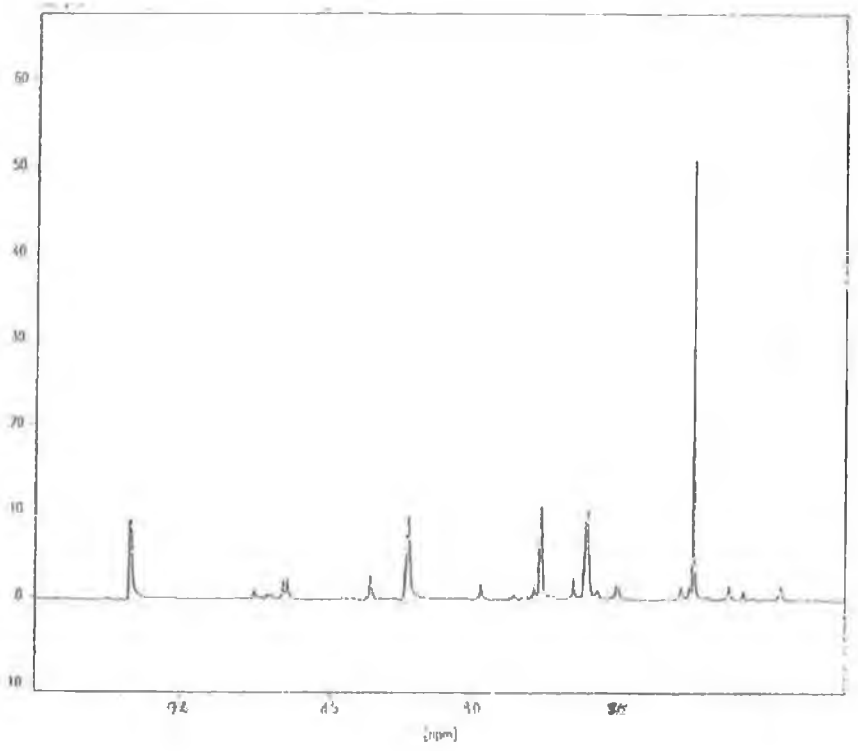

Figure 10 ^{1}H NMR of deuteriated phen in 1 cm^3 of $CDCl_3$

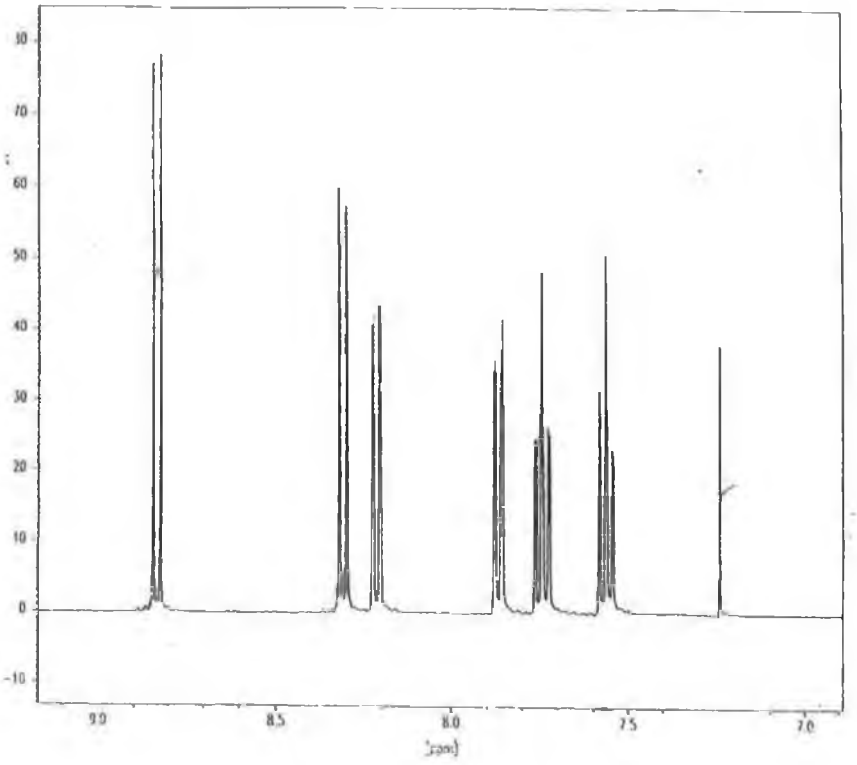

Figure 11 ^{1}H NMR of undeuteriated biq in 1 cm^3 of $CDCl_3$

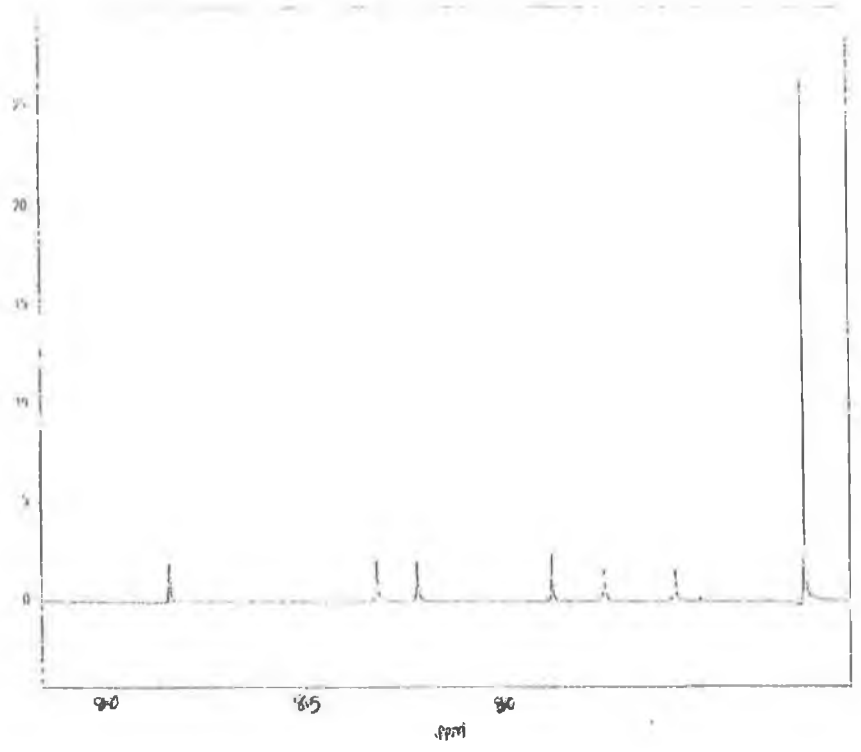

Figure 12 ^{1}H NMR of deuteriated biq in 1 cm^3 of $CDCl_3$

3.3.3.2 ^{1}H NMR of Hpytr complexes containing h_8-bpy and d_8-bpy

The ^{1}H NMR spectra of the N2-isomer of $[Ru(bpy)_2pytr]^{2+}$, $[Ru(d_8\text{-}bpy)_2pytr]^{2+}$ and $[Ru(bpy)_2d_5\text{-}pytr]^{2+}$ are presented in Figure 13, Figure 14 and Figure 15 respectively. The elucidation of the spectra is greatly facilitated by the deuteriation of the ligands.

COMPOUND	H^3 (ppm)	H^4 (ppm)	H^5 (ppm)	H^6 (ppm)	$H^{5'}$ (ppm)
Hpytr	8.09 (d)	7.98 (t)	7.51 (t)	8.70 (d)	8.27 (s)
$[Ru(bpy)_2pytr]^+$ Iso 1	8.08(-0.01)	7.84(-0.14)	7.11(-0.40)	7.49(-1.21)	7.90(-0.37)
$[Ru(bpy)_2pytr]^+$ Iso 2	8.32(+0.23)	7.99(+0.01)	7.34(-0.17)	7.57(-1.13)	8.11(-0.16)
$[Ru(d_8\text{-}bpy)_2pytr]^+$ Iso 1	8.08(-0.01)	7.84(-0.14)	7.11(-0.40)	7.49(-1.21)	7.90(-0.37)
$[Ru(d_8\text{-}bpy)_2pytr]^+$ Iso 2	8.32(+0.23)	7.99(+0.01)	7.34(-0.17)	7.57(-1.13)	8.11(-0.16)

Table 1: 400 MHz ^{1}H NMR resonances for the $[Ru(bpy)_2pytr]^{2+}$ mononuclear complexes. All measurements were carried out in d_3-Acetonitrile except free ligand measured in d_6-DMSO. Values in parenthesis are the chemical shifts compared with the free ligand. (s = singlet, d = doublet, t = triplet and m = multiplet). (Iso 1 is the N4 bound isomer and Iso 2 is the N2 bound isomer).

Table 1illustrates the chemical shifts of the H^3, H^4, H^5 and H^6 Hpytr protons on complexation to the Ru moiety. When comparing the proton shifts of the isomers the $H^{5'}$ signal is the most indicative shift. For N4-isomer (-0.37), which is double of that for N2-isomer (-0.16). The signal of the $H^{5'}$ proton of the triazole ring undergoes a large shift upfield when the $Ru(bpy)_2$ moiety is coordinated to the N^4 coordination site. The ring current effect of the adjacent bipyridyls is experienced by the $H^{5'}$ when it is in such close vicinity.

The $H^{5'}$ of N2-isomer is also shifted upfield by 0.16 ppm on coordination to the N^2 site, which is due to the negative charge present on the triazolate ligand, resulting in a higher electron density on the ligand. The ^{1}H NMR of the $[Ru(d_8\text{-}bpy)_2(d_5\text{-}pytr)]^+$ isomers are not listed as in this case all of the proton signals are suppressed. The complexes $[Ru(bpy)_2(d_5\text{-}pytr)]^+$ and $[Ru(d_8\text{-}bpy)_2(d_5\text{-}pytr)]^+$ are not useful tools in spectral elucidation but may prove useful in the identification of the excited state.

3.3.3.3 ^{1}H NMR of Hpztr complexes containing h_8-bpy and d_8-bpy.

The ^{1}H NMR resonances of the two isomers of $[Ru(bpy)_2pztr]^+$ are significantly different as shown by Hage et al. The deuteriation of the bpy ligand has facilitated the elucidation of the spectra greatly and enables the interpretation of the ligand shifts without the presence of the bipyridyl signals. Isolation of the pztr mononuclear coordination isomers $[Ru(bpy)_2pztr]^+$, $[Ru(d_8\text{-}bpy)_2pztr]^+$ and $[Ru(d_8\text{-}bpy)_2d_4\text{-}pztr]^+$ was achieved through the use of neutral alumina columns with 100% acetonitrile to elute N2-isomer and 100% methanol to elute N4-isomer.^{1}H NMR spectra were obtained for each isomer in deuteriated acetonitrile. The chemical shifts of these isomers are shown in Table 2. The shifts of the complex $[Ru(d_8\text{-}bpy)_2(d_4\text{-}pztr)]^+$ are not shown in this table as all the C-H signals are replaced by C-D signals and hence all of the complex peaks are suppressed in the ^{1}H NMR spectra.

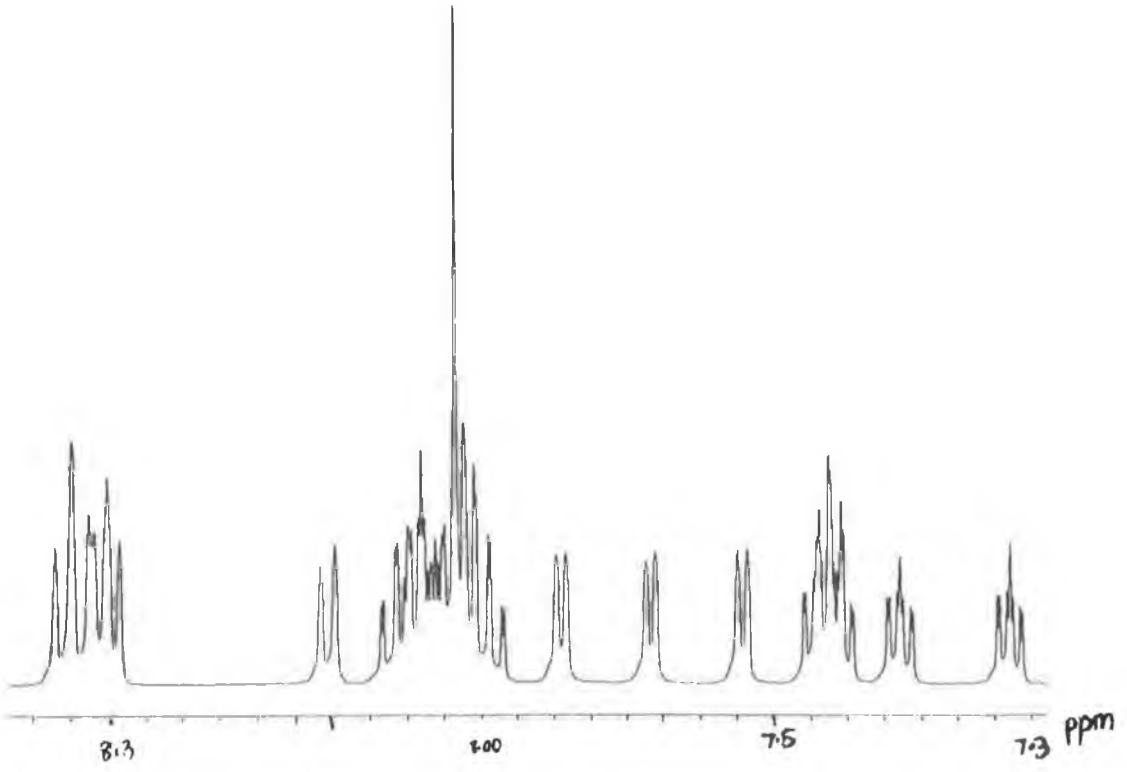

Figure 13: ^{1}H NMR of $[Ru(bpy)_2pytr]^{2+}$ N2-isomer in d_3-acetonitrile.

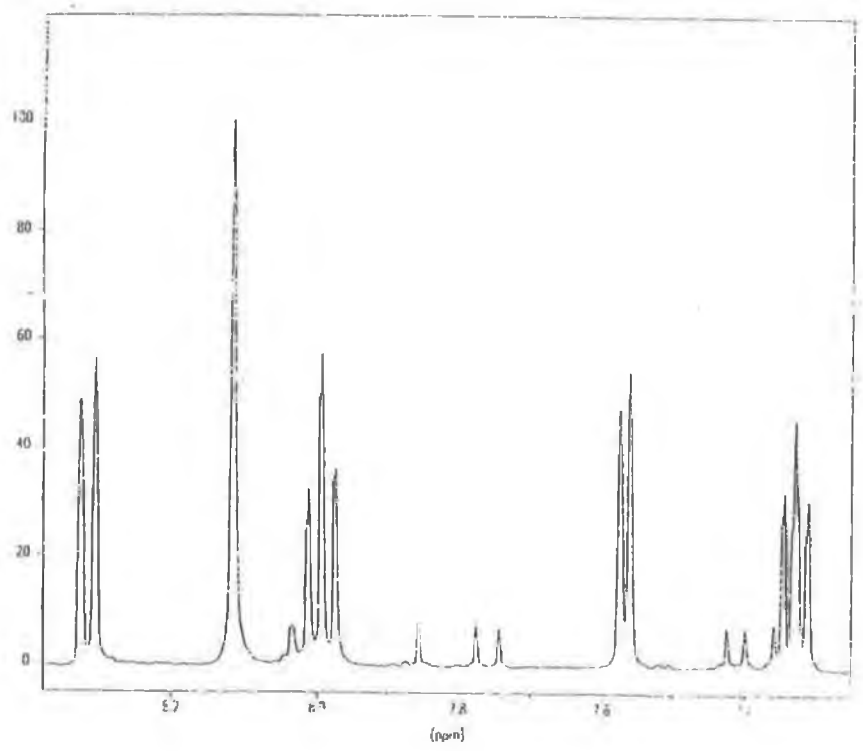

Figure 14 ^{1}H NMR of [Ru(d_8-bpy)$_2$pytr]$^+$ N2-isomer in d_3-acetonitrile..

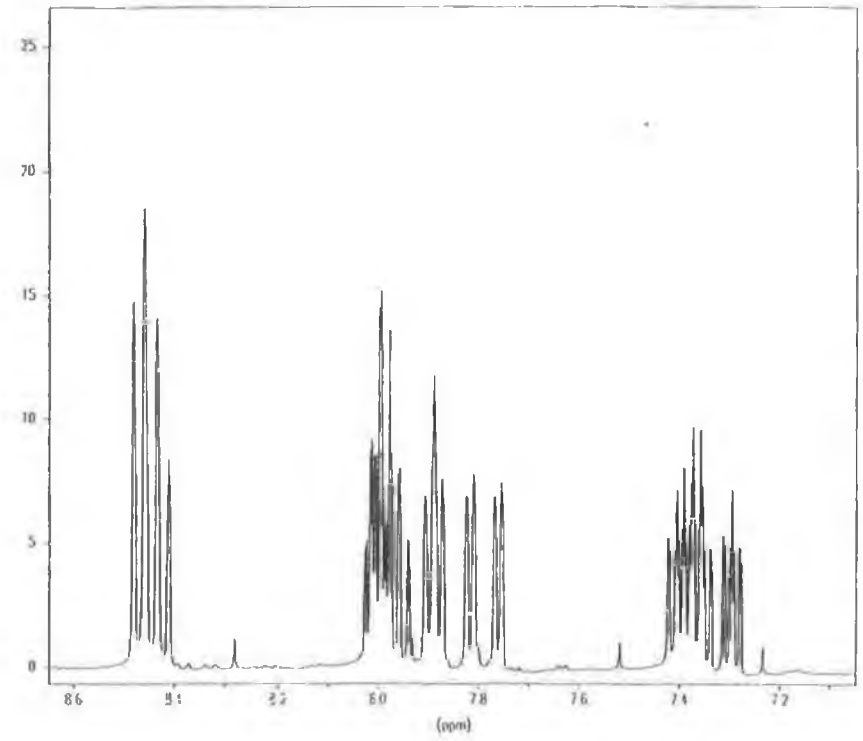

Figure 15 ^{1}H NMR of [Ru(bpy)$_2$$d_5$-pytr]$^+$ N2-isomer in d_3-acetonitrile

To determine the coordination mode of the pyrazine-triazole ligand in the mononuclear complexes the ^{1}H NMR spectra were compared. Figure 16 and 17 show the ^{1}H NMR spectra of N4-isomer and N2-isomer of the $[Ru(bpy)_2pztr]^+$ complexes respectively. The partially deuteriated $[Ru(d_8\text{-}bpy)_2pztr]^+$ complexes facilitate the interpretation of the ligand shifts for each isomer, ^{1}H NMR spectra for the partially deuteriated complex shown in Figure 18 and Figure 19. The H^3 proton is observed as a sharp singlet, hence assignment of this proton is straightforward. In Figure 16 it may be observed that for H^5 its chemical shift is at much higher field than that observed in Figure 17 for N2-isomer. Structural models reveal that when the triazole ring is bound via N^4 the $H^{5'}$ proton will be directed to the neighbouring bpy ring, but for the N^2 bound isomer this proton will not be located as near to the bipyridyls. [30] The above elucidation shows that N4-isomer is bound via N^4 of the triazole and isomer 2 via N2, which may be clarified by the crystal structure of N2-isomer in Figure 35.

COMPOUND	H^3 (ppm)	H^5 (ppm)	H^6 (ppm)	$H^{5'}$ (ppm)
Hpztr	9.47 (s)	8.71 (d)	8.65 (d)	8.24 (s)
$[Ru(bpy)_2pztr]^+$ Iso 1	9.52(+0.05)	8.07 (-0.64)	8.60 (-0.05)	8.94 (+0.70)
$[Ru(bpy)_2pztr]^+$ Iso 2	9.50 (-0.03)	8.10 (-0.61)	8.54 (-0.11)	8.74 (+0.50)
$[Ru(d_8\text{-bpy})_2pztr]^+$ Iso 1	9.52(+0.05)	8.07 (-0.64)	8.60 (-0.05)	8.94 (+0.70)
$[Ru(d_8\text{-bpy})_2pztr]^+$ Iso 2	9.44 (-0.03)	8.10 (-0.61)	8.54 (-0.11)	8.74 (+0.50)
$[Ru(phen)_2pztr]^+$ Iso 1	9.35 (-0.12)	8.10 (-0.61)	8.20 (-0.45)	7.36 (-0.88)
$[Ru(phen)_2pztr]^+$ Iso 2	9.25 (-0.22)	8.08 (-0.63)	8.18 (-0.47)	7.98 (-0.26)
$[Ru(d_8\text{-phen})_2pztr]^+$ Iso 1	9.35 (-0.12)	8.10 (-0.61)	8.20 (-0.45)	7.36 (-0.88)
$[Ru(d_8\text{-phen})_2pztr]^+$ Iso 2	9.25 (-0.22)	8.08 (-0.63)	8.18 (-0.47)	7.98 (-0.26)
$[Ru(biq)_2pztr]^+$ Iso 1	8.57 (-0.90)	7.80 (-0.91)	8.49 (-0.16)	7.50 (-0.74)
$[Ru(biq)_2pztr]^+$ Iso 2	8.32 (-1.15)	7.61 (-1.10)	8.28 (-0.37)	7.78 (-0.46)
$[Ru(d_{12}\text{-biq})_2pztr]^+$ Iso 1	8.57 (-0.90)	7.80 (-0.91)	8.49 (-0.16)	7.50 (-0.74)
$[Ru(d_{12}\text{-biq})_2pztr]^+$ Iso 2	8.32 (-1.15)	7.61 (-1.10)	8.28 (-0.37)	7.78 (-0.46)

Table 2: 400 MHz ^1H NMR resonances for the mononuclear complexes. All measurements were carried out in d_3-Acetonitrile except free ligand measured in d_6-DMSO. Values in parenthesis are the chemical shifts compared with the free ligand. (s = singlet, d = doublet, t = triplet and m = multiplet). In all cases isomer 1 is N4 bound and isomer 2 is N2 bound.

3.3.3.4 ^{13}C NMR of Hpztr complexes containing h_8-bpy and d_8-bpy

Deuteriation involves the exchange of the C-H to C-D, which has always been reflected in the ^1H NMR spectrum and has aided in elucidation of the spectrum, here we will observe its effect on the ^{13}C spectrum. The effect of deuteriation on the ^{13}C spectra has never been previously considered for the inorganic complexes with deuteriated ligands.

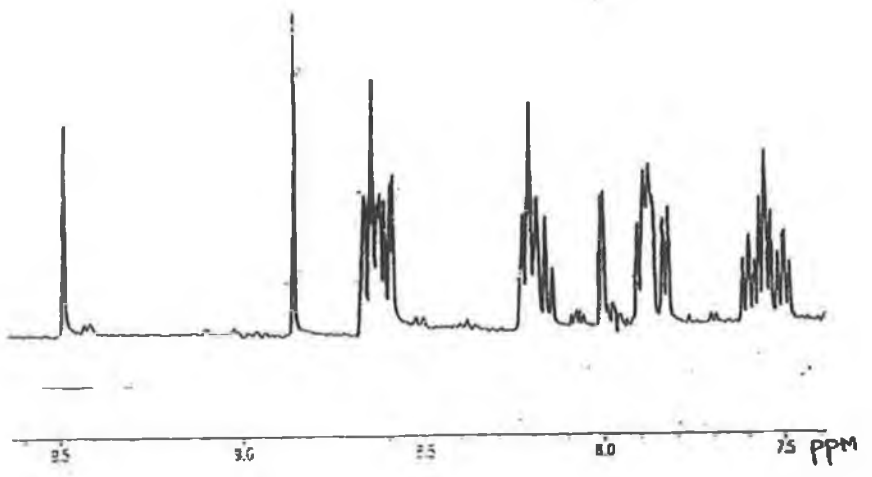

Figure 16 ^{1}H NMR of [Ru(bpy)$_2$pztr]$^+$ N4-isomer in d_3-acetonitrile

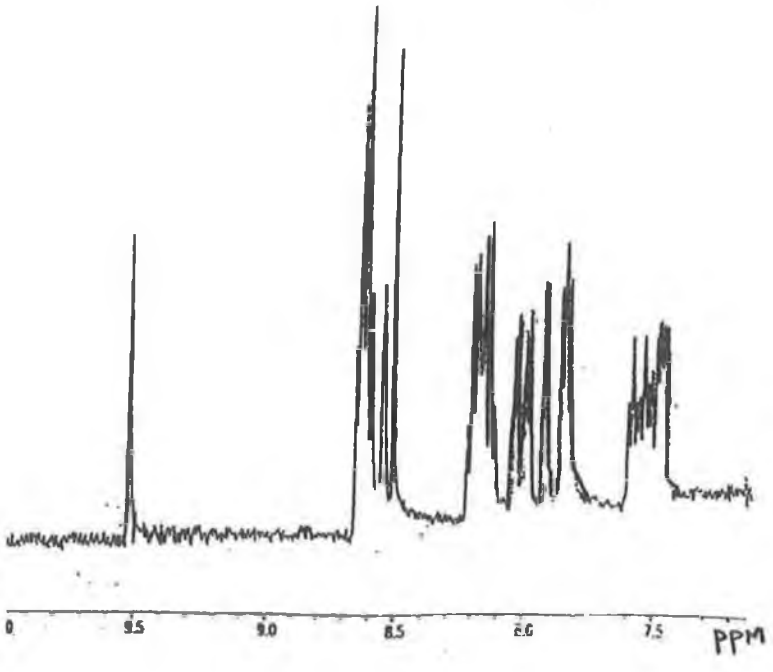

Figure 17 ^{1}H NMR of [Ru(bpy)$_2$pztr]$^+$ N2-isomer in d_3-acetonitrile

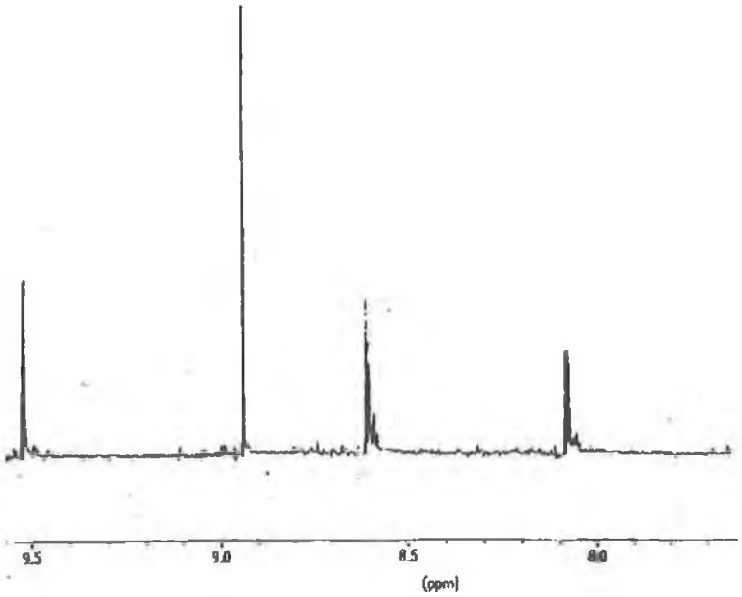

Figure 18: ^{1}H NMR of [Ru(d_8-bpy)$_2$pztr]$^+$ N4-isomer in d_3-acetonitrile

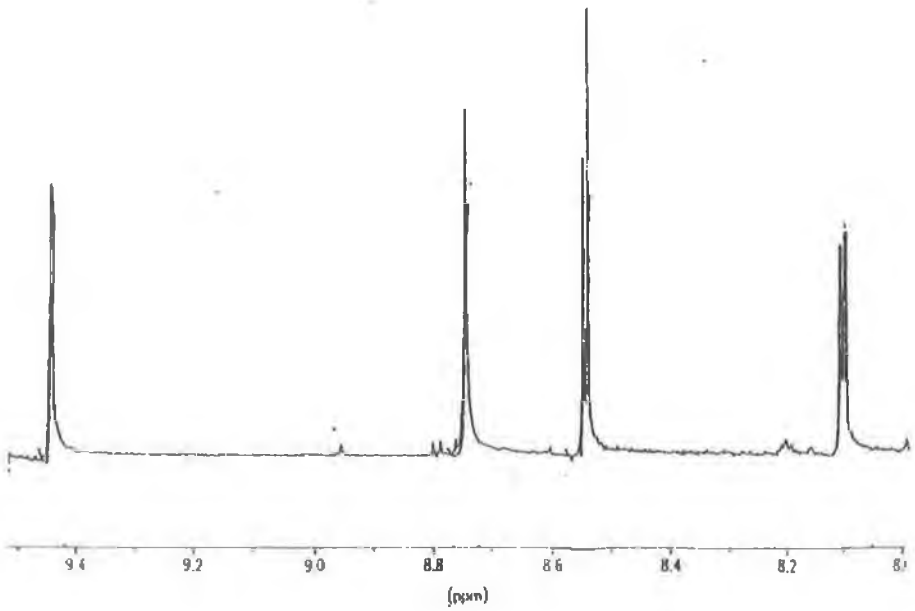

Figure 19: ^{1}H NMR of [Ru(d_8-bpy)$_2$pztr]$^+$ N2-isomer in d_3-acetonitrile

For organic compounds however where selective deuteriation has been encountered the use of the ^{13}C spectrum has proven most useful [31,32]. Recently O'Callaghan et al.[33], observed a substantial diminution in the height of the carbon signals, and nearby carbon signals of the ^{13}C spectra for polyheterocyclic compounds upon deuteriation. The decrease in the signal intensity of the ^{13}C has been attributed to various factors: loss of heteronuclear Overhauser effect (NOE), the fact that C-D coupling constants are smaller than C-H coupling constants, and signal 'splitting' owing to the presence of partially and fully deuteriated species. Figure 20, Figure 21 and Figure 22 are the ^{13}C spectra of $[Ru(bpy)_2pztr]^+$, $[Ru(d_8\text{-}bpy)_2pztr]^+$ and $[Ru(d_8\text{-}bpy)_2d_5\text{-}pztr]^+$ respectively. The ^{13}C spectra have not been assigned for the complexes. However in Figure 20 we see that there is a range of ^{13}C signals between 175 and 200 ppm. On comparison of Figure 20 with Figure 21 we see a large difference as the C-D signals of the deuteriated bipyridyls have been suppressed only revealing the C-H signals of the $pztr^-$ ligand. Figure 22 illustrates the ^{13}C of the fully deuteriated complex which has only solvent peaks remaining. This clearly illustrates the effect of deuteriation on the partially and fully deuteriated complexes.

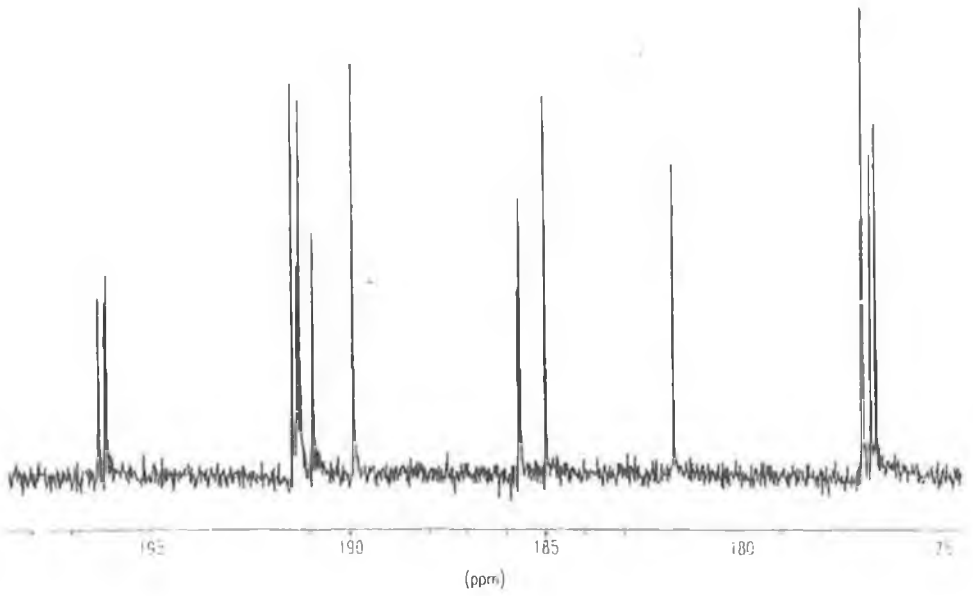

Figure 20 ^{13}C NMR of $[Ru(bpy)_2pztr]^+$ N2-isomer in d_3-acetonitrile.

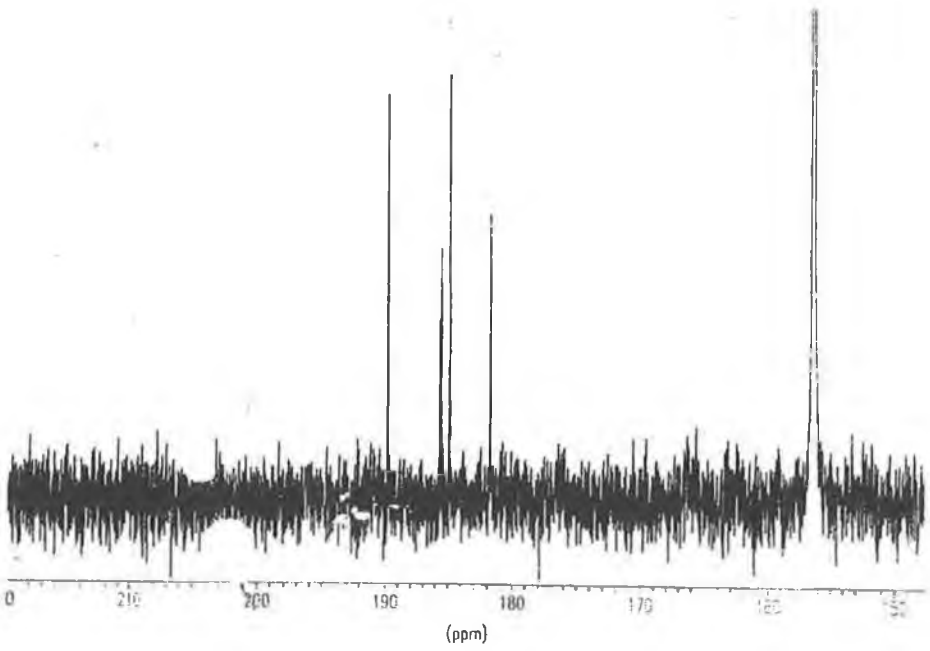

Figure 21 ^{13}C NMR of $[Ru(d_8\text{-bpy})_2pztr]^+$ N2-isomer in d_3-acetonitrile.

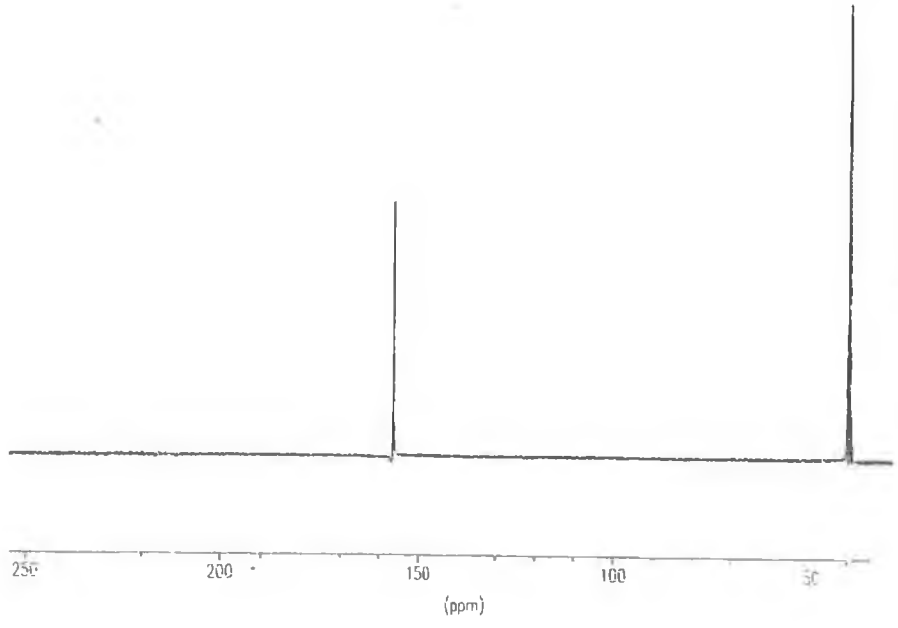

Figure 22 ^{13}C NMR of $[Ru(d_8\text{-bpy})_2d_5\text{-pztr}]^+$ N2-isomer in d_3-acetonitrile.

3.3.3.5 ^{1}H NMR of Hpztr complexes containing h_8-phen and d_8-phen

The complex $[Ru(phen)_2pztr]^+$ also forms coordination isomers which were visible on elution down a hplc column. The N2 and N4 coordination isomers are identified via ^{1}H NMR by observing the chemical shift of the H5' triazole signal. The H5' signal is known as being sensitive to ring current effect when a peripheral ligand (i.e. bpy, phen, biq) is nearby. For the complex $[Ru(phen)_2pztr]^+$, N4-isomer appears to be the N4 bound coordination isomer as it has the most significant shift of the H5' triazole proton of the two isomers. A shift of -0.88 ppm is experienced by the H5' proton of the N4 isomer compared to -0.26 ppm for the N2 isomer with respect to the Hpztr ligand shifts.

The other 3 Hpztr ligand protons (H3, H5 and H6) of the pyrazine ring in both N2 and N4 have chemical shifts quite similar in magnitude. The H5' shift of the N4 isomer of $[Ru(phen)_2pztr]^+$ is shifted -0.88 ppm on complexation to the metal. However, in the case of $[Ru(bpy)_2pztr]^+$ for the N4 isomer a shift of + 0.70 ppm is observed for the H5'.

Figure 23 and Figure 24 are 'H NMR spectra of the two coordination isomers of $[Ru(phen)_2pztr]^+$, N4 and N2 respectively. Figure 25 and Figure 26 are the ^{1}H NMR spectra of the N2 bound isomer of $[Ru(d_8\text{-phen})_2pztr]^+$ and $[Ru(phen)_2d_5\text{-pztr}]^+$ which illustrate effectively the use of partial deuteriation in the elucidation of ^{1}H NMR spectra of phenanthroline containing compounds. The spectra of $[Ru(d_8\text{-phen})_2pztr]^+$ only contains the signals of the Hpztr ligand protons, whereas the $[Ru(phen)_2d_5\text{-pztr}]^+$ shows only the proton signals of the phenanthroline complex. The phenanthroline ligand as previously stated is a difficult ligand to deuteriate but fortunately clear ^{1}H NMR spectra were obtained. The chemical shifts for the N2 and N4 isomers of $[Ru(phen)_2pztr]^+$ are listed in Table 2.

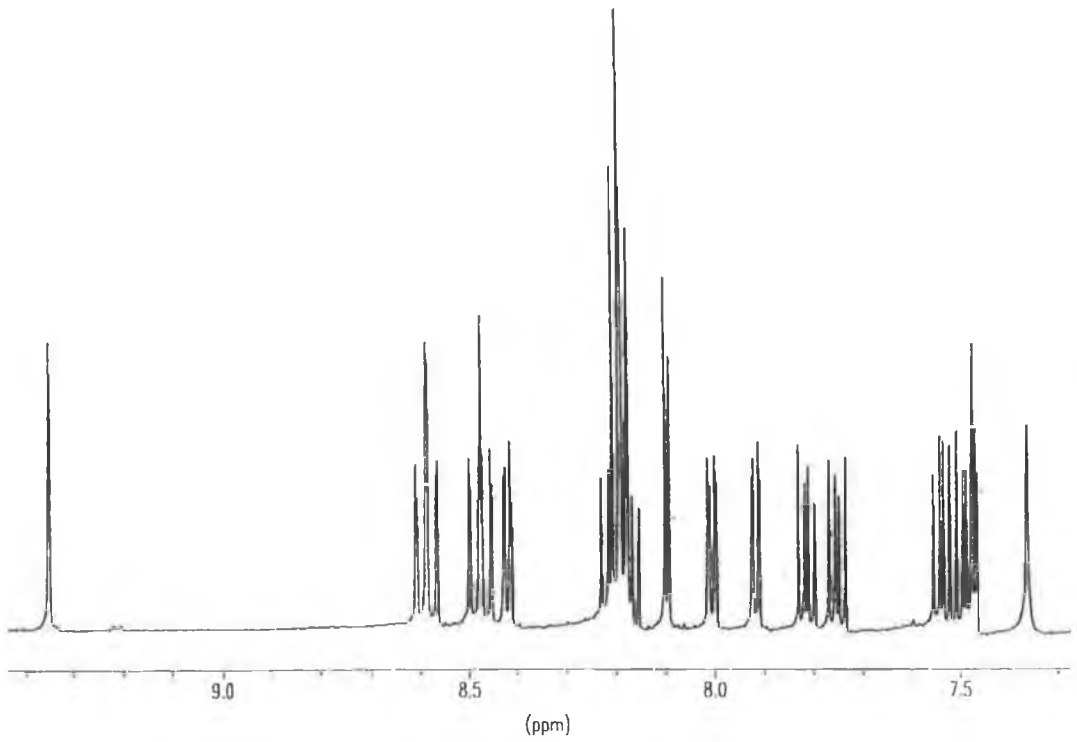

Figure 23: ^{1}H NMR of [Ru(phen)$_2$pztr]$^+$ N4-isomer in d_3-acetonitrile.

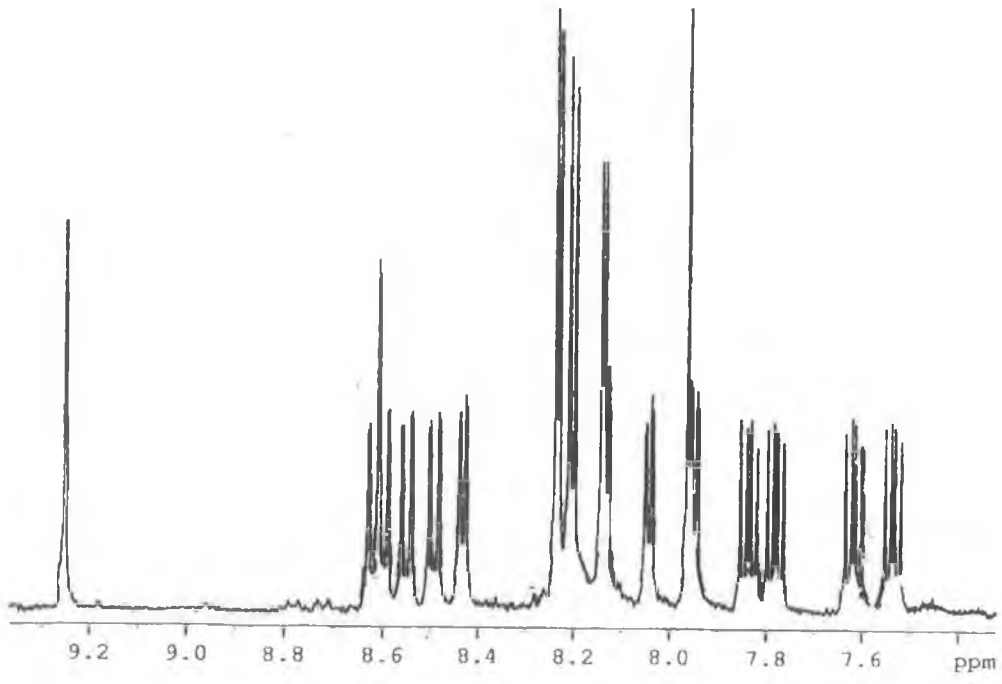

Figure 24: ^{1}H NMR of [Ru(phen)$_2$pztr]$^+$ N2-isomer in d_3-acetonitrile.

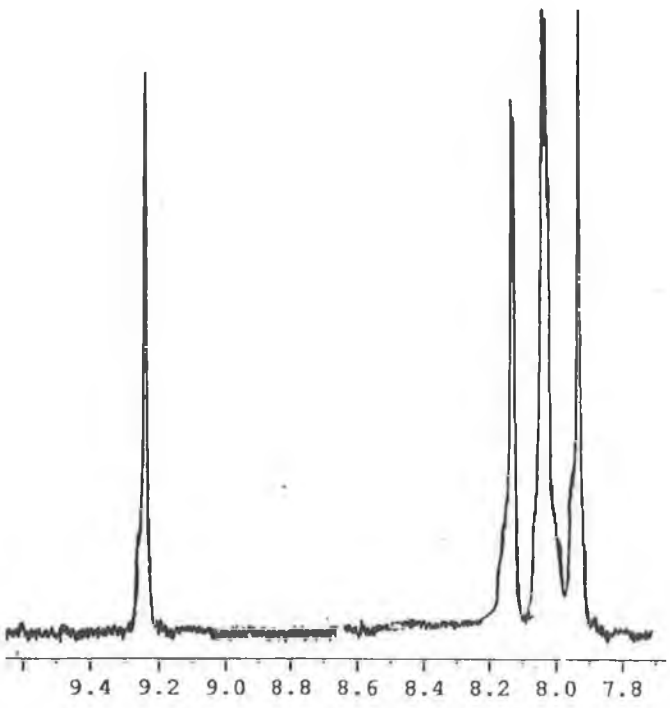

Figure 25: ^{1}H NMR of [Ru(d_8-phen)$_2$pztr]$^+$ N2-isomer in d_3-acetonitrile.

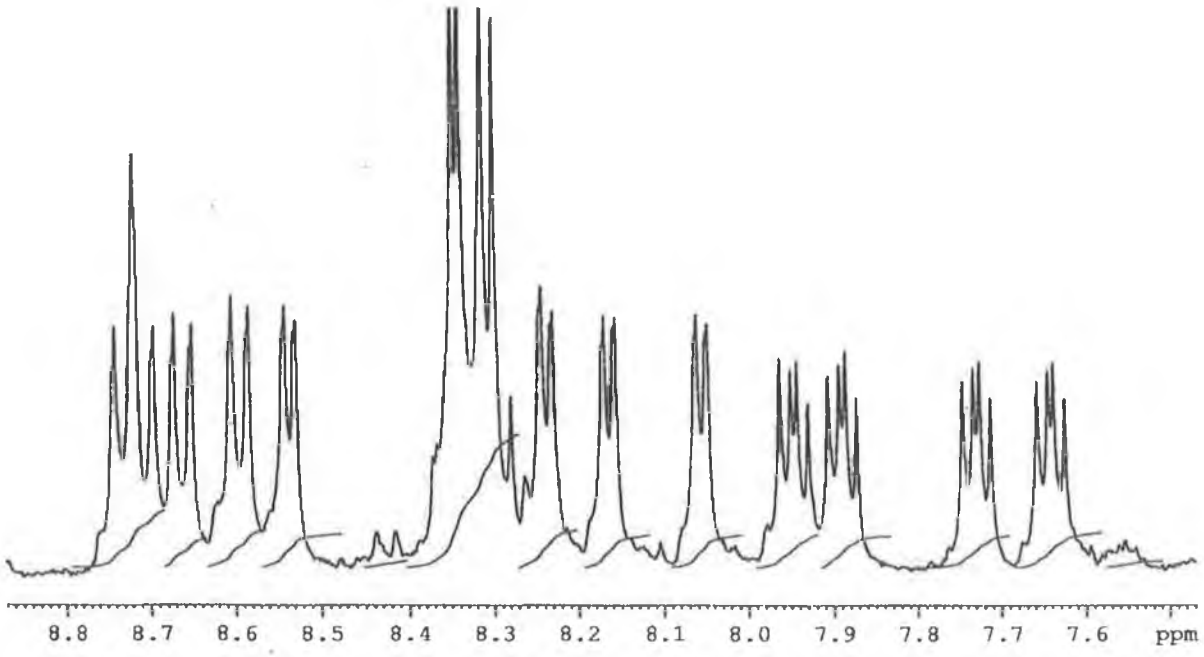

Figure 26: ^{1}H NMR of [Ru(phen)$_2$$d_5$-pztr]$^+$ N2-isomer in d_3-acetonitrile.

3.3.3.6 ^{1}H NMR of Hpztr complexes containing h_{12}-biq and d_{12}-biq

It was hoped on synthesis of the dark purple $[Ru(biq)_2pztr]^+$ monomer that the size of the biquinoline ligand would sterically hinder the formation of both coordination isomers. A ratio of 1:20 of N4-isomer:N2-isomer was found on isolation by column chromatography, which suggests that in fact the N4-bound isomer is sterically hindered.

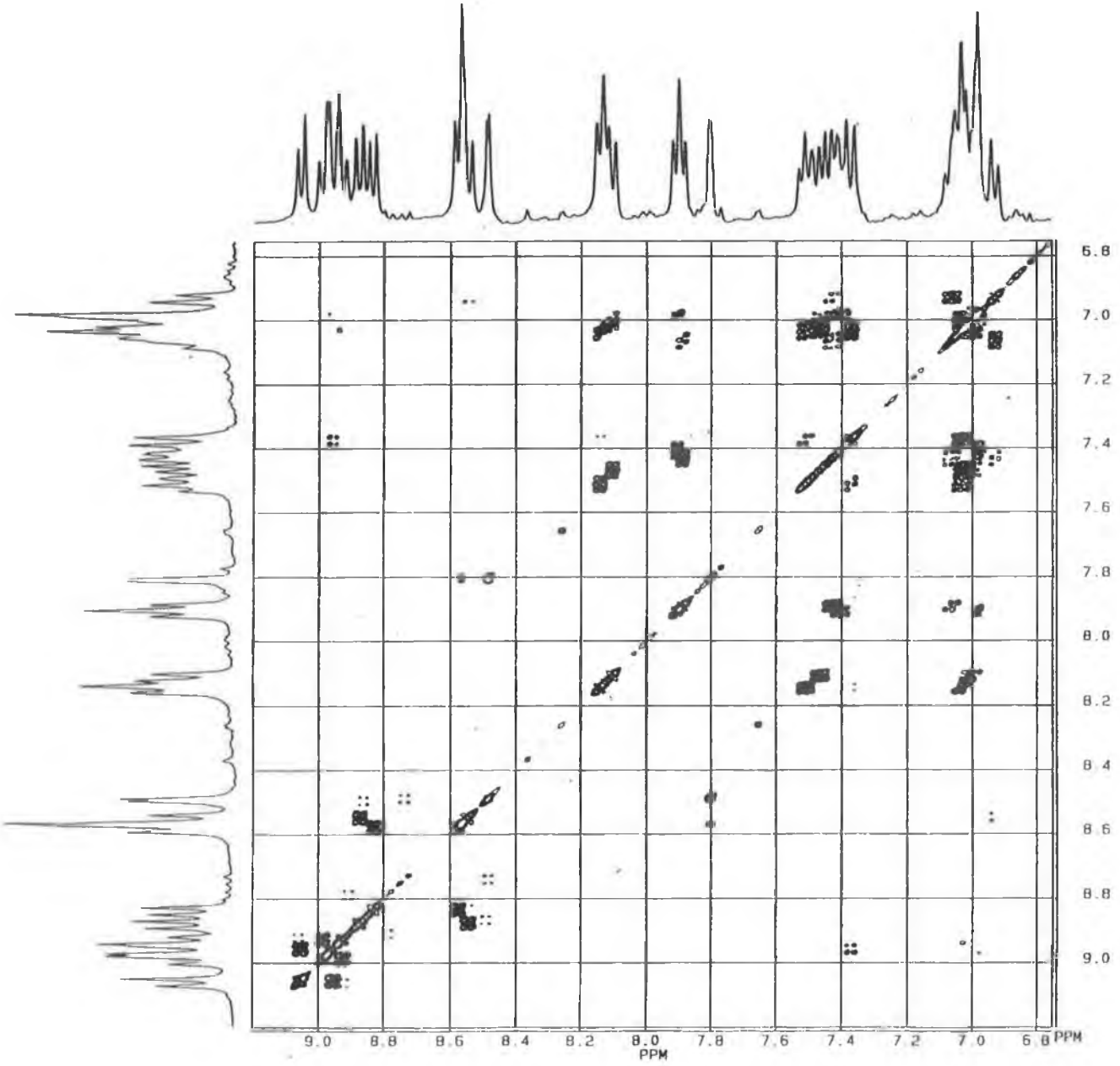

Figure 27: COSY NMR of $[Ru(biq)_2pztr]^+$ N4-isomer in d_3-acetonitrile.

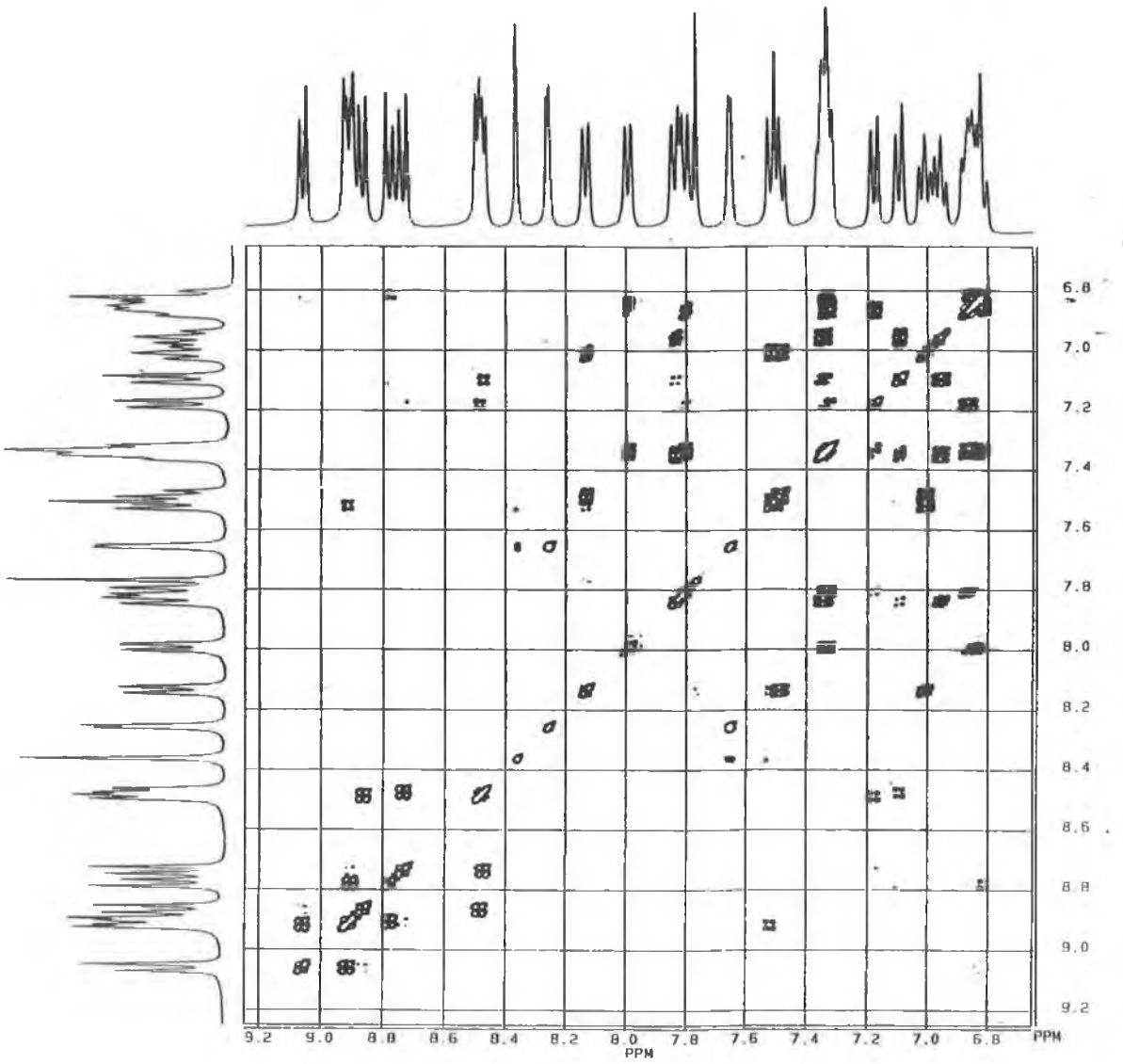

Figure 28: COSY NMR of $[Ru(biq)_2pztr]^+$ N2-isomer in d_3-acetonitrile.

Separation was achieved using neutral alumina and 100% Acetonitrile followed by 100% Methanol to elute the second fraction. The hplc trace only revealed one peak for the product. Once the isomers were isolated, COSY NMRs were obtained which are shown in Figure 27 and Figure 28. The use of COSY NMR facilitated greatly in the assignment of the ligand shifts, which are listed in Table 2.

A partially deuteriated complex confirmed the assignment of the COSY. The findings were that three proton peaks of the pyrazine ring H5 (d), H6 (d) and H3 (s) are at 7.61, 8.28 and 8.32 ppm respectively are all coupled to each other as expected, whereas the H5' of the triazole ring, is not coupled to another proton. From the chemical shift data presented in Table 2 it is suggested that N4-isomer is the N4 bound isomer and isomer 2 is the N2 bound. This is because the H5' signal of the triazole ring for the N4 isomer undergoes a shift of -0.74 ppm compared to the N2 isomer of -0.46 ppm. Another observation is that the entire proton shifts for the N2 isomer are greater than that of the N4 isomer, excluding the H5' of the triazole ring.

3.3.3.7 ^{99}Ru NMR Spectra

^{1}H NMR is widely known as being a powerful tool in the elucidation of Ru(II) structures. More recent studies have delved into the use of other nuclei in their analysis such as ^{57}Fe, ^{103}Rh, ^{187}Os and ^{55}Mn [34], and a more common probe in use is that of ^{15}N which is a great asset in the interpretation of heterocyclic ligand based complexes[35]. In this section the use of ^{99}Ru NMR as an analytical tool to identify coordination isomers in a mixture of a Ru(II) complex is proposed. Ruthenium NMR was carried out in collaboration with the Universiteit van Amsterdam[36]. The results are shown in Table 3 for the ruthenium shifts on coordination to the different ligands. ^{99}Ru NMR gave two distinct signals for the monomer of the $[Ru(bpy)_2pytr]^+$ containing both coordination isomers.

COMPOUND	^{99}Ru (ppm)
$[Ru(bpy)_2pytr]^+$ N4	4853
$[Ru(bpy)_2pytr]^+$ N2	4700
$[Ru(bpy)_2pztr]^+$ N4	4817
$[Ru(bpy)_2pztr]^+$ N2	4678

Table 3: 300 MHz ^{99}Ru resonances for the mononuclear complexes of pyridine- and pyrazine-triazole in d_3-acetonitrile.

On comparison with the NMR spectra of the isolated isomers the signal assigned to isomer 1-N4 bound was at 4853 ppm and isomer 2-N2 bound was at 4700 ppm. N2-isomer is shifted upfield compared to that of N4-isomer due to its coordination site N2, as the N2 site is a greater σ-donor than the N4 site causing an upfield shift for N2-isomer. Also the fact that it is a pyridine ring bound to a triazole ring has an effect which will be discussed in chapter 4.

For the complexes $[Ru(bpy)_2pztr]^+$ two peaks were observed isomer 2, N2 bound was at 4678 ppm. N2-isomer is shifted upfield compared to N4-isomer. The pKa values correspond to the upfield shifts of the different isomers. The pKa of the N4 bound isomers in both the $pytr^-$ and $pztr^-$ complexes has a less acidic pKa value than the N2 site. This is in direct agreement with the shifts that occur in the ^{99}Ru NMR and is based on the greater σ-donating properties of the N2 coordination site compared to that of the N4 site. Another pattern observed is the pK_a values for the $pztr^-$ isomers are lower than that of the $pytr^-$ and this is the same case for the corresponding upfield shift of the $pztr^-$ isomers in this ^{99}Ru NMR. Additional results are shown in Appendix 2, and further discussion on ^{99}Ru NMR may be found in Appendix 1 paper 2.

3.3.4 Electronic and Photophysical properties.

3.3.4.1 Absorption and Emission of Hpytr complexes.

The absorption, emission and luminescent lifetime(room temperature) properties of Ru(II) pyridine triazole complexes and their deuteriated analogues are listed in Table 4. The electronic absorption spectra of all these Ru(II) dinuclear complexes are quite similar and are dominated in the visible region by $d\pi - \pi^*$ metal-to-ligand charge transfer (MLCT) transitions typical of complexes of this type[37] and in the UV region (250-350 nm) by intense $\pi - \pi^*$ transitions associated with the bipyridyl and bridging ligands. The absorption of the deprotonated species are all red-shifted with respect to $[Ru(bpy)_3]^{2+}$ as a result of strong σ-donation of the negatively charged triazole moiety.

Compound	[a]Abs (nm) (log ε)	[a]Em (nm) (300K)	[a,b]Lifetime (τ/ns)(300K)
$[Ru(bpy)_2(pytr)]^+$ N4	470 (4.03)	660	---
$[Ru(bpy)_2(Hpytr)]^{2+}$ N4	450 (3.95)	615	---
$[Ru(bpy)_2(pytr)]+$ N2	465 (3.96)	650	145
$[Ru(bpy)_2(Hpytr)]^{2+}$ N2	437 (3.89)	620	----
$[Ru(d_8\text{-}bpy)_2(pytr)]^+$ N4	475 (4.07)	665	---
$[Ru(d_8\text{-}bpy)_2(Hpytr)]^{2+}$ N4	445 (3.80)	613	---
$[Ru(d_8\text{-}bpy)_2(pytr)]^+$ N2	468 (3.89)	654	250
$[Ru(d_8\text{-}bpy)_2(Hpytr)]^{2+}$ N2	440 (4.01)	622	----
$[Ru(bpy)_2(d_5\text{-}pytr)]^+$ N4	468 (3.99)	658	---
$[Ru(bpy)_2(d_5\text{-}Hpytr)]^{2+}$ N4	442 (3.87)	610	---
$[Ru(bpy)_2(d_5\text{-}pytr)]^+$ N2	470 (4.04)	654	142
$[Ru(bpy)_2(d_5\text{-}Hpytr)]^{2+}$ N2	441 (3.92)	614	----
$[Ru(d_8\text{-}bpy)_2(d_5\text{-}pytr)]^+$ N4	463 (3.96)	668	---
$[Ru(d_8\text{-}bpy)_2(d_5\text{-}Hpytr)]^{2+}$ N4	448 (3.87)	619	---
$[Ru(d_8\text{-}bpy)_2(d_5\text{-}pytr)]^+$ N2	472 (3.95)	652	250
$[Ru(d_8\text{-}bpy)_2(d_5\text{-}Hpytr)]^{2+}$ N2	441 (3.83)	622	----

Table 4: Absorption, emission and luminescent properties of the mononuclear complexes [a]measured in acetonitrile, [b]degassed with nitrogen. Protonation and deprotonation of the complexes were carried out with trifluoroacetic acid or diethylamine respectively. All laser measurements were carried out under nitrogen atmosphere in acetonitrile with an error of ±10%. The lifetimes which do not appear for the Hpytr complexes are too short (<20ns) to be measured with the laser system available. (N4 is isomer 1 and N2 is isomer 2).

When the complexes are protonated the coordinated ligand becomes a weaker σ-donor and a stronger π-acceptor. As a consequence, the metal dπ (t_{2g}) orbitals are stabilised and the t_{2g} – ^{3}MLCT energy gap is increased, resulting in the observed blue shift in the absorption spectrum. In all the pyridine triazole complexes the absorption maxima occurred between 435 and 470 nm. Deuteriation has no affect on the absorption maxima. The pyridine triazole complexes exhibit emission at room temperature in acetonitrile in their protonated and deprotonated forms. For the deprotonated species the emission maxima occurs at lower energy than that of the $[Ru(bpy)_3]^{2+}$. This can be explained by the strong σ-donor properties of the anionic bridging ligand, leading to increased electron density on the metal centre, and as a consequence decreasing the t_{2g} - ^{3}MLCT energy gap which in turn lowers the emission energy. The luminescent lifetime properties of these complexes will be discussed in section 3.3.5.

3.3.4.2 Absorption and emission of pyrazine triazole complexes

3.3.4.2.1 $[Ru(bpy)_2pztr]^+$

The absorption, emission (300 K), emission (77 K) and luminescent lifetime (room temperature) properties of Ru(II) pyrazine triazole complexes and their deuteriated analogues are listed in Table 5. The same spectra were observed as expected for the deuteriated and non-deuteriated complexes with respect to $[Ru(bpy)_3]^{2+}$ as a result of strong σ-donation of the negatively charged triazole moiety. When the complexes are protonated the coordinated ligand becomes a weaker σ-donor and a stronger π-acceptor. Figure 39 illustrates the shift in the absorption spectra on protonation. As a consequence, the metal dπ (t_{2g}) orbitals are stabilised and the t_{2g} –^{3}MLCT energy gap is increased, resulting in the observed blue shift in the absorption spectrum. In all the pyrazine triazole complexes the absorption maxima occurred around 450 nm.

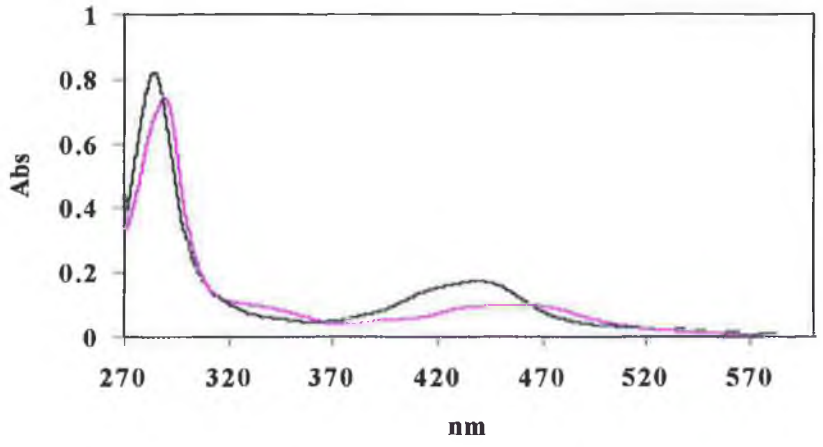

Figure 7 Absorption spectra of $[Ru(bpy)_2pztr]^+$ (pink, 460 nm) and $[Ru(bpy)_2Hpztr]^{2+}$ (blue, 440 nm) in acetonitrile.

Pyrazine triazole complexes exhibit emission at room temperature (300 K) and at low temperature (77 K) in acetonitrile in their protonated and deprotonated forms. For the deprotonated species the emission maxima occurs at lower energy than that of the $[Ru(bpy)_3]^{2+}$. This can be explained by the strong σ-donor properties of the anionic bridging ligand, leading to increased electron density on the metal centre, and as a consequence decreasing the t_{2g} - ^{3}MLCT energy gap which in turn lowers the emission energy.

At 77 K all the complexes exhibit a strong emission with vibrational structure. This vibrational fine structure is due to relaxation via bipyridine-based vibrations, [38]which is common in ruthenium polypyridyl complexes. On cooling to 77 K a blue shift is observed in the emission maxima for both the protonated and deprotonated species. This is associated with a phenomenon termed "rigidchromism" by Wrighton and coworkers who were one of the first to report on it [39]. In the alcoholic glasses formed at 77 K, the solvent dipoles are immobile on the timescale of the excited state and therefore cannot respond to the change in electronic configuration between the ground and excited state.

Compound	[a]Abs (nm) (log ε)	[a]Em (nm)(300K)	[c]Em (nm)(77 K)	[a,b]Lifetime (τ/ns)(300K)
$[Ru(bpy)_2(pztr)]^+$ N4	458 (3.99)	669	640	---
$[Ru(bpy)_2(Hpztr)]^{2+}$ N4	440 (4.14)	657	615	---
$[Ru(bpy)_2(pztr)]^+$ N2	456 (3.81)	668	640	228
$[Ru(bpy)_2(Hpztr)]^{2+}$ N2	441 (4.12)	658	620	230
$[Ru(d_8\text{-}bpy)_2(pztr)]^+$ N4	460 (3.70)	664	635	---
$[Ru(d_8\text{-}bpy)_2(Hpztr)]^{2+}$ N4	439 (3.93)	656	619	---
$[Ru(d_8\text{-}bpy)_2(pztr)]^+$ N2	455 (3.63)	661	641	283
$[Ru(d_8\text{-}bpy)_2(Hpztr)]^{2+}$ N2	440 (3.87)	654	620	230
$[Ru(bpy)_2(d_4\text{-}pztr)]^+$ N4	459 (3.96)	670	638	---
$[Ru(bpy)_2(d_4\text{-}Hpztr)]^{2+}$ N4	442 (3.85)	656	615	---
$[Ru(bpy)_2(d_4\text{-}pztr)]^+$ N2	459 (3.74)	667	643	210
$[Ru(bpy)_2(d_4\text{-}Hpztr)]^{2+}$ N2	440 (3.64)	660	619	467
$[Ru(d_8\text{-}bpy)_2(d_4\text{-}pztr)]^+$ N4	461 (4.02)	664	639	---
$[Ru(d_8\text{-}bpy)_2(d_4\text{-}Hpztr)]^{2+}$ N4	440 (3.75)	652	617	---
$[Ru(d_8\text{-}bpy)_2(d_4\text{-}pztr)]^+$ N2	455 (3.86)	667	645	290
$[Ru(d_8\text{-}bpy)_2(d_4\text{-}Hpztr)]^{2+}$ N2	437 (3.69)	653	622	480

Table 5: Absorption, emission and luminescent properties of the mononuclear complexes [a]measured in acetonitrile, [b]deaerated with nitrogen, [c]measured in 80:20 ethanol: methanol. Protonation and deprotonation of the complexes were carried out with 1 drop of dil. trifluoroacetic acid or diethylamine respectively. Laser lifetime measurements have an error of +/- 10 %.

The result is an increase in the emission energy, which is confirmed in a blue shift in the emission spectra. Another observation at low temperature is the increase in emission intensity of the complexes. This is attributed to two factors, the first being solvent dependent. At low temperature, the complex and its environment are rigid, making it less susceptible to vibronic coupling to low frequency, high amplitude Ru – N vibrations, which contribute to radiationless decay, k_{nr}.

Solvent interactions, which may contribute to k_{nr} are also considerably reduced in the frozen matrix, as too is quenching of the excited state by oxygen, since diffusion of oxygen to the excited state is restricted. The second factor is related to the ^{3}MLCT – ^{3}MC energy gap. Since this transition is thermally activated at 77 K there will be insufficient thermal energy to populate the ^{3}MC level, and as a consequence, the intensity of the emission increases. The emission maxima for the complex $[Ru(bpy)_2pztr]^+$ is in the region of 660 nm at room temperature and at 77 K 630 nm.

3.3.4.2.2 $[Ru(phen)_2pztr]^+$

The absorption, emission (300 K), emission (77 K) and luminescent lifetime (room temperature) properties of Ru(II) pyrazine triazole complexes and their deuteriated analogues containing phen are listed in Table 6.

These complexes were not previously prepared, hence a systematic characterisation was carried out in order to compare the effect of ligand substitution. As expected the protonated species is at higher energy than the deprotonated species for the same reasons as discussed previously. By replacing the bipyridyl moiety with the phen moiety, there is a change in the π-acceptor and σ-donor properties of the ligand systems, which alters the electronic and photophysical properties[30]. This is evident in the in the blue shift observed on going from the bipyridyl to the phenanthroline containing complex.

The blue shift may be attributed to the stronger σ- donor properties of phenanthroline as compared to bipyridine, which results in lower absorption and emission energies and higher metal based reduction potentials than $[Ru(bpy)_3]^{2+}$[37]. A difference in the shape of the absorption spectra from that of the bpy on substitution of the phen is observed which may be seen in Figure 30. The absorption maxima for the $[Ru(phen)_2pztr]^+$ complex is in the region of 430 nm.

Compound	[a]Abs (nm) (log ε)	[a]Em (nm) (300K)	[c]Em (nm)(77K)	[a,b]Lifetime (τ/ns)(300K)
$[Ru(phen)_2(pztr)]^+$ N4	431 (3.83)	667	602	120
$[Ru(phen)_2(Hpztr)]^{2+}$ N4	414 (3.75)	643	592	---
$[Ru(phen)_2(pztr)]^+$ N2	430 (3.68)	654	596	130
$[Ru(phen)_2(Hpztr)]^{2+}$ N2	415 (3.79)	642	582	---
$[Ru(d_8\text{-phen})_2(pztr)]^+$ N4	430 (3.58)	660	605	210
$[Ru(d_8\text{-phen})_2(Hpztr)]^{2+}$ N4	420 (3.88)	645	590	---
$[Ru(d_8\text{-phen})_2(pztr)]^+$ N2	431 (3.91)	655	600	150
$[Ru(d_8\text{-phen})_2(Hpztr)]^{2+}$ N2	416 (4.02)	640	585	---
$[Ru(phen)_2(d_5\text{-pztr})]^+$ N4	429 (3.85)	669	603	280
$[Ru(phen)_2(d_5\text{-Hpztr})]^{2+}$ N4	416 (3.92)	645	591	---
$[Ru(phen)_2(d_5\text{-pztr})]^+$ N2	431(3.80)	653	598	170
$[Ru(phen)_2(d_5\text{-Hpztr})]^{2+}$ N2	417 (3.75)	640	581	---
$[Ru(d_8\text{-phen})_2(d_5\text{-pztr})]^+$ N4	432 (3.84)	669	600	235
$[Ru(d_8\text{-phen})_2(d_5\text{-Hpztr})]^{2+}$N4	415(3.86)	642	594	---
$[Ru(d_8\text{-phen})_2(d_5\text{-pztr})]^+$ N2	432 (3.59)	651	598	210
$[Ru(d_8\text{-phen})_2(d_5\text{-Hpztr})]^{2+}$N2	418 (3.95)	640	581	---

Table 6 Absorption, emission and luminescent properties of the mononuclear complexes [a]measured in acetonitrile, [b]deaerated with nitrogen, [c]measured in 80:20 ethanol:methanol. Protonation and deprotonation of the complexes were carried out with 1 drop of dil. trifluoroacetic acid or diethylamine, respectively. Laser lifetime measurements have an error of +/- 10 %. Lifetimes were not carried out under protonated conditions as they were outside experimental error.

The emission maxima for the $[Ru(phen)_2pztr]^+$ complex is in the region of 650 nm at room temperature and 600 nm at low temperature. Factors attributing to the blue shift observed on going from bpy to phen have already been mentioned and also the circumstances under which the emission increases in energy on decreasing temperature have been discussed. Deuteriation did not show any change in the absorption or emission energies of the $[Ru(d_8\text{-phen})_2pztr]^+$ complexes. The luminescent lifetimes of the $[Ru(phen)_2pztr]^+$ complexes will be discussed in section 3.3.5.

3.3.4.2.3 $[Ru(biq)_2pztr]^+$

The absorption, emission (300 K), emission (77 K) and luminescent lifetime (room temperature) properties of Ru(II) pyrazine triazole complexes containing biq and their deuteriated analogues are listed in Table 7. Comparisons may be drawn with similar $[Ru(biq)_2L]^+$ type complexes i.e. $Ru(biq)_2X$-Mepytr (where X = 1 or 3).[39]

Biquinoline is a strong π-accepting ligand which is found to exhibit less negative reduction potentials that are (biq) based, lower absorption and emission energies, and higher metal-based oxidation potentials than $[Ru(bpy)_3]^{2+}$[40,41,42,43]. Comparing the biquinoline containing complexes to that of the phen or bpy we see a significant difference in the photophysical properties. This dark purple complex absorbs over a broad region of the spectrum, which is the desired objective of this research, as a complex which absorbs a wide range of the solar spectrum would be an ideal sensitiser for the use in efficient solar energy conversion.

The absorption spectra of this complex may be see in Figure 41. However, even though biquinoline is a strong π-acceptor it is also a weak σ-donor, less than that of bpy, which leads to diminished ligand field strength. Due to this weaker ligand field the ^3MC states are closer in energy to the ^3MLCT states and consequently such compounds tend to be photolabile. Preliminary photolysis studies showed that this complex was photolabile in acetonitrile, dichloromethane and acetone containing 0.01M LiCl, however in 100% acetone it did not appear to photodecompose.

Compound	[a]Abs (nm) (log ε)	[a]Em (nm) (300K)	[c]Em (nm) (77K)	[a,b]Lifetime (τ/ns)(300K)
$[Ru(biq)_2(pztr)]^+$ N4	584 (3.58)	787	746	190
$[Ru(biq)_2(Hpztr)]^{2+}$ N4	548 (3.79)	730	713	---
$[Ru(biq)_2(pztr)]^+$ N2	576 (4.01)	782	742	220
$[Ru(biq)_2(Hpztr)]^{2+}$ N2	550 (3.67)	746	720	---
$[Ru(d_{12}\text{-}biq)_2(pztr)]^+$ N4	582 (3.56)	793	752	210
$[Ru(d_{12}\text{-}biq)_2(Hpztr)]^{2+}$ N4	544 (3.67)	735	717	---
$[Ru(d_{12}\text{-}biq)_2(pztr)]^+$ N2	580 (3.66)	787	752	270
$[Ru(d_{12}\text{-}biq)_2(Hpztr)]^{2+}$ N2	550 (3.85)	750	725	---
$[Ru(biq)_2(d_5\text{-}pztr)]^+$ N4	590 (3.75)	790	750	260
$[Ru(biq)_2(d_5\text{-}Hpztr)]^{2+}$ N4	550 (3.83)	738	715	---
$[Ru(biq)_2(d_5\text{-}pztr)]^+$ N2	572 (3.67)	777	740	240
$[Ru(biq)_2(d_5\text{-}Hpztr)]^{2+}$ N2	546 (3.75)	740	717	---
$[Ru(d_{12}\text{-}biq)_2(d_5\text{-}pztr)]^+$N4	586 (3.58)	789	756	210
$[Ru(d_{12}\text{-}biq)_2(d_5\text{-}Hpztr)]^{2+}$N4	537 (3.65)	729	719	---
$[Ru(d_{12}\text{-}biq)_2(d_5\text{-}pztr)]^+$ N2	577 (3.76)	792	749	---
$[Ru(d_{12}\text{-}biq)_2(d_5\text{-}Hpztr)]^{2+}$ N2	542 (3.86)	747	717	---

Table 7 Absorption, emission and luminescent properties of the mononuclear complexes [a]measured in acetonitrile, [b]deaerated with nitrogen, [c]measured in 80:20 ethanol: methanol. Protonation and deprotonation of the complexes were carried out with 1 drop of dil. trifluoroacetic acid or diethylamine respectively. Laser lifetime measurements have an error of +/- 10 %. Lifetimes were not carried out under protonated conditions as they were outside experimental error.

The absorption maxima for the $[Ru(biq)_2pztr]^+$ complexes is in the region of 550 nm which is 4000 cm^{-1} lower in energy than those of the analogous $Ru(bpy)_2$ compounds.

The emission properties of the biquinoline complexes are quite low in energy. For room temperature (300 K) the emission maxima is in the region of 760 nm and the low temperature (77 K) at 720 nm shown in *Table 7*. These values are in agreement with those found for the $[Ru(biq)_2Mepytr]^+$ type complexes and are red shifted compared to the bpy and phen values due to the stronger π-accepting properties of the biq and the decrease in the ligand field strength. The luminescent lifetimes of these complexes will be looked at further in section 3.3.5.

The absorption spectra of $[Ru(bpy)_2pztr]^+$, $[Ru(phen)_2pztr]^+$ and $[Ru(biq)_2pztr]^+$ is shown in Figure 42 and this illustrates clearly the σ-donor/ π-acceptor properties of the ligands. The bpy and phen containing complexes do not differ greatly as they are good σ-donors with phen being slightly stronger σ-donor than bpy.

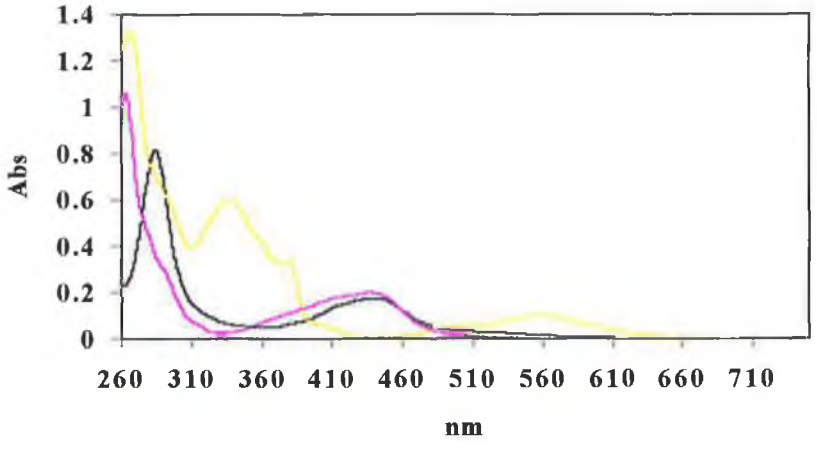

Figure 30 Absorption spectra of $[Ru(bpy)_2pztr]^+$ (blue), $[Ru(phen)_2pztr]^+$ (pink) and $[Ru(biq)_2pztr]^+$ (green).

The biq ligand is a good π-acceptor ligand and this is shown by the dramatic red shift to lower energy for both the π-π* band and the MLCT (dπ-π*) band. Shifts in the spectrum such as these observed in Figure 30 is the reason for ligand substitution in Ru(II) polypyridyl complexes in order to 'fine tune' their photophysical properties. Through ligand substitution complexes with stable photophysical properties may be

achieved and through investigating a series of complexes as portrayed in this text a suitable complex may be achieved by means of elimination.

3.3.5 Luminescence properties

In this section, the photophysical properties of a series of selectively deuteriated mixed ligand complexes will be discussed. The increase in the luminescent lifetime of $[Ru(bpy)_3]^{2+}$ upon deuteriation of the bpy ligands has been well documented, but to date no systematic study of the effect of selective deuteriation on the lifetimes of the mixed ligand ruthenium polypyridyl complexes has ever been carried out. Keyes et al.[44] previously proposed that the emission lifetime was only increased if the excited state was located on the ligand that was deuteriated.

The effect of deuteriation has contributed to the location of the excited state electron in mixed ligand systems. This increase in lifetime is related to the non-radiative relaxation of the excited state, k_{nr}. k_{nr} may be derived from the equation;

$$\tau = k_r + k_{nr}$$

where, τ is the luminescent lifetime, k_r is the radiative decay and k_{nr} the non-radiative decay.

The relationship with deuteriation and longer lifetimes is based on the phenomena of slower vibrational relaxation of the excited electron on the bipyridyl. In this situation the C-H stretch are replaced with the C-D stretch on the bipyridyls.

It has been recognised by Siebrands theory[45,46] that C-H vibrations are important promoting modes for transition and hence the deuteriation will cause a dramatic change on these transitions. Less vibrational energy is lost as the frequency of the C-D oscillations is increased, leading to a less efficient k_{nr}, which results in an increase in lifetime.

The complexes of the ligands Hpytr and Hpztr are sensitive to protonation and for this purpose the lifetimes were not carried out in a protonated medium. The lifetimes for the complex $[Ru(bpy)_2pytr]^+$ are listed in Table 4.

The use of selective deuteriation was best demonstrated for this complex as the N2 bound isomer gave an increase in lifetime when the bpy was deuteriated and when the whole complex was deuteriated. The $[Ru(bpy)_2pytr]^+$ complex gave a lifetime of 145 ns and this remained the same in the case of the $[Ru(bpy)_2d_6\text{-}pytr]^+$, hence suggesting that the excited state is not based on the $pytr^-$ ligand.

An increase in lifetime was observed for the $[Ru(d_8\text{-}bpy)_2pytr]^+$ and $[Ru(d_8\text{-}bpy)_2d_6\text{-}pytr]^+$ up to 250 ns. This increase confirms that the excited state emission is firmly based on the bpy ligands.

It was previously proposed[47] that the excited state of the $[Ru(bpy)_2pztr]^+$ complexes was bpy based, in which case a significant increase of the lifetime of the deuteriated bpy analogues should be observed. Table 5 lists the luminescent lifetimes of the $pztr^-$ complexes. The complexes $[Ru(bpy)_2pztr]^+$ and $[Ru(bpy)_2d_5\text{-}pztr]^+$ gave an emission lifetime of 220 ns, however, the complexes $[Ru(d_8\text{-}bpy)_2pztr]^+$ and $[Ru(d_8\text{-}bpy)_2d_5\text{-}pztr]^+$ gave a lifetime of 280 ns. This is an increase but not as substantial as for the $pytr^-$ containing complexes[48]. Detailed temperature dependence studies were carried out in order to rationalise this behaviour, and it was found that for the deprotonated complex $[Ru(bpy)_2pztr]^+$, in the temperature range 120-250 K, the emission is resolved into two distinct bands of intensity ratio 1:2 at 600 nm and 700 nm respectively.

This will be discussed in section 3.3.5.1. It has been proposed [13] that the presence of two closely linked excited states might account for the fact that there was no marked increase in the emission lifetime of the $[Ru(bpy)_2pztr]^+$ complex on deuteriation of the bpy as if there is an equilibrium between two triplet states based on different ligands, the deuteriation of one of these ligands is not going to have the same effect as when the excited states in question are non-coupled.

The complex $[Ru(phen)_2pztr]^+$ did not give any more insight into the excited state location. For the deprotonated N2 isomer a lifetime of 130 ns was observed which when the phen was deuteriated remained at 150 ns.

However the $[Ru(phen)_2d_5\text{-pztr}]^+$ gave an emission lifetime of only 170 ns and the fully deuteriated complex gave a lifetime of 210 ns. In order to obtain conclusive results for the $pztr^-$ containing complexes the protonated species must be studied and at various temperatures.

Table 7 lists the emission lifetimes for the complex $[Ru(biq)_2pztr]^+$ and the selectively deuteriated analogues. The deprotonated N4 isomer has a lifetime of 190 ns for the fully undeuteriated complex $[Ru(biq)_2pztr]^+$, 210 ns for the deuteriated biq complex $[Ru(d_{12}\text{-biq})_2pztr]^+$, 260 ns for the deuteriated $pztr^-$ complex $[Ru(biq)_2d_5\text{-pztr}]^+$ and 210 ns for $[Ru(d_{12}\text{-biq})_2d_5\text{-pztr}]^+$.

Again for the biq analogues we only see a slight increase in the deuteriated $pztr^-$ complex. The investigation into the photophysical properties of the Hpztr ligand has developed through means of resonance raman and the fact that selective deuteriation is not successful for the $pztr^-$ complexes suggests that temperature dependence luminescence may aid in the elucidation of the $pztr^-$ excited states. One can expect that the presence of two strongly coupled emitting states, based on different ligands, will limit the effect of partial deuteriation on the emission lifetime [48]. However, in the system reported here the limited effect of deuteriation is explained by the presence of two weakly coupled emitting states, the deactivation of one of which is not strongly influenced by vibrational coupling [13]. The photophysical properties for $pztr^-$ containing complexes are thus very unusual.

3.3.5.1 Dual emission of $pztr^-$ complexes

The following results were obtained after a temperature dependent emission study was carried out on $[Ru(bpy)_2pztr]^+$ isomers. Prior to this finding an extensive study was carried out on the luminescent lifetimes, which proved to be incoherent, hence a more in depth study was performed on the emission properties where, evidence of dual emission was detected. The results which are discussed in depth in paper 1[13], Appendix 1, show that on cooling to 90 K a typical emission is observed at 617 nm and after laser excitation at 355 nm a single exponential lifetime was obtained.

An increase in temperature to 145 K gave two distinct emission bands at 710 nm and 590 nm. The luminescent signal is not single exponential. When luminescent temperature dependence studies were carried out on the two signals, a difference was found in their lifetimes. Above 260 K shows that population of only the bipyridyl triplet manifold is observed and a single exponential decay of the emission signal is found.

Based on these results obtained, the dual emission occurs in the complex $[Ru(bpy)_2pztr]^+$ due to the similarity in energy levels of the pyrazine and bipyridyl MLCT states. It has been suggested that the highest energy emitting state between 120 and 260 K is pyrazine based. After excitation to the ^{1}MLCT level, efficient intersystem crossing to the lowest, strongly coupled bipyridyl based triplet state is observed.

The lower energy components of this manifold are weakly coupled to a pyrazine state, and population of the pyrazine state occurs thermally between 120 and 260 K. To conclude it is suggested that Ru(II) polypyridyl complexes with ligands containing pyrazine may show unusual photophysical properties due to close lying excited states.

3.3.6 Acid-base properties

Investigations into the acid-base behaviour of their $[Ru(L)_2X]^+$ (where L = bpy, phen or biq, and X = $pytr^-$ or $pztr^-$) complexes, can yield important information about their electronic properties. In ruthenium polypyridyl complexes the Ru-N bond is mainly σ in nature, but in addition it is stabilised by backbonding between the t_{2g} and π^* orbitals of the metal and ligand, respectively. Determination of the pK_a of a complex yields information about the extent of the backbonding from the metal and the σ-donor and π-acceptor properties of the ligands, while determination of the excited state pK_a, pK_a^*, offers an insight into the nature of the emitting state.

The acid-base properties of the excited state can give information about the charge redistribution, which occurs upon excitation, and furthermore, the excited state acidity can be related to the nature of the emitting state. By monitoring the spectral changes as a function of pH, titration curves were obtained from which were determined pK_a values. The pK_a values of the $Ru(bpy)_2$ type complexes of the pyridine[49,50] and pyrazine triazole were previously studied but had not been as expected so further research was carried out to confirm the results. The pK_a values of the pyridine triazole and pyrazine triazole complexes are cited in Table 8. The pK_a values were calculated for the deuteriated complexes also which only differ in the calculation of the $pK_a^*(1)$ as the luminescent lifetimes of the complexes is required to calculate the value.

The following equations were used to determine the pK_a^* of the excited state:

$$pK_a^*(1) = pH_i + \log(\tau_a/\tau_b) \qquad eqn.\ 1$$

where τ_a is the lifetime of the protonated species and τ_b is the lifetime of the deprotonated species. This equation 1 has not been incorporated into this study as the lifetime of the complexes in a protonated media was not obtained and will be examined in future studies.

The point of inflection in the emission titration curves do not represent real excited-state pK_a values, or pK_a *, because they need to be corrected for the different lifetimes of the protonated and deprotonated species[51].

An estimate of the pK_a * value can also be obtained from the ground-state pK_a values from the absorption titration and the emission energies of the protonated and deprotonated species, using the Förster equation , eqn. 2[52,53,54,55].

$$pK_a^* (2) = pK_a + 0.625(\upsilon_a - \upsilon_b) / T \quad \text{eqn. 2}$$

where υ_a and υ_b are the emission maxima of the deprotonated and protonated species respectively and T is the experimental temperature. (This equation is susceptible to error due to the stokes shifts in the emission spectra.)

$[Ru(bpy)_2pytr]^+$ and $[Ru(bpy)_2pztr]^+$

The protonation and deprotonation of the pyridine-triazole and pyrazine-triazole ligands alters their σ-donor and π-acceptor properties. The emission properties of the $[Ru(bpy)_2pztr]^+$ complexes are listed in Table 5. The excited state acidity has been investigated by a study of the pH dependence of the emitting properties of the compounds. The emission titrations were carried out by excitation into the appropriate isosbestic point. By investigating the acid-base behaviour of this type of ruthenium compound important information about their electronic properties can be obtained. The ground state behaviour tends to be a measure of the amount of electron donation from the ligand to the metal, while the excited state measurements can give information about the nature of the emitting state. Upon coordination to ruthenium, the acidity of the triazole proton in the ground state increases considerably, which is generally explained by σ donation from the ligand to the metal centre. As N2 isomer is considerably more acidic than the N4 isomer, the coordination site of N2 appears to be a better σ donor.

Compound	PK_a (G.S.)	PH_i (Ex.S)	PK_a*(2)
$[Ru(bpy)_2pytr]^{2+}N4$	5.95	4.22	6.04
$[Ru(bpy)_2pytr]^{2+}N2$	4.07	2.12	4.13
$[Ru(d_8\text{-}bpy)_2pytr]^{2+}N4$	6.0	4.2	6.09
$[Ru(d_8\text{-}bpy)_2pytr]^{2+}N2$	4.1	2.2	4.16
$[Ru(bpy)_2d_5\text{-}pytr]^{2+}N4$	6.0	4.2	6.09
$[Ru(bpy)_2d_5\text{-}pytr]^{2+}N2$	4.09	2.12	4.15
$[Ru(bpy)_2pztr]^{+}N4$	5.2	2.5	5.22
$[Ru(bpy)_2pztr]^{+}N2$	3.7	2.0	3.52
$[Ru(d_8\text{-}bpy)_2pztr]^{+}N4$	5.3	2.5	5.31
$[Ru(d_8\text{-}bpy)_2pztr]^{+}N2$	3.6	2.0	3.61
$[Ru(d_8\text{-}bpy)_2d_4\text{-}pztr]^{+}N4$	5.25	2.6	5.26
$[Ru(d_8\text{-}bpy)_2d_4\text{-}pztr]^{+}N2$	3.55	1.9	3.51

Table 8 Ground state pK_a, excited state pH_i and corrected pK_a* values, carried out in Britton Robinson buffer with conc. NaOH and conc. H_2SO_4.

The difference between the ground state and the excited state pK_a values of the $[Ru(bpy)_2pztr]^+$ complexes is in all cases very small. This observation suggests that the deprotonation of the $pztr^-$ ligand does not participate in the emission process. However, this is not true in this case and can not be clearly stated whether or not the $pztr^-$ ligand is the emitting state as more recent studies[48] have shown that the emission appears to come from two strongly coupled emitting states, based on different ligands. Hence the location of the emitting state is not as straightforward as hoped, as the photophysical properties of the complex are quite complicated.

$[Ru(phen)_2pztr]^+$ and $[Ru(biq)_2pztr]^+$

The pK_a titration results for the ground and excited state properties of $[Ru(phen)_2pztr]^+$ and $[Ru(biq)_2pztr]^+$ are listed in Table 9. The phenanthroline containing complexes reveal that the pK_a of the excited state is more acidic than that of the ground state pK_a. The only result that may be suggested for the pK_a titrations is that there is a similar behaviour for the bpy, phen and biq containing complexes as for each complex the excited state pK_a is more acidic than the ground state. The ground state pK_a titration of $[Ru(biq)_2pztr]^+$ is shown in Figure 43.

The magnitude of the acidity of the complex varies between each complex and this may be attributed to the greater σ-donor properties of the bpy and phen containing complexes compared to that of the biq. Based on the pK_a results of the $[Ru(bpy)_2pztr]^+$ and $[Ru(phen)_2pztr]^+$ it is suggested that the $pztr^-$ ligand acts as a spectator ligand and does not actively participate in the emission processes. After excitation of the ruthenium polypyridyl complex, an electron is promoted from the metal to the bpy ligand. This results in a ruthenium centre with a formal valence of 3+, with a consequent increase in σ-donation from the triazole ligand to the metal ion. This causes a higher acidity for the ligand when the complex is excited. Formation of the complex $[Ru(biq)_2pztr]^+$ causes an electron flow from the triazole ligand to the ruthenium centre, yielding a lowering of the pK_a value of the Hpztr ligand.

Compound	PK_a (G.S.)	pH_i (Ex.S.)	PK_a*(2)
$[Ru(phen)_2pztr]^+N4$	5.00	2.30	5.05
$[Ru(phen)_2pztr]^+N2$	3.50	1.80	3.52
$[Ru(d_8\text{-phen})_2pztr]^+N4$	5.10	2.35	5.05
$[Ru(d_8\text{-phen})_2pztr]^+N2$	3.45	1.82	3.52
$[Ru(phen)_2d_5\text{-pztr}]^+N4$	5.05	2.30	5.05
$[Ru(phen)_2d_5\text{-pztr}]^+N2$	3.51	1.90	3.52
$[Ru(biq)_2pztr]^+N4$	3.70	3.10	3.92
$[Ru(biq)_2pztr]^+N2$	3.60	2.00	3.67
$[Ru(d_{12}\text{-biq})_2pztr]^+N4$	3.81	3.20	3.92
$[Ru(d_{12}\text{-biq})_2pztr]^+N2$	3.60	2.00	3.67
$[Ru(biq)_2d_5\text{-pztr}]^+N4$	3.80	3.20	3.92
$[Ru(biq)_2d_5\text{-pztr}]^+N2$	3.60	2.00	3.67

Table 9 Ground state and excited state acid- base properties, carried out in Britton Robinson buffer with conc. NaOH and conc. H_2SO_4.

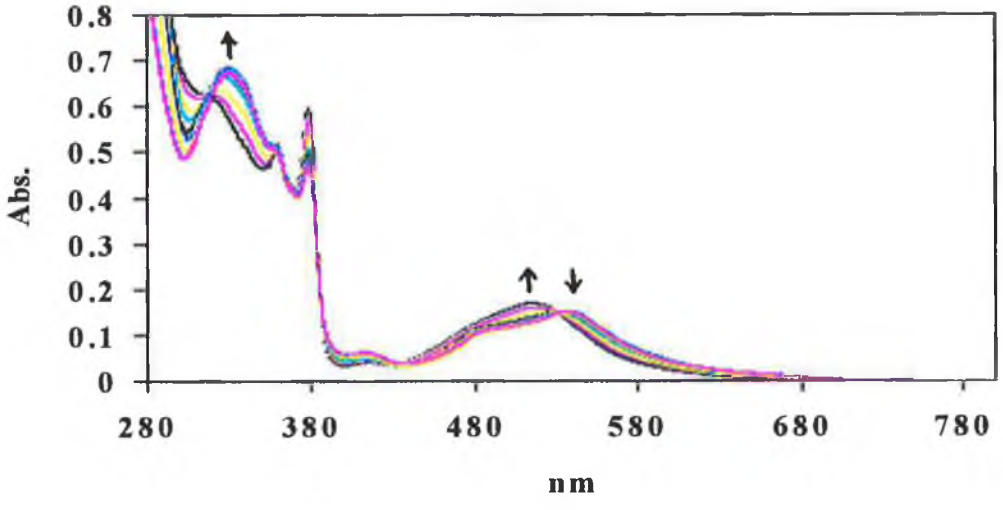

Figure 31 Absorption acid-base titration of $[Ru(biq)_2pztr]^+$ N4-isomer. Measurements carried out in the pH range 1 to 7.

Since biq is a stronger π-acceptor and a weaker σ-donor ligand than bpy, less electron density is present at the ruthenium centre for the $Ru(biq)_2$ system than for the $Ru(bpy)_2$ moiety, leading to an increase of electron donation from $pztr^-$ to the Ru(II) for the $[Ru(biq)_2pztr]^+$ complex. Figure 31 illustrates the ground state pK_a titration of the complex $[Ru(biq)_2pztr]^+$ for N4-isomer.

3.3.7 Electrochemical properties

A number of investigations have been carried out on mono- and polynuclear complexes containing polypyridine-type ligands from which it is well established that oxidation and reduction processes are metal centred and ligand-centred, respectively[1].

Compound	Ru(II/III)oxid.(V) (V vs S.C.E)	Ligand based red.(V) (V vs S.C.E)	
$[Ru(bpy)_2(pztr)]^+$ N4	1.10	-1.43	-1.66
$[Ru(bpy)_2(Hpztr)]^{2+}$ N4	1.30	-1.4	-1.51
$[Ru(bpy)_2(pztr)]+$ N2	1.01	-1.44	-1.67
$[Ru(bpy)_2(Hpztr)]^{2+}$ N2	1.25	-1.21	-1.55
$[Ru(d_8\text{-bpy})_2(pztr)]^+$ N4	1.00	-1.42	-1.67
$[Ru(d_8\text{-bpy})_2(Hpztr)]^{2+}$ N4	1.31	-1.39	-1.50
$[Ru(d_8\text{-bpy})_2(pztr)]^+$ N2	1.10	-1.45	-1.68
$[Ru(d_8\text{-bpy})_2(Hpztr)]^{2+}$ N2	1.25	-1.20	-1.54
$[Ru(d_8\text{-bpy})_2(d_4\text{-pztr})]^+$ N4	1.00	-1.44	-1.68
$[Ru(d_8\text{-bpy})_2(d_4\text{-Hpztr})]^{2+}$ N4	1.32	-1.41	-1.51
$[Ru(d_8\text{-bpy})_2(d_4\text{-pztr})]^+$ N2	1.10	-1.43	-1.69
$[Ru(d_8\text{-bpy})_2(d_4\text{-Hpztr})]^{2+}$ N2	1.25	-1.22	-1.56

Table 10 Electrochemical data of the Ru(II) complexes obtained in acetonitrile containing 0.1M TEAP. Values obtained by Cyclic Voltammetry. Potentials in Volts versus SCE. Protonation occurred via addition of 1 drop of $HClO_4$. Scanrate of 0.1 V/ sec.

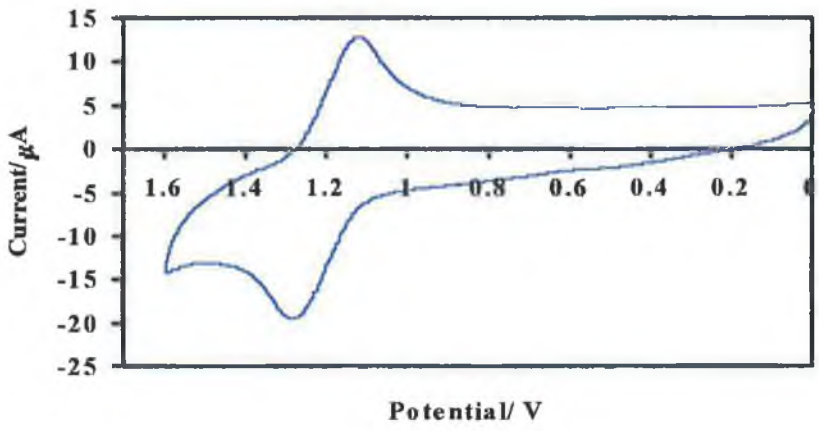

Figure 8 Cyclic voltammogram of the oxidation of [Ru(bpy)$_2$pztr]$^+$ N4-isomer in 0.1 M TEAP in acetonitrile with a scan rate of 100 mV/ sec. Scanrate of 0.1 V/ sec.

The oxidation and reduction potentials for $[Ru(bpy)_2pztr]^+$, $[Ru(phen)_2pztr]^+$ and $[Ru(biq)_2pztr]^+$ are given in Table 10, Table 11 and Table 12 respectively. All values have been corrected using the redox potential of ferrocene under the same experimental conditions as a secondary reference. Its potential was taken to be +0.38 V vs SCE.The anodic region of the cyclic voltammogram Figure 46 features reversible metal-centred oxidation, while the cathodic region is poorly defined waves resulting from the reduction of the coordinated polypyridyl ligands. The oxidation potentials are significantly lower than that of $[Ru(bpy)_3]^{2+}$ ($E_{1/2}$ = 1.26 V vs SCE) for the $[Ru(L)_2pztr]^+$ complexes(where L = bpy, or phen) which may be seen in Table 10 and Table 11, which indicates that pyrazine-triazole is a stronger σ-donor ligand than bpy or phen. On protonation of the complexes the bpy and phen complexes show an anodic shift of between 200 and 300 mV compared to the deprotonated species. Since in its protonated form the coordinated ligand is a better π-acceptor and weaker σ-donor, this results in a decrease in electron density at the metal centre which then becomes more difficult to oxidise. The oxidation potentials of the N2-bound, N2-isomer are slightly lower than those of the N4 bound, N4-isomer shown in Table 10. electrochemical properties of the complexes.

Compound	Ru(II/III)oxid.(V) (V vs S.C.E)	Ligandbased red.(V) (V vs S.C.E)
$[Ru(phen)_2(pztr)]^+$ N4	0.94	-1.4
$[Ru(phen)_2(Hpztr)]^{2+}$ N4	0.86	---
$[Ru(phen)_2(pztr)]+$ N2	0.87	-1.5
$[Ru(phen)_2(Hpztr)]^{2+}$ N2	0.82	—
$[Ru(d_8\text{-phen})_2(pztr)]^+$ N4	0.92	-1.35
$[Ru(d_8\text{-phen})_2(Hpztr)]^{2+}$ N4	0.84	---
$[Ru(d_8\text{-phen})_2(pztr)]^+$ N2	0.85	-1.4
$[Ru(d_8\text{-phen})_2(Hpztr)]^{2+}$ N2	0.81	---

Table 11 Electrochemical data of the Ru(II) complexes obtained in acetonitrile containing 0.1M TEAP. Values obtained by Cyclic Voltammetry. Potentials in Volts versus SCE. Protonation occurred via addition of 1 drop of $HClO_4$. Scanrate of 0.1 V/sec.

This may be assigned to the stronger σ-donor properties of the N2 site, which leads to a higher electron density on the metal centre and, therefore, a lower oxidation potential[1]. As it may be observed in Table 10 the deuteriation of the ligands has no effect on the electrochemical properties of the complexes. The σ-donor properties of the phenanthroline ligand are not very different from that of the bipyridyl ligand and this is reflected in the oxidation potentials of the $[Ru(phen)_2pztr]^+$ complexes listed in Table 11. Due to the difficulty observed in obtaining satisfactory reduction potentials in acidic solutions, such as adsorption on the electrode surface, no clear reduction waves could be produced. The N2 isomer again is oxidised more readily compared to that of the N4 isomer due to the greater σ-donor strength of the N2 site.

Compound	Ru(II/III)oxid.(V) (V vs S.C.E)	Ligand based red.(V) (V vs S.C.E)
$[Ru(biq)_2(pztr)]^+$ N4	1.04	-1.05, -1.39
$[Ru(biq)_2(Hpztr)]^{2+}$ N4	1.29	-1.10, -1.39
$[Ru(biq)_2(pztr)]+$ N2	1.02	-1.23, -1.40
$[Ru(biq)_2(Hpztr)]^{2+}$ N2	0.75	---
$[Ru(d_{12}\text{-}biq)_2(pztr)]^+$ N4	1.03	-1.06, -1.38
$[Ru(d_{12}\text{-}biq)_2(Hpztr)]^{2+}$ N4	1.25	-1.09, -1.37
$[Ru(d_{12}\text{-}biq)_2(pztr)]^+$ N2	1.01	-1.25, -1.41
$[Ru(d_{12}\text{-}biq)_2(Hpztr)]^{2+}$ N2	0.78	---

Table 12 Electrochemical data of the Ru(II) complexes obtained in acetonitrile containing 0.1M TEAP. Values obtained by Cyclic Voltammetry. Potentials in Volts versus SCE. Protonation occurred via addition of 1 drop of $HClO_4$. c

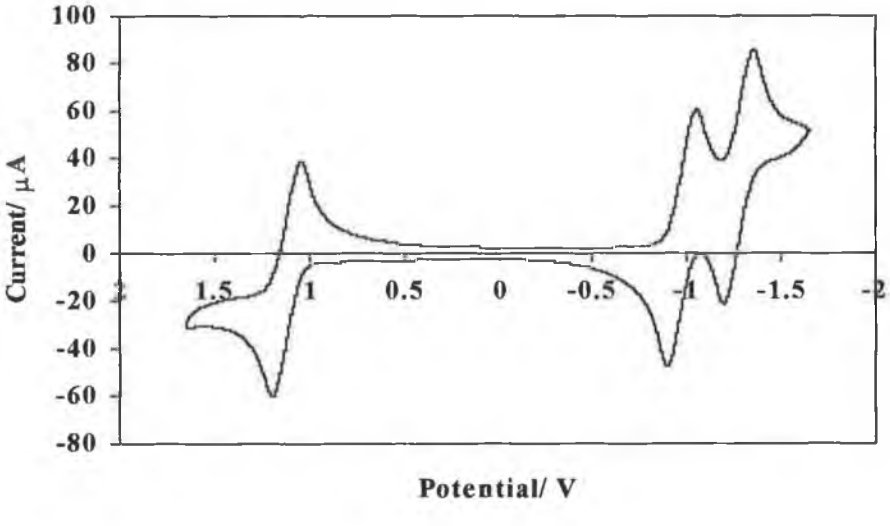

Figure 9 Cyclic voltammogram of the oxidation of $[Ru(biq)_2pztr]^+$ N2-isomer in 0.1 M TEAP in acetonitrile with a scan rate of 100 mV/ sec. Scanrate of 0.1 V/ sec.

The $[Ru(biq)_2pztr]^+$ complexes are listed in Table 12. All complexes exhibit reversible oxidation and reduction processes as deduced from the cyclic voltammogram in Figure 33. In general the oxidation potentials of the $[Ru(biq)_2pztr]^+$ complexes are 100 mV higher than those of the analogous $Ru(bpy)_2$ complexes. The σ-donor properties of biq are significantly weaker than those of bpy or phen, leading to a raise of the oxidation potential i.e. stabilisation of the dπ orbitals. The N2 isomer is also easier to oxidise than the N4 for the biq containing complexes. In general the biq containing $pztr^-$ complexes are more difficult to oxidise and reduce compared to the bpy and phen analogues due to the weaker σ-donor strength of the biq ligand. This effect has also been observed for the electronic properties of the complex.

3.3.8 X- Ray Crystallography of $[Ru(bpy)_2pztr]^{2+}$ Isomer 2-N2 bound

The crystal of $[Ru(bpy)_2pztr]^{2+}$ N2-isomer was obtained after the separation of the mononuclear isomers on a neutral alumina column. On isolation of the isomers they were subsequently recrystallised in acetone: water (2:1). The physical structure of the isomers is of utmost importance to clarify the coordination sites of the ligand Hpztr.

The following data, Figure 48 collected by Dr. J.G Gallagher, Dublin City University, is related to the complex which has been identified as $[Ru(bpy)_2pztr]^+$ N2-isomer from its retention time and ^1H NMR spectra. The following data gathered have illustrated that the coordination site is N2 of the triazole ring to the pyrazine ring for N2-isomer which confirms ^1H NMR predictions. It seems to hydrogen bond between each unit cell, which may be seen in Appendix 1, which also includes relevant data. Each unit cell was inter linked with $[PF_6]_{3/2}$ salt units which was in agreement with the C, H, N analysis. From the data it can be seen that the crystal is orthorhombic, space group B2cb, a = 17.4944(13) Å, b = 17.5143(15) Å, c = 19.5605(20) Å, $\alpha = 90^0$, $B = 90^0$, $\lambda = 90^0$, V = 5993.4(9) $Å^3$.

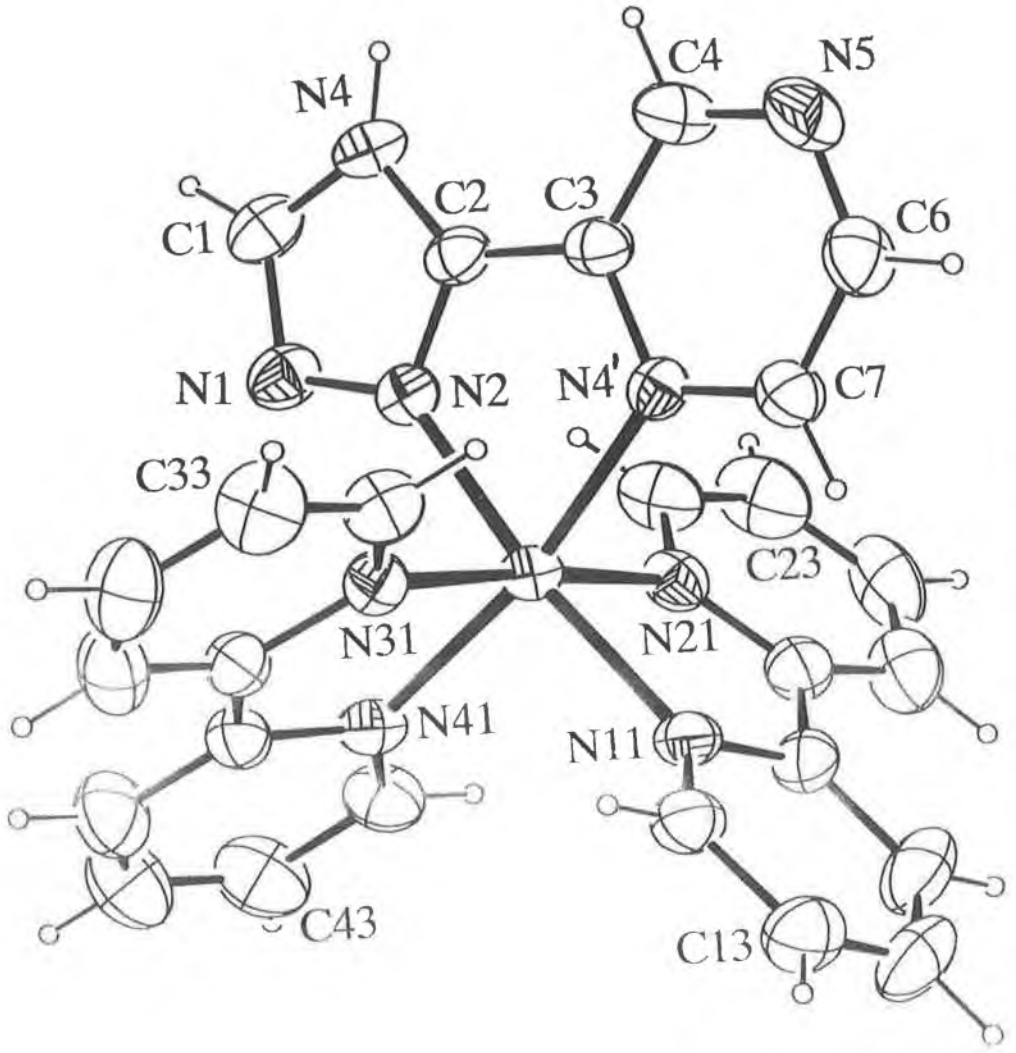

Figure 34 X-Ray Crystal structure of $[Ru(bpy)_2pztr]^{2+}$ N2 bound.

Bond length(Å)	$[Ru(bpy)_2pztr]^{2+}$ N2(Å)	$[Ru(bpy)_23Mepytr]^{+}$ N2(Å)
Ru – N(2)	2.023(4)	2.050(5)
C(5) – C(52)	1.440(7)	1.456(8)
N1 – N2	1.368(6)	1.374(6)
C2 – N4	1.346(6)	1.334(7)
N1 – C1	1.331(7)	1.317(7)

Table 13 Selected bond lengths of $[Ru(bpy)_2pztr]^{2+}$ N2 bound and $[Ru(bpy)_23Mepytr]^{+}$ N2 bound.

The structure of $[Ru(bpy)_2pztr]^{2+}$ N2 bound can be compared with the bond angles and lengths obtained for bis(2,2'-bipyridine)[3-methyl-5-(pyridin-2-yl)-1,2,4-triazole] ruthenium hexafluorophosphate tetrahydrate crystal structure [1].

Bond angles(^{0})	$[Ru(bpy)_2pztr]^{2+}$ N2(^{0})	$[Ru(bpy)_23Mepytr]^{+}$ N2(^{0})
N2 – Ru –N4'	78.2(2)	78.0(2)
N4' – Ru – N21	88.6(2)	90.9(2)
N41 – Ru – N21	97.4(2)	90.5(2)
N2 – Ru – N41	92.6(2)	87.4(2)
N41 – Ru – N31	79.0(2)	79.4(2)

Table 14 Selected bond angles of $[Ru(bpy)_2pztr]^{2+}$ N2 bound and $[Ru(bpy)_23Mepytr]^{+}$ N2 bound.

In Table 13 a direct comparison of the bond lengths of both crystals are shown. Each contains a 1,2,4- triazole ring linked to an aromatic ring i.e. pyridine or pyrazine so similarities should appear in the bond lengths and bond angles. Figure 35 illustrates the hydrogen bonding of the $[Ru(bpy)_2pztr]^{+}$, which reveals that there is evidence of intramolecular hydrogen bonding via the N4 sites of the triazole ring.

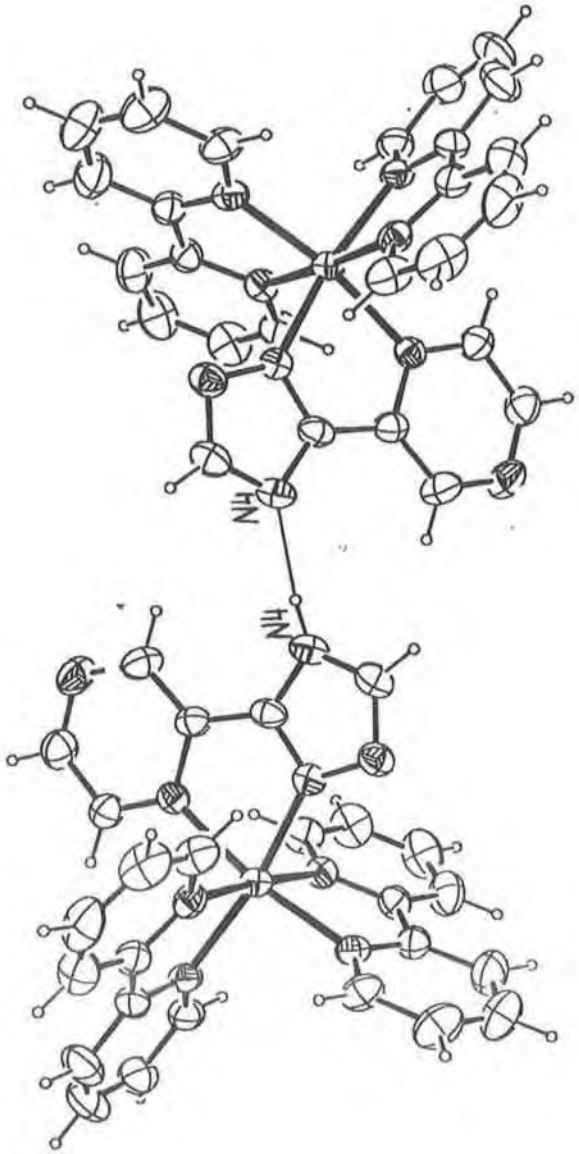

Figure 35 X-Ray Crystal structure of $[Ru(bpy)_2pztr]^{2+}$ N2 bound showing Hydrogen bonding.

This hydrogen bonding results in the presence of $[PF_6]_{3/2}$ for each complex in the CHN analysis as the complexes share a proton between them via the N4 site of the triazole. Refer to Appendix 4 for complete set of crystal data.

3.4 References

1 R. Hage, Ph. D. Thesis, Leiden University, The Netherlands, **1991**.

2 H.P. Hughes, Ph. D. Thesis, Dublin City University, Ireland, **1993**.

3 B. Buchanan, E. Mc Govern, P. Harkin and J.G Vos, Inorg. Chim. Acta., **1988**,*154*, 1.

4 B. Buchanan, R. Wang, J.G. Vos, R. Hage, J.G. Haasnoot and J. Reedijk, Inorg. Chem., **1990**, *29*, 3263 .

5 R. Hage, J. Haasnoot, D. Stufkens, T. Snoeck, J.G. Vos and J. Reedijk, Inorg. Chem., **1989**, *28*, 1413.

6 B. Buchanan, J.G. Vos, M. Kaneko, W. van der Putten, J. Kelly, R. Hage, R. de Graaf, R. Prins, J. Haasnoot and J. Reedijk, J. Chem. Soc., Dalton Trans., **1990**, 2425.

7 B. Buchanan, H. Hughes, J. van Diemen, R. Hage, J. Haasnoot, J. Reedijk and J.G. Vos, J. Chem. Soc., Chem. Comm., **1991**, 300.

8 B. Buchanan, P. Degn, J. Velasco, H. Hughes, B. Creaven, C. Long, J. G. Vos, R. Howie, R. Hage, J. van Diemen, J. Haasnoot and J. Reedijk, J. Chem. Soc., Dalton Trans., **1992**, 1177.

9 R. Wang, J.G. Vos, R. Schmehl and R. Hage, J. Am. Chem. Soc., **1992**, *114*, 1964.

10 R. Hage, R. Prins, J. Haasnoot, J. Reedijk and J. G. Vos, J. Chem. Soc., Dalton Trans., **1987**, 1389.

11 R. Hage, J. Haasnoot, H. Nieuwenhuis, J. Reedijk, R. Wang and J.G. Vos, J. Chem. Soc., Dalton Trans., **1991**, 3271.

12 R. Hage, H. Lempers, J. Haasnoot, J. Reedijk, F. Weldon and J.G. Vos, Inorg. Chem., **1997**, *36*, 3139.

13 T. Keyes, C.M. O'Connor, J.G. Vos, Chem. Comm., **1998**, 889.

14 T. Keyes, J.G. Vos, J. Kolnaar, J. Haasnoot, J. Reedijk and R. Hage, Inorg. Chim. Acta., **1996**, *245*, 237.

15 B.P. Sullivan, D.J. Salmon and T.J. Meyer, Inorg. Chem., **1978**, *17*, 3334.

16 R. Hage, A. Dijkhuis, J. Haasnoot, R. Prins, J. Reedijk, B. Buchanan and J.G. Vos, Inorg. Chem., **1988**, *27*, 2185.

17 E. Riesgo, A. Credi, L. De Cola, and R. Thummel, Inorg. Chem., **1998**, *37*, 2145.

18 B. Patterson and F. Keene, Inorg. Chem., **1998**, *37*, 645.

19 N. Fletcher and F. Keene, J. Chem. Soc., Dalton Trans., **1998**, 2293.

20 P. Belser, S. Bernhard, E. Jandrasics, A. von Zelewsky, L. De Cola and V. Balzani, Coord. Chem. Rev., **1997**, *159*, 1.

21 S. Campagna, S. Serroni, S. Bodige and F. Mac Donnell, Inorg. Chem., **1999**, *38*, 692.

22 F. Gasparrini, D. Misiti, C.M. O'Connor, J.G. Vos and C. Villani, awaiting acceptance.

23 F. Gasparrini, D. Misiti, W. Still, C. Villani and H. Wennemers, J. Org. Chem., **1997**, *62*, 8221.

24 F. Gasparrini, D. Misiti, M. Pierini and C. Villani, Tetrahedron; Asymmetry, **1997**, *8*, 12, 2069.

25 H. Nieuwenhuis, J. Haasnoot, R. Hage, J. Reedijk, T. Snoeck, D. Stufkens and J. G. Vos, Inorg. Chem., **1991**, *30*, 48.

26 P. J. Steel and E.C. Constable, J. Chem. Soc., Dalton Trans., **1990**, 1389.

27 E. Constable, R. Henney, T. Leese and D. Tocher, J. Chem. Soc., Dalton Trans., **1990**, 443.

28 C. Cathey, E. Constable, M. Hannon, D. Tocher and M. Ward, J. Chem. Soc., Chem. Comm., **1990**, 621.

29 E. Carraway, J. Demas, B. de Graff and J. Bacon, Anal. Chem., **1991**, *63*, 337.

30 A. Juris, V. Balzani, F. Barigelletti, S. Campagna, P. Belser and A. von Zelewsky, Coord. Chem. Rev., **1988**, *84*, 85.

31 R. Echols and G. Levy, J. Org. Chem., **1974**, *39*, 9, 1321.

32 M. Shapiro, M. Kolpak and T. Lemke, J. Org. Chem., **1984**, *49*, 187.

33 J. O'Brien, T.B Mc Murry and C. O'Callaghan, J. Chem. Research, (S), **1998**, 448.

34 W. von Philipsborn, Chem. Soc. Rev., **1999**, *38*, 973.

35 Y. Chen, F. Lin and R. Shepherd, Inorg. Chem., **1999**, *28*, 973.

36 S. Gaemers, J. van Slageren, C.M. O' Connor, J.G. Vos, R. Hage and C.J. Elsevier, awaiting acceptance.

37 R.S. Lumpkin, E.M. Kober, L.Worl, Z. Murtaza and T.J. Meyer, J. Phys. Chem., **1990**, *94*, 239.

38 M. Wrighton and D.L.Morse, J.Am.Chem.Soc., **1974**, *96*, 996.

39 T. Keyes, J.G. Vos, J. Kolnaar, J.G. Haasnoot, J. Reedijk and R. Hage, Inorg. Chim. Acta., **1996**, *245*, 237.

40 S.D Ernst and W. Kaim, Inorg. Chem., **1989**, *28*, 1520.

41 F. Barigelletti, A.Juris, V. Balzani, P. Belser and A. von Zelewsky, Inorg. Chem., **1987**, *26*, 4115.

42 A. Juris, S. Campagna, V. Balzani, G. Gremaud and A.von Zelewsky, Inorg. Chem., **1988**, *27*, 3652.

43 V. Balzani, F. Barigelletti and L. De Cola, Top. Current Chem., **1990**, *158*, 31.

44 T.E. Keyes, F. Weldon, E. Muller, P. Pechy, M. Gratzel and J.G. Vos, J. Chem. Soc., Dalton Trans., **1995**, *16*, 2705.

45 W.J. Siebrand, J. Chem. Phys., **1967**, *46*, 440.

46 W.J. Siebrand, J. Chem. Phys., **1971**, *55*, 5843.

47 W. Humbs, H. Yersin, Inorg. Chim. Acta., **1997**, *265*, 139.

48 T. Keyes, C.M. O'Connor, U. O'Dwyer, C.G. Coates, P. Callaghan, J. Mc Garvey and J.G. Vos, awaiting acceptance.

49 R. Wang, J.G. Vos, R.H. Schmehl and R. Hage, J. Am. Chem. Soc., **1992**, *114*, 1964.

50 B. Buchanan, J.G. Vos, M. Kaneko, W. Van Putten, J. Kelly, R. Hage, R. de Graff, R. Prins, J. Haasnoot and J. Reedijk, J. Chem. Soc., Dalton Trans, **1990**, 2425.

51 M.K. Nazeeruddin and K. Kalyanasundaram, Inorg. Chem., **1989**, *28*, 4251.

52 T. Forster, Nature, **1989**, *36*, 186.

53 J.F. Ireland and P. Wyatt, Adv. Phys. Org. Chem., **1976**, *12*, 131.

54 N. Lasser and J. Feitelson, J. Phys. Chem., **1973**, *77*, (8), 1011.

55 J.J. Aaron and J.D. Winefordner, Photochem. and Photobiol., **1973**, *18*, 97.

Chapter 4

THE SYNTHESIS AND CHARACTERISATION OF RU(II) MONONUCLEAR COMPLEXES CONTAINING 3-(PYRIDINE-2-YL)-5- (PYRAZINE-2-YL)-1,2,4-TRIAZOLE (HPPT).

4.1 INTRODUCTION

Supermolecules have attracted much interest due to their potential use in artificial photosynthesis processes and also in areas such as molecular electronics[1,2,3,4,5]. Molecular devices are often based on metal-containing building blocks that exhibit suitable ground and excited state properties, and bridging ligands capable of linking the building blocks to form the appropriate supramolecular structures. A large problem associated with the use of Ru(II)polypyridyl complexes as photomolecular devices is their photostability due to population of low-lying ^{3}MC excited states[6,7,8]. In order to isolate the ^{3}MC state (the deactivating state) from the ^{3}MLCT excited state (the state responsible for luminescence), it is necessary to increase the energy-gap between these two states as much as possible[9,10,11,12]. A ligand capable of increasing this energy gap is strived for, hence a series of ligands and their mono- and dinuclear complexes are prepared to ascertain the perturbation of their effects on the energy gap.

It is hoped by combining the strong σ-donor pyridyltriazole ring and the strong π-accepting pyrazine ring in this ligand that the ^{3}MC state will be perturbed enough that its population will be prevented. The ^{3}MC energy level tends to be increased when strong σ-donating ligands are involved, but destabilisation of the t_{2g} energy level may occur due to the possible decrease of the t_{2g}-^{3}MLCT energy gap[13,14,15]. Ligands such as these do not get directly involved in the emission process and are referred to as a spectator ligand. Good π-accepting ligands may also serve to enlarge the ^{3}MLCT-^{3}MC energy gap, but decrease of the t_{2g}-^{3}MLCT energy gap is possible[16,17,18]. These ligands are expected to be directly involved in the electrochemical and emission processes by lowering the energy of the ^{3}MLCT level. The location of the excited state in this study is facilitated through the use of deuteriated bipyridyl moieties of the complexes.

In 1988 Hage et al reported the synthesis and characterisation of the Hbpt ligand (3,5-bis (pyridin-2-yl)-1,2,4-triazole)[19]. Purification of these pyridyl-triazole type complexes commenced on semi-preparative hplc in order to isolate the coordination isomers[20]. Protonation of the bpt$^-$ complex leads to a shift of higher energy for the lowest MLCT band. Similar behaviour was previously observed for a series of compounds containing imidazole, pyrazole and 1,2,4-triazole moieties and is explained by the increased σ-donor capacity of the deprotonated ligand[21]. The bpt$^-$ monomer is a greater σ-donor than the pyridyl-triazole complexes, which has been deemed due to the presence of the extra pyridine ring.

Studies of the anionic bridging ligand (bpt$^-$) have revealed that the two nitrogen atoms of the triazole ring have quite different σ-donor properties and are therefore inequivalent and also that interaction between the two metal centres is very efficient[19,22,23,24]. On the basis of this observation it was postulated that in dinuclear complexes of $[Ru(L_2)bptRu(L_2)]^{3+}$, the emitting state is located on the ruthenium centre bound to the N1 site of the triazole ring, while photosubstitution occurs at the N4 site of the bridging ligand [25]. Further investigations were pursued using mixed ligand bpy/ phen dinuclear complexes, where it was found that the emitting state was bpy based. The results also indicated that the nature of the emitting charge transfer states is solely determined by the nature of the polypyridyl ligand, but that on the other hand, the location of the first metal based oxidation is controlled by the asymmetry of the bpt$^-$ ligand. Photochemical experiments in MeCN suggested strongly that the ^{3}MC level of the ruthenium unit at the N4 triazole atom is lowest in energy[26].

In contrast with the Hbpt ligand studies, the studies into the ligand Hbpzt (3,5-bis(pyrazin-2-yl)-1,2,4-triazole) revealed that on complexation of the dinuclear species there was direct evidence for electron localisation within the reduced $bpzt^-$ bridging ligand. The $bpzt^-$ mononuclear complexes shows perturbations of the electronic environment which is effected by either protonation of the $bpzt^-$ ligand or the addition of a second Ru(II) centre, resulting in a switch of the ligand on which the LUMO is based. As for the asymmetry reported in the electronic nature of the bpt^- ligand[27,28], the $bpzt^-$ ligand shows charge polarisation toward one pyrazine of the reduced bpzt bridge in the ^{3}MLCT state of the dinuclear complexes[29,30].

In this chapter, the synthesis, characterisation, photochemical and photophysical properties of a series of mononuclear Ru(II)polypyridyl complexes and their deuteriated analogues containing 3-(pyrazin-2-yl)-5-(pyridin-2-yl)-1,2,4-triazole (Hppt) Figure 1 are prepared.

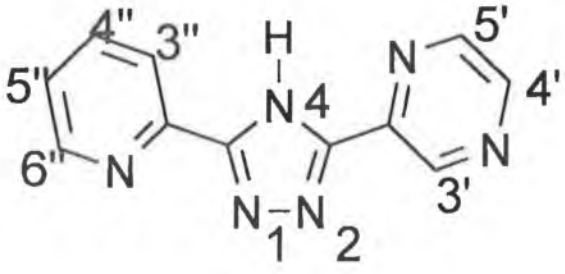

Figure 1 Structure of 3-(pyrazin-2-yl)-5-(pyridin-2-yl)-1,2,4-triazole (Hppt)

It is of interest to examine the effect of increasing the asymmetry in this ligand due to the two, very different coordination sites i.e. one pyrazine based, one pyridine based as this will greatly influence the photophysical properties.

There are a potential four binding sites on the Hppt ligand in Figure 1 for a $Ru(bpy)_2$ moiety to coordinate to, hence the four isomers possible are:

- N1 of triazole and N of pyridine ring (Isomer 1)
- N4 of triazole and N of pyridine ring
- N2 of triazole and N of pyrazine ring (Isomer 2)
- N4 of triazole and N of pyrazine ring

The synthesis of the mononuclear complex yields four isomers, two of which are more prominent and are later shown to be the N1 and N2 bound isomers, denoted isomer 1 and isomer 2 above. The N4 isomer of both the pyridine and pyrazine coordination sites of the ppt$^-$ ligand are visible on hplc as a shoulder of the N1 and N2 peaks and are removed during purification. The isomers are isolated to create dinuclear species, in the following chapter the isolated isomers will be "complexes used as ligands" to form the dinuclear species the indirect route.

The direct route for the synthesis of the dinuclear complexes yields two isomers, which are inseparable due to the close similarities of their properties. In order to investigate the properties of the ppt$^-$ dinuclear complexes, the purified monomers are reacted with a second moiety of $Ru(bpy)_2$, which is known as the indirect method . This will be discussed further in chapter 5. It is envisaged that due to the asymmetry of the ligand Hppt that vectorial electron or energy transfer may be controlled and mediated via this bridging ligand.

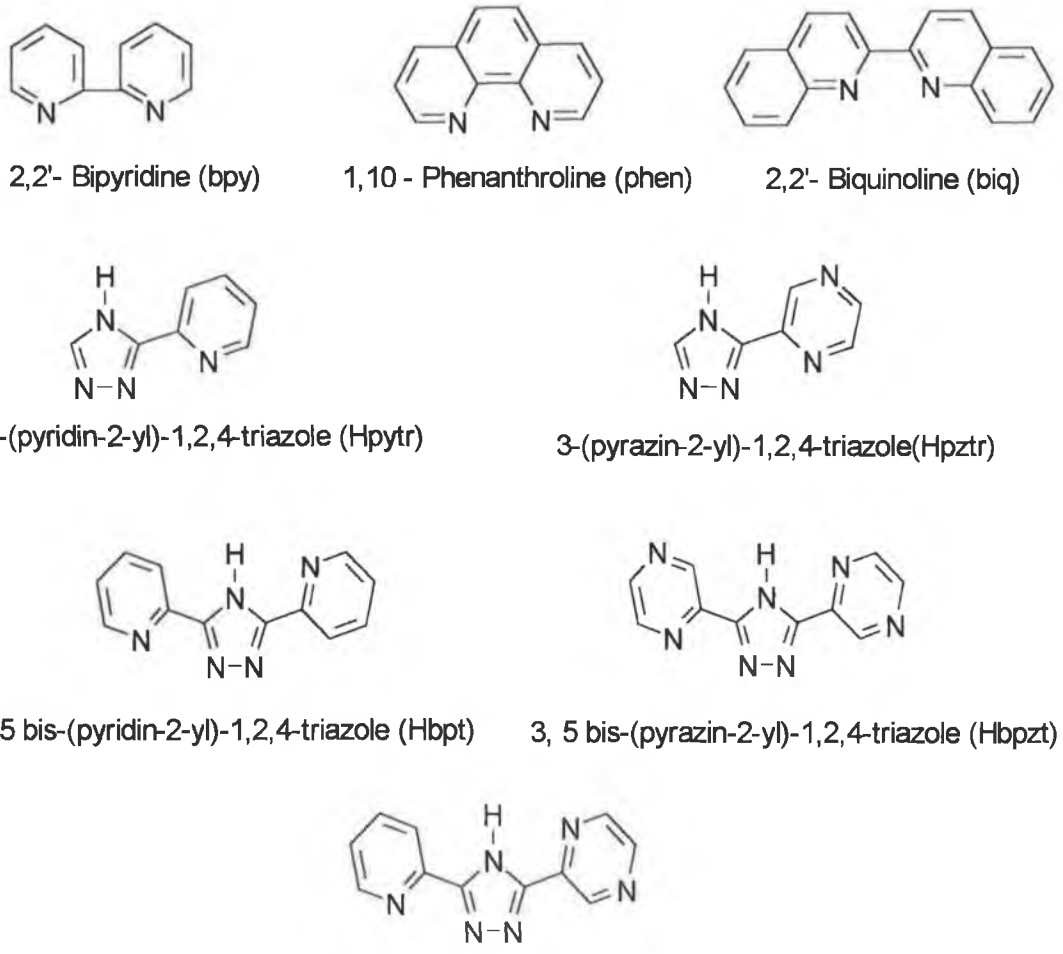

Figure 2 Ligands cited in this chapter

It is of interest to examine the effect of increasing the asymmetry in this ligand due to the two, very different coordination sites i.e. one pyrazine based, one pyridine based as this will greatly influence the photophysical properties. The ppt⁻ mononuclear complexes investigated in this chapter have been designed with bpy, phen, biq and their deuteriated analogues. The excited state of this ligand is a complicated one, and in order to perturb the energy levels of the complexes the different ligands were incorporated. Also in order to facilitate the ^{1}H NMR studies and luminescent lifetime elucidation the complexes have been selectively deuteriated. It is hoped that some insight can be shown into the photophysical properties of the compounds.

4.2 EXPERIMENTAL

Cis-$[Ru(bpy)_2Cl_2].2H_2O$ and *Cis*-$[Ru(d_8\text{-}bpy)_2Cl_2].2H_2O$ were prepared as described in section 3.2, chapter 3.

4.2.1 Preparation of Hppt ligand

3-(pyridin-2-yl)-5(pyrazin-2-yl)-1,2,4-triazole (Hppt)

The following synthesis is a modified method of that previously reported. (15 g; 0.12 mol) 2-pyrazylcarboxylic acid was dissolved in 90 cm^3 ethanol and 15 cm^3 concentrated H_2SO_4 and heated under reflux for 3 hours. The solution was neutralised with a saturated solution of Na_2CO_3 and then filtered to remove side products. Most of the ethanol was removed and the remaining solution was extracted with dichloromethane to yield a yellow product. The fractions were dried over $MgSO_4$. The dichloromethane was evaporated off to yield the ester, which crystallised after a few minutes. The ester was weighed and an equimolar amount of hydrazine monohydrate (use in fume hood) was weighed out. The ester was dissolved in ethanol and then dropped into the hydrazine monohydrate and the pyrazylhydrazide crystalised out overnight in the freezer (-4^0C). The pyrazylhydrazide was filtered and weighed. An equimolar amount of 2-cyanopyridine (as to the pyrazylhydrazide) was weighed out and dissolved in 30 cm^3 of methanol and 0.7 g sodium and was heated under reflux for 3 hours to form the pyridyl-imidate. The pyrazylhydrazide was added to the solution and heated for 15 min. The precipitate (yellow intermediate) was heated under reflux for 1 hour in a minimal quantity of ethylene glycol to yield the Hppt ligand. The ligand (white) was recrystalised in hot ethanol. (A schematic diagram of the Hppt synthesis is shown in Figure 3).

Yield: 14 g (52%), M.P.: 250-252 ^0C [31]

Other routes for the synthesis of this ligand exist but were not investigated.

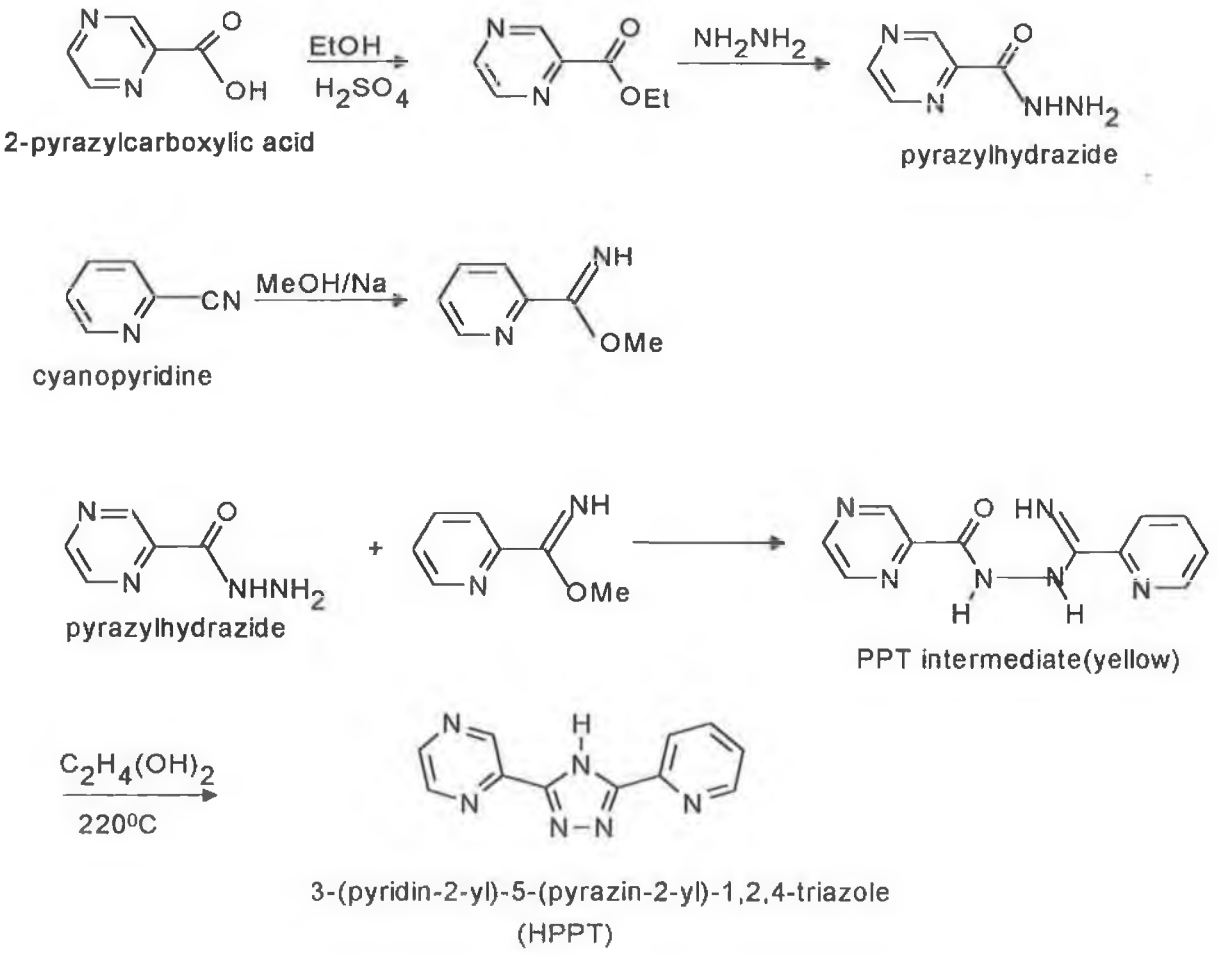

Figure 3 Synthesis of 3-(pyrazyl-2-yl)-5-(pyridin-2-yl)-1,2,4-triazole (Hppt).

Characterisation of Hppt Ligand

This reaction was monitored by ^{1}H NMR at three different stages. The first checkpoint is the formation of the pyrazylhydrazide. The ^{1}H NMR for this product was carried out in d_6-DMSO shown in Figure 4, the protons were assigned to: N-H, 10.15 ppm (s), C-H, 9.11 ppm (s), C-H, 8.81 ppm (d), C-H, 8.67 ppm (d), N-H_2, 4.65 ppm (s).

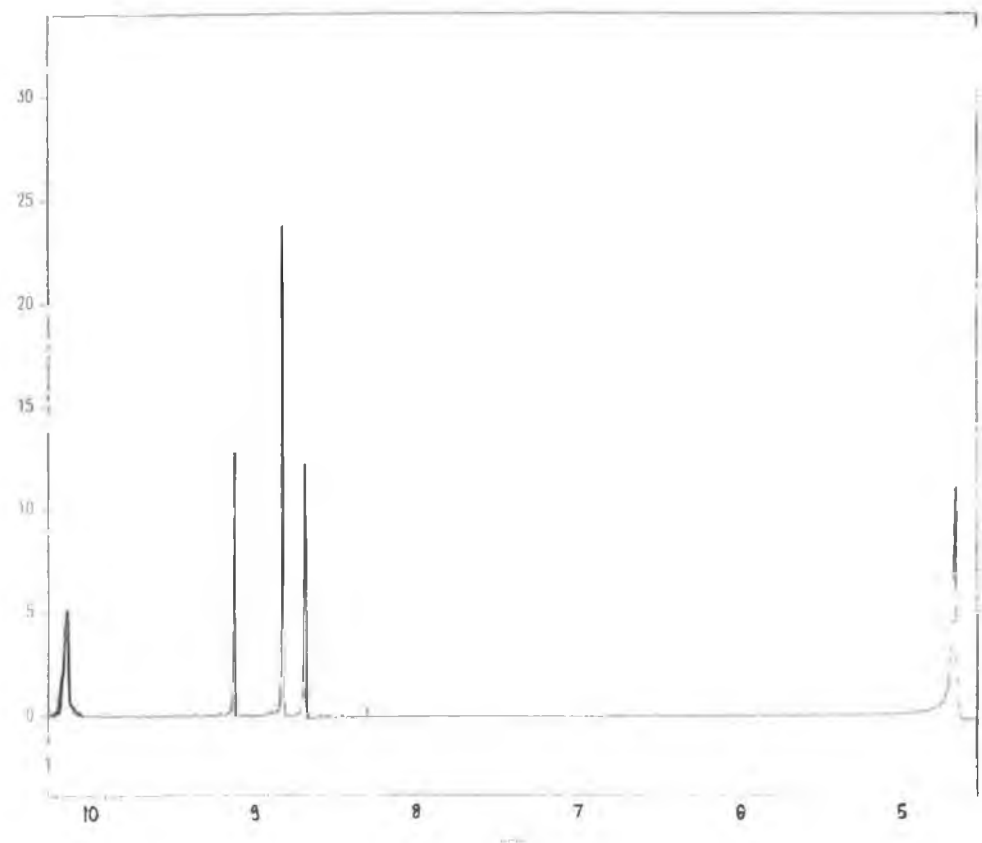

Figure 4 ^{1}H NMR of pyrazylhydrazide in d_6-dmso

The ^{1}H NMR of the Hppt intermediate (yellow) product is shown in Figure 5. The protons were assigned as follows: (pyrazine ring) H3, 9.19 ppm; H5, 8.73 ppm; H6, 8.60 ppm; (pyridine ring) H3, 8.19 ppm; H4, 7.90 ppm; H5, 7.51 ppm; H6, 8.84 ppm.

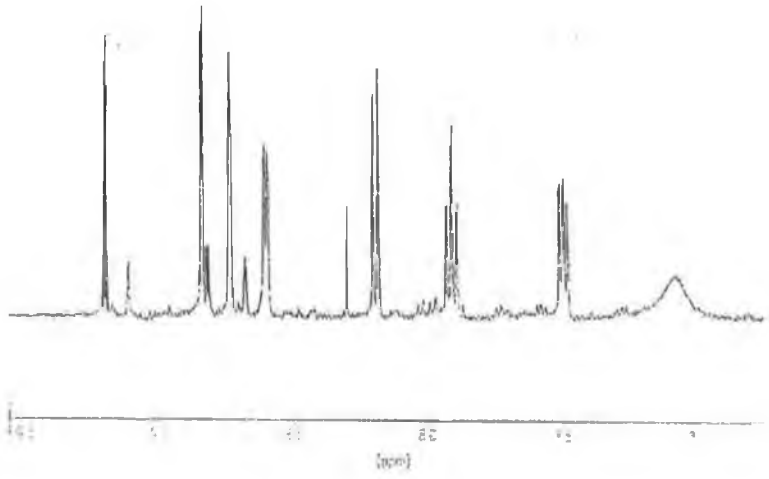

Figure 5 ^{1}H NMR of the Hppt intermediate in d_6-dmso.

After the intermediate was cyclised in ethylene glycol the result was the Hppt ligand. The ^{1}H NMR of the Hppt ligand is shown in Figure 6 and the protons are assigned as follows : (Pyrazine ring) H3, 9.33 ppm(s); H5 and H6, 8.72ppm(m); (Pyridine ring) H3, 8.17ppm(d); H4, 8.01ppm(t); H5, 7.54ppm(t); H6, 8.77ppm(d). As can be seen from ^{1}H NMR the ligand is very pure once recrystallised.

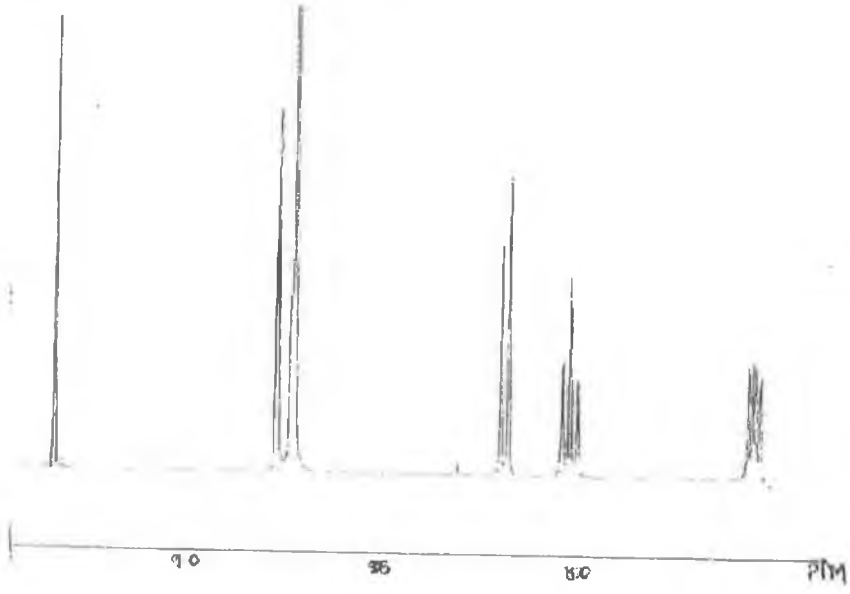

Figure 6 ^{1}H NMR of the ligand 3-(pyrazin-2-yl)-5-(pyridin-2-yl)-1,2,4-triazole in d_6-dmso.

4.2.2 Preparation of the mononuclear complexes

$[Ru(bpy)_2ppt][PF_6]_{3/2}.5H_2O$

Cis-$[Ru(bpy)_2Cl_2].2H_2O$ (520 mg;1 mmol) and Hppt ligand (224 mg; 1 mmol) were heated under reflux for 6 hours in 40 cm^3 ethanol and 10 cm^3 water. The solution was evaporated to dryness and the residue then dissolved in 10 cm^3 water and precipitated by addition of aqueous NH_4PF_6. This resulted in a mixture of two isomers. The complex was recrystallised in a mixture of acetone: water 1:1 (v/v). The isomers were separated by column chromatography on a neutral alumina column. Isomer 1 eluted off the column using 100% acetonitrile, and isomer 2 eluted off using 100% methanol.
Yield of combined fractions: 888 mg (95%). CHN: Found C, 39.75; H, 2.95; N, 13.8. $RuC_{31}H_{33}N_{10}O_5P_{3/2}F_9$ requires C, 39.60; H, 3.10; N, 14.90 %.

$[Ru(d_8\text{-}bpy)_2Hppt][PF_6]_2.2H_2O.NH_4PF_6$

Cis-$[Ru(d_8\text{-}bpy)_2Cl_2].2H_2O$ (540 mg; 1 mmol)and Hppt(224mg;1mmol) were heated under reflux for 6 hours in 40 cm^3 ethanol and 10 cm^3 water. The solution was evaporated to dryness and the residue then dissolved in 10 cm^3 water and precipitated by addition of aqueous NH_4PF_6. The resulting complex was a mixture of two isomers. The complex was recrystallised in a mixture of acetone: water 1:1(v/v). The isomers were separated by column chromatography on a neutral alumina column. Isomer 1 eluted off the column using 100% acetonitrile, and isomer 2 eluted off using 100% methanol. Yield of combined fractions: 712 mg (93%). CHN: Found C, 33.50; H, 2.64; N, 13.24. $RuC_{31}D_{16}H_{16}N_{11}O_2P_3F_{18}$ requires C, 32.58; H, 2.82; N, 13.48 %.

[Ru(bpy)$_2$d$_7$-ppt][PF$_6$]$_{3/2}$.1H$_2$O

Cis-[Ru(bpy)$_2$Cl$_2$].2H$_2$O (520 mg; 1 mmol)and d$_8$-ppt(231mg;1mmol) were heated under reflux for 6 hours in 40 cm^3 ethanol and 10 cm^3 water. The solution was evaporated to dryness and the residue then dissolved in 10 cm^3 water and precipitated by addition of aqueous NH_4PF_6. The resulting complex was a mixture of two isomers. The complex was recrystallised in a mixture of acetone: water 1:1(v/v). The isomers were separated by column chromatography on a neutral alumina column. Isomer 1 eluted off the column using 100% acetonitrile, and isomer 2 eluted off using 100% methanol. Yield of combined fractions: 730 mg (97%). CHN: Found C, 42.54; H, 2.82; N, 15.01. $RuC_{31}H_{18}N_{10}O_1P_{3/2}F_9D_7$ requires C, 42.34; H, 2.86; N, 15.90. (Isomer 2)

[Ru(d$_8$-bpy)$_2$d$_7$-ppt][PF$_6$]$_{3/2}$.3H$_2$O

Cis-[Ru(d$_8$-bpy)$_2$Cl$_2$].2H$_2$O (540 mg; 1 mmol)and d$_8$-ppt(231mg;1mmol) were heated under reflux for 6 hours in 40 cm^3 ethanol and 10 cm^3 water. The solution was evaporated to dryness and the residue then dissolved in 10 cm^3 water and precipitated by addition of aqueous NH_4PF_6. The resulting complex was a mixture of two isomers. The complex was recrystallised in a mixture of acetone: water 1:1(v/v). The isomers were separated by column chromatography on a neutral alumina column. Isomer 1 eluted off the column using 100% acetonitrile, and isomer 2 eluted off using 100% methanol. Yield of combined fractions: 725 mg (94%). CHN: Found C, 39.60; H, 2.71; N,15.61. $RuC_{31}H_6D_{23}O_1P_{3/2}F_9N_{10}$ requires C, 39.97; H, 3.14; N, 15.04. (Isomer 2)

$[Ru(phen)_2ppt][PF_6]_{3/2}.H_2O$

Cis-$[Ru(phen)_2Cl_2].2H_2O$ (568 mg; 1 mmol)and Hppt(224mg;1mmol) were heated under reflux for 6 hours in 40 cm^3 ethanol and 10 cm^3 H_2O. The solution was evaporated to dryness and the residue then dissolved in 10 cm^3 water and precipitated by addition of aqueous NH_4PF_6. The resulting complex was a mixture of two isomers. The complex was recrystallised in a mixture of acetone: water 1:1(v/v). The isomers were separated by column chromatography on a neutral alumina column. Isomer 1 eluted off the column using 100% acetonitrile, and isomer 2 eluted off using 100% methanol. Yield of combined fractions: 754 mg (95%). CHN was not obtained for this complex, however, this complex was made in an identical manner to that of $[Ru(phen)_2d_7$-ppt$]_{3/2}[PF_6]$ and was found to be hplc pure and ^1H NMR pure.

$[Ru(d_8$-phen$)_2ppt][PF_6]_{3/2}.H_2O$

Cis-$[Ru(d_8$-phen$)_2Cl_2].2H_2O$ (576 mg; 1 mmol)and Hppt (269 mg;1.2 mmol) were heated under reflux for 6 hours in 40 cm^3 ethanol and 10 cm^3 H_2O. The solution was evaporated to dryness and the residue then dissolved in 10 cm^3 water and precipitated by addition of aqueous NH_4PF_6. The resulting complex was a mixture of two isomers. The complex was recrystallised in a mixture of acetone: water 1:1(v/v). The isomers were separated by column chromatography on a neutral alumina column. Isomer 1 eluted off the column using 100% acetonitrile, and isomer 2 eluted off using 100% methanol. Yield of combined fractions: 790 mg (93%). CHN was not obtained for this complex, however, this complex was made in an identical manner to that of $[Ru(phen)_2d_7$-ppt$]_{3/2}[PF_6]$ and was found to be hplc pure and ^1H NMR pure.

$[Ru(phen)_2d_7$-ppt$][PF_6]_{3/2}.2H_2O$

Cis-$[Ru(phen)_2Cl_2].2H_2O$ (240 mg; 0.45 mmol)and d_8-ppt (115 mg;0.5mmol) were heated under reflux for 6 hours in 40 cm^3 ethanol and 10 cm^3 H_2O. The solution was

evaporated to dryness and the residue then dissolved in 10 cm^3 water and precipitated by addition of aqueous NH_4PF_6.

The resulting complex was a mixture of two isomers. The complex was recrystallised in a mixture of acetone: water 1:1(v/v). The isomers were separated by column chromatography on a neutral alumina column. Isomer 1 eluted off the column using 100% acetonitrile, and isomer 2 eluted off using 100% methanol. Yield of combined fractions: 290 mg (84%). CHN: Found C, 45.13; H, 2.60; N, 14.48. $RuC_{35}D_7H_{20}N_{10}O_2P_{3/2}F_9$ requires C, 44.47; H, 2.87; N, 14.82 %.

$[Ru(d_8\text{-phen})_2d_7\text{-ppt}][PF_6]_{3/2}.5H_2O$

Cis-$[Ru(d_8\text{-phen})_2Cl_2].2H_2O$ (60 mg; 0.102 mmol)and d_8-ppt (22 mg; 0.1mmol) were heated under reflux for 6 hours in 40 cm^3 ethanol and 10 cm^3 H_2O. The solution was evaporated to dryness and the residue then dissolved in 10 cm^3 water and precipitated by addition of aqueous NH_4PF_6. The resulting complex was a mixture of two isomers. The complex was recrystallised in a mixture of acetone: water 1:1(v/v). The isomers were separated by column chromatography on a neutral alumina column. Isomer 1 eluted off the column using 100% acetonitrile, and isomer 2 eluted off using 100% methanol. Yield of combined fractions: 75 mg (91%). CHN: Found C, 41.45; H, 2.65; N, 13.13. $RuC_{35}H_{10}D_{23}N_{10}O_5P_{3/2}F_9$ requires C, 41.40; H, 3.28; N, 13.80. (Isomer-2).

$[Ru(biq)_2Hppt][PF_6]_2.H_2O$

Cis-$[Ru(biq)_2Cl_2].2H_2O$ (500 mg; 0.694 mmol)and Hppt (187 mg; 0.833 mmol) were heated under reflux for 6 hours in 40 cm^3 ethanol and 10 cm^3 H_2O. The solution was evaporated to dryness and the residue then dissolved in 10 cm^3 water and precipitated by addition of aqueous NH_4PF_6. The resulting complex was a mixture of two isomers. The complex was recrystallised in a mixture of acetone: water 1:1(v/v). The isomers were separated by column chromatography on a neutral alumina column. isomer 1 eluted off

the column using 100% Acetonitrile, and isomer 2 eluted off using 100% Methanol. Yield of combined fractions: 650 mg (95%). CHN: Found C, 49.47; H, 2.91; N, 12.55. $RuC_{47}H_{34}N_{10}O_1P_2F_{12}$ requires C, 49.30; H, 2.90; N, 12.23%.

$[Ru(d_{12}\text{-biq})_2Hppt][PF_6]_2.5H_2O$

Cis-$[Ru(d_{12}\text{-biq})_2Cl_2].2H_2O$ (250 mg; 0.34 mmol)and Hppt (92 mg; 0.408 mmol) were heated under reflux for 6 hours in 40 cm^3 ethanol and 10 cm^3 H_2O. The solution was evaporated to dryness and the residue then dissolved in 10 cm^3 water and precipitated by addition of aqueous NH_4PF_6. The resulting complex was a mixture of two isomers. The complex was recrystallised in a mixture of acetone: water 1:1(v/v). The isomers were separated by column chromatography on a neutral alumina column. isomer 1 eluted off the column using 100% Acetonitrile, and isomer 2 eluted off using 100% Methanol. Yield of combined fractions: 310 mg (90%). CHN: Found C, 45.40; H, 2.85; N, 12.13. $RuC_{47}D_{24}H_{18}N_{10}O_4P_2F_{12}$ requires C, 46.04; H, 3.45; N, 11.43 %.

$[Ru(biq)_2d_7\text{-ppt}][PF_6].3H_2O$

Cis-$[Ru(biq)_2Cl_2].2H_2O$ (468 mg; 0.65 mmol)and d_8-ppt (161 mg; 0.7 mmol) were heated under reflux for 6 hours in 40 cm^3 ethanol and 10 cm^3 H_2O. The solution was evaporated to dryness and the residue then dissolved in 10 cm^3 water and precipitated by addition of aqueous NH_4PF_6. The resulting complex was a mixture of two isomers. The complex was recrystallised in a mixture of acetone: water 1:1(v/v). The isomers were separated by column chromatography on a neutral alumina column. isomer 1 eluted off the column using 100% Acetonitrile, and isomer 2 eluted off using 100% Methanol. Yield of combined fractions: 595 mg (95%). CHN: Found C, 54.62; H, 3.22; N, 13.37. $RuC_{47}D_7H_{30}N_{10}O_3PF_6$ requires C, 54.12; H, 3.58; N, 13.43 %.

$[Ru(d_{12}\text{-biq})_2d_7\text{-ppt}][PF_6]_{3/2}.5H_2O$

Cis-$[Ru(d_{12}\text{-biq})_2Cl_2].2H_2O$ (100 mg; 0.137 mmol) and d_8-ppt (47 mg; 0.20 mmol) were heated under reflux for 6 hours in 40 cm^3 ethanol and 10 cm^3 H_2O.

The solution was evaporated to dryness and the residue then dissolved in 10 cm^3 water and precipitated by addition of aqueous NH_4PF_6. The resulting complex was a mixture of two isomers. The complex was recrystallised in a mixture of acetone: water 1:1(v/v). The isomers were separated by column chromatography on a neutral alumina column. isomer 1 eluted off the column using 100% Acetonitrile, and isomer 2 eluted off using 100% Methanol. Yield of combined fractions: 125 mg (85%). CHN: Found C, 47.38; H, 3.24; N, 13.97. $RuC_{47}H_6D_{31}N_{10}O_5P_{3/2}F_9$ requires C, 47.97; H, 3.60; N, 11.90. (Isomer-2).

4.3 RESULTS AND DISCUSSION

4.3.1 Synthetic analysis

The ppt$^-$ mononuclear complexes form four different coordination isomers due to the various coordination sites of the Hppt ligand. Of these four isomers , two have been studied (N1 of the triazole to the pyridine ring {isomer 1} and N2 of the triazole ring to pyrazine {isomer 2}) as the two N4 bound isomers of the Hppt ligand are too difficult to isolate. The ppt$^-$ complexes may be formed in a protonated or deprotonated manner, as previously seen for the pztr$^-$ complexes. From CHN analysis of the various bpy, phen and biq, ppt$^-$ complexes there is a difference in the counter ion content [PF_6]. This may have been avoided if a drop of base had been added to the complex during recrystallisation. This does not effect any of the measurements as all measurements were carried out in acidic and basic media. The only difference that was noticed is during UV spectrum analysis of the complex, prior to addition of acid or base the spectrum obtained will give you a mixture of the two species. The presence of $[PF_6]_{3/2}$ may be attributed to hydrogen bonding via the complexes resulting in a sharing of the counter ion between unit cells. This was not evident in the crystal structure obtained for isomer 2 of the ppt$^-$ complex, as data was unable to be collected for this crystal. One complex was found to contain excess NH_4PF_6 salt. As the complex is isolated as a PF_6 salt, in some cases there is evidence of excess PF_6 remaining after recrystallisation as the complexes are recrystallised from acetone and water and the PF_6 salt is water soluble. The presence of excess PF_6 is evident in the ^{1}H NMR spectrum as three NH_4 quaternary ammonium signals. The presence of the excess salt does not interfere with measurements.

4.3.2 Isis draw structures of the mononuclear Hppt isomers.

The following structures were investigated purely for a visual purpose. It is important to ascertain which proton of the ppt⁻ ligand is adjacent to a peripheral ligand, i.e. bpy, phen or biq in order to confirm ^{1}H NMR shifts.

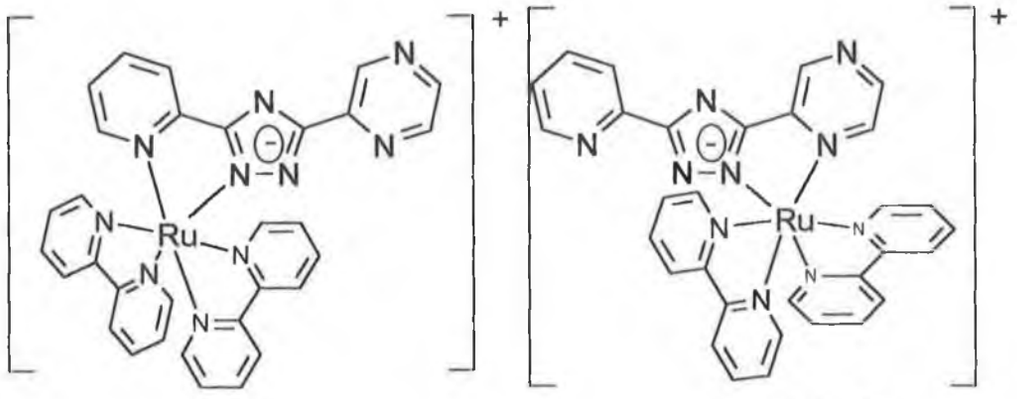

Figure 7 Isis draw structure of $[Ru(bpy)_2ppt]^+$ N1/N2-bound coordination isomers

It is known that when a proton of these bridging ligands is in close vicinity to the bpy ligand that a shift arises due to a ring current effect [35,36]. The ppt⁻ ligand also has four potential binding sites, hence four different isomers may be formed. It was hoped that the use of biquinoline may cause some steric hindrance and cut down on the amount of isomers formed.

In both cases for the pyridine and pyrazine isomers in Figure 7, their H6 proton is hanging directly over the bpy rings, hence this is the proton to observe when identifying the different isomers.

We can also see that the unbound ring is free to rotate and the ligand is not rigid or of a planar fashion. The N4 isomers are not characterised in the text as they are too difficult to isolate when mixed with the analogous N1/N2 bound isomers. The N4 isomers are only present as a shoulder of the N1 and N2 bound isomers, and the retention times of the N4 bound isomers are slightly longer than that of their respective N1 and N2 bound isomers. This separation was only clear on semi-preparative hplc. Also the N4 isomers seem to be produced in a smaller ratio than that of the N1/ N2 isomers. However, the N4 isomers are also formed on complexation and should be noted.

For the phenanthroline containing complexes $[Ru(phen)_2ppt]^+$, the pyridine and pyrazine bound isomers of the N1/N2 triazole position are shown in Figure 8. In both cases their H6 proton is hanging directly over the phen rings, hence this proton will be shifted more upfield than the adjacent protons.

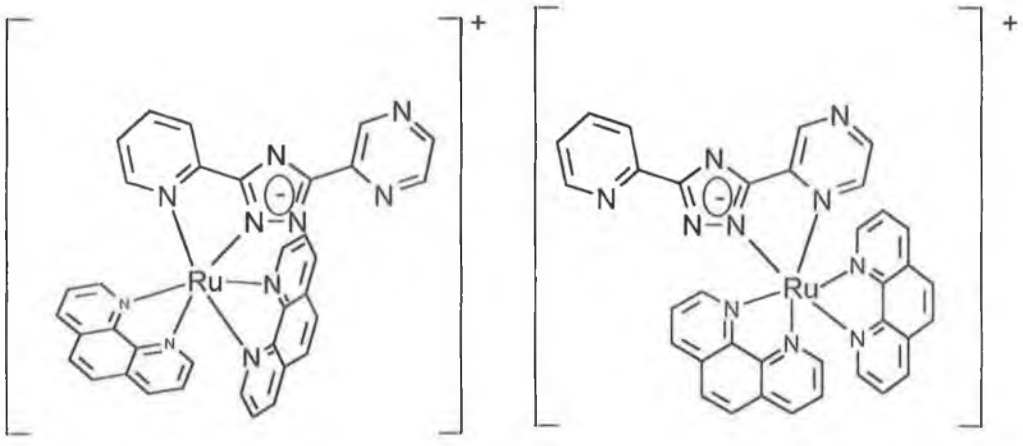

Figure 8 Isis draw structure of $[Ru(phen)_2ppt]^+$ N1/N2-bound coordination isomers

It is suggested that the pyrazine bound analogue experiences the usual H6 shift of the pyrazine ring. However, in the case of the $[Ru(biq)_2ppt]^+$ complex the pyridine bound isomer experiences a shift of both the H6 and the H3 protons of the pyridine ring are due to the coordination of the peripheral biquinoline ligand, however this was not observed. The biquinoline isomers of the $[Ru(biq)_2ppt]^+$ complex in Figure 9 again shows the same type of coordination, and the H6 proton of the bound ring (pyridine/ pyrazine) will be shifted upfield. The spatial alignment of the biquinoline complexes is slightly different to that of the bpy and phen isomers.

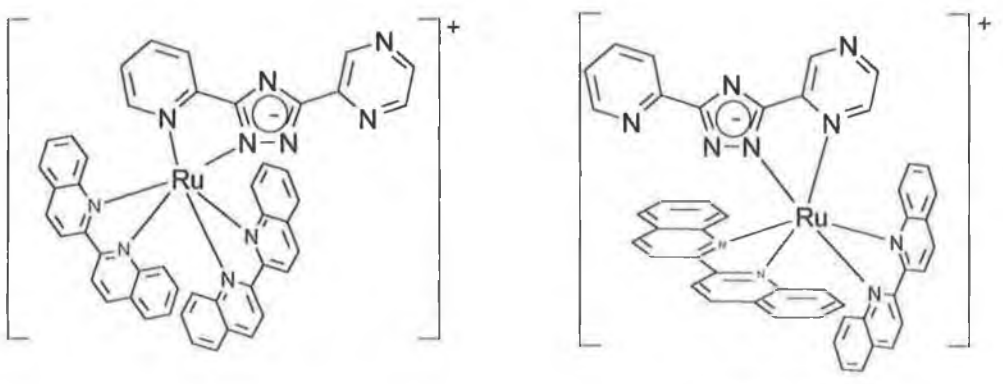

Isomer 1 Isomer 2

Figure 9 Isis draw structure of $[Ru(biq)_2ppt]^+$ N1/N2-bound coordination isomers

In the interpretation of the ^1H NMR of these complexes there does not appear to be any dramatic steric effects caused by the size of biquinoline but $[Ru(phen)_2ppt]^+$ complex, the H6 proton of both the pyridine ring (N1-bound isomer) and pyrazine ring (N2-bound isomer) will be shifted substantially due to the ring current effect experienced by the adjacent protons. As previously mentioned in chapter 3 the coordination isomers have a Δ and Λ enantiomer each.

4.3.3 Chromatographic interpretation

Initially the mononuclear compounds were run on an analytical hplc using a SCX cation exchange column and a mobile phase of 0.12M $LiClO_4$, 80:20 acetonitrile: water, flowrate of 2 cm^3/min and a detector wavelength of 280 nm.

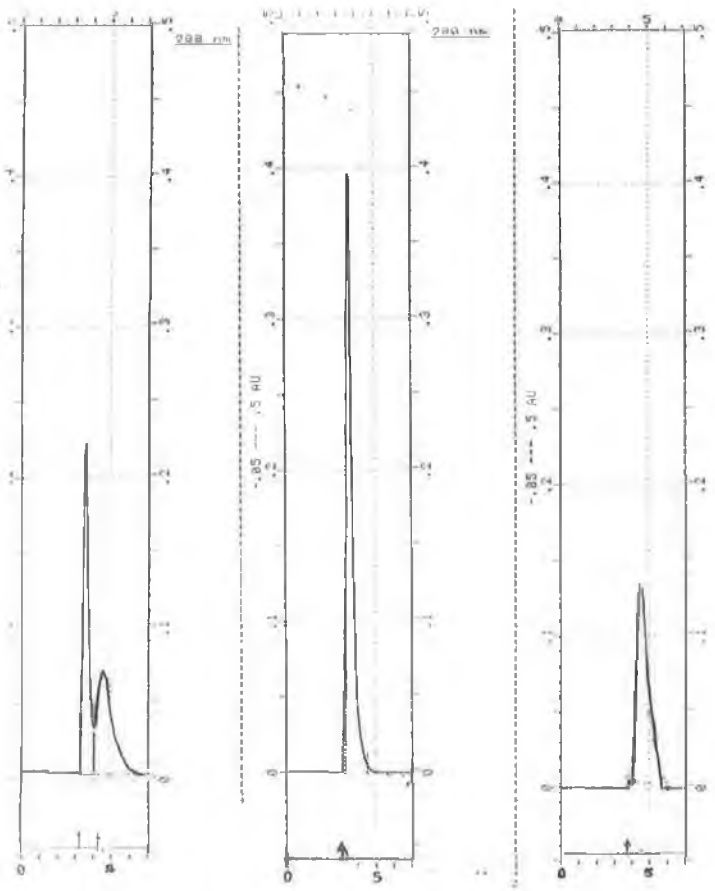

Figure 10 Analytical hplc trace of the mononuclear [Ru(bpy)2ppt]$^{+}$ and its isolated coordination isomers, 0.12 M $LiClO_4$, 80:20 MeCN:H_2O at 2 cm^3/ min.

The hplc trace of the monomer is presented in Figure 10, which portrays the two isomers at different retention times and the separated coordination isomers after isolation either by means of semi-preparative hplc or by neutral alumina columns. The retention time for the isomers 1 and 2 are 4.08 min. and 4.99 min. respectively. Deuteriation does not have any effect on retention time. The isolation of the ppt coordination isomers is more difficult than that of the pyridine-/ pyrazine-triazole complexes, as the resolution of the isomers is not as good. It may be suggested that the difficulty in separation is due to the interaction of free nitrogen atoms on the cationic column. Also more importantly the only difference is that one isomer is bound via the pyridine ring and the other via the pyrazine ring but the coordination sites to the triazole ring of both isomers have equal properties. It was noted that all the biquinoline containing complexes have very short retention times in comparison to that of the bipyridyl containing analogues and that a slower flowrate is required (1.5 cm^3/ min) in order to see any resolution of the isomers. The biquinoline isomers were adequately isolated on the neutral alumina column in a ratio of 90:10 for isomer 1:isomer 2, however, the bipyridyl and phenanthroline isomers required semi-preparative separation as insufficient purification was achieved on column chromatography.

4.3.4 ^{1}H NMR spectroscopy

The 3-(pyrazin-2-yl)-5-(pyridin-2-yl)-1,2,4 triazole ligand has proven to be complicated in ascertaining the coordination mode of the purified compounds as the only difference lying between isomer 1 and isomer 2 is the fact that they are pyridine or pyrazine bound [31]. Due to the isomerisation obtained during the synthesis of the mononuclear ppt complexes, it is essential that correct assignment be given to each isomer in order to interpret their coordination sites to the ppt bridging ligand. The use of ^{1}H NMR enables the elucidation of the structure and aids in the determination of the coordination modes of the complex. The complexes and their deuteriated analogues were synthesised as described in Section 4.2.

Mononuclear complexes

$[Ru(bpy)_2ppt]^+$

^1H NMR resonances for the ppt^- ligand and complexes are shown in Table 1. The coordination isomers that will be dealt with in this text are the N1 of the triazole to the pyridine ring and the N2 of the triazole to the pyrazine ring. The N4 isomers were not isolated for this study. The interpretation of the $[Ru(bpy)_2bpt]^+$ and $[Ru(bpy)_2bpzt]^+$ complexes will not involve coordination isomers, mononuclear coordination occurs via the N2 site of the triazole ligand, hence a shift of the H6 proton of the pyridine and pyrazine should be observed respectively.

Further evidence of the coordination of the ppt^- isomers will be verified using ^1H NMR spectroscopy. Isomer 1 has been assigned to coordinate via N1 of the triazole and the pyridine ring. For this isomer the H^6 proton of the pyridine ring experiences an upfield shift in relation to the H^6 of the pyrazine ring. The upfield shift has been associated with a ring current effect of an adjacent bpy which a H^6 proton of the pyridine (or pyrazine) will experience when a $Ru(bpy)_2$ (or $Os(bpy)_2$) moiety is coordinated to it [32,33,34]. Due to the effect of the negatively charged triazole ring on the coordinated ppt^- ligand, more electron density is located on the pyridine and pyrazine rings resulting in an overall upfield shift of all the protons compared to that of the free ligand. The assignment of the protons of the coordinated ppt^- ligand was facilitated by deuteriation of the bipyridyls prior to synthesis of the mononuclear complex. Hence, it may be concluded that coordination for isomer 1 does take place via the N1 of the triazole ring and the N of the pyridine.

For isomer 2 a similar result is observed as in this case it is the pyrazine ring protons which experience the shift upfield due to the coordinated $Ru(bpy)_2$ moiety. H^6 and H^5 of the pyrazine ring are strongly shifted upfield due to the proximity of the adjacent bipyridyls[35,36].

Compound	H3	H4	H5	H6
Hppt prz	9.33 (s)	(---)	8.72 (d)	8.72 (d)
pyr	8.17 (d)	8.01 (t)	7.54 (t)	8.77 (d)
$[Ru(bpy)_2ppt]^+$ Iso 1 prz	9.19(-0.14), s	(---)	8.46(-0.26),m	8.32(-0.40),m
pyr	7.78(-0.39), d	8.00(-0.01), m	7.18(-0.36),t	7.51(-1.26),d
$[Ru(d_8\text{-}bpy)_2ppt]^+$ Iso 1 prz	9.19(-0.14), s	(---)	8.46(-0.26),m	8.32(-0.40),m
pyr	7.78(-0.39), d	8.00(-0.01), m	7.18(-0.36),t	7.51(-1.26),d
$[Ru(bpy)_2ppt]^+$ Iso 2 prz	9.31(-0.02),s	(---)	8.38(-0.34),d	8.18(-0.54),d
pyr	7.88(-0.29),m	7.77(-0.24),t	7.25(-0.29),t	8.49(-0.28),d
$[Ru(d_8\text{-}bpy)_2ppt]^+$ Iso 2 prz	9.31(-0.02),s	(---)	8.38(-0.34),d	8.18(-0.54),d
pyr	7.88(-0.29),m	7.77(-0.24),t	7.25(-0.29),t	8.49(-0.28),d
$[Ru(phen)_2ppt]^+$ Iso 1 prz	9.14(-0.19),s	(---)	8.53(-0.19),m	8.37(-0.35),d
pyr	7.93(-0.24),m	8.08(+0.07),m	7.19(-0.35),t	8.12(-0.65),m
$[Ru(phen)_2ppt]^+$ Iso 2 prz	9.40(+0.07),s	(---)	8.40(-0.32),d	8.20(-0.52),m
pyr	8.03(-0.14),m	8.00(+0.01),m	7.21(-0.33),t	8.59(-0.18),m
$[Ru(biq)_2ppt]^+$ Iso 1 prz	9.20(-0.13),s	(---)	8.88(+0.16),d	8.50(-0.22),m
pyr	8.22(+0.05),d	7.86(-0.15),t	7.68(+0.14),t	8.05(-0.72),d
$[Ru(d_{12}\text{-}biq)_2ppt]^+$Iso 1 prz	9.20(-0.13),s	(---)	8.88(+0.16),d	8.50(-0.22),d
pyr	8.22(+0.05),d	7.86(-0.15),t	7.68(+0.14),t	8.05(-0.72),d

Table 1 400 MHz ^1H NMR resonances observed for the complexes containing the ppt⁻ ligand in d_3-Acetonitrile. Hppt was measured in d_6-DMSO. Values in parenthesis are the chemical shifts compared with the free ligand. (s = singlet, d = doublet, t = triplet and m = multiplet). (Pyr represents the pyridine ring and prz the pyrazine ring)

The resonances of the uncoordinated pyridine ring show a small upfield shift due to the electron density influenced by the deprotonated triazole ring. Figure 11 and Figure 12 illustrate the ^{1}H NMR spectra of $[Ru(bpy)_2ppt]^+$ and $[Ru(d_8\text{-}bpy)_2ppt]^+$ respectively for the N1-pyridine bound isomer (isomer 1). This (Figure 12) is a good example of the advantages of deuteriation in ^{1}H NMR elucidation, as we can see the bipyridyl proton signals are completely suppressed and a clear interpretation may be made of the Hppt ligand shifts after coordination.

$[Ru(phen)_2ppt]^+$

Table 1 lists the chemical shifts for the complexes $[Ru(phen)_2ppt]^+$ isomer 1 and 2. The complex $[Ru(phen)_2ppt]^+$ was purified as stated for the bpy analogue and the resulting ^{1}H NMR spectra are shown for isomer 1 and isomer 2 in Figure 13 and Figure 15. Isomer 1 has been assigned as being bound to N1 of the triazole to the pyridine as the H6 signal of the pyridine ring undergoes the maximum shift of -0.65 ppm and the H5 of the same ring shifts -0.35 ppm. Figure 14 is the ^{1}H NMR spectrum of $[Ru(phen)_2d_7\text{-}ppt]^+$ which presents the phenanthroline protons without the ppt$^-$ ligand signals as they are deuteriated. This enables a clear view of the phenanthroline protons after complexation and can be subtracted from the fully undeuteriated $[Ru(phen)_2ppt]^+$ to determine the ppt$^-$ shifts. Isomer 2, shown in Figure 15, has been assigned as being N2 of the triazole to the pyrazine as the H6 signal of the pyrazine ring is shifted by -0.52 ppm. This upfield shift is attributed to the ring current effect experienced by the H6 proton from the adjacent phenanthroline rings. The corresponding $[Ru(phen)_2d_7\text{-}ppt]^+$ for isomer 2 is shown in Figure 16. There is a distinct difference in the spectra of $[Ru(phen)_2d_7\text{-}ppt]^+$ isomer 1 and isomer 2. The shift observed is that of the phenanthroline protons and occurs on complexation to the Hppt ligand. This confirms that there are two coordination isomers present.

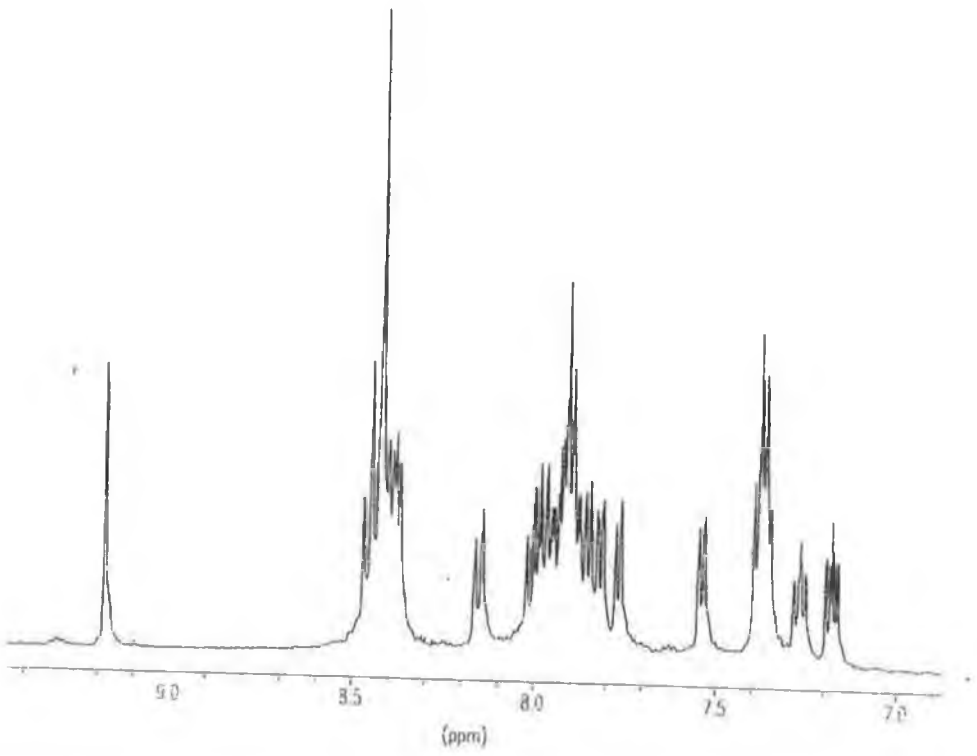

Figure 11 ^{1}H NMR of $[Ru(bpy)_2ppt]^{+}$ pyridine bound in d_3-acetonitrile

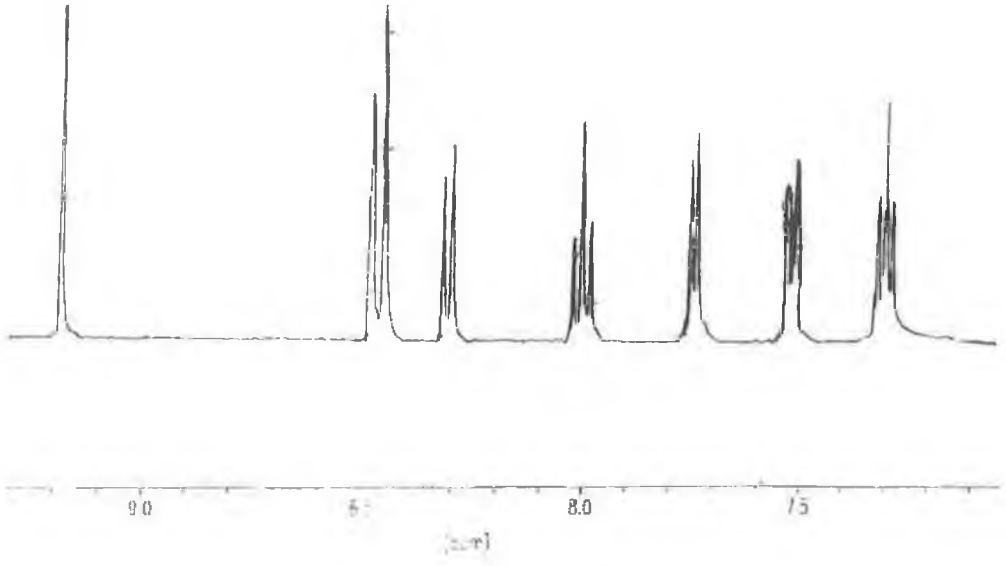

Figure 12 ^{1}H NMR of $[Ru(d_8\text{-}bpy)_2ppt]^{+}$ pyridine bound in d_3-acetonitrile

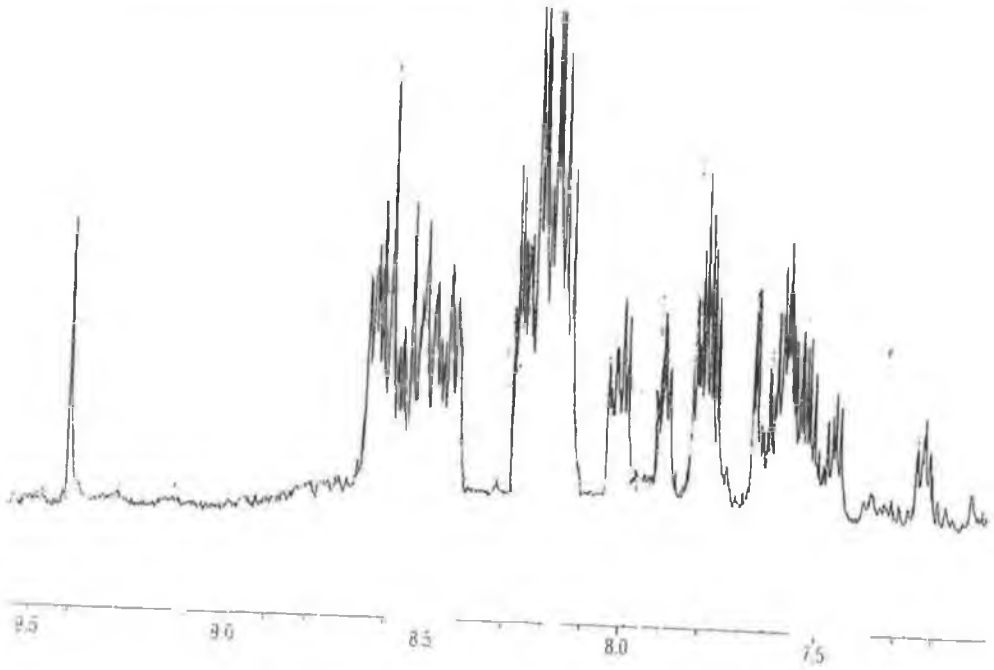

Figure 13 ^{1}H NMR of [Ru(phen)2ppt]$^{+}$ pyridine bound in d3-acetonitrile

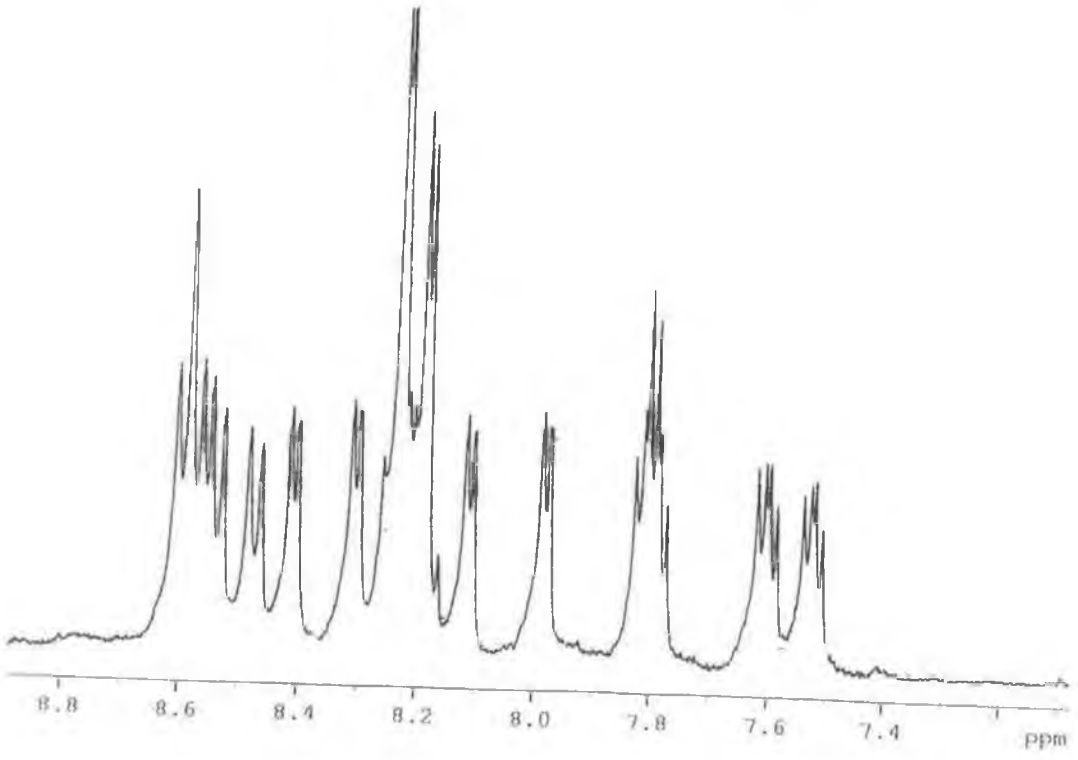

Figure 14 ^{1}H NMR of [Ru(phen)2d7-ppt]$^{+}$ pyridine bound in d3-acetonitrile

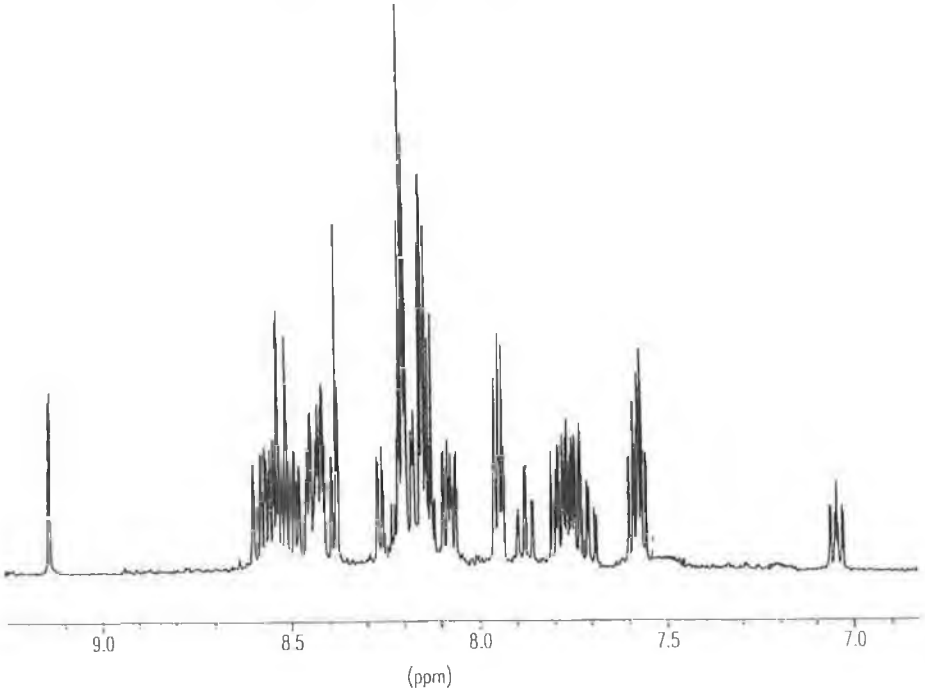

Figure 15 ^{1}H NMR of [Ru(phen)2ppt]$^{+}$ pyrazine bound in d3-acetonitrile

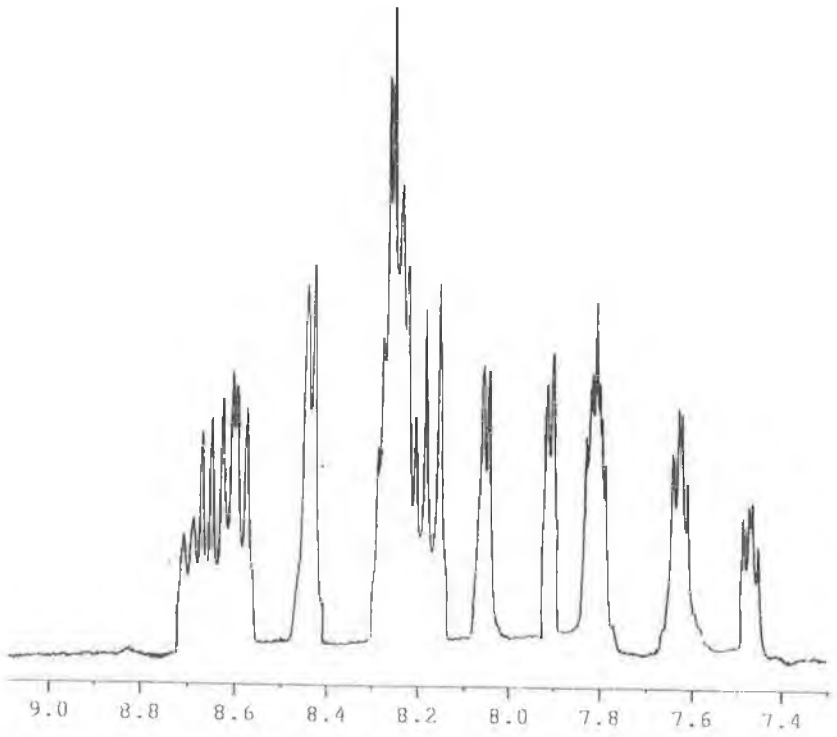

Figure 16 ^{1}H NMR of [Ru(phen)2d7-ppt]$^{+}$ pyrazine bound in d3-acetonitrile

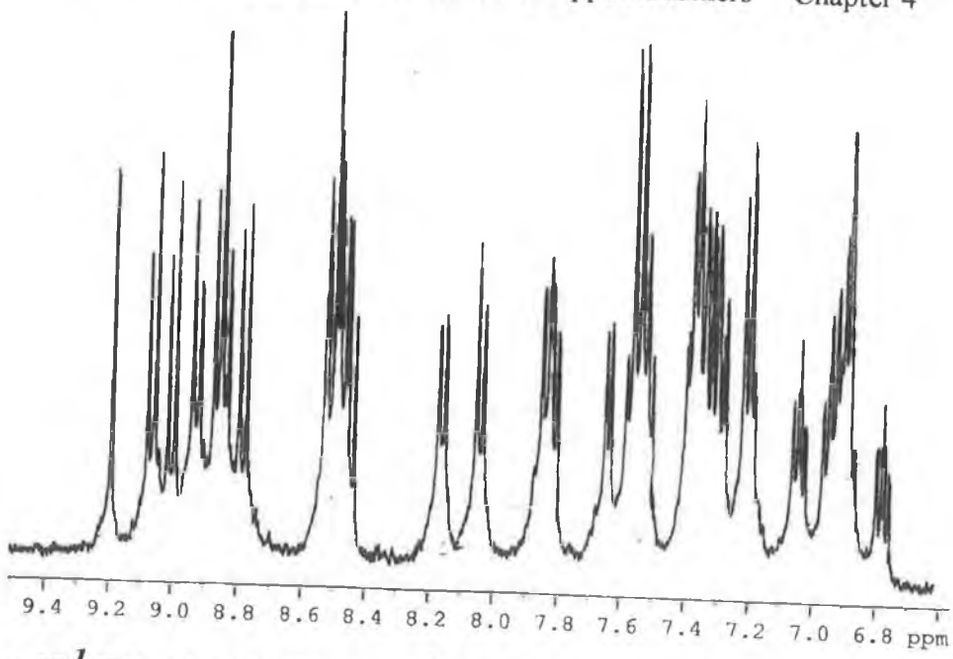

Figure 17 ^{1}H NMR of [Ru(biq)2ppt]$^{+}$ pyridine bound in d3-acetonitrile

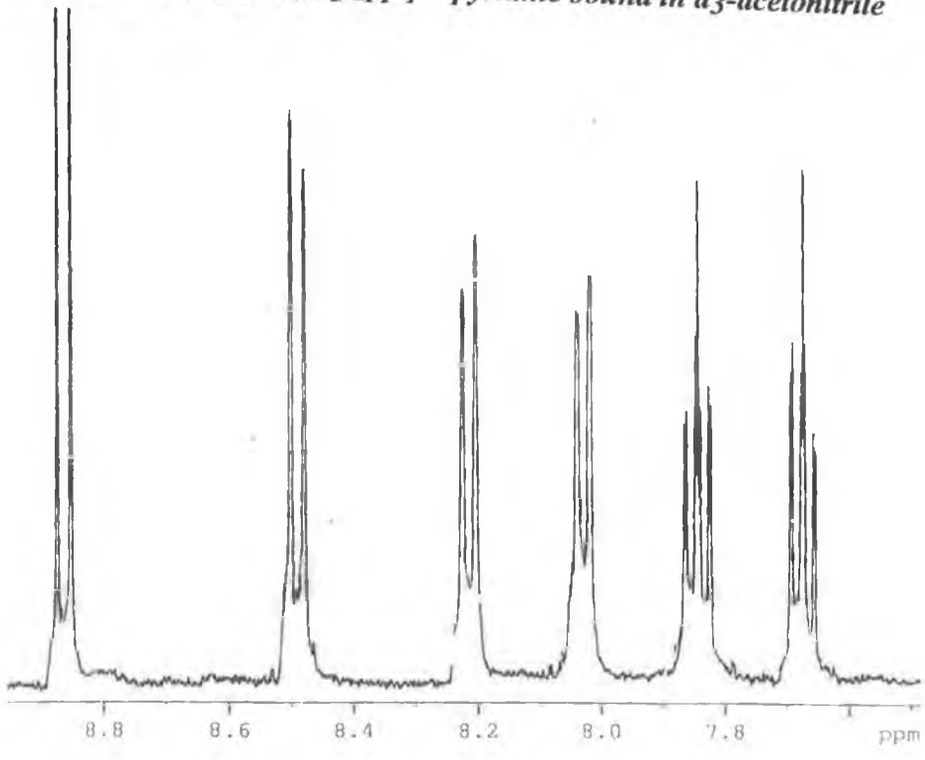

Figure 18 ^{1}H NMR of [Ru(d12-biq)2ppt]$^{+}$ pyridine bound in d3-acetonitrile

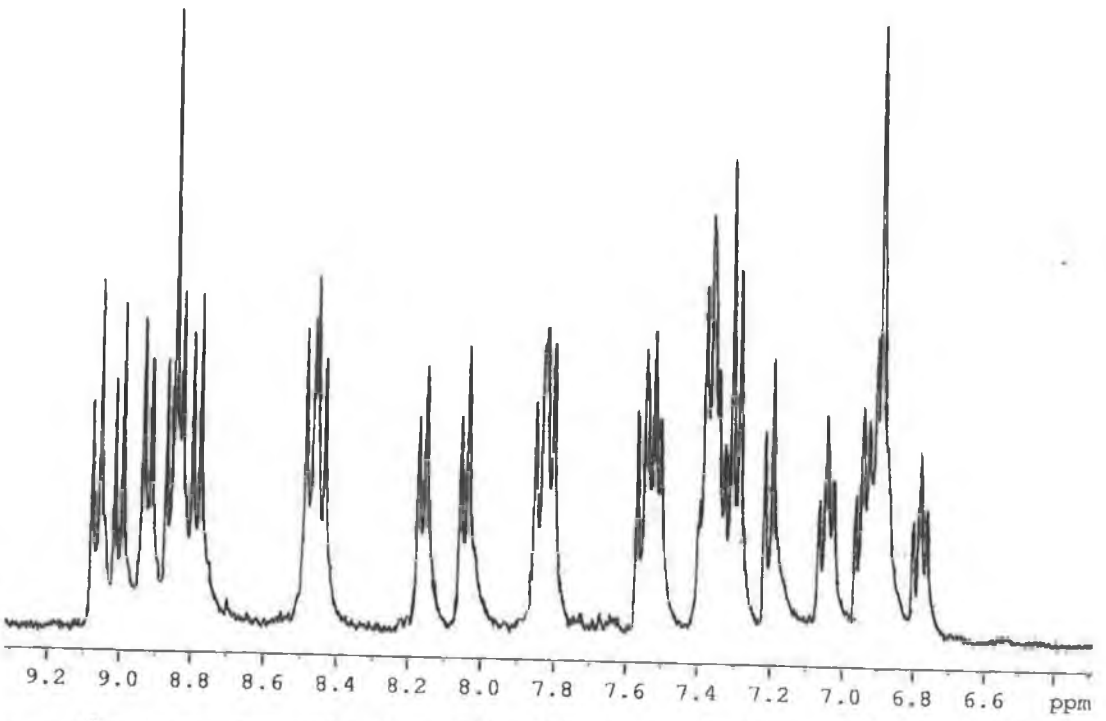

Figure 19 ^{1}H NMR of [Ru(biq)$_2$d$_7$-ppt]$^+$ pyridine bound in d$_3$-acetonitrile

[Ru(biq)$_2$ppt]$^+$

The chemical shifts for the complex [Ru(biq)$_2$ppt]$^+$ are listed in Table 1. It appears that on complexation to the Hppt ligand that the biquinoline ligand does actually cause steric hindrance which promotes the presence of one isomer over the other.

Two isomers were isolated from the alumina column in a ratio of 90:10 hence only isomer 1 is characterised by ^{1}H NMR. Isomer 1 has been assigned to the N1 of the triazole to the pyridine bound isomer. A shift of -0.72 ppm is experienced by the H6 proton of the pyridine ring. The spectrum of [Ru(biq)$_2$ppt]$^+$ isomer 1 is shown in Figure 17, and the partially deuteriated analogues [Ru(d$_{12}$-biq)$_2$ppt]$^+$ and [Ru(biq)$_2$d$_7$-ppt]$^+$ are shown in Figure 18 and Figure 19 respectively. In Figure 19 the H3 singlet of the pyrazine ring of [Ru(d$_{12}$-biq)$_2$ppt]$^+$ is off the scale at 9.20 ppm but the other six ppt protons are present.

This spectrum clearly illustrates the shifts for the ppt$^-$ ligand on complexation to the biquinoline moiety. Figure 19 presents the biquinoline protons only as the ppt$^-$ ligand was deuteriated. Addition of the spectra in Figure 18 and 19 will give the same spectrum as that shown in Figure 17. It has been clearly illustrated here that the use of deuteriation in the elucidation of ^{1}H NMR is highly advantageous. Also from the spectra shown in this chapter we can see that the bpy, phen, biq and ppt$^-$ ligands were all successfully deuteriated and to my knowledge only the bpy ligand has previously been deuteriated. Hence we have shown also that deuteriation is applicable to various heterocyclic ligands.

4.3.4.1 ^{99}Ru NMR of [Ru(bpy)$_2$ppt]$^+$ coordination isomers

The following data was obtained by Gaemers et al[37] of the University of Amsterdam. Recent studies have shown that ^{99}Ru NMR is a powerful tool for the analysis of ruthenium(II) complexes in addition to well established techniques. The data in Figure 20 is a summary of the results obtained for the complexes in this chapter and chapter 3. A comparison is drawn between the pyridine triazole (highlighted in red) complex and the pyrazine triazole (highlighted in blue) complex as shown in chapter 3 and from these complexes we see that the stronger σ-donor N2 coordination site leads to a lower ruthenium chemical shift.

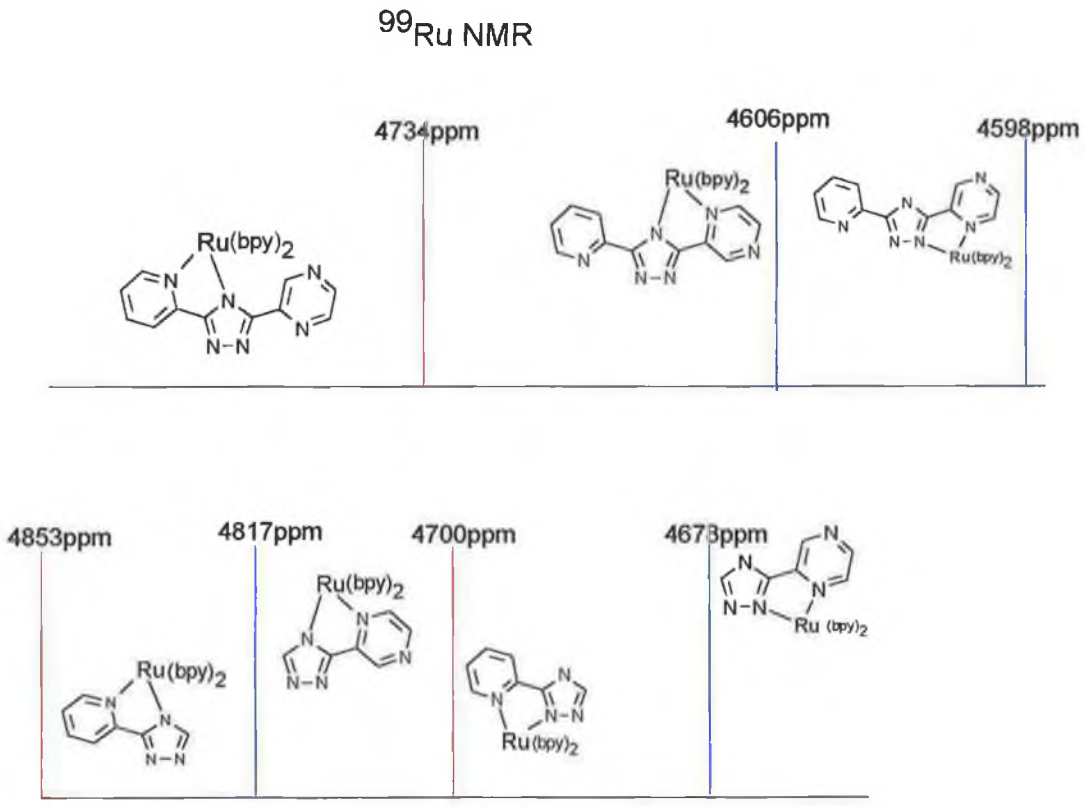

Figure 22 Schematic layout of the Ru shifts in d_3-acetonitrile.

The same applies for the ppt$^-$ complexes an example of which is shown in Figure 27. On going from the N2 to the N4 isomer of the pyrazine-triazole isomer there is a shift of 140 ppm and for the pyridine-triazole isomers a shift of 153 ppm. A similar shift exists for the N2/ N4 pyrazine-bound isomers of the Hppt complex of 136 ppm. This concurs with the redox potentials of these complexes. It may also be noticed that the pyrazine bound isomers of the pztr$^-$ and ppt$^-$ complexes are at lower chemical shifts than that of the pyridine bound which may be compared with the higher redox potentials of the pyrazine complexes. Pyrazine is a greater π-acceptor than pyridine and will cause an upfield shift. This technique may be used in the identification process of coordination isomers in various compounds.

Also for complexes containing polydentate nitrogen ligands it is found that complexes with higher redox potentials have higher ^{99}Ru chemical shifts, possibly allowing the prediction of electronic properties of this type of complex based on ^{99}Ru-NMR spectroscopy. The relevant paper [37] may be found in appendix 1 paper 3. Data gathered for this study is presented in appendix 2.

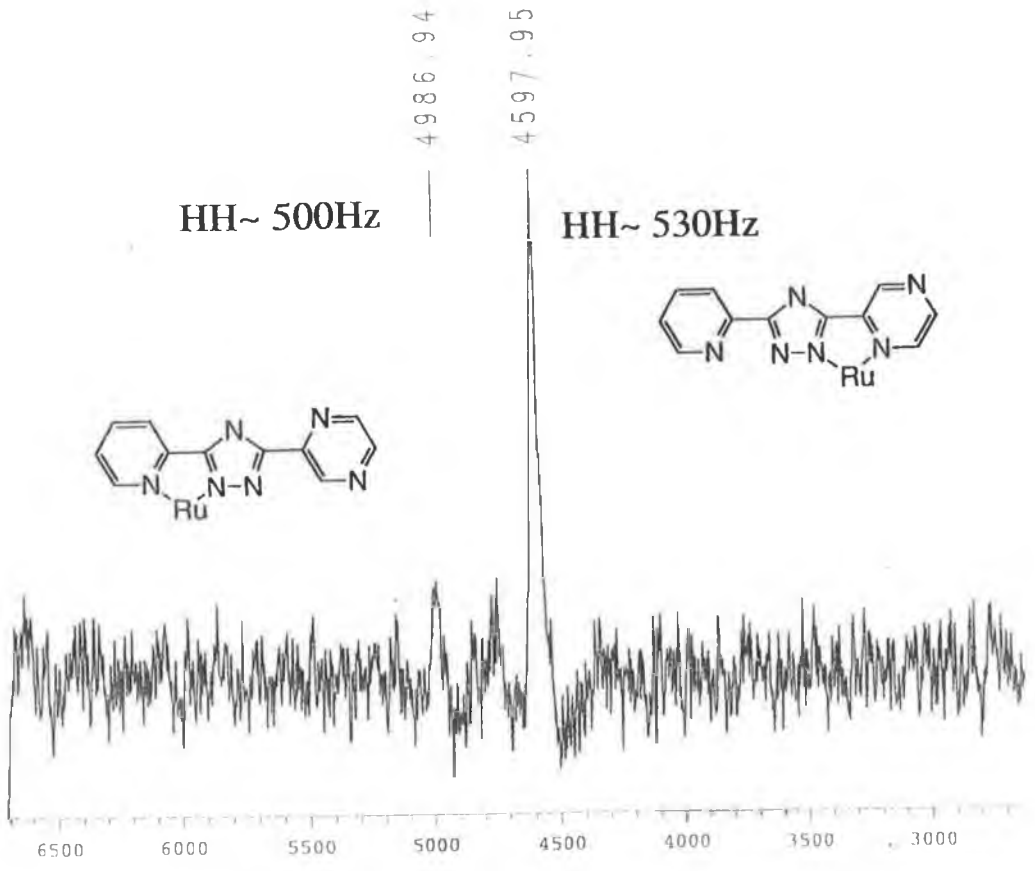

Figure 21 ^{99}Ru NMR spectra of [Ru(bpy)$_2$ppt]$^+$ isomer 2 in d_3-acetonitrile.

4.3.4 Absorption and Emission properties

$[Ru(bpy)_2ppt]^+$

In Table 2 the absorption and emission maxima (298 and 77 K) of the $[Ru(bpy)_2ppt]^+$ complexes and their luminescent lifetimes at room temperature (298K) are listed. As expected the complexes absorb in the visible region (Figure 28) between 350 and 500nm as expected for Ruthenium polypyridyl complexes[38,39,40,41] which is characteristic of their $d\pi$-π^*, metal to ligand charge transfer (MLCT). From the table of results it is evident that deuteriation has no effect on the absorption and emission measurements of the complexes.

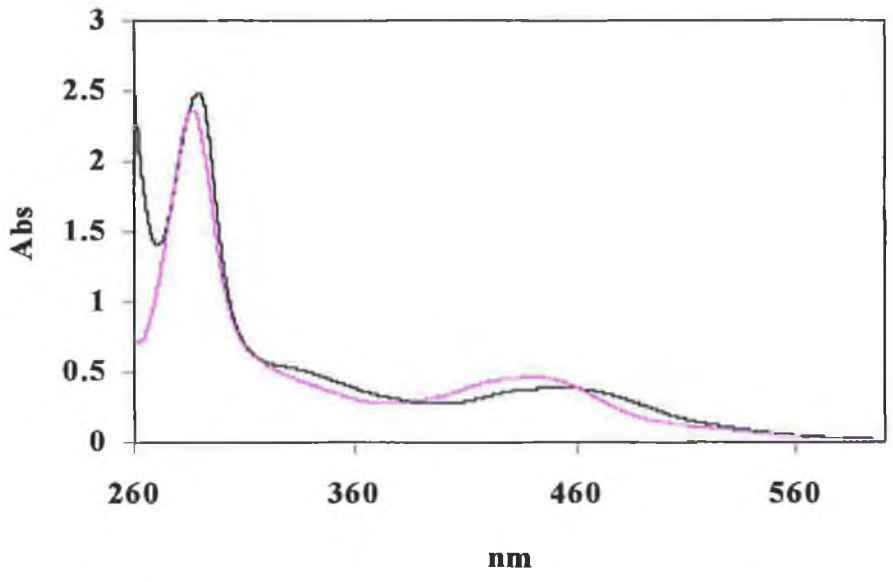

Figure 24 Absorption spectrum of $[Ru(bpy)_2ppt]^+$ (blue, 461 nm) $[Ru(bpy)_2Hppt]^{2+}$ (pink, 441 nm.) in acetonitrile.

Compound	[a]Abs(nm) (log ε)	[a]Em (nm) (298K)	[c]Em (nm) (77K)	[a,b]Lifetime (τ/ns)(298K)
$[Ru(bpy)_2(ppt)]^+$Iso 1	461(4.04)	671	615	217
$[Ru(bpy)_2(Hppt)]^{2+}$Iso 1	441(3.95)	612	580	(---)
$[Ru(bpy)_2(ppt)]^+$Iso 2	457(4.35)	658	600	140
$[Ru(bpy)_2(Hppt)]^{2+}$Iso 2	432(4.13)	669	615	(---)
$[Ru(d_8\text{-}bpy)_2(ppt)]^+$Iso 1	465(4.15)	670	615	220
$[Ru(d_8\text{-}bpy)_2(Hppt)]^{2+}$Iso 1	436(4.20)	612	580	(---)
$[Ru(d_8\text{-}bpy)_2(ppt)]^+$Iso 2	457(4.19)	658	600	130
$[Ru(d_8\text{-}bpy)_2(Hppt)]^{2+}$Iso 2	422(3.99)	669	615	(---)
$[Ru(bpy)_2(d_7\text{-}ppt)]^+$Iso 1	465(3.95)	670	615	580
$[Ru(bpy)_2(d_7\text{-}Hppt)]^{2+}$Iso 1	436(4.02)	613	580	(---)
$[Ru(bpy)_2(d_7\text{-}ppt)]^+$Iso 2	457(4.16)	660	600	110
$[Ru(bpy)_2(d_7\text{-}Hppt)]^{2+}$Iso 2	422(4.05)	670	615	(---)
$[Ru(d_8\text{-}bpy)_2(d_7\text{-}ppt)]^+$Iso 1	465(3.98)	671	615	220
$[Ru(d_8\text{-}bpy)_2(d_7\text{-}Hppt)]^{2+}$Iso 1	436(4.08)	613	580	(---)
$[Ru(d_8\text{-}bpy)_2(d_7\text{-}ppt)]^+$Iso 2	457(3.95)	660	600	165
$[Ru(d_8\text{-}bpy)_2(d_7\text{-}Hppt)]^{2+}$Iso 2	422(4.02)	670	615	(---)

Table 2 Electronic properties of the mononuclear complexes of the partially deuteriated $[Ru(bpy)_2ppt]^+$ coordination isomers [a] measured in acetonitrile, [b] degassed with Argon and [c] 80: 20 ethanol: methanol. Protonation and deprotonation of the complexes were carried out on addition of trifluoroacetic acid or diethylamine respectively. Lifetime error +/- 6 %.

A higher shift in energy is observed on going from $[Ru(bpy)_2ppt]^+$ isomer 1 to isomer 2 due to the better π-acceptor capabilities of the pyrazine ring compared with that of the pyridine ring. Emission occurs from ^{3}MLCT excited states[42,43]. The emission values for these complexes are found between 600 and 680 nm. The acid/base chemistry of these complexes influences its electronic properties. Protonation of the complexes arises in a shift to higher energy of the MLCT bands both in the absorption and emission values which is due to a decrease in σ-donor capacity of the protonated ligand resulting in destabilisation of the d-orbitals[19,21,44]. The emission values obtained at low temperature are found at higher energy than those measured at room temperature. The blue shift on going from the 298 K emission measurements to the 77 K analogues is based on the fact that at low temperature the excited state energy levels experience less vibrational energy loss and this results in an increase of emitting energy of the complex.

$[Ru(phen)_2ppt]^+$

In Table 3 the absorption and emission maxima (298 and 77 K) of the $[Ru(phen)_2ppt]^+$ complexes and their luminescent lifetimes at room temperature (298K) are listed. The electronic properties of the $[Ru(phen)_2ppt]^+$ complexes are generally not that different from those of the $[Ru(bpy)_2ppt]^+$ complexes, however a blue shift in the MLCT band of the absorption and emission spectra exists as phenanthroline is a greater σ-donor than that of bipyridyl. Figure 23 is an example of an absorption spectra of $[Ru(phen)_2ppt]^+$ protonated and deprotonated.

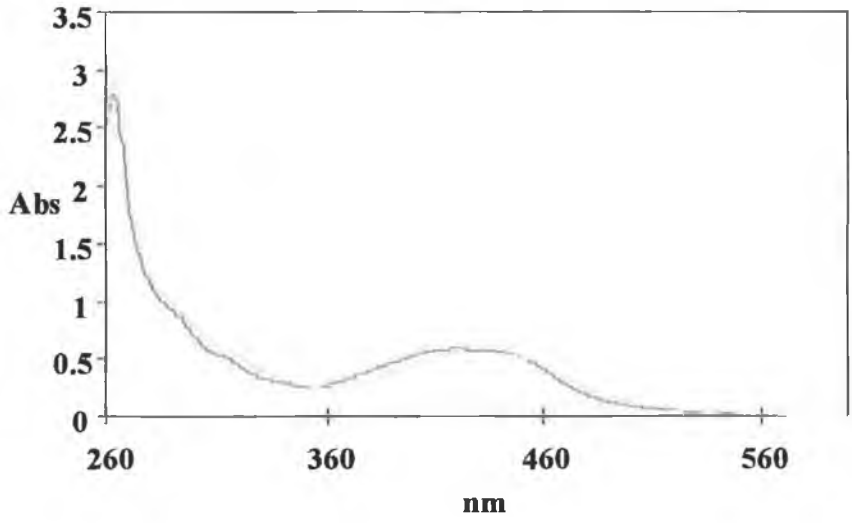

Figure 25 Absorption spectra for [Ru(phen)$_2$ppt]$^+$ (yellow, 429 nm) [Ru(phen)$_2$Hppt]$^{2+}$ (red, 404 nm.) in acetonitrile.

Protonation causes an increase in energy and a blue shift compared to the deprotonated species. Low temperature emission measurements are at higher energy than the values measured at room temperature. The effect of substituting bpy with phen will be further discussed in the luminescent lifetime section, however, no dramatic deviation from the bpy complexes is expected for the phen analogues.

[Ru(biq)$_2$ppt]$^+$

In Table 4 the absorption and emission maxima (298 and 77 K) of the [Ru(biq)$_2$ppt]$^+$ complexes and their luminescent lifetimes at room temperature (298 K) are listed.

Compound	[a]Abs (nm) (log ε)	[a]Em (nm) (298K)	[c]Em (nm) (77K)	[a,b]Lifetime (τ/ns)(298K)
$[Ru(phen)_2(ppt)]^+$Iso 1	429(3.95)	658	592	650
$[Ru(phen)_2(Hppt)]^{2+}$Iso 1	404(3.99)	610	569	(---)
$[Ru(phen)_2(ppt)]^+$Iso 2	428(3.87)	655	592	170
$[Ru(phen)_2(Hppt)]^{2+}$Iso 2	407(3.82)	630	567	(---)
$[Ru(d_8\text{-phen})_2(ppt)]^+$Iso 1	429(3.97)	658	592	950
$[Ru(d_8\text{-phen})_2(Hppt)]^{2+}$Iso 1	404(3.89)	610	569	(---)
$[Ru(d_8\text{-phen})_2(ppt)]^+$Iso 2	428(3.79)	655	592	335
$[Ru(d_8\text{-phen})_2(Hppt)]^{2+}$Iso 2	407(3.85)	630	567	(---)
$[Ru(phen)_2(d_7\text{-ppt})]^+$Iso 1	429(3.90)	658	592	640
$[Ru(phen)_2(d_7\text{-Hppt})]^{2+}$Iso 1	404(3.88)	610	569	(---)
$[Ru(phen)_2(d_7\text{-ppt})]^+$Iso 2	428(3.78)	655	592	215
$[Ru(phen)_2(d_7\text{-Hppt})]^{2+}$Iso 2	407(3.85)	630	567	(---)
$[Ru(d_8\text{-phen})_2(d_7\text{-ppt})]^+$Iso 1	429(3.76)	658	592	480
$[Ru(d_8\text{-phen})_2(d_7\text{-Hppt})]^{2+}$Iso 1	404(3.75)	610	569	(---)
$[Ru(d_8\text{-phen})_2(d_7\text{-ppt})]^+$Iso 2	428(3.72)	655	592	1000
$[Ru(d_8\text{-phen})_2(d_7\text{-Hppt})]^{2+}$Iso 2	406(3.80)	630	567	(---)

Table 3 Electronic properties of the mononuclear complexes of the partially deuteriated $[Ru(phen)_2ppt]^+$ coordination isomers [a]measured in acetonitrile, [b]degassed with Argon and [c] 80: 20 ethanol: methanol. Protonation and deprotonation of the complexes were carried out on addition of trifluoroacetic acid or diethylamine respectively. Lifetime error +/- 6 %.

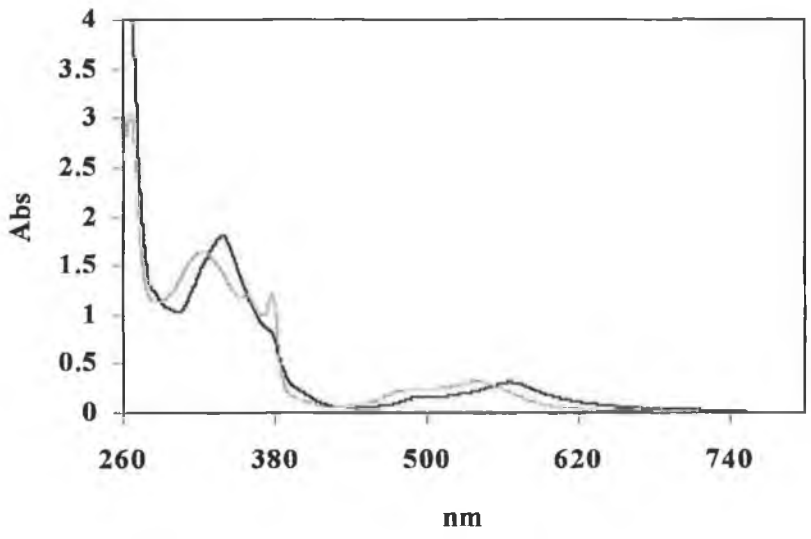

Figure 26 Absorption spectra for $[Ru(biq)_2ppt]^+$ (blue, 576 nm) $[Ru(biq)_2Hppt]^{2+}$ (pink, 555 nm.) in acetonitrile.

Biquinoline is a weaker σ-donor than bipyridyl or phenanthroline and this leads to a decrease in energy, hence the MLCT band is red shifted to 550nm. The other peaks observed in the absorption spectrum are LC (ligand centred), π-π* in the UV region at 260 nm. The absorption band at 370 nm is also assigned to MLCT (metal to ligand charge transfer) d π-π* and there also may be contributions from LMCT (ligand to metal charge transfer) π-d π*. The absorption and emission values are very sensitive towards deprotonation of the triazole ring and upon deprotonation the MLCT is shifted to a lower energy. On going from ground state to excited state there is a red shift in energy of > 200 nm.

Compound	[a]Abs (nm) (log ε)	[a]Em (nm) (298K)	[c]Em (nm) (77K)	[a,b]Lifetime (τ/ns)(298K)
$[Ru(biq)_2(ppt)]^+$Iso 1	576(4.20)	810	765	340
$[Ru(biq)_2(Hppt)]^{2+}$Iso 1	555(4.25)	786	723	(---)
$[Ru(biq)_2(ppt)]^+$Iso 2	550(4.16)	790	739	260
$[Ru(biq)_2(Hppt)]^{2+}$Iso 2	542(4.17)	770	718	(---)
$[Ru(d_{12}\text{- biq})_2(ppt)]^+$Iso 1	574(4.18)	810	765	320
$[Ru(d_{12}\text{- biq})_2(Hppt)]^{2+}$Iso 1	554(4.20)	786	723	(---)
$[Ru(d_{12}\text{- biq})_2(ppt)]^+$Iso 2	551(4.19)	790	739	240
$[Ru(d_{12}\text{- biq})_2(Hppt)]^{2+}$Iso 2	542(4.15)	770	718	(---)
$[Ru(biq)_2(d_7\text{-ppt})]^+$Iso 1	574(4.18)	810	765	320
$[Ru(biq)_2(d_7\text{-Hppt})]^{2+}$Iso 1	556(4.16)	786	723	(---)
$[Ru(biq)_2(d_7\text{-ppt})]^+$Iso 2	553(4.12)	790	739	380
$[Ru(biq)_2(d_7\text{-Hppt})]^{2+}$Iso 2	540(4.15)	770	718	(---)
$[Ru(d_{12}\text{- biq})_2(d_7\text{-ppt})]^+$Iso 1	575(4.20)	810	765	140
$[Ru(d_{12}\text{- biq})_2(d_7\text{-Hppt})]^{2+}$Iso 1	553(4.22)	786	723	(---)
$[Ru(d_{12}\text{- biq})_2(d_7\text{-ppt})]^+$Iso 2	552(4.19)	790	739	185
$[Ru(d_{12}\text{- biq})_2(d_7\text{-Hppt})]^{2+}$Iso 2	542(4.21)	770	718	(---)

Table 4 Electronic properties of the mononuclear complexes of the partially deuteriated $[Ru(biq)_2ppt]^+$ coordination isomers [a]measured in acetonitrile, [b]degassed with Argon and [c] 80: 20 ethanol: methanol. Protonation and deprotonation of the complexes were carried out on addition of trifluoroacetic acid or diethylamine respectively. Lifetime error +/ - 6 %.

The low temperature emission measurements are shifted to a higher energy due to less efficient vibrational energy loss in a frozen medium. A shift to higher energy is observed for isomer 2 due to the better π-acceptor capabilities of the pyrazine ring as opposed to the pyridine ring (isomer 1).

It is hoped that using ligands such as these that a photostable, regenerative complex will be achieved. Sufficient perturbation of the ^{3}MC state is required in order to stabilise such Ru(II) complexes. One such complex has been observed but only in its deprotonated state[45]. The complex $[Ru(biq)_2(3Mepytr)]^+$ was found to be photostable but however this property was pH dependent and on protonation photolabilisation of the ligand 3Mepytr was observed.

4.3.6 Luminescent lifetime measurements

Luminescent measurements at room temperature of $[Ru(bpy)_2ppt]^+$, $[Ru(phen)_2ppt]^+$ and $[Ru(biq)_2ppt]^+$ are presented in Table 2, Table 3 and Table 4 respectively. The protonated species were not investigated in this study as they are more sensitive to pH than the deprotonated form and are more difficult to ascertain. A series of selectively deuteriated complexes were synthesised in order for the excited state of the complexed ppt$^-$ monomers to be located. All the measurements were repetitively carried out under the same conditions. It was hoped that by selectively deuteriating the ligands of the ppt$^-$ complexes on excitation a visible increase would be observed if the excited state was based on the deuteriated ligand.

This increase in lifetime is related to the non-radiative relaxation of the excited state, k_{nr},k_{nr} may be derived from the equation;

$$\tau = k_r + k_{nr}$$

where, τ is the luminescent lifetime,

k_r is the radiative decay and k_{nr} is the non-radiative decay

The relationship with deuteriation and longer lifetimes is based on the phenomena of slower vibrational relaxation of the excited electron on the bipyridyl. Inthis situation the C-H stretch are replaced with the C-D stretch on the bipyridyls. It has been recognised by Siebrands theory[46,47] that C-H vibrations are important promoting modes for transition and hence the deuteriation will cause a dramatic change on these transitions.

For the complex $[Ru(bpy)_2ppt]^+$ the lifetimes for the pyridine bound isomer will be discussed first. Based on the lifetimes of the first three analogues $[Ru(bpy)_2ppt]^+$, $[Ru(d_8\text{-}bpy)_2ppt]^+$ and $[Ru(bpy)_2d_7\text{-}ppt]^+$, it would suggest that the excited state is based on the ppt^- ligand. This is based on the increase of lifetime on going from $[Ru(bpy)_2ppt]^+$, 217 ns to $[Ru(bpy)_2d_7\text{-}ppt]^+$, 580 ns. The complex $[Ru(d_8\text{-}bpy)_2ppt]^+$ has a lifetime of 220 ns, hence no change when the bpy is deuteriated, however, the complex $[Ru(d_8\text{-}bpy)_2d_7\text{-}ppt]^+$ gives a lifetime of 220 ns which does not correlate with the other results as it should show some increase if the Hppt ligand is deuteriated. The only suggestion that may be made without further studies is that for the fully deuteriated complex the excited states are weakly coupled as previously seen for the $pztr^-$ complexes. If this is the case there may be a deactivation process occurring via the ^{3}MLCT of the bpy when the complex is fully deuteriated, hence there would be no increase observed.

The pyrazine bound isomer of $[Ru(bpy)_2ppt]^+$ had no pattern at all. The lifetimes obtained were as follows $[Ru(bpy)_2ppt]^+$; 140 ns, $[Ru(d_8\text{-}bpy)_2ppt]^+$; 130 ns, $[Ru(bpy)_2d_7\text{-}ppt]^+$; 110 ns and $[Ru(d_8\text{-}bpy)_2d_7\text{-}ppt]^+$; 165 ns. Because this is the pyrazine bound isomer the photophysics would be expected to be complexed based, based on the results observed for the $[Ru(bpy)_2pztr]^+$ complexes in chapter 3. The use of the selective deuteriation has given no insight into the photophysical properties of this isomer, all that can be suggested at this moment is that there is two deactivation pathways competing with each other which limits the effect of deuteriation on increasing the lifetime.

The phenanthroline containing complexes are slightly better in that there is some sort of pattern involved after selective deuteriation. For the pyridine bound isomer of

$[Ru(phen)_2ppt]^+$ it would be suggested that the excited state of the complex is based on the phenanthroline ligand as the lifetime of $[Ru(phen)_2ppt]^+$ is 650 ns, $[Ru(d_8\text{-}phen)_2ppt]^+$ is 950 ns and $[Ru(phen)_2d_7\text{-}ppt]^+$ is 640 ns, hence an increase is observed for the deuteriated phenanthroline complex. However, the fully deuteriated complex $[Ru(d_8\text{-}phen)_2d_7\text{-}ppt]^+$ has a lifetime of 480 ns. Again it may be suggested that in the case of fully deuteriated mixed ligand systems that there is a competitive deactivation process occurring which results in a decrease in the lifetime. The pyrazine bound isomer of $[Ru(phen)_2ppt]^+$ has much shorter lifetimes than that of the pyridine bound. Again it may be suggested that the excited state lifetime is based on the phenanthroline ligand as the lifetimes show an increase for the deuteriated phen complex as the lifetime of $[Ru(phen)_2ppt]^+$ is 170 ns, $[Ru(d_8\text{-}phen)_2ppt]^+$ is 335 ns, $[Ru(phen)_2d_7\text{-}ppt]^+$ is 210 ns and the fully deuteriated complex $[Ru(d_8\text{-}phen)_2d_7\text{-}ppt]^+$ is 1000 ns. For the whole series of substituted ligands this is the only fully deuteriated complex to give an increase in lifetime. This lifetime of 1000 ns may be attributed to the deuteriated phenanthroline and it may suggest that when the Hppt was deuteriated that the excited states of the ppt^- and the phen were isolated from each other allowing for a clear deactivation process from the phen ^{3}MLCT. For the $[Ru(d_8\text{-}phen)_2ppt]^+$ complex the lifetime is only 335 ns and this may be due to an interaction of weakly coupled excited states, when only the phen is deuteriated.

The biquinoline analogues were also prepared and the results were also quite scattered. For the pyridine bound isomer of $[Ru(biq)_2ppt]^+$ a lifetime of 340 ns was obtained. For the rest of this series the lifetimes are 320 ns for $[Ru(d_{12}\text{-}biq)_2ppt]^+$, 320 ns for $[Ru(biq)_2 d_7\text{-}ppt]^+$ and 140 ns for $[Ru(d_{12}\text{-}biq)_2d_7\text{-}ppt]^+$. No conclusions may be determined on the location of the excited state from these results. A similar pattern is observed for the pyrazine bound isomer.

The use of selective deuteriations may have applications in the location of the excited state, but the photophysical properties of pyrazine-triazole and ligands containing pyrazine-triazole have turned out to be more complicated than previously thought.

Hence, a larger investigation will have to be carried out on this series of complexes by temperature dependence luminescent studies and resonance raman in order for a model of the photophysical properties of the ppt$^-$ complexes to be derived.

4.3.7 Acid-Base properties

The acid-base properties for the complexes $[Ru(bpy)_2ppt]^+$, $[Ru(phen)_2ppt]^+$, $[Ru(biq)_2ppt]^+$ are listed in Table 5, Table 6 and Table 7 respectively. The following equations were used to determine the pK_a^* of the excited species.

$$pK_a^*(1) = pH_i + \log(\tau_a/\tau_b) \qquad \text{eqn. 1}$$

where τ_a is the lifetime of the protonated species and τ_b is the lifetime of the deprotonated species.

The point of inflection in the emission titration curves do not represent real excited-state pK_a values, or pK_a^*, because they need to be corrected for different lifetimes of the protonated and deprotonated species[48]. An estimate of the pK_a^* value can also be obtained from the ground-state pK_a values from the absorption titration and the emission energies of the protonated and deprotonated species, using the Forster equation, equation 2 [49,50,51,52]

$$pK_a^*(2) = pk_a + 0.625(\nu_a - \nu_b) \qquad \text{eqn. 2}$$

where ν_a and ν_b are the emission maxima of the deprotonated and protonated species respectively and T is the experimental temperature. (This equation is susceptible to error due to the stokes shifts in the emission spectra).

The pK_a of the ground state for both isomers of the $[Ru(bpy)_2ppt]^+$ complex is lower than in the excited state. This suggests that the excited state is based on the ppt^- ligand. This assumption is based on the knowledge that upon excitation of a ruthenium polypyridyl complex, a metal-based electron is promoted to a ligand-based π^* orbital.

Compound	pK_a	pH_i*	pK_a*(1)	pK_a*(2)
$[Ru(bpy)_2(ppt)]^+$ Iso 1	2.7 (2.7)	3.0	2.26	2.82
$[Ru(bpy)_2(ppt)]^+$ Iso 2	3.6 (3.8)	3.8	4.18	3.57
$[Ru(d_8\text{-bpy})_2(ppt)]^+$ Iso 1	2.7	3.0	2.15	2.82
$[Ru(d_8\text{-bpy})_2(ppt)]^+$ Iso 2	3.6	3.8	4.01	3.57
$[Ru(bpy)_2(bpt)]^+$	*4.2*	*3.9*	*3.3*	*2.8*
$[Ru(bpy)_2(bpzt)]^+$	*2.0*	*4.9*	*3.8*	*1.3*

Table 5 Ground state pK_a and excited state pK_a * values of the mononuclear ppt complexes containing bipyridyl and some related compounds. pK_a *(1) and pK_a *(2) were calculated using eqn. 1 and eqn. 2 respectively. All measurements are carried out in Britton Robinson buffer. All values ± 0.1. Values in italics[31].

This results in the creation of a ruthenium centre with a formal valence of 3+. A decreased basicity is then explained by a reduced electron density on the ppt^- ligand as a result of electron donation to the metal centre. The fact that the pK_a* values are higher or equal to the pK_a values suggest that the electron is excited into the ppt^- ligand so that the ligand does not just act as a spectator ligand. Similar acid-base behaviour was observed for the mononuclear $[Ru(bpy)_2bpzt]^+$ [31] and $[Ru(bpy)_2pztr]^+$ [53]. Hence, it may be suggested that the pK_a of the ppt^- complex is strongly influenced by the pyrazine ring especially for the pyrazine bound isomer.

The values for the phen containing analogues are listed in Table 6. The pK_a values for the ground state $[Ru(phen)_2ppt]^+$ isomers are more acidic or almost equivalent to that of the excited state suggesting that the excited state electron is ppt^- based.

Compound	pK_a	pH_i*	pK_a*(1)	pK_a*(2)
$[Ru(phen)_2(ppt)]^+$ Iso 1	2.5	2.8	---	2.6
$[Ru(phen)_2(ppt)]^+$ Iso 2	3.4	3.6	---	3.45
$[Ru(d_8\text{-phen})_2(ppt)]^+$ Iso 1	2.5	2.8	---	2.6
$[Ru(d_8\text{-phen})_2(ppt)]^+$ Iso 2	3.4	3.6	---	3.45
$[Ru(phen)_2(bpt)]^+$	*3.4*	*3.9*	*3.3*	*3.7*

Table 6 Ground state pK_a and excited state pK_a * values of the mononuclear ppt complexes containing phenanthroline. pK_a *(1) and pK_a *(2) were calculated using eqn. 1 and eqn. 2 respectively. All measurements are carried out in Britton Robinson buffer. All values ± 0.1. Values in italics[31].

Compound	pK_a	pH_i*	pK_a*(1)	pK_a*(2)
$[Ru(biq)_2(ppt)]^+$ Iso 1	4.0	3.3	---	4.05
$[Ru(biq)_2(ppt)]^+$ Iso 2	3.34	1.95	---	3.39
$[Ru(d_{12}\text{-biq})_2(ppt)]^+$ Iso 1	4.0	3.3	---	4.05
$[Ru(d_{12}\text{-biq})_2(ppt)]^+$ Iso 2	3.35	1.98	---	3.39

Table 7 Ground state pK_a and excited state pK_a * values of the mononuclear ppt complexes containing biquinoline. pK_a *(1) and pK_a *(2) were calculated using eqn. 1 and eqn. 2 respectively. All measurements are carried out in Britton Robinson buffer. All values ± 0.1.

For the complex $[Ru(bpy)_2bpt]^+$ the ground state was found to be less acidic than the excited state and this lead to the excited state electron being bpy based. The analogous phen complex $[Ru(phen)_2bpt]^+$ possessed the same pK_a values as the bpy species and hence the excited state electron was based on the phen. The pK_a values of $[Ru(bpy)_2ppt]^+$ and $[Ru(phen)_2ppt]^+$ do not differ greatly and this may be attributed to

the similarity in the electronic properties of the bpy and phen ligands. The pK_a values for the isomers of the complex $[Ru(biq)_2ppt]^+$ and their deuteriated analogues are listed in Table 7. The pK_a values tell a different story for the $[Ru(biq)_2ppt]^+$ isomers. In all cases the excited state is more acidic than the ground state and this would suggest that the excited state electron is based on the biquinoline. The pK_a values of all the complexes in general reflect the σ-donor and π-acceptor properties of the ligands with $[Ru(phen)_2ppt]^+$ having the more acidic pK_a values due to its good σ-donor properties and $[Ru(biq)_2ppt]^+$ having the more basic pK_a values due to the biq π-accepting properties.

4.3.8 Electrochemical properties

The electrochemical potentials obtained for all the $[Ru(bpy)_2ppt]^+$ complexes are shown in Table 8. It may be observed that the isomer 2 species has a metal-based oxidation at a higher potential than the analogous isomer 1. This is due to the weaker σ-donor properties of the pyrazine ligand, less electron density is present on the metal and therefore it is harder to oxidise[54,55]. The reduction potentials observed for the mononuclear deprotonated complexes may be assigned to the bipyridyls[27,56]. The metal-based oxidation potential of the $[Ru(bpy)_2ppt]^+$ is significantly lower than that of the $[Ru(bpy)_3]^{2+}$, which has an oxidation potential of 1.26 v SCE[57].

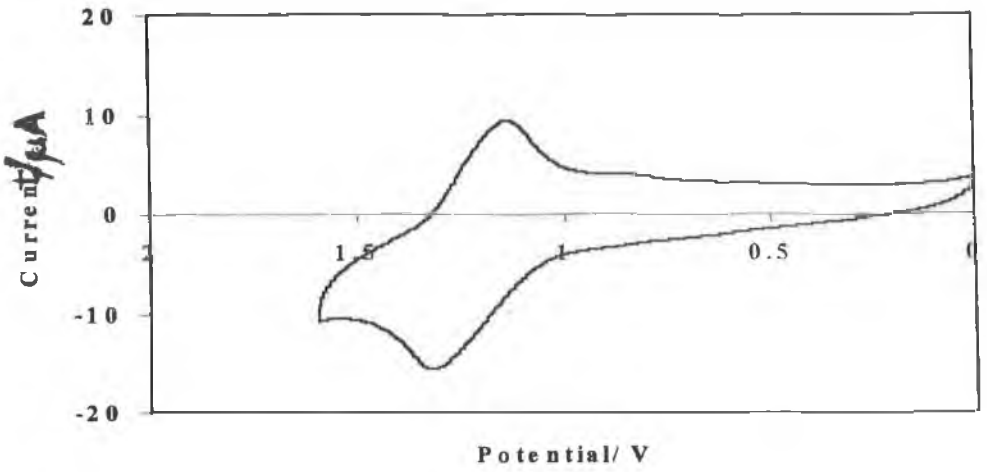

Figure 25 ***Cylic voltammongram of $[Ru(bpy)_2Hppt]^{2+}$ isomer 1, 0.1 M TEAP in acetonitrile with one drop of H_2SO_4 and a scanrate of 0.1 V/ sec.***

This is due to the increased σ-donor ability of the deprotonated triazole ligand compared to that of the bpy. An increase in oxidation potential is observed when the triazole ligand is protonated. This is due to the decreased σ-donor strength abilities of the protonated ligand, with a consequent decrease in the electron density at the metal centre. This means that the metal centre is more difficult to oxidise than in the deprotonated case. The oxidation and reduction potentials for the protonated and deprotonated phen complexes are listed in Table 9.

Compound	Oxid. Pot. (V) (V vs S.C.E.)	Red. Pot. (V) (V vs S.C.E.)
$[Ru(bpy)_2(ppt)]^+$ Iso 1	0.95	-1.45, -1.70
$[Ru(bpy)_2(Hppt)]^{2+}$ Iso 1	1.25	---
$[Ru(bpy)_2(ppt)]^+$ Iso 2	1.05	-1.50, -1.75
$[Ru(bpy)_2(Hppt)]^{2+}$ Iso 2	1.20	---
$[Ru(d_8\text{-}bpy)_2(ppt)]^+$ Iso 1	0.95	-1.45, -1.70
$[Ru(d_8\text{-}bpy)_2(Hppt)]^{2+}$ Iso 1	1.25	---
$[Ru(d_8\text{-}bpy)_2(ppt)]^+$ Iso 2	1.05	-1.50, -1.75
$[Ru(d_8\text{-}bpy)_2(Hppt)]^{2+}$ Iso 2	1.20	---
$[Ru(d_8\text{-}bpy)_2(d_7\text{-}ppt)]^+$ Iso 1	0.95	-1.45, -1.70
$[Ru(d_8\text{-}bpy)_2(d_7\text{-}ppt)]^{2+}$ Iso 1	1.25	---
$[Ru(d_8\text{-}bpy)_2(d_7\text{-}ppt)]^+$ Iso 2	1.05	-1.50, -1.75
$[Ru(d_8\text{-}bpy)_2(d_7\text{-}ppt)]^{2+}$ Iso 2	1.20	---

Table 8 Electrochemical data of the Ru(II) bipyridyl complexes containing the Hppt ligand obtained in MeCN containing 0.1M TEAP. Values obtained by cyclic voltammetry. Potentials in Volts versus S.C.E. Protonation occurred via addition of 1 drop of H_2SO_4. Scanrate of 0.1 V/ sec.

Compound	Oxid. Pot. (V) (V vs S.C.E.)	Red. Pot. (V) (V vs S.C.E.)
$[Ru(phen)_2(ppt)]^+$ Iso 1	0.96	-1.48, -1.78
$[Ru(phen)_2(Hppt)]^{2+}$ Iso 1	1.30	---
$[Ru(phen)_2(ppt)]^+$ Iso 2	1.06	-1.52, -1.80
$[Ru(phen)_2(Hppt)]^{2+}$ Iso 2	1.27	---
$[Ru(d_8\text{-phen})_2(ppt)]^+$ Iso 1	0.95	-1.48, -1.78
$[Ru(d_8\text{-phen})_2(Hppt)]^{2+}$ Iso 1	1.31	---
$[Ru(d_8\text{-phen})_2(ppt)]^+$ Iso 2	1.07	-1.52, -1.80
$[Ru(d_8\text{-phen})_2(Hppt)]^{2+}$ Iso 2	1.25	---
$[Ru(phen)_2(d_7\text{-ppt})]^+$ Iso 1	0.95	-1.48, -1.78
$[Ru(phen)_2(d_7\text{-ppt})]^{2+}$ Iso 1	1.29	---
$[Ru(phen)_2(d_7\text{-ppt})]^+$ Iso 2	1.06	-1.52, -1.80
$[Ru(phen)_2(d_7\text{-ppt})]^{2+}$ Iso 2	1.28	---
$[Ru(d_8\text{-phen})_2(d_7\text{-ppt})]^+$ Iso 1	0.97	-1.48, -1.78
$[Ru(d_8\text{-phen})_2(d_7\text{-ppt})]^{2+}$ Iso 1	1.30	---
$[Ru(d_8\text{-phen})_2(d_7\text{-ppt})]^+$ Iso 2	1.05	-1.52, -1.80
$[Ru(d_8\text{-phen})_2(d_7\text{-ppt})]^{2+}$ Iso 2	1.27	---

Table 9 Electrochemical data of the Ru(II) phenanthroline complexes containing the Hppt ligand obtained in MeCN containing 0.1M TEAP. Values obtained by cyclic voltammetry. Potentials in Volts versus S.C.E. Protonation occurred via addition of 1 drop of H_2SO_4. Scanrate of 0.1 V/ sec.

Compound	Oxid. Pot. (V) (V vs S.C.E.)	Red. Pot. (V) (V vs S.C.E.)
$[Ru(biq)_2(ppt)]^+$ Iso 1	1.06	-1.04, -1.35
$[Ru(biq)_2(Hppt)]^{2+}$ Iso 1	1.32	---
$[Ru(biq)_2(ppt)]^+$ Iso 2	1.15	-1.00, -1.45
$[Ru(biq)_2(Hppt)]^{2+}$ Iso 2	1.30	---
$[Ru(d_{12}\text{-}biq)_2(ppt)]^+$ Iso 1	1.05	-1.04, -1.35
$[Ru(d_{12}\text{-}biq)_2(Hppt)]^{2+}$ Iso 1	1.31	---
$[Ru(d_{12}\text{-}biq)_2(ppt)]^+$ Iso 2	1.16	-1.00, -1.45
$[Ru(d_{12}\text{-}biq)_2(Hppt)]^{2+}$ Iso 2	1.32	---
$[Ru(biq)_2(d_7\text{-}ppt)]^+$ Iso 1	1.05	-1.04, -1.35
$[Ru(biq)_2(d_7\text{-}ppt)]^{2+}$ Iso 1	1.35	---
$[Ru(biq)_2(d_7\text{-}ppt)]^+$ Iso 2	1.12	-1.00, -1.45
$[Ru(biq)_2(d_7\text{-}ppt)]^{2+}$ Iso 2	1.31	---
$[Ru(d_{12}\text{-}biq)_2(d_7\text{-}ppt)]^+$ Iso 1	1.06	-1.04, -1.35
$[Ru(d_{12}\text{-}biq)_2(d_7\text{-}ppt)]^{2+}$ Iso 1	1.32	---
$[Ru(d_{12}\text{-}biq)_2(d_7\text{-}ppt)]^+$ Iso 2	1.14	-1.00, -1.45
$[Ru(d_{12}\text{-}biq)_2(d_7\text{-}ppt)]^{2+}$ Iso 2	1.30	---

Table 10 Electrochemical data of the Ru(II) biquinoline complexes containing the Hppt ligand obtained in MeCN containing 0.1M TEAP. Values obtained by cyclic voltammetry. Potentials in Volts versus S.C.E. Protonation occurred via addition of 1 drop of H_2SO_4. Scanrate of 0.1 V/ sec.

On comparing the $[Ru(phen)_2ppt]^+$ with the $[Ru(bpy)_2ppt]^+$ there is a shift to a higher potential for the phen complexes, which is particularly observed in the case of the protonated species. This shift has been previously observed for the complexes $[Ru(bpy)_2bpt]^+$ and $[Ru(phen)_2bpt]^+$[31].

The complexes containing biquinoline are listed in Table 10. It may be observed that the metal based oxidation potentials for the biq containing complexes are higher than those of bpy or phen. The σ-donor properties of biq are significantly than that of bpy or phen leading to a raise of the oxidation potential (i.e. stabilisation of the d-orbitals). The reduction potentials of the biq complexes are significantly less negative than those of the bpy and phen complexes, due to the strong π-accepting properties of the biq ligand. All complexes exhibit reversible oxidation and reduction processes as deduced from the cyclic voltammograms. Deuteriation does not appear to affect the electrochemical properties of Ru(II) polypyridyl complexes.

4.3.9 X-Ray Crystallography of $[Ru(bpy)_2ppt]^+$ pyrazine bound

Figure 26 illustrated the crystal structure of the N2 of the triazole to the pyrazine bound coordination isomer of $[Ru(bpy)_2ppt]^+$.

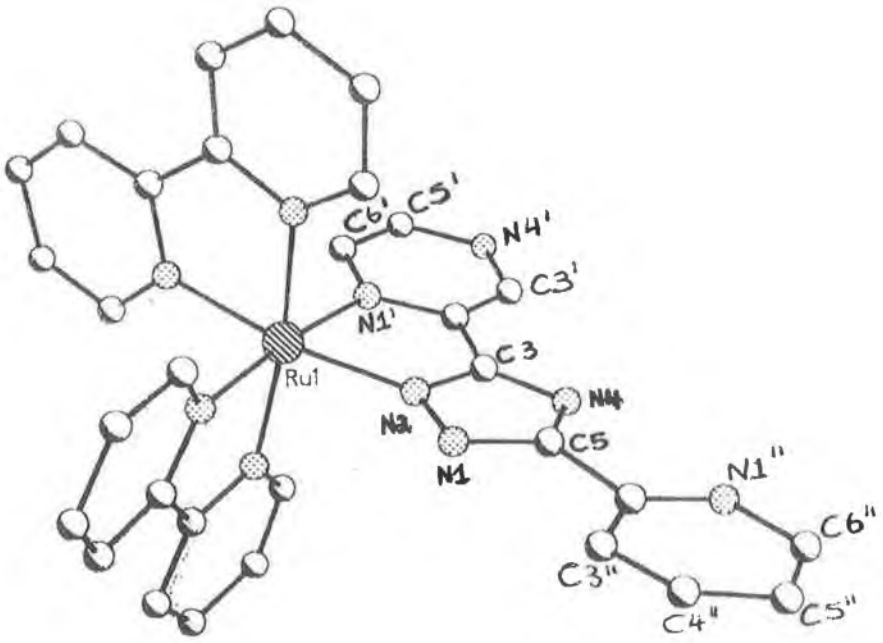

Figure 26 X-Ray Crystallography of $[Ru(bpy)_2ppt]^+$ (N2 of the triazole to the pyrazine ring coordination).

The structure could not be solved to great detail due to spatial disorders in the crystal lattice. The quality of the crystal prevented bond length and angles from being calculated. However, the data obtained is sufficient for the confirmation of the coordination site of isomer 2 (N2 bound to the pyrazine). A comparison of the bond lengths and angles of this structure with that of the $[Ru(bpy)_2bpt]^+$ or $[Ru(bpy)_2bpzt]^+$ would be desirable but unfortunately the data were not collected for this structure. The data were collected under the following conditions: Temperature -90^0C, Instrument: Cappa CCD, Phi-Scan (180 frames, $\Delta phi = 1^0$, t = 30 s per frame).

4.4 References

1 V. Balzani and F. Scandola, Supramolecular Photochemistry, Ellis Horwood, **1991**.

2 J.R. Norris and P. Gast, J. Photochem., **1985**, *29*, 185.

3 V. Balzani, Pure and Appl. Chem., **1990**, *62*, 6, 1099.

4 V. Balzani, L Moggi and F. Scandola, Supramolecular Photochemistry, Reidel publishing company, **1987**, 1.

5 S. Campagna, G. Denti, S. Serroni, M. Ciano and V. Balzani, Inorg. Chem., **1991**, *30*, 3728.

6 T.J. Meyer, Pure and Appl. Chem., **1986**, *58*, (9), 1193.

7 J. Van Houten and R.J. Watts, J. Am. Chem. Soc., **1976**, *98*, (16), 4853.

8 M.A. Ollino and A.J. Rest, J. Photochem and Photobiol., A:Chem, **1992**, *69*, 73.

9 Y. Kawanishi, N. Kitamura and S. Tazuke, Inorg. Chem., **1989**, *28*, 2968.

10 W.F. Wacholtz, R.A. Auerbach and R.H. Schmehl, Inorg. Chem., **1987**, *26*, 2989.

11 J.R. Kirchoff, D.R. Mc Millan, P.A. Marnot and J.P. Sauvage, J. Am. Chem. Soc., **1985**, *107*, 1138.

12 F. Barigelletti, A. Juris, V. Balzani, P. Belser and A von Zelewsky, Inorg. Chem., **1987**, *26*, 1138.

13 M. Haga, Inorg. Chim. Acta., **1980**, *45*, 183.

14 A.M. Bond and M. Haga, Inorg. Chem., **1986**, *25*, 4507.

15 P. Day and N. Saunders, J. Chem. Soc., A, **1967**, 1536.

16 J.D. Peterson, W.R. Murphy Jnr., R. Sahai, K.J. Brewer, R.R. Ruminski, Coord. Chem. Rev., **1985**, *64*, 261.

17 Y. Fuchs, S. Lofters, T. Deiter, W. Shi, R. Morgan, T.C. Strekas, H.D. Gaffney and A.D. Baker, J. Am. Chem. Soc., **1987**, *109*, 2691.

18 S. Ernst, V. Kasack and W. Kaim, Inorg. Chem., **1988**, *27*, 1146.

19 R. Hage, A.H.J. Dijkhuis, J.G. Haasnoot, R. Prins, J. Reedijk, B.E. Buchanan and J.G. Vos, Inorg. Chem., **1988**, *27*, 2185.

20 B.E. Buchanan, R. Wang, J.G. Vos, R. Hage, J.G. Haasnoot and J. Reedijk, Inorg. Chem., **1990**, *29*, 3263.

21 R. Hage, R. Prins, J.G. Haasnoot and J.G. Vos, J. Chem., Soc., Dalton Trans, **1987**, 1389.

22 R. Hage, J.G. Haasnoot, H.A. Nieuwenhuis, J. Reedijk, D.J. De Ridder and J.G. Vos, J. Am. Chem. Soc., **1990**, *112*, 9245.

23 L. De Cola, F. Barigelletti, V. Balzani, R. Hage, J.G. Haasnoot, J. Reedijk and J.G. Vos, Chem. Phys. Lett., **1991**, *178*, 491.

24 F. Barigelletti, L. De Cola, V. Balzani, R. Hage, J.G. Haasnoot, J. Reedijk and J.G. Vos, Inorg. Chem., **1991**, *30*, 641.

25 F. Barigelletti, L. De Cola, V. Balzani, R. Hage, J.G. Haasnoot, J. Reedijk, and J.G. Vos, Inorg. Chem., **1989**, *28*, 4344.

26 H.P. Hughes, D. Martin, S. Bell, J. Mc Garvey and J.G. Vos, Inorg. Chem., **1993**, *32*, 4402.

27 R. Hage, J.G. Haasnoot, D. Stufkens, T. Snoeck, J.G. Vos and J. Reedijk, Inorg. Chem., **1989**, *28*, 1413.

28 H.P. Hughes and J.G. Vos, Inorg. Chem., **1995**, *34*, 4001.

29 C. Coates, T.E. Keyes, H.P. Hughes, P.M. Jayaweera, J.J. Mc Garvey and J.G. Vos, J. Phys Chem., **1998**, *102*, 5013.

30 C. Coates, T.E. Keyes, H.P. Hughes, P.M. Jayaweera, J.J. Mc Garvey and J.G. Vos, Coord. Chem. Rev., **1998**, *171*, 323.

31 H.P. Hughes, Ph. D. Thesis, Dublin City University, Ireland, **1993**.

32 G. Bryant and J. Fergusson, Aust. J. Chem., **1971**, *24*, 441.

33 Y. Ohsawa, M. De Armond, K. Hanck and C. Moreland, J. Am. Chem. Soc., **1985**, *107*, 5383.

34 J. De Wolf, R. Hage, J.G. Haasnoot, J. Reedijk and J.G. Vos, New J. Chem., **1991**, *15*, 501.

35 P. Belser and A von Zelewsky, Helv. Chim. Acta., **1980**, *63*, 1675.

36 E. Constable and J. Lewis, Inorg. Chim. Acta., **1983**, *70*, 251.

37 S. Gaemers, J. Van Slageren, C.M. O'Connor, J.G. Vos, R. Hage and C.

Elsevier, awaiting acceptance.

38 K. Kalyanasundaram, M. Nazeeruddin, M. Gratzel, G. Viscardi, P. Savarino and E. Barni, Inorg. Chim. Acta, **1992**, *198*, 831.

39 R. Stainewicz and D. Hendricker, J. Amer. Chem. Soc., **1977**, *99*, (20), 6581.

40 R. Berger, Inorg. Chem., **1990**, *29*, 1920.

41 J. Kelly, C.Long, C. O'Connell, J.G. Vos and A. Tinnemans, Inorg. Chem., **1983**, *22*, (20), 2818.

42 R. Harrigan and G. Crosby, J. Chem. Phys., **1973**, *59*, (7), 3468.

43 D. Sandrini, M. Maestri, V. Balzani, U. Maeder and A. von Zelewsky, Inorg. Chem. **1988**, *27*, 2640.

44 M. Haga, T. Matsumura-Inoue and S. Yamabe, Inorg. Chem., **1987**, *26*, 4148.

45 T. Keyes, J.G. Vos, J. Kolnaar, J.G. Haasnoot, J. Reedijk and R. Hage, Inorg. Chim. Acta., **1996**, *245*, 237.

46 W. Siebrand, J. Phys. Chem., **1967**, *46*, 440.

47 W. Siebrand, J. Phys. Chem., **1971**, *55*, 5843.

48 M. Nazeeruddin and K. Kalyanasundaram, Inorg. Chem., **1989**, *28*, 4251.

49 T. Forster, Nature, **1989**, *36*, 186.

50 J. Ireland and P. Whyatt, Adv. Phys. Org. Chem., **1976**, *2I*, 131.

51 N. Lasser and J. Feilelson, J. Phys. Chem., **1973**, *77*, (8), 1011.

52 J. Aaron and J. Winefordner, Photochem. and Photobiol., **1973**, *18*, 97.

53 R. Hage, Ph. D. Thesis, Leiden University, The Netherlands, **1991**.

54 E. Dodsworth and A . Lever, Chem. Phys. Lett., **1986**, *124*, (2), 152.

55 D. Rillema, G. Allen, T. Meyer and D. Conard, Inorg. Chem., **1983**, *22*, 1617.

56 C. Elliot and E. Hershenhart, J. Amer. Chem. Soc., **1982**, *104*, 7519.

57 N. Takvoryan, R. Hemingway and A. Bard. J. Amer. Chem. Soc., **1973**, *95*, 6582.

Chapter 5

THE SYNTHESIS AND CHARACTERISATION OF RU(II) DINUCLEAR COMPLEXES CONTAINING 3-(PYRIDINE-2-YL)-5- (PYRAZINE-2-YL)-1,2,4-TRIAZOLE (HPPT).

5.1 INTRODUCTION

There is continuing interest in the photophysical properties of the Ru(II) polpyridyl complexes due to their well-recognised role in useful, photochemically driven devices.[1] Tailoring of the excited state properties of these complexes is central to their adaptation for useful practical application. Numerous studies have been carried out on Ru(II) complexes coordinated to a bridging ligand demonstrate perturbation of their photophysical properties due to electronic communication between individual components. The extent of perturbation depends on factors such as the σ-donor/ π-acceptor properties of the ligands and/ or the identity of the metal centres. Central to the investigation of the components (metals, bridging ligands and peripheral ligands) is the necessity for effective spectroscopic probes of excited-state properties, which will be sensitive to changes resulting from either slight chemical or other modifications to the immediate external environment.[2,3,4,5]

In the design of supramolecular assemblies many factors must be considered and the most basic of those and maybe the most important is the synthetic strategy especially if directional energy control is involved. This requires:

(i) knowledge of electronic, and electrochemical properties of each individual metal unit,

(ii) knowledge of the extent to which the properties of each component are affected by the order of nuclearity,

(iii) the availability of synthetic strategies for the preparation of polynuclear compounds with different units.

The idea of "complexes as ligands" has been a useful approach in the synthesis of the polynuclear compounds[6,7]. This concept has allowed for the synthesis of polynuclear complexes of the dpp (bis-(2-pyridyl)pyrazine) ligand, which controlled migration of electronic energy in a desired direction. This concept was also incorporated into the 'indirect' synthesis of the dinuclear complexes in this chapter.

The bridging ligand in polynuclear systems is of great importance, as its chemical nature controls the electronic communication between the metal centres. With their coordination sites they contribute to determining the spectroscopic and redox properties of the metal-based units. The size and coordination modes of the bridging ligands determine the whole structure of the supramolecular system. A range of rigid bridging ligands and spacers have been investigated over the years examples of which are: PAP (2,6-adamantanebis-(1,1,3,3-tetramethyl-1,3-dihydro-7,8-diaza) cyclopenta [1] phenanthrene-2-ylidene)[8], Tpy (2,2':6',2"-terpyridine) in conjunction with ph (1,4-phenylene)[9], Tpphz (tetrapyrido-[3,2-a: 2',3'-c: 3", 2" -h: 2"', 3"'-j]phenazine][10] and Bqpy (bis-{dipyrido[3, 2-f:2', 3'-h] quinoxalo}-[2, 3-e: 2', 3' -l]pyrene)[11], shown in Figure 1.

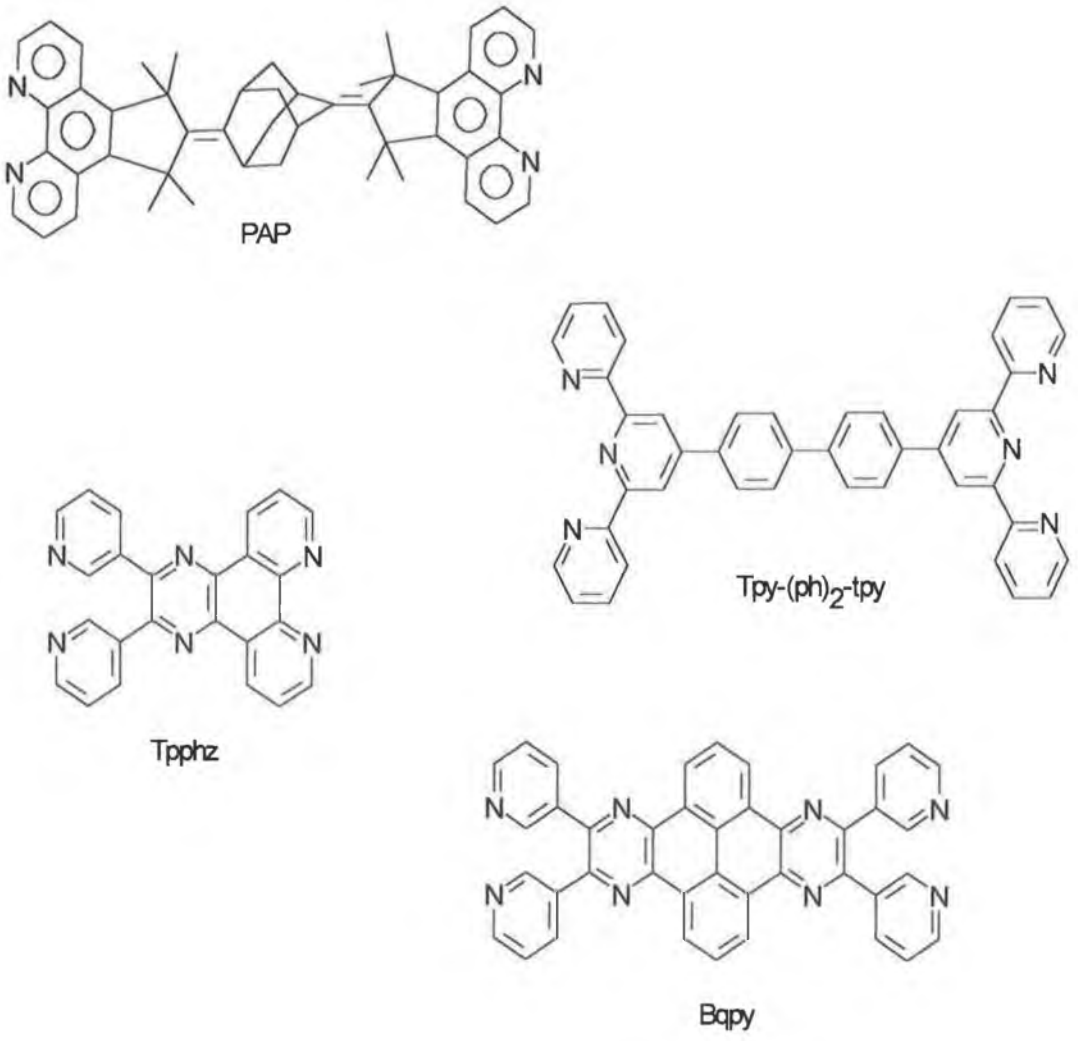

Figure 1 Examples of rigid bridging ligands.

In rigid rodlike species the key role played by the bridging ligand is 2-fold, because (i) it gives the desired rigidity to the molecular backbone by fixing the distance and, to a certain extent, the relative orientation between the reacting centres and (ii) it can contain different molecular subunits with either conducting or isolating electronic properties. The asymmetry of the Hppt ligand has potential with regard to vectorial energy or electronic transfer within photomolecular devices. Meyer et al. have incorporated the use of unsymmetrical ligands into their studies to investigate firstly, in multiple chelates which ligand is the ultimate acceptor. Secondly, in complexes with two or more identical acceptor ligands, is the excited state electron localised on one ligand or is it delocalised over both[12]. For this reason selective deuteriation was incorporated into the synthesis of the indirect dinuclear complexes of the Hppt ligand cited in this chapter.

In the search for a suitable bridging ligand, a systematic study has been carried out which involved the study of other bridging ligands. Previous studies in dinuclear complexes show that by using ligands such as 3,5-bis(pyridin-2-yl)-1,2,4-triazole (Hbpt)[13], the lowest excited state is located on the polypyridine ligands, while with the ligand 3,5-bis(pyrazin-2-yl)-1,2,4-triazole (Hbpzt)[15] the emitting state is located on the pyrazine ligand . The Hppt ligand is of interest since the two coordination sites on the bridge are very different from each other. Based on the Hbpt[13] type complexes the pyridine bound isomer of the Hppt complex is expected to show bpy based photophysical properties, while the pyrazine coordinated Hppt isomer can lead to both a pyrazine or a bpy based excited state chemistry similar to that of Hpztr[14] and Hbpzt[15] complexes.

The Hppt ligand has proven to be a very complex and useful bridging ligand. Results given in the following chapter will demonstrate the potential applications for the ppt dinuclear dimers in areas such as (a) supramolecular assemblies, (b) molecular switches and (c) photosensitisers.

The applications for such molecules in supramolecular chemistry will be based on the fact that there is a suitable synthetic strategy developed i.e. 'complexes as ligands'. For the dinuclear species, the coordination sites can vary the structure of the system and lead to interesting spectroscopic results and also the mono- and dinuclear characteristics are known for the complex. More recent revelations have also shown that the enantiomers[18] can be isolated on hplc for the dinuclear ppt complexes which is desirable for photophysical measurements in large assemblies.

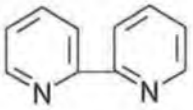

2,2'- Bipyridine (bpy)

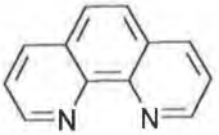

1,10 - Phenanthroline (phen)

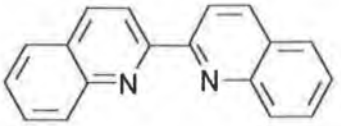

2,2'- Biquinoline (biq)

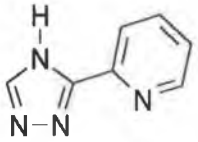

3-(pyridin-2-yl)-1,2,4-triazole (Hpytr)

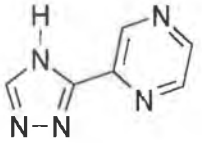

3-(pyrazin-2-yl)-1,2,4-triazole (Hpztr)

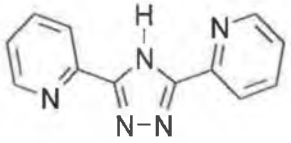

3, 5 bis-(pyridin-2-yl)-1,2,4-triazole (Hbpt)

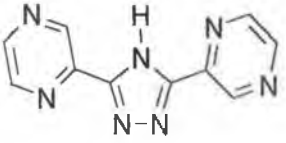

3, 5 bis-(pyrazin-2-yl)-1,2,4-triazole (Hbpzt)

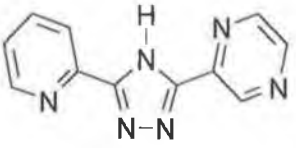

3-(pyridin-2-yl)-5-(pyrazin-2-yl)-1,2,4-triazole (Hppt)

Figure 2 Ligands cited in this chapter

Current research relating to 'molecular switches' is presently focussed on acid-base controllable devices[16] which is directly relevant to the studies in this text as the acid/ base dependency of the spectroscopic features of the Hppt dinuclear complex are sensitive to the pH of their environment which may be used as an ON/ OFF trigger for systems such as these. Due to the reversible redox properties and long luminescent lifetimes of the ppt dinuclear complexes, there may be application for them as photosensitisers in solar cells. Results will be further discussed in the experimental section

5.2 EXPERIMENTAL

5.2.1 Preparation of the Hppt dinuclear complexes

5.2.1.1 Direct Method

The synthetic route taken to prepare the direct dinuclear complexes is to use one mole of the bridging ligand (Hppt) and 2 moles of the $[Ru(L)_2]Cl_2$, where L is bipyridyl, phenanthroline or biquinoline and their deuteriated analogues (as shown in chapter 3).

$[(Ru(bpy)_2)_2ppt]\,[PF_6]_3.4H_2O$ [RuRu]

This compound was prepared by dissolving (112 mg; 0.5 mmol) Hppt in 50 cm^3 ethanol: water 2:1 (v/v). An excess of $[Ru(bpy)_2Cl_2].2H_2O$ (570 mg;1.1 mmol) was added and heated under reflux for 8 hours. The solvent was removed by rotary evaporation and the residue dissolved in 10 cm^3 water. The complex was precipitated by addition of an aqueous solution of NH_4PF_6.
The complex was recrystalised in acetone: water 1:1(v/v).
Yield after purification: 0.6 g (82%), CHN: Found C, 39.94; H, 2.75; N, 11.67; $Ru_2C_{51}H_{47}N_{14}O_4P_3F_{18}$ requires C, 39.33; H, 3.04; N, 12.59 %.

$[(Ru\ (d_8\text{-}bpy)_2)_2ppt]\,[PF_6]_3$

This compound was prepared by dissolving (112 mg; 0.5 mmol) Hppt in 50 cm^3 ethanol: water 2:1 (v/v). An excess of $[Ru(d_8\text{-}bpy)_2Cl_2].2H_2O$ (590 mg;1.1 mmol) was added and heated under reflux for 8 hours. The solvent was removed by rotary evaporation and the residue dissolved in 10 cm^3 water. The complex was precipitated by addition of an aqueous solution of NH_4PF_6.The complex was recrystalised in acetone: water 1:1(v/v).
Yield after purification: 0.61 g(87%) CHN: Found C, 41.15; H, 2.86; N, 11.58; $Ru_2C_{51}D_{32}H_7N_{14}P_3F_{18}$ requires C, 40.37; H, 2.72; N, 12.93 %.

$[(Ru(phen)_2)_2ppt]\ [PF_6]_3.6H_2O$

This compound was prepared by dissolving (112 mg; 0.5 mmol) Hppt in 50 cm^3 ethanol: water 2:1 (v/v). $[Ru(phen)_2Cl_2].2H_2O$ (568 mg;1 mmol) was added and heated under reflux for 8 hours. The solvent was removed by rotary evaporation and the residue dissolved in 10 cm^3 water. The complex was precipitated by addition of an aqueous solution of NH_4PF_6.The complex was recrystalised in acetone: water 1:1(v/v).

Yield after purification:0.58 g(85%) CHN: Found C, 41.25; H, 2.34; N, 11.46; $Ru_2C_{59}H_{51}N_{14}O_6P_3F_{18}$ requires C, 41.90; H, 3.04; N, 11.61 %.

$[(Ru(d_8\text{-}phen)_2)_2ppt]\ [PF_6]_3.7H_2O$

This compound was prepared by dissolving (112 mg; 0.5 mmol) Hppt in 50 cm^3 ethanol: water 2:1 (v/v). $[Ru(d_8\text{-}phen)_2Cl_2].2H_2O$ (576 mg;1 mmol) was added and heated under reflux for 8 hours. The solvent was removed by rotary evaporation and the residue dissolved in 10 cm^3 water. The complex was precipitated by addition of an aqueous solution of NH_4PF_6.The complex was recrystalised in acetone: water 1:1(v/v). CHN was not obtained for this complex, however, this complex was made in an identical manner as the $[Ru((phen)_2)_2ppt]^{3+}$ complex and was found to be hplc pure and ^1H NMR pure (just showing the isomers of the dinuclear complexes).

$[(Ru(biq)_2)_2ppt]\ [PF_6]_3.H_2O$

This compound was prepared by dissolving (47 mg; 0.208 mmol) Hppt in 50 cm^3 ethanol: water 2:1 (v/v). $[Ru(biq)_2Cl_2].2H_2O$ (300 mg; 0.416 mmol) was added and heated under reflux for 8 hours. The solvent was removed by rotary evaporation and the residue dissolved in 10 cm^3 water. The complex was precipitated by addition of an aqueous solution of NH_4PF_6.The complex was recrystalised in acetone:water 1:1(v/v).

Yield after purification: 0.28 g (81%) CHN: Found C, 52.35; H, 2.72; N, 10.06; $Ru_2C_{83}H_{57}N_{14}OP_3F_{18}$ requires C, 52.36; H, 3.01; N, 10.30 %.

$[(Ru(d_{12}\text{-biq})_2)_2ppt]\ [PF_6]_3.4H_2O$

This compound was prepared by dissolving (38 mg; 0.17 mmol) Hppt in 50 cm^3 ethanol: water 2:1 (v/v). $[Ru(d_{12}\text{-biq})_2Cl_2].2H_2O$ (250 mg; 0.34 mmol) was added and heated under reflux for 8 hours. The solvent was removed by rotary evaporation and the residue dissolved in 10 cm^3 water. The complex was precipitated by addition of an aqueous solution of NH_4PF_6.The complex was recrystalised in acetone: water 1:1(v/v). Yield after purification: 0.25 g (87%) CHN: Found C, 48.88; H, 3.15; N, 10.31; $Ru_2C_{83}D_{48}H_{15}N_{15}O4P_3F_{18}$ requires C, 49.35; H, 3.14; N, 10.40 %.

5.2.1.2 Indirect method

The synthetic route taken to prepare the indirect dinuclear complexes is to use 1 mole of the metal complex $[Ru(L)_2(L')]^+$ and 1 mole of the $[Ru(L)_2]Cl_2$, where L is bipyridyl and L' is the ligand Hppt. Their deuteriated analogues of the ligands were also incorporated, hence a number of analogues ensued. All mononuclear isomers were previously purified as described in chapter 4.

$[Ru(bpy)_2ppt1Ru(bpy)_2][PF_6]_3.5H_2O$ [Ru1Ru]

(100 mg; 0.104 mmol) $[Ru(bpy)_2ppt]$ isomer 1 was dissolved in 50 cm^3 ethanol: water 2:1 (v/v). An equimolar equivalent of $[Ru(bpy)_2Cl_2].2H_2O$ (54 mg; 0.104 mmol) was added and heated under reflux for 8 hours. The solvent was removed by rotary evaporation and the residue dissolved in 10 cm^3 water. The complex was precipitated by addition of an aqueous solution of NH_4PF_6.The complex was recrystalised in acetone: water 1:1(v/v). Yield after purification: 0.120 g (78%) CHN: Found C, 39.40; H, 2.62; N, 11.65; $Ru_2C_{51}H_{49}N_{14}O_5P_3F_{18}$ requires C, 38.88; H, 3.13; N, 12.45 %.

$[Ru(bpy)_2ppt2Ru(bpy)_2]$ $[PF_6]_3.9H_2O$ [Ru2Ru]

(100 mg; 0.104 mmol) $[Ru(bpy)_2ppt]$ isomer 2 was dissolved in 50 cm^3 ethanol: water 2:1 (v/v). An equimolar equivalent of $[Ru(bpy)_2Cl_2].2H_2O$ (54 mg; 0.104 mmol) was added and heated under reflux for 8 hours. The solvent was removed by rotary evaporation and the residue dissolved in 10 cm^3 water. The complex was precipitated by addition of an aqueous solution of NH_4PF_6.The complex was recrystalised in acetone: water 1:1(v/v). Yield after purification: 0.128 g(83%) CHN: Found C, 36.94; H, 2.58; N, 11.72; $Ru_2C_{51}H_{41}N_{14}O_9P_3F_{18}$ requires C, 37.23; H, 3.36; N, 11.92%.

$[Ru(bpy)_2ppt1Ru(d_8\text{-}bpy)_2]$ $[PF_6]_3.14H_2O$

(95 mg;0.1 mmol) $[Ru(bpy)_2ppt]$ isomer 1 was dissolved in 50 cm^3 ethanol: water 2:1 (v/v). An equimolar equivalent of $[Ru(d_8\text{-}bpy)_2Cl_2].2H_2O$ (56 mg; 0.1 mmol) was added and heated under reflux for 8 hours. The solvent was removed by rotary evaporation and the residue dissolved in 10 cm^3 water. The complex was precipitated by addition of an aqueous solution of NH_4PF_6.The complex was recrystalised in acetone:water 1:1(v/v).

Yield after purification: 0.135 g(89%) CHN: Found C, 34.38; H, 2.44; N, 11.21; $Ru_2C_{51}H_{51}D_{16}N_{14}O_{14}P_3F_{18}$ requires C, 34.93; H, 3.85; N, 11.19 %.

$[Ru(bpy)_2ppt2Ru(d_8\text{-}bpy)_2][PF_6]_3.6H_2O$

(85 mg; 0.09 mmol) $[Ru(bpy)_2ppt]$ isomer 2 was dissolved in 50 cm^3 ethanol: water 2:1 (v/v). An equimolar equivalent of $[Ru(d_8\text{-}bpy)_2Cl_2].2H_2O$ (51 mg; 0.09 mmol) was added and heated under reflux for 8 hours. The solvent was removed by rotary evaporation and the residue dissolved in 10 cm^3 water. The complex was precipitated by addition of an aqueous solution of NH_4PF_6.The complex was recrystalised in acetone: water 1:1(v/v). Yield after purification: 0.10 g (73%) CHN: Found C, 38.84; H, 2.61; N, 11.38. $Ru_2C_{51}H_{35}D_{16}N_{14}O_2P_3F_{18}$ requires C, 38.45; H, 3.2; N, 12.3 %.

$[Ru(d_8\text{-bpy})_2ppt1Ru(bpy)_2][PF_6]_3.5H_2O$

(88 mg; 0.09 mmol) $[Ru(d_8\text{-bpy})_2ppt]$ isomer 1 was dissolved in 50 cm^3 ethanol: water 2:1 (v/v). An equimolar equivalent of $[Ru(bpy)_2Cl_2].2H_2O$ (47 mg; 0.09 mmol) was added and heated under reflux for 8 hours. The solvent was removed by rotary evaporation and the residue dissolved in 10 cm^3 water. The complex was precipitated by addition of an aqueous solution of NH_4PF_6.The complex was recrystalised in acetone: water 1:1(v/v). Yield after purification: 0.115 g(85%) CHN: Found C, 38.85; H, 2.73; N, 11.52; $Ru_2C_{51}H_{33}D_{16}N_{14}O_5P_3F_{18}$ requires C, 38.44; H, 3.20; N, 12.31%.

$[Ru(d_8\text{-bpy})_2ppt2Ru(bpy)_2]\ [PF_6]_3.XH_2O$

(100 mg; 0.103 mmol) $[Ru(d_8\text{-bpy})_2ppt]$ isomer 2 was dissolved in 50 cm^3 ethanol: water 2:1 (v/v). An equimolar equivalent of $[Ru(bpy)_2Cl_2].2H_2O$ (58 mg; 0.103 mmol) was added and heated under reflux for 8 hours. The solvent was removed by rotary evaporation and the residue dissolved in 10 cm^3 water. The complex was precipitated by addition of an aqueous solution of NH_4PF_6.The complex was recrystalised in acetone: water 1:1(v/v). Yield after purification: 0.132 g(83%) CHN was not obtained for this complex, however, this complex was made in an identical manner as the $[Ru(bpy)_2ppt2Ru(bpy)_2]$ complex and was found to be hplc pure and ^1H NMR pure.

$[Ru(d_8\text{-bpy})_2ppt1Ru(d_8\text{-bpy})_2][PF_6]_3.11H_2O$

(50 mg; 0.05 mmol) $[Ru(d_8\text{-bpy})_2ppt]$ isomer 1 was dissolved in 50 cm^3 ethanol: water 2:1 (v/v). An equimolar equivalent of $[Ru(d_8\text{-bpy})_2Cl_2].2H_2O$ (28 mg; 0.05 mmol) was added and heated under reflux for 8 hours. The solvent was removed by rotary evaporation and the residue dissolved in 10 cm^3 water. The complex was precipitated by addition of an aqueous solution of NH_4PF_6.The complex was recrystalised in acetone: water 1:1(v/v).

Yield after purification: 0.060 g(77%) CHN: Found C, 36.19; H, 2.22; N, 10.12; $Ru_2C_{51}H_{29}D_{32}N_{14}O_{11}P_3F_{18}$ requires C, 35.70; H, 3.58; N, 11.03 %.

$[Ru(d_8\text{-}bpy)_2ppt2Ru(d_8\text{-}bpy)_2][PF_6]_3.XH_2O$

(70 mg; 0.072 mmol) $[Ru(d_8\text{-}bpy)_2ppt]$ isomer 2 was dissolved in 50 cm^3 ethanol: water 2:1 (v/v). An equimolar equivalent of $[Ru(d_8\text{-}bpy)_2Cl_2].2H_2O$ (40 mg; 0.072 mmol) was added and heated under reflux for 8 hours. The solvent was removed by rotary evaporation and the residue dissolved in 10 cm^3 water. The complex was precipitated by addition of an aqueous solution of NH_4PF_6.The complex was recrystalised in acetone: water 1:1(v/v). Yield after purification: 0.088 g(80%)
CHN was not obtained for this complex, however, this complex was made in an identical manner as the $[Ru(bpy)_2ppt2Ru(bpy)_2]$ complex and was found to be hplc pure and ^1H NMR pure.

$[Ru(bpy)_2d_7\text{-}ppt1Ru(bpy)_2][PF_6]_3.2H_2O$

(60 mg; 0.062 mmol) $[Ru(bpy)_2d_7\text{-}ppt]$ isomer 1 was dissolved in 50 cm^3 ethanol: water 2:1 (v/v). An equimolar equivalent of $[Ru(bpy)_2Cl_2].2H_2O$ (32 mg; 0.062 mmol) was added and heated under reflux for 8 hours. The solvent was removed by rotary evaporation and the residue dissolved in 10 cm^3 water. The complex was precipitated by addition of an aqueous solution of NH_4PF_6.The complex was recrystalised in acetone: water 1:1(v/v).
Yield after purification: 0.075 g(81%) CHN: Found C, 39.91; H, 2.67; N, 12.92; $Ru_2C_{51}H_{36}D_7N_{14}O_2P_3F_{18}$ requires C, 40.08; H, 3.30; N, 12.84 %.

$[Ru(bpy)_2d_7\text{-}ppt2Ru(bpy)_2][PF_6]_3.XH_2O$

(70 mg; 0.072 mmol) $[Ru(bpy)_2d_7\text{-}ppt]$ isomer 2 was dissolved in 50 cm^3 ethanol: water 2:1 (v/v). An equimolar equivalent of $[Ru(bpy)_2Cl_2].2H_2O$ (37 mg; 0.072 mmol) was added and heated under reflux for 8 hours. The solvent was removed by rotary evaporation and the residue dissolved in 10 cm^3 water. The complex was precipitated by addition of an aqueous solution of NH_4PF_6.The complex was recrystalised in acetone: water 1:1(v/v). Yield after purification: 0.082 g(76%)

CHN was not obtained for this complex, however, this complex was made in an identical manner as the $[Ru(bpy)_2ppt2Ru(bpy)_2]$ complex and was found to be hplc pure and ^1H NMR pure.

5.3 RESULTS AND DISCUSSION

5.3.1 Chromatographic interpretation

The dinuclear ppt$^-$ complexes were analysed on analytical hplc using an SCX cation exchange column and a mobile phase of 0.12M $LiClO_4$ in 80: 20 acetonitrile: water with a flowrate of 2.0 cm^3 min^{-1} and a detector wavelength of 280 nm. From the hplc chromatograms it was found that the direct dinuclear complexes only revealed one peak. In a previous study[17] it was suggested that 'self assembly' occurred on synthesis of the ppt$^-$ direct dimer. However, it may be shown by use of the uv/ vis detector that by viewing the uv/ vis spectrum at either side of the dimer peak the uv/ vis spectra are clearly different. ^{1}H NMR spectra of the direct dimer are quite complicated but suggest the presence of two isomers.

To clarify that the direct dimer presented two coordination isomers a study on the stereoisomers was carried out by Villani et al[18] on the direct dimer of the ppt$^-$ and twice the amount of stereoisomer peaks were obtained on chiral hplc than were expected (refer to appendix 3). In comparison to the chiral hplc of the stereoisomers of the dinuclear bpt$^-$ complex run under the same conditions but yielding half the amount of hplc peaks, hence, it may be concluded that there is no evidence of 'self assembly'. To further explore the direct dimer synthesis larger ligands (1,10-phenanthroline and 2,2'- biquinoline) were incorporated to investigate if any steric hindrance would occur and encourage the route to 'self assembly'. Chromatograms of the larger dinuclear systems did not show any difference in comparison to the bipyridyl analogues. Attempts to isolate one of the two coordination dinuclear complexes were not successful, this may be attributed to the large similarities of the physical and electronic properties of the complexes.

Another angle was taken on the synthesis of the dinuclear complexes via an indirect route illustrated in Figure 3. The coordination isomers of the Hppt mononuclear complexes were isolated as described in Chapter 4. The pyridine bound isomer and

the pyrazine bound isomer of the ppt$^-$ are reacted with an equivalent molar of $Ru(bpy)_2Cl_2$ or $Ru(d_8\text{-}bpy)_2Cl_2$ to form the respective dinuclear systems.

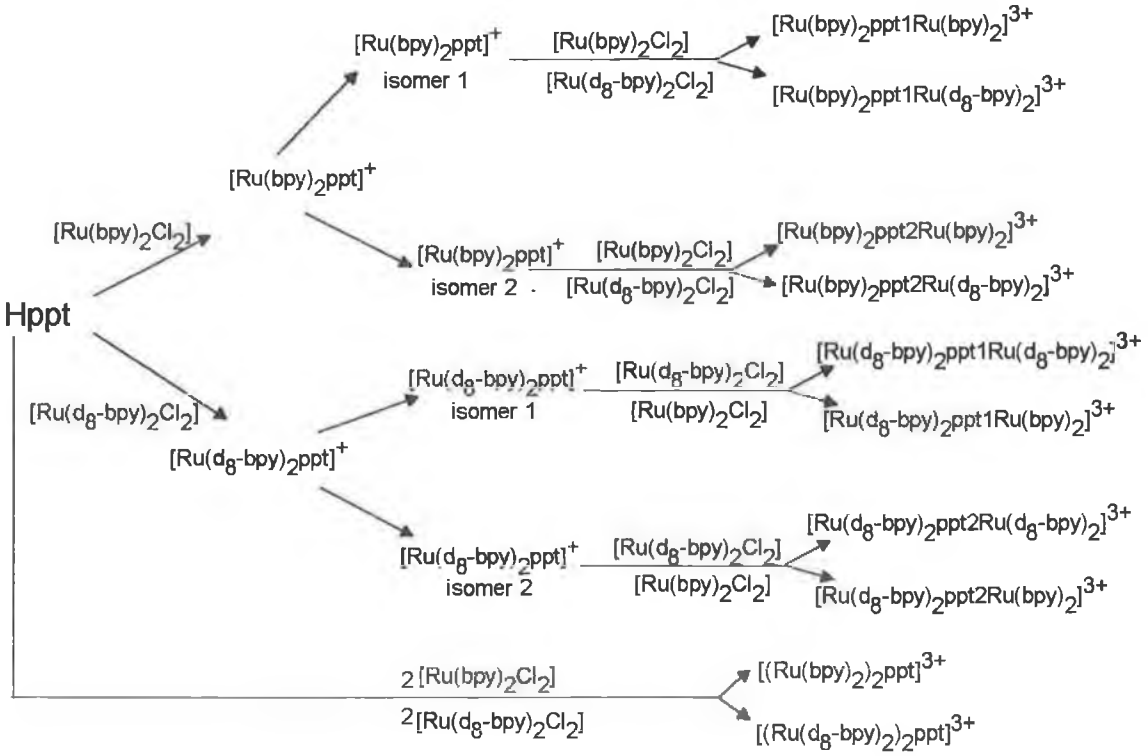

Figure 3 Synthetic routes of the Hppt dinuclear complexes.

The indirect synthesis to produce the individual dinuclear complexes can isolate the dinuclear complexes as one peak was revealed on the hplc chromatogram and was found to be pure when analysed using the photodiode array detector at different points of the peak.

Column chromatography may be used to purify dinuclear complexes using neutral alumina with 100% acetonitrile to remove any monomer remaining and 100%

methanol to bring down the dimer. Any remaining $[Ru(L)_2Cl_2].xH_2O$ (where L is h_8-bipyridyl or d_8-bipyridyl) will stick to the top of the column.

To remove any excess ligand or NH_4PF_6 after synthesis, the complex is dissolved in dry acetone and filtered under vacuum, the filtrate was collected and recrystallised from acetone: water 2:1. Purification may also be achieved by semi-preparative hplc using a mobile phase of 0.12 M KNO_3 in 80:20 acetonitrile: water and a flowrate of 2.5 cm^3/ min.

5.3.1.1 Stereoisomer separation

The interest in isolating enantiomerically pure isomers is of current interest[19,20,21] as it is suggested that in order to achieve accurate results for luminescent lifetimes of Ru(II) complexes they would have to be stereoisomer pure. This of course is of great importance in the area of supramolecular chemistry[22,23], as it would have an amplified effect in such systems. As previously mentioned, the enantiomeric separation of some of the complexes cited in this text has been carried out by Villani et al[18]. The development of a hplc stationary phase[24,25] which is capable of separating enantiomers would be a great advantage in the synthesis and purification of Ru(II) complexes both for mononuclear and supramolecular studies.

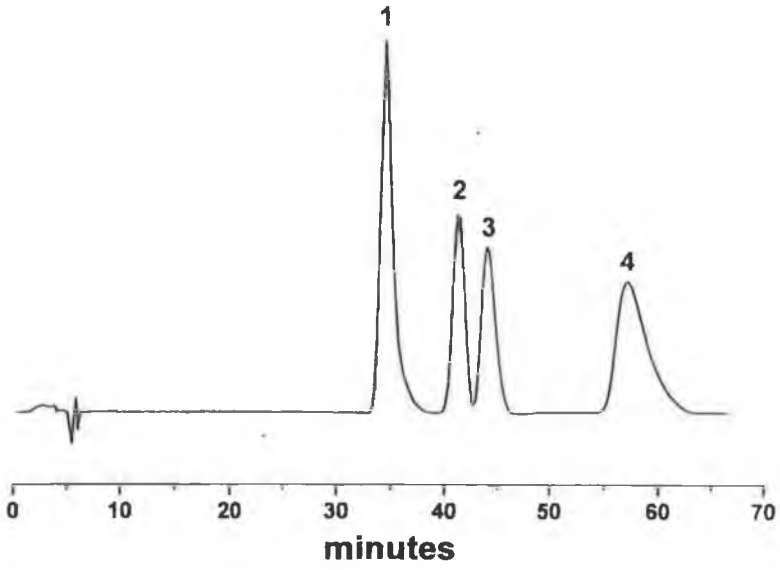

Figure 4 Chromatogram of enantiomeric separation of $[(Ru(bpy)_2)_2bpt]^{3+}$, where peak 1 and 4 are the homochiral species $\Lambda\Lambda$ and $\Delta\Delta$, and peak 2 and 3 are $\Lambda\Delta$ and $\Delta\Lambda$ heterochiral species respectively[18]

The study carried out used a new stationary phase (silica-bound Teicoplanin) which enables high efficient chromatographic resolution of chiral mono- and dinuclear Ru(II) complexes. A set of results were obtained for the direct dinuclear complexes of $[(Ru(bpy)_2)_2bpt]^{3+}$ and $[(Ru(bpy)_2)_2ppt]^{3+}$. The results obtained for the $[(Ru(bpy)_2)_2bpt]^{3+}$ dinuclear complexes revealed 4 peaks as shown in Figure 4

On a cation exchange column one peak is obtained for this direct dinuclear complexes. The explanation for the presence of four peaks for the bpt dinuclear complexes is that, for each chiral Ru(II) dinuclear complexes there exists two diastereoisomers and for each of these diastereoisomers there are two corresponding enantiomers, hence four peaks in all. However on carrying out the same chromatogram under the same conditions for the $[(Ru(bpy)_2)_2ppt]^{3+}$ dinuclear complexes 7 peaks were observed. The reason being that, the direct

dinuclear complexes synthesis produces two geometric isomers which each form two diastereoisomers (4 in total) and each of the diastereoisomers contain two enantiomers, leading to a total of 8 peaks. In the chromatogram shown in Figure 5, 7 peaks are observed as two of the enantiomer peaks may overlap. The presence of two sets of enantiomers existing for the ppt dinuclear complexes confirmed that self assembly does not occur on direct dinuclear complexes synthesis, i.e. that under the single peak observed on cation exchange chromatogram two dinuclear isomers exist. Corresponding data may be found in appendix 3, relevant paper is presented in appendix 1, paper 4.

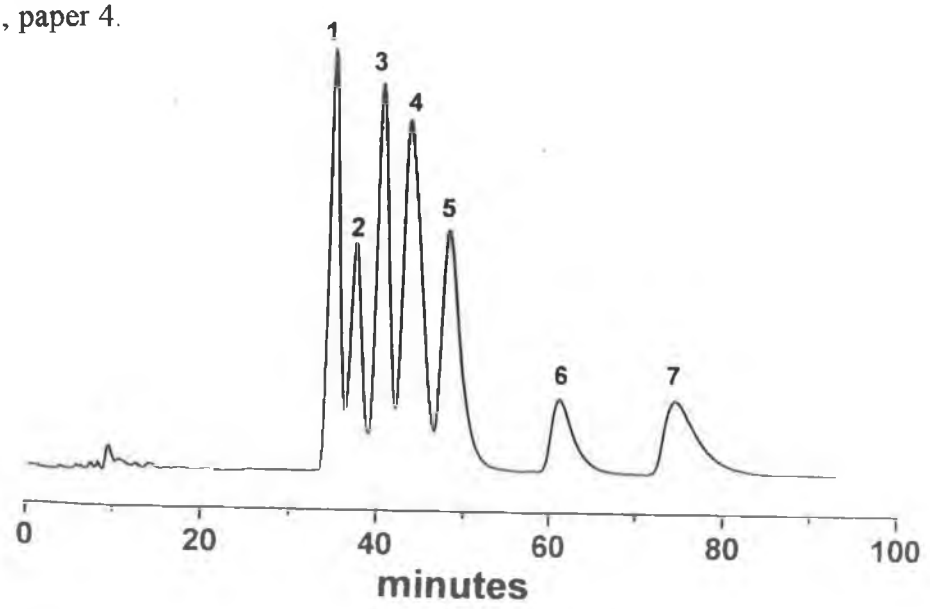

Figure 5 Chromatogram of enantiomeric separation of $[(Ru(bpy)_2)_2ppt]^{3+}$ [18]

5.3.2 ^{1}H NMR Spectroscopy.

^{1}H NMR elucidation of Ru(II) dinuclear complexes[17,33] has proven complicated due to the large quantity of bipyridyl protons. Deuteriation has shown to be quite an effective tool in ^{1}H NMR elucidation [26,29] as illustrated in previous chapters.

5.3.2.1 Indirect Dinuclear Complexes.

Synthesis was also carried out via the indirect route to eliminate the formation of the second dinuclear coordination isomer. The reaction pathway which is illustrated in

Figure 3 involves isolating a mononuclear isomer and reacting with another $Ru(bpy)_2$ moiety. In this manner isomer 1 yields Ru1Ru and isomer 2 yields Ru2Ru. Selective deuteriation of the bipyridyl ligands and the Hppt ligand was incorporated into this study as it will enhance visually from ^1H NMR which isomers are present and will aid in the elucidation of the spectra. The complexes were also designed through selective deuteriation for photophysical purposes which will be discussed in section 5.3.4.2. The ^1H NMR shifts for the coordination isomers of the dinuclear complexes is shown in *Table 1*.

Compound	H^3(ppm)	H^4(ppm)	H^5(ppm)	H^6(ppm)
Hppt pyz	9.35, s	(---)	8.72, d	8.72, d
pyr	8.20, d	8.03, t	7.56, t	8.79, d
Ru1Ru pyz	9.15(-0.20)	(---)	8.30(-0.42)	7.40(-1.32)
pyr	8.32(+0.12)	7.48(-0.55)	7.08(-0.48)	7.10(-1.69)
Ru2Ru pyz	9.10(-0.25)	(---)	8.50(-0.22)	7.54(-1.18)
pyr	8.42(+0.22)	7.57(-0.46)	7.15(-0.41)	7.00(-1.79)

Table 1 ^1H NMR of the indirect dinuclear ppf complexes in d_3-acetonitrile (values in brackets represent chemical shifts of the ligand on complexation to the two Ru centres).

The complex referred to, as Ru1Ru is the indirect dinuclear complexes, which was formed from the pyridine, bound monomer. The pyridine bound monomer has been assigned as being coordinated via N1 of the triazole ring. Hence, when a second moiety of $Ru(bpy)_2$ is added to this complex the second metal unit coordinates via N4 of the triazole to the free pyrazine ring. This observed in the ^1H NMR shifts in Table 1, for the pyrazine ring the H6 proton is shifted significantly, as it is coordinated via the N4 site.

This shift may be attributed to the H6 proton of the pyrazine ring hanging in close proximity to the bpy rings, also the N4 site is a weaker σ-donor than the N2 site causing a larger shift upfield for the N4 bound isomers. The H5 proton of the

assigned as being N1 of the triazole to the pyridine ring, coordinated. This is the coordination of the mononuclear isomer that was used to form the indirect dinuclear complexes and may be confirmed by the chemical shifts observed in the ^{1}H NMR. The H4 and H5 protons of the pyridine ring undergo upfield shifts, however, it is the H6 proton of the pyridine ring which undergoes the most substantial shift. Hence based on this data it is suggested that Ru1Ru is N1to the pyridine for the first metal centre and N4 to the pyrazine for the second metal centre.

The complex referred to as Ru2Ru was produced from the monomer $[Ru(bpy)_2ppt]^+$ N2 bound to the pyrazine. Complexation of the second moiety of $Ru(bpy)_2$ leads to the coordination of a second metal centre at N4 to the free pyridine ring. This may be observed from the ^{1}H NMR data, as the H6 proton of the pyrazine ring is shifted but not as much as in Ru1Ru. However, for the H6 of the pyridine ring a larger shift is experienced than in the case of Ru1Ru. In the Ru2Ru complex the pyridine is N4 coordinated to the metal centre. All upfield shifts may be attributed to ring current effect experienced by the ppt$^-$ protons from the adjacent bpy rings, and the σ-donating strength also contributes to such shifts. It may be suggested that the dinuclear complex is coordinated N2 to the pyrazine and N4 to the pyridine.

Examples of the selectively deuteriated dinuclear complexes ^{1}H NMR are shown in Figure 6 to Figure 11. Figure 6 and 7 illustrate the two isomers without the use of deuteriation. The ^{1}H NMR of the partially deuteriated complex formed after synthesis of a undeuteriated monomer with a $Ru(d_8\text{-bpy})_2$ moiety are presented for both isomers in Figure 8 and 9. The dinuclear complexes prepared with the deuteriated d_7-ppt ligand are shown in Figure 10 and Figure 11. For each ^{1}H NMR displayed the top spectrum is Ru1Ru and the bottom spectrum is Ru2Ru.

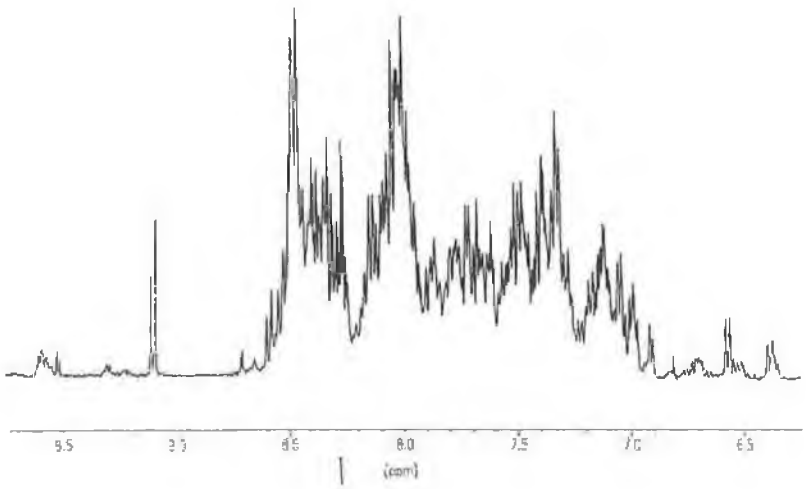

Figure 6 ^{1}H NMR of $[Ru(bpy)_2ppt1Ru(bpy)_2]^{3+}$ in d_3-acetonitrile [Ru1Ru]

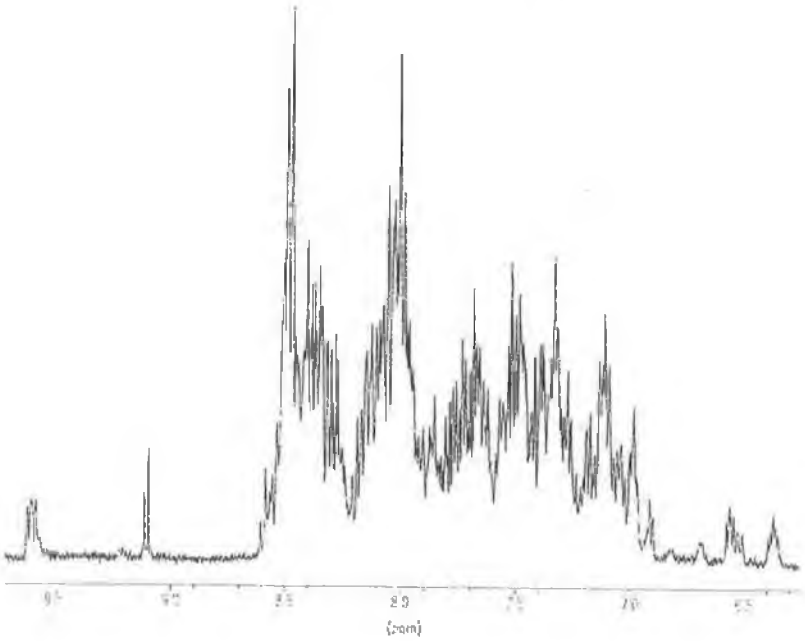

Figure 7 ^{1}H NMR of $[Ru(bpy)_2ppt2Ru(bpy)_2]^{3+}$ in d_3-acetonitrile [Ru2Ru]

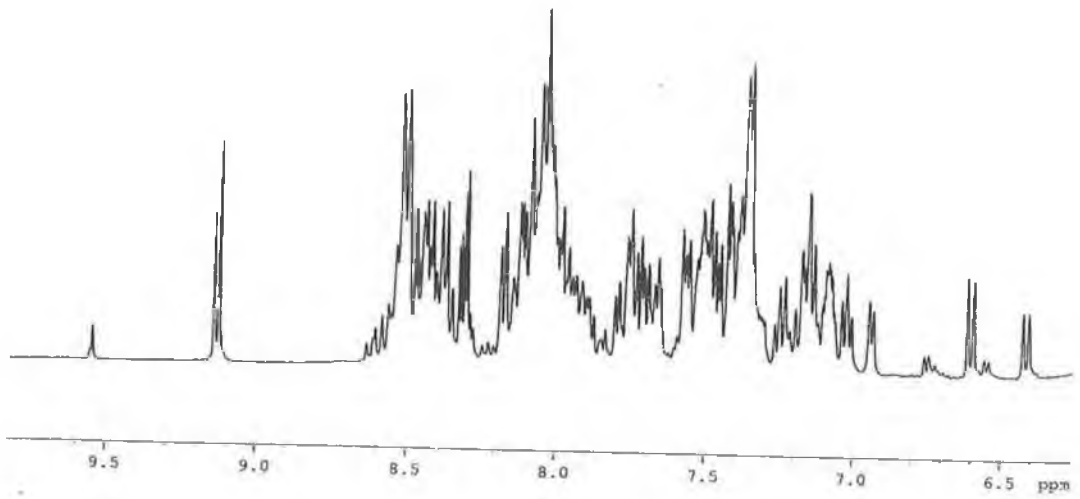

Figure 8 ^1H NMR of $[Ru(bpy)_2ppt1Ru(d_8\text{-}bpy)_2]^{3+}$ in d_3-acetonitrile.

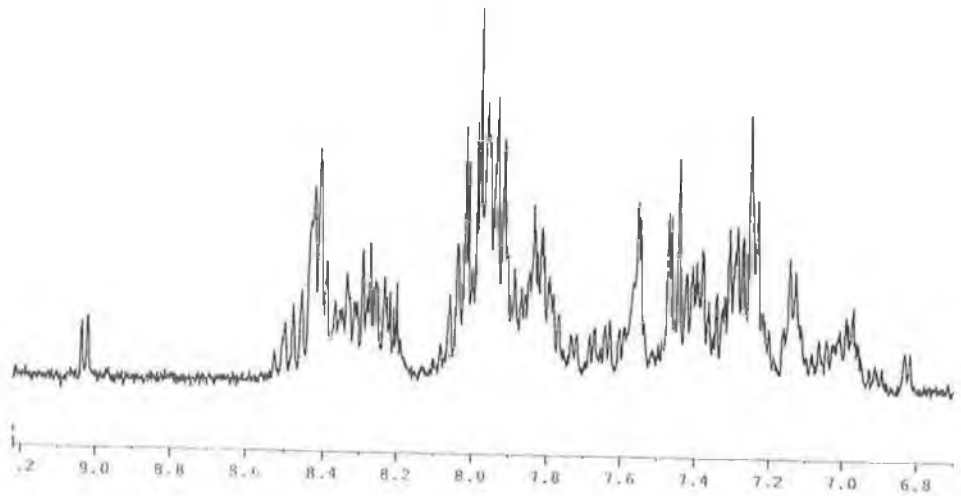

Figure 9 ^1H NMR of $[Ru(bpy)_2ppt2Ru(d_8\text{-}bpy)_2]^{3+}$ in d_3-acetonitrile.

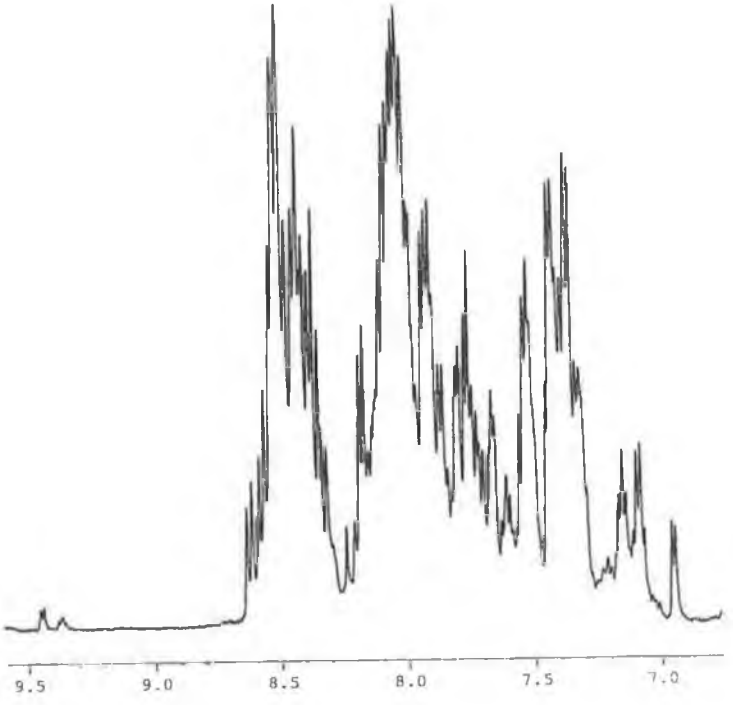

Figure 10 ^{1}H NMR of [Ru(bpy)$_2$d$_7$-ppt1Ru(bpy)$_2$]$^{3+}$ in d$_3$-acetonitrile.

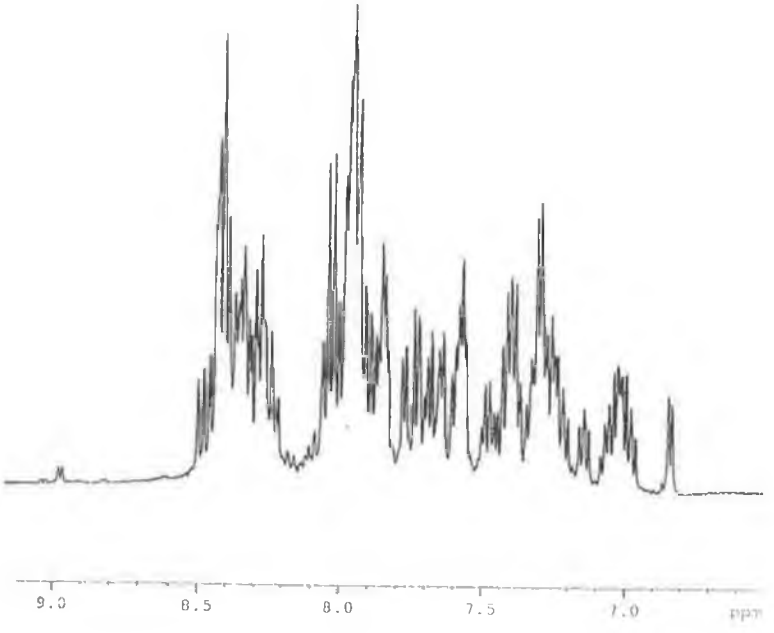

Figure 11 ^{1}H NMR of [Ru(bpy)$_2$d$_7$-ppt2Ru(bpy)$_2$]$^{3+}$ in d$_3$-acetonitrile.

5.3.2.2 Direct dinuclear complexes compounds

It has been observed that only one hplc peak is obtained on synthesis by taking the direct synthetic route or by indirectly preparing the dinuclear species from that of the isolated mononuclear species. Figure 12 portrays the three coordination isomers of the Hppt ligand. The isomer 1 and isomer 2 will be dealt with in this study but isomer 3, will not be dealt with as there is no evidence it exists and it is suggested that due to steric hindrance that it is not feasible.

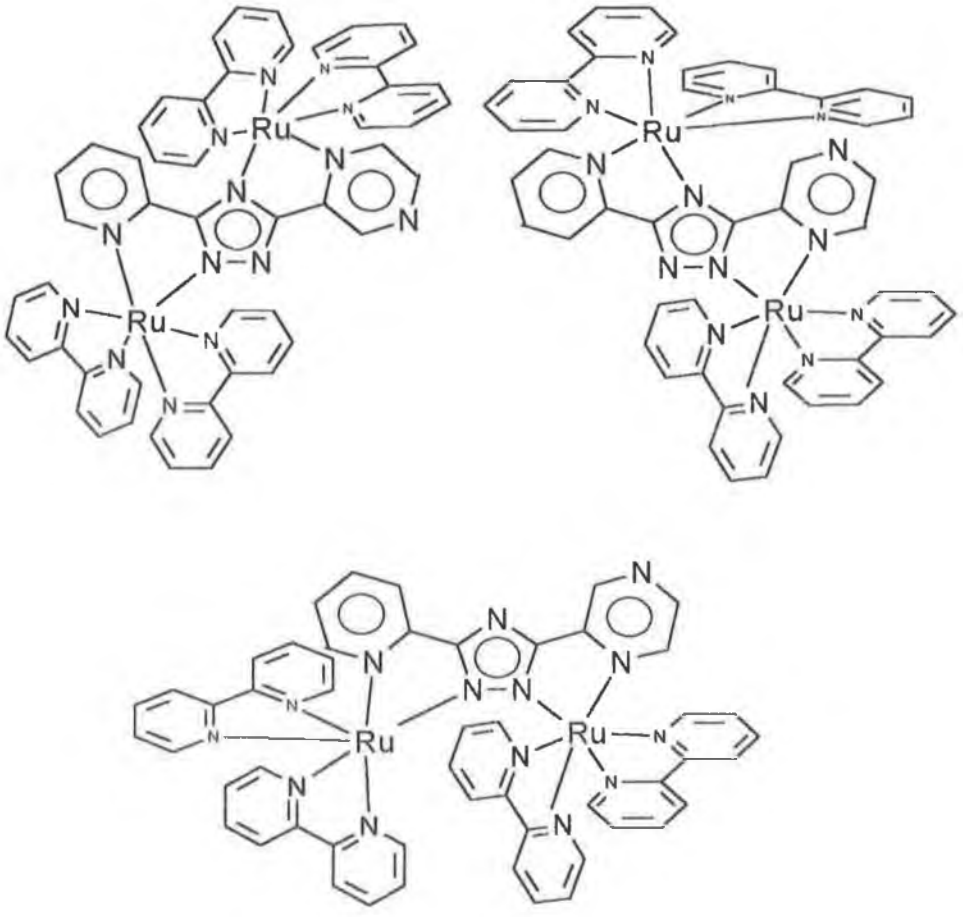

Figure 12 Three possible coordination isomers for the ppt dinuclear complexes.

* N4 of the triazole to pyrazine & N1 of triazole to pyridine
* N2 of the triazole to pyrazine & N4 of triazole to pyridine
* N2 of the triazole to pyrazine & N1 of triazole to pyridine

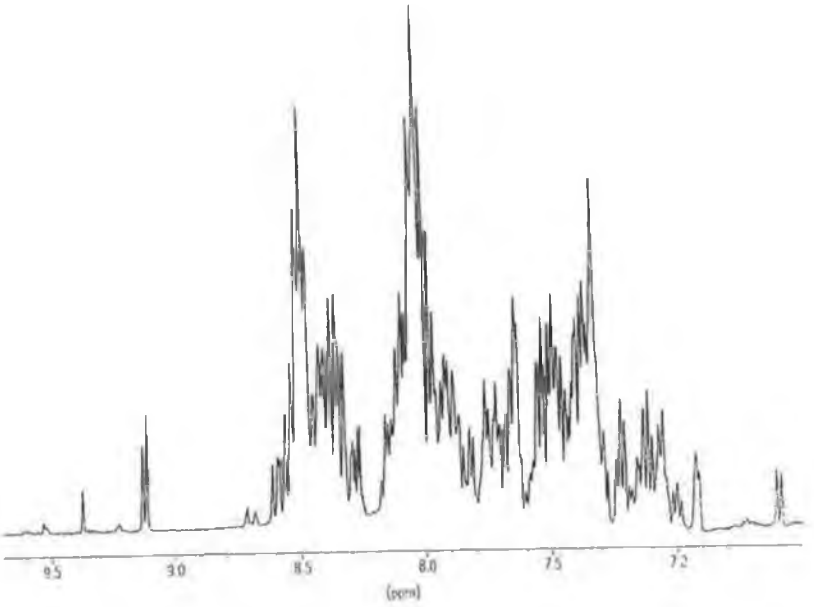

Figure 13 ^1H NMR of $[(Ru(bpy)_2)_2ppt]^{3+}$ in d_3-acetonitrile

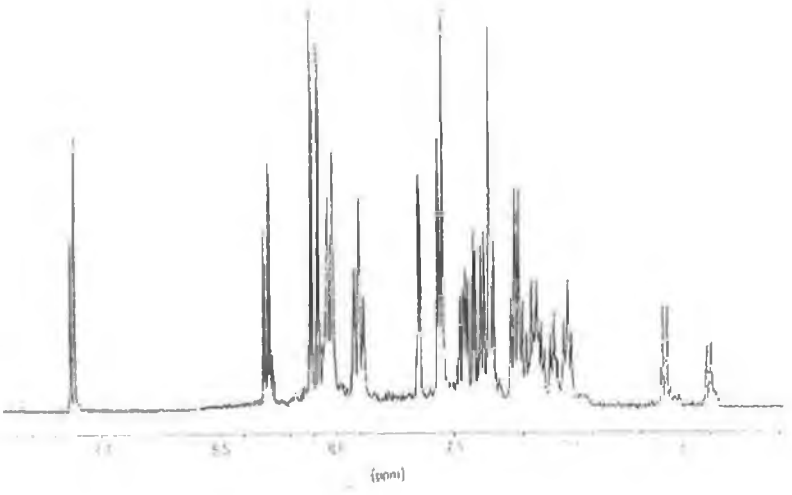

Figure 14 ^1H NMR of $[(Ru(d_8\text{-}bpy)_2)_2ppt]^{3+}$ in d_3-acetonitrile

For the directly synthesised dinuclear complexes it is evident that H3 of the pyridine ring and H5 of the pyrazine ring are both strongly shifted upfield due to the magnetic anistrophic effect of adjacent bipyridyl rings.

The ^{1}H NMR of the directly synthesised dinuclear compounds (2 $[Ru(bpy)_2Cl_2]$ equivalents with 1 Hppt ligand) are quite complicated. This is due to the presence of two isomers in this complex. Hence it is not possible to give an accurate assignment of the proton shifts as the are twice the number of protons present. Figure 13 shows the ^{1}H NMR of the direct dinuclear complexes of the $[(Ru(bpy)_2)_2ppt]^{3+}$ which is quite complicated. The deuteriated version of this complex $[(Ru(d_8\text{-}bpy)_2)_2ppt]^{3+}$ shown in Figure 14. The phenanthroline direct dinuclear complexes gives a similar complicated spectrum as for the bpy.

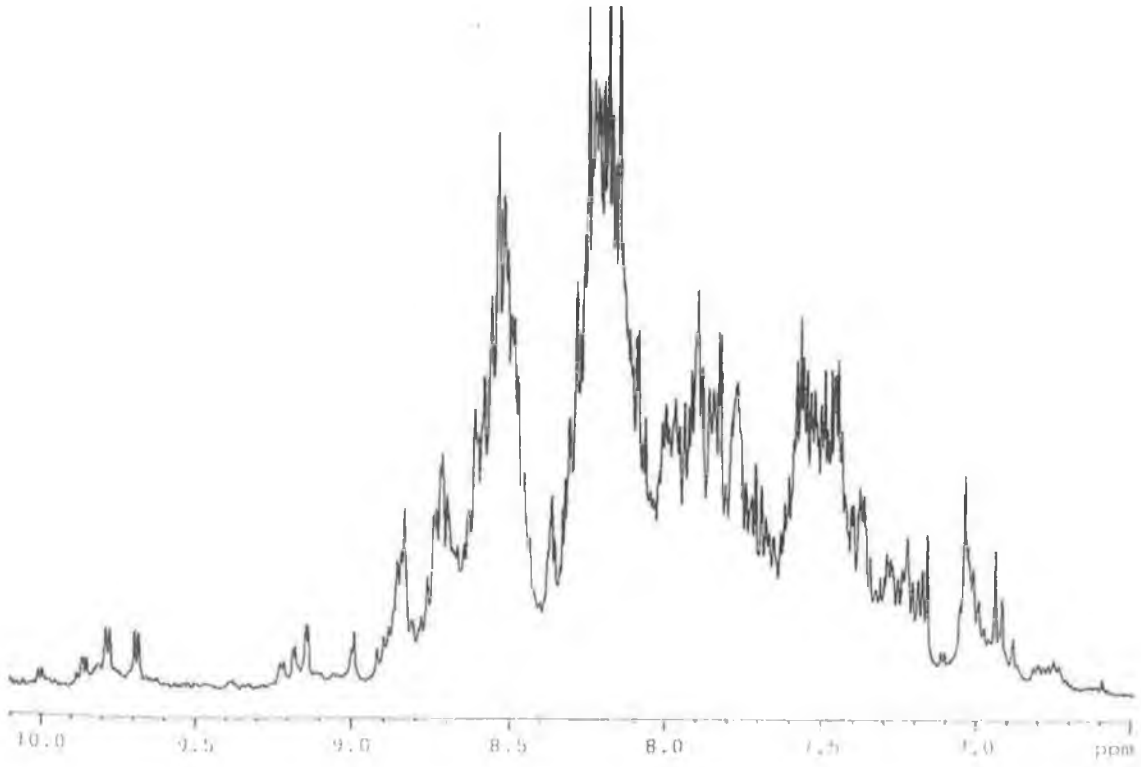

Figure 15 ^{1}H NMR of $[(Ru(phen)_2)_2ppt]^{3+}$ in d_3-acetonitrile

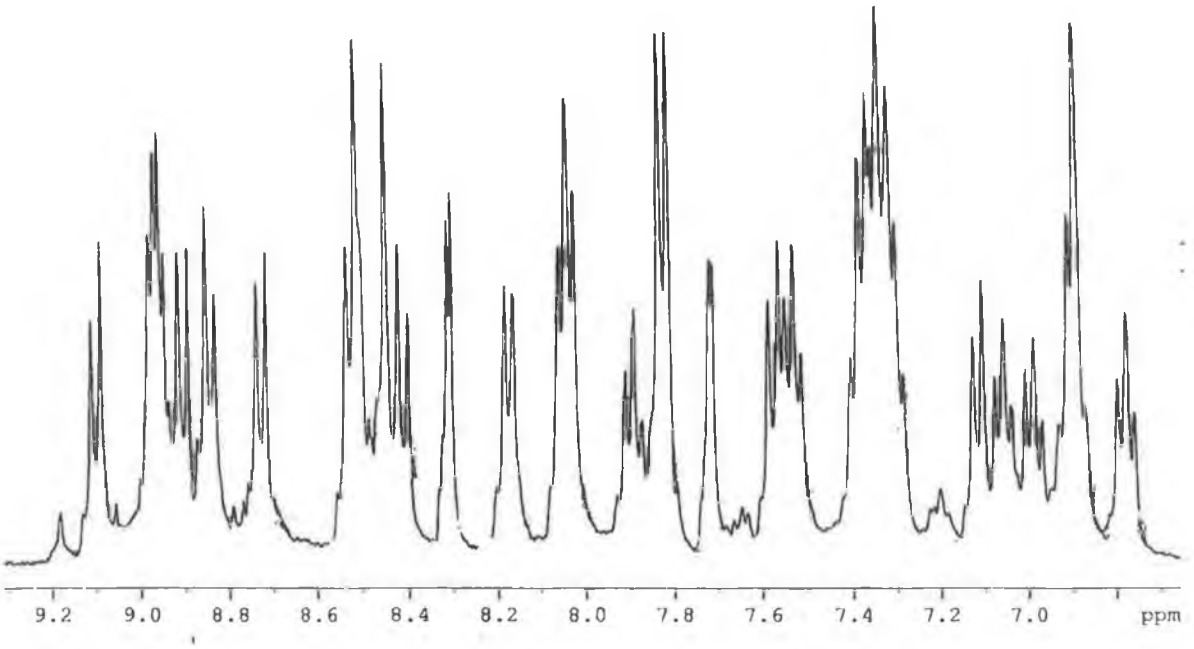

Figure 16 ^1H NMR of $[(Ru(biq)_2)_2ppt]^{3+}$ in d_3-acetonitrile

5.3.3 Electronic and photophysical properties

5.3.3.1 Absorption and Emission of ppt dinuclear complexes.

Indirect dinuclear complexes

The absorption, emission and luminescent lifetime (room temperature) properties of Ru(II) ppt⁻ indirect dinuclear complexes complexes and their deuteriated analogues are listed in Table 2. The absorption and emission spectra of the indirect dinuclear complexes were not affected by the deuteriation of the ligands. All the complexes exhibit an absorption band in the visible region between 400 and 550 nm which is expected for the dπ-π* metal-to-ligand charge transfer (MLCT) band characteristic of Ru(II) polypyridyl complexes[27,28]. On comparison to the ppt⁻ mononuclear compounds there is a shift to higher energy on addition of the second $Ru(bpy)_2$ moiety, which causes the negative charge of the triazole anion to be shared between the two metal centres.

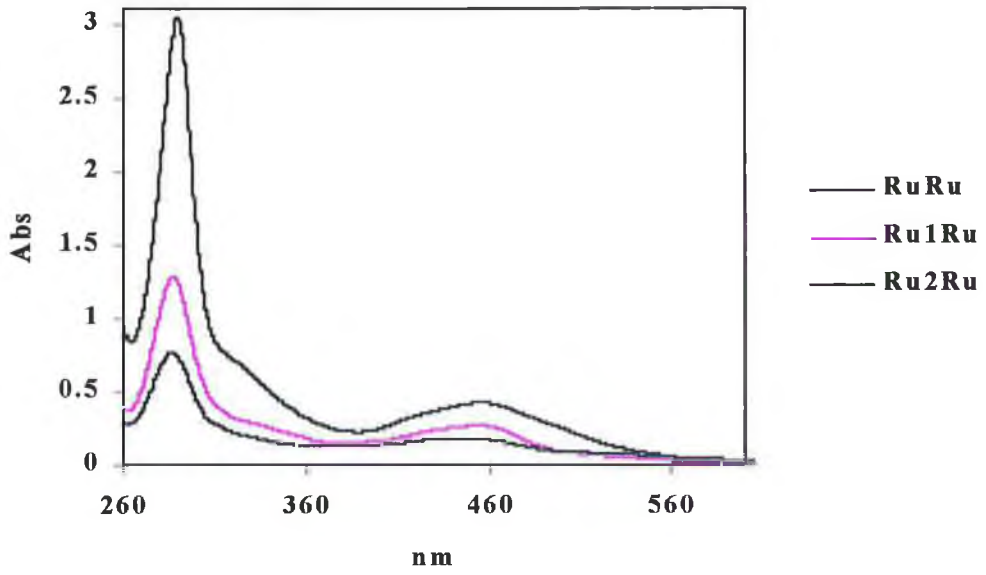

Figure 17 Absorption spectra of the $[(Ru(bpy)_2)_2ppt]^{3+}$;[RuRu] direct dinuclear complexes and the two indirect dinuclear complexes [Ru1Ru] and [Ru2Ru], equimolar concentrations (0.2×10^{-4} M) in acetonitrile.

This results in a decrease of the electron density on the metal centre causing a blue shift of the MLCT band. This is also observed for the complexes $[(Ru(bpy)_2)_2bpt]^{3+}$ and $[(Ru(bpy)_2)_2bpzt]^{3+}$. The absorption spectra of the dinuclear species $[(Ru(bpy)_2)_2bpt]^{3+}$ and $[(Ru(bpy)_2)_2bpzt]^{3+}$ have the same absorption maxima (+/ - 3 nm) as the $[(Ru(bpy)_2)_2ppt]^{3+}$ which is to be expected as they all have similar structural and chemical properties.

The absorption spectra of the direct dinuclear complexes $[(Ru(bpy)_2)_2ppt]^{3+}$ and the two indirect dinuclear complexes $[Ru(bpy)_2ppt1Ru(bpy)_2]^{3+}$ and $[Ru(bpy)_2ppt2Ru(bpy)_2]^{3+}$ are shown in Figure 17. This is to illustrate the presence of the two isomers in the direct dinuclear complexes species and to show the effect on isolating the isomers through the indirect synthesis. Eventhough they absorb in the same region of the spectrum the shape of the absorption band is different.

Compound	[a]Abs (nm) (log ε)	[a]Em (nm) (298K)	[c]Em (nm) (77K)	[a,b]Lifetime(τ/ns) (298K)
$[Ru(bpy)_2ppt]^+$ 1	461 (4.04)	671	615	217
$[Ru(bpy)_2ppt]^+$ 2	457 (4.35)	659	600	140
$[Ru(bpy)_2ppt1Ru(bpy)_2]^{3+}$	451 (4.31)	670	645	150
$[Ru(bpy)_2ppt2Ru(bpy)_2]^{3+}$	449 (4.29)	662	647	170
$[Ru(bpy)_2ppt1Ru(d_8\text{-}bpy)_2]^{3+}$	449 (4.32)	670	644	161
$[Ru(bpy)_2ppt2Ru(d_8\text{-}bpy)_2]^{3+}$	447 (4.28)	662	649	142
$[Ru(d_8\text{-}bpy)_2ppt1Ru(bpy)_2]^{3+}$	450 (4.34)	668	644	175
$[Ru(d_8\text{-}bpy)_2ppt2Ru(bpy)_2]^{3+}$	445 (4.31)	664	643	103
$[Ru(d_8\text{-}bpy)_2ppt1Ru(d_8\text{-}bpy)_2]^{3+}$	455 (4.30)	675	642	154
$[Ru(d_8\text{-}bpy)_2ppt2Ru(d_8\text{-}bpy)_2]^{3+}$	450 (4.29)	660	648	131
$[Ru(bpy)_2d_7\text{-}ppt1Ru(bpy)_2]^{3+}$	452 (4.35)	673	643	108
$[Ru(bpy)_2d_7\text{-}ppt2Ru(bpy)_2]^{3+}$	448 (4.39)	660	645	145
$[Ru(bpy)_2bpt]^+$	*475 (4.05)*	*650*	*624*	*354*
$[(Ru(bpy)_2)_2bpt]^{3+}$	*452 (4.30)*	*642*	*603*	*85*
$[Ru(bpy)_2bpzt]^+$	*450 (4.09)*	*666*	*605*	*290*
$[(Ru(bpy)_2)_2bpzt]^{3+}$	*452 (4.43)*	*671*	*617*	*260*

Table 2 Electronic properties of the indirect dinuclear complexes [a] measured in acetonitrile, [b] degassed with Argon, [c]80:20 ethanol: methanol. Lifetime error +/- 6 %. Values in italics for the bpt and bpzt complexes[17].

There is a characteristic emission band observed for the indirect dinuclear complexes in the region of 660 nm to 670 nm. The difference in the emission maxima on going from monomer to dinuclear species of the ppt complexes is only a few nm and this was also observed for the bpt and bpzt species. The emission value for the bpzt dinuclear species is 671 nm at 300 K, which is similar to that of the ppt dinuclear complexes whereas the bpt complex emits at higher energy around 640 nm. However at low temperature for the bpzt and the bpt species both emit at higher energy than

that of the ppt⁻ dinuclear complexes. The emission spectra undergoes a blue shift on going from room temperature to low temperature which can be explained by the phenomenon of 'rigidchromism' as explained in previous chapters.

Further temperature dependent emission studies are required in order to investigate if the dinuclear complex undergoes dual emission as for the pyrazine-triazole complexes.

5.3.3.2 Luminescent lifetime properties

The luminescent lifetime measurements were not carried out on the direct dinuclear complexes, as a true lifetime would not be attainable due to the presence of the two isomers. This was the reason for the synthesis of the indirect dinuclear complexes and hence a study of the photophysics of the dinuclear complexes could be achieved. The dinuclear complexes were designed using the technique of selective deuteriation purposely to use as a probe to locate the excited state of the ppt dinuclear complexes. A systematic investigation of the complexes was carried out in deaerated acetonitrile, at room temperature and monitored by CCD detection.

The results shown in *Table 2* for both Ru1Ru and Ru2Ru moieties shows that on selective deuteriation of the ligands that no particular enhancement of the lifetime is observed. This at first would suggest that the use of deuteriation is pointless however that is not the case. Observation shows that for all complexes containing the d_8-bpy moieties, on comparison with the Ru1Ru and Ru2Ru fully undeuteriated dinuclear complexes there is no enhancement of lifetime for the deuteriated bipyridyl ligands. This suggests that, the excited state is based on the ppt ligand, as there is no dramatic effect over a wide range of selectively deuteriated complexes. So far the interpretation is clear but on observation of the lifetime obtained repetitively for the dinuclear isomers containing d_7-ppt the dramatic enhancement of this lifetime as expected does not occur. In order to clarify that the complexes are fully deuteriated, the ^{1}H NMR of the complexes are shown in section 5.3.2.2 in this chapter and show clearly that the compound is deuteriated. There are two phenomena which may be used in the explanation of this result.

Firstly, previous studies of selectively deuteriated complexes shown in Chapter 3 have also portrayed insensitivity to deuteriation. The pyrazine-triazole complexes were shown to have dual emission properties over a wide temperature range[14], which was explained, by close-lying excited states of the pyrazine-triazole and the bpy ligands. Further resonance raman studies acknowledge the close lying states and showed them to be weakly-coupled emitting states, one of which has a deactivation process not strongly influenced by vibrational coupling[29]. Hence from this interpretation a similar one may be developed for the Hppt dinuclear system that on deprotonation of the complex the excited state is based on the Hppt ligand but is not clearly defined by selectively deuteriating the ligands due to weakly-coupled emitting states.

Secondly, would be to suggest that the excited state is Hppt based as already stated however, the fact that it is insensitive to deuteriation as previously mentioned suggests that the excited state is localised around the pyrazine of the Hppt ligand and that the pyrazine-triazole moiety of the ligand may govern the location of the excited state energies. It has been shown that for the $[(Ru(bpy)_2)_2bpzt]^{3+}$ complex that the excited state of the complex was localised towards one of the pyrazine rings of the reduced Hbpzt ligand[13]. Of course this cannot be clearly stated until further studies are carried out. Also, it is known that for the pyridyl-triazole complexes irrespective of the protonation state of the triazole ring has excited states which are bpy-based[30,31,32]. Hence, the fact that no bipyridyl enhancement was observed on the deprotonation of the Hppt ligand may suggest that there is no contribution to the excited state from the pyridine-side of the Hppt ligand. This is only hypothetical and further investigations would be required.

5.3.4 Electrochemical properties

The electrochemistry of the direct dinuclear complexes was not investigated, as an accurate voltammogram is not achievable due to the presence of two isomers. For dinuclear complexes communication between the metal centres may be observed via electrochemistry.

Two oxidation peaks are observed in the cyclic voltammogram of Ru1Ru. For the indirect dinuclear complexes of Ru1Ru and Ru2Ru type species each complex exhibits two reversible metal-based oxidation processes shown in *Table 3*. A difference of 290 mV exists for the oxidation potentials between the two ruthenium centres which is expected for this bridging ligand[17].

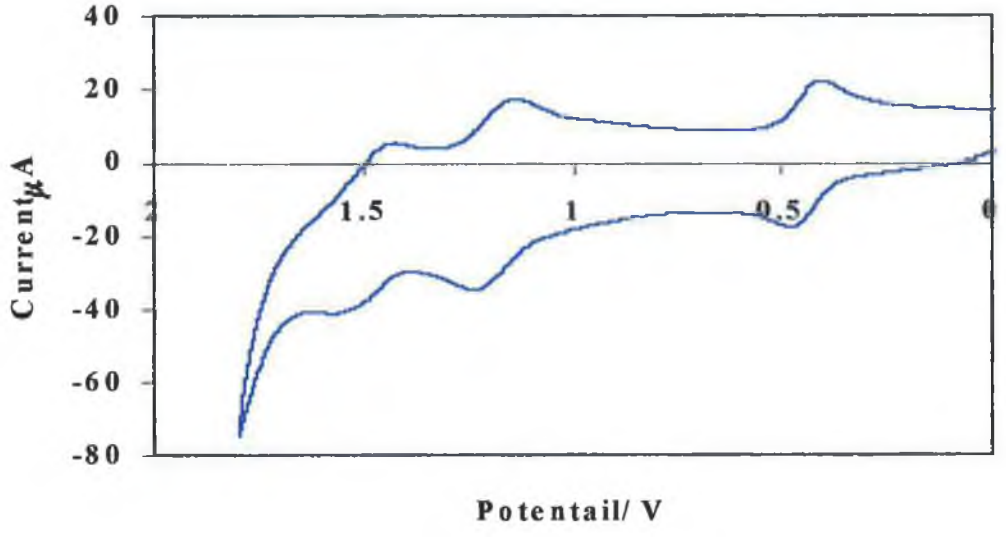

Figure 3 Cyclic Voltammogram of $[Ru(bpy)_2ppt1Ru(bpy)_2]^{3+}$ in MeCN containing 0.1M TEAP(internal reference: Ferrocene). Scan rate 0.1 V sec^{-1}.

Compound	Oxidation Pot. (V)	Reduction Pot. (V)
$[Ru(bpy)_2ppt]^+$ 1	0.94	-1.47/ -1.71
$[Ru(bpy)_2ppt]^+$ 2	1.03	-1.51/ -1.74
$[Ru(bpy)_2bpt]^+$	0.85	-1.44/ -1.68
$[Ru(bpy)_2bpzt]^+$	1.00	-1.41/ -1.66
$[Ru(bpy)_2ppt1Ru(bpy)_2]^{3+}$	1.06/ 1.35	-0.87/ -1.37/ -1.49/ -1.63/ -1.78
$[Ru(bpy)_2ppt2Ru(bpy)_2]^{3+}$	1.11/ 1.45	-1.04/ -1.45/ -1.56/-1.71
$[(Ru(bpy)_2)_2bpt]^{3+}$	*1.06/ 1.38*	*-1.42/ -1.67*
$[(Ru(bpy)_2)_2bpzt]^{3+}$	*1.19/ 1.50*	*-1.27/ -1.39/ -1.59*

Table 3 Electrochemical data of the Ru(II) indirect dinuclear complexes of the ppt complexes obtained in MeCN containing 0.1M TEAP. Values obtained by using cyclic voltammetry (internal reference: Ferrocene). Potentials in Volts versus SCE. Scanrate of 0.1 V/ sec. Values in italics[17].

The difference in oxidation potentials of the two ruthenium centres is due to an increased electron negativity on the ppt ligand after the oxidation of the first metal centre making it more difficult to oxidise the second metal centre. As can be seen from the data that for all indirect dinuclear complexes isomer 1 the N1-pyridine bound/ N4 pyrazine bound is at a higher metal-based oxidation potential than the analogous isomer 2 N1-pyrazine bound/ N4 pyridine bound. This may be attributed to the weaker σ-donor properties of the pyrazine ligand, hence less electron density is present on the metal and therefore it is harder to oxidise. This is also experienced on going from isomer 1 (pyridine bound) to isomer 2 (pyrazine bound) of the ppt$^-$ mononuclear complex and is evident on going from the bpt$^-$ to the bpzt$^-$ mononuclear and dinuclear complexes.

The reduction potentials obtained for all of the dinuclear species indicates that the first reduction potential must be ppt$^-$ based, as it is found at a less negative potential than that of the bpt$^-$ analogue[33].

Similar behaviour occurs for the ppt⁻ ligand as for the bpzt⁻ ligand, that in the mononuclear species a bpy-based reduction is only observed (bpy-based LUMO). For the same species in the dinuclear form the π^* level is lowered for the ppt⁻ ligand on addition of the second $Ru(bpy)_2$ moiety. Consequently, due to the lowering of the π^* level of the ppt⁻ ligand a less negative reduction potential (-0.87 V) is observed for the ligand compared to that of the bpy's. Based on the electrochemical data given here it is proposed that the lowest MLCT state is localised on the ppt⁻ ligand. This confirms suggestions made to explain the photophysical properties of the dinuclear species in section 5.3.3.2.

5.4 References

1 V. Balzani and F. Scandola, *Supramolecular Photochemistry*, Horwood: Chichester, U.K., **1991**.

2 A. Nieuwenhuis, D.J. Stufkens, R.A. Mc Nicholl, J.J. Mc Garvey, C.G. Coates, .H. Al-Obaidi, J.R. Westwell, M.W. George and J.J. Turner,; J. Am. Chem. Soc., **1995**, *117*, 5579.

3 C.G. Coates, L. Jacquet, J.J. Mc Garvey, S.E. Bell, A.H. Al-Obaidi and J.M. Kelly; J. Am. Chem. Soc., **1997**, *119*, 7130.

4 K.F. Mongey, J.G. Vos, B.D. Mac Graith, C.M. Mc Donagh, C.G. Coates and J.J. Mc Garvey; J. Mater. Chem., **1997**, *7*, 1473.

5 K. Maruszewski and J.R. Kincaid; Inorg. Chem., **1995**, *34*, 2002.

6 G. Denti, S. Campagna, L. Sabatino, S. Serroni, M. Ciano and V. Balzani, Inorg. Chem., **1990**, *29*, 4750.

7 S. Campagna, G. Denti, S. Serroni, M. Ciano and V. Balzani, Inorg. Chem., **1991**, *30*, 3728.

8 V. Balzani, F. Barigelletti, P. Belser, S. Bernhard, L. De Cola and L. Flamigni, J. Phys. Chem., **1996**, *100*, 16786.

9 L. Hammarstrom, F. Barigelletti, L. Flamigni, M. Indelli, N. Armaroli, G. Calogero, M. Guardigli, A. Sour, J.P. Collin and J.P. Sauvage, J. Phys. Chem., A, **1997**, *101*, 9061.

10 E. Ishow, A. Gourdon, J.P. Launay, P. Lecante, M. Verelst, C. Chiorboli, F. Scandola and C. Bignozzi, Inorg. Chem., **1998**, *37*, 3603.

11 E. Ishow, A. Gourdon, J.P. Launay, C. Chiorboli and F. Scandola, Inorg. Chem., **1999**, *38*, 1504.

12 K. Omberg, G. Smith, D. Kavaliunas, P. Chen, J. Treadway, J. Schoonover, R. Palmer and T.J. Meyer, Inorg. Chem., **1999**, *38*, 951.

13 C.G. Coates, T.E. Keyes, H.P. Hughes, P.M. Jayaweera, J.J. Mc Garvey and J.G. Vos, J. Phys. Chem. A, **1998**, *102*, 5013.

14 T.E. Keyes, C.M. O'Connor and J.G. Vos, Chem. Comm., **1998**, 889.

15 C.G. Coates, T.E. Keyes, J.J. Mc Garvey, H.P. Hughes, J.G. Vos and P.M. Jayaweera, Coord. Chem. Rev., **1998**, *171*, 323.

16 E. Ishow, A. Credi, V. Balzani, F. Spadola and L. Mandolini, Chem. Eur. J., **1999**, *5*, 3, 984.

17 H.P. Hughes, Ph. D. Thesis, Dublin City University, Ireland.

18 F. Gasparrini, D. Misiti, C.M. O'Connor, J.G. Vos and C. Villani, awaiting acceptance.

19 E. Riesgo, A. Credi, L. De Cola, and R. Thummel, Inorg. Chem., **1998**, *37*, 2145.

20 B. Patterson and F. Keene, Inorg. Chem., **1998**, *37*, 645.

21 N. Fletcher and F. Keene, J. Chem. Soc., Dalton Trans., **1998**, 2293.

22 P. Belser, S. Bernhard, E. Jandrasics, A. von Zelewsky, L. De Cola and V. Balzani, Coord. Chem. Rev., **1997**, *159*, 1.

23 S. Campagna, S. Serroni, S. Bodige and F. Mac Donnell, Inorg. Chem., **1999**, *38*, 692.

24 F. Gasparrini, D. Misiti, W. Still, C. Villani and H. Wennemers, J. Org. Chem., **1997**, *62*, 8221.

25 F. Gasparrini, D. Misiti, M. Pierini and C. Villani, Tetrahedron; Asymmetry, **1997**, *8*, 12, 2069.

26 S. Chirayil and R. Thummel, Inorg. Chem., **1989**, *28*, 813.

27 K. Kalyanasundaram, M. Nazeeruddin, M. Gratzel, G. Viscardi, P. Savarino and E. Barni, Inorg. Chim. Acta., **1992**, *198*, 831.

28 R.M. Berger, Inorg. Chem., **1990**, *29*, 1920.

29 T. Keyes, C. O'Connor, U. O'Dwyer, C. Coates, P. Callaghan, J.J. Mc Garvey and J.G. Vos, awaiting acceptance.

30 R. Hage, R. Prins, J.G. Haasnoot, J. Reedijk and J.G. Vos, J. Chem. Soc., Dalton Trans., **1987**, 1389.

31 B. Buchannan, R. Wang, J.G. Vos, R. Hage, J.G. Haasnoot and J. Reedijk, Inorg. Chem., **1990**, *29*, 3263.

32 R. Wang, J.G. Vos, R. Schmehl and R. Hage, J. Amer. Chem. Soc., **1992**, *114*, 1964.

33 R. Hage, A. Dijkhuis, J.G. Haasnoot, R. Prins, J. Reedijk, B. Buchannan and J.G. Vos, Inorg. Chem., **1988**, *27*, 2185.

Chapter 6

CONCLUSION AND FUTURE WORK

6.1 CONCLUSION

In this work, the synthesis and characterisation of a number of novel Ruthenium (II) mononuclear and dinuclear complexes containing 1,2,4-triazole ligands is described. Synthesis has played a large role of this study, as a selection of heteroligand complexes were prepared which all form coordination complexes. The use of 'synthetic strategy' was used during this study in order to attempt to tune the excited states of the complexes through the use of ligand substitution. It was hoped through the use of deuteriation of the heteroligand complexes that the excited states would be pinpointed but in the case of the Hpztr and Hppt ligands their photophysical properties revealed to be more complicated than first thought. Also for the formation of Hppt dinuclear complexes two synthetic routes were involved, both direct and indirect.

Characterisation of the $pztr^-$ complexes was determined by hplc, UV, emission, ^1H NMR, electrochemistry and also ^{99}Ru NMR and stereoisomerism through collaborative work. The use of selective deuteriation was best demonstrated for the $[Ru(bpy)_2pytr]^+$ complex which suggested that the excited state was bpy based. In the case of the $[Ru(bpy)_2pztr]^+$ complex the photophysical properties turned out to be much more complicated as there were no dramatic effects noticed after selectively deuteriating the complex. After temperature dependence studies of the emission properties of the pztr complex it has been proposed that the complex has dual emission properties i.e. that two close-lying excited states may exist. The phenanthroline and biquinoline analogues of the $pztr^-$ complex did not show any enhancement after deuteriation hence further studies are required into their photophysical properties. The electrochemistry of the $pztr^-$ complexes shows that the σ-donor properties of the biquinoline complex are significantly weaker than those of the bipyridyl and phenanthroline species. This leads to a raise of the oxidation potential of the biq species due to the stabilisation of the dπ-orbitals. In all cases the N2 isomer was easier to oxidise than the N4 isomer due to the greater σ-donor strength of the N2 site. A crystal structure was obtained of $[Ru(bpy)_2pztr]^+$ N2 bound which confirms the structure of the complex, the coordination sites of the isomers and the hydrogen bonding occurring in the complexes.

The Hppt complexes proved to be more complicated than the Hpztr complexes as the Hppt type have a potential of four coordination isomers forming on synthesis. Semi-preparative hplc was very useful in the isolation of the N1 and N2 isomers of the ppt$^-$ complexes. ^{1}H NMR and ^{99}Ru NMR were used to identify the isomers. The use of selective deuteriation for the bpy, phen and biq ppt$^-$ complexes did not give much insight into the photophysical properties of the complexes, as there was no dramatic effects on deuteriation of the ligands. Resonance Raman and temperature dependence studies is necessary in aprotic and protic media in order for further insight to be obtained. The acid-base properties of the ppt$^-$ complexes suggest that the ppt$^-$ ligand is not a spectator ligand as the pK_a* is higher than that of the ground state pK_a. Similar results were found for the phen-containing analogue however the biq species gave the opposite result, i.e. that the excited state is based on the biq ligand. An X-Ray crystal structure of the pyrazine bound $[Ru(bpy)_2ppt]^+$ was achieved which confirms the coordination isomers depicted form the ^{1}H NMR.

The study of the dinuclear complexess of Hppt incorporated two different synthetic routes, one in which was the direct approach i.e. 2 $[Ru(bpy)_2Cl_2]$ moieties with 1 Hppt moiety. Whereas the indirect approach was more difficult in that the mononuclear coordination isomer had to be isolated prior to synthesis with 1 moiety of $[Ru(bpy)_2Cl_2]$ to form the indirect dinuclear complexes. It was found that the direct dinuclear complexes formed two inseparable dinuclear coordination dinuclear complexes with almost identical chemical properties. This was confirmed by the presence of double the amount of stereoisomers present in the sample and by hplc-photodiode array detection. From the photophysical properties it suggests that the excited state may be based on the ppt$^-$ ligand and maybe even localised around the pyrazine ring. This is suggested as the pyrazine-triazole complexes proved to be insensitive to the effects of selective deuteriation due to its close lying excited states. This may also be the case for the Hppt ligand. Also the Hbpzt ligand was found to have its excited state localised around one pyrazine ring of the ligand. In the case of Hpytr and Hbpt the excited state has been mainly bpy based. We have seen no evidence of bpy-enhancement hence this may suggest that the excited state is ppt$^-$ based. Electrochemical evidence thus far suggests that the lowest MLCT state is localised on the ppt$^-$ ligand. Further investigations are required.

In general the molecular modelling was found to be quite useful in the visual understanding of both the coordination isomers and the stereoisomers. Also the use of deuteriation does not appear to alter the hplc, UV and electrochemical properties of all the complexes cited in this text. Much experience has been obtained in synthesis, purification, recrystallisation and deuteriation, which is outlined in the relevant chapters. Also a variety of analytical techniques have been incorporated in the characterisation, in which training in new techniques such as laser spectroscopy with CCD detection was obtained. New concepts such as photophysics and photochemistry were also examined in relation to Ru(II) chemistry. As a result of this study a series of complexes with varying ligands and selectively deuteriated moieties have been prepared and are available for a more in-depth study into the photophysical and electrochemical behaviour of these Ru(II) complexes.

6.2 Future Work

From this study develops new projects which are necessary in completing the study of the HPPT and Hpztr ligand investigation. Some of the concepts are as follows;

1. Temperature dependence studies in acidic and basic media of the mononuclear ppt$^-$ complexes both emission and laser spectroscopy for the bpy, phen and biq analogues.
2. Temperature dependence studies of the photophysical behaviour of the Hppt indirect dinuclear complexes.
3. A more in-depth electrochemical study of the ppt$^-$ mono- and dinuclear Complexes
4. Spectroelectrochemistry of the indirect dinuclear complexes of Hppt.
5. Another area, which may be useful to prevent isomerisation, is the use of quarternisation. The aim would be to selectively methylate one nitrogen on either the pyridine or the pyrazine ring. A similar ligand dpp was previously quarternised by Serroni et al[1] with the use of trimethyloxonium tetrafluoroborate, which selectively methylated one of the pyridine rings as shown in Figure 1.

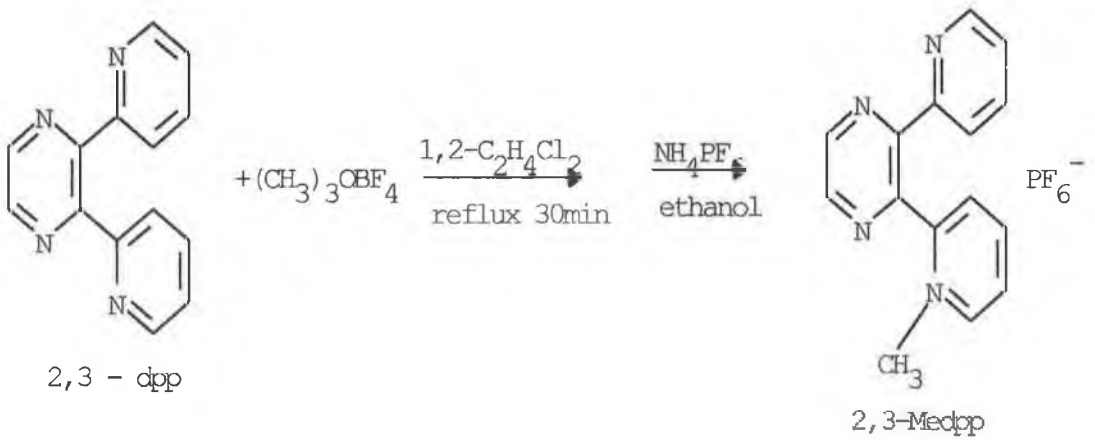

***Figure 1: Quarternisation of the ligand Dpp using trimethyloxonium tetrafluoroborate*[1].**

6. Partial deuteriation of the Hppt ligand i.e. deuteriation of the pyrazine or pyridine ring prior to synthesis of the Hppt ligand.
7. Synthesis of the indirect Hppt dinuclear complexes completely deuteriated, may see some enhancement of the ppt⁻ ligand.
8. Solvatochromic study of the $[Ru(biq)_2pztr]^+$ and $[Ru(biq)_2ppt]^+$ complexes.
9. Photochemical study of all the mono- and dinuclear complexes of Hppt.
10. Photochemical study of $[Ru(biq)_2pztr]^+$ complexes. Thus far the $pztr^{-2}$ complexes containing biq have been found to be unstable and the ppt⁻ monomers have shown to be photostable. $[Ru(biq)_2pytr]^+$ have been previously been found to be photostable[3], hence it may be the presence of the pyridine-ring on the Hppt ligand that aids in its biq complexes photostability.
11. Preparation of mixed ligand indirect ppt⁻ dinuclear complexes i.e. $[Ru(bpy)_2pptRu(biq)_2]^{3+}$.

6.3 References

1 S. Serroni, G. Denti, Inorg. Chem., **1992**, *31*, 21,4251.

2 A. Brennan and Olaffs, Photochemistry projects, **1998** and **1999**.

3 T. Keyes, J.G. Vos, J. Kolnaar, J. Haasnoot, J. Reedijk and R. Hage, Inorg. Chim. Acta.,**1996**, *245*, 237.

APPENDIX I

POSTERS, PRESENTATIONS AND PUBLICATIONS

Posters

1. The synthesis, purification and characterisation of ruthenium 3-(pyrazin-2-yl)-2-(pyridin-2-yl)-1,2,4-triazole (Hppt), Ru-Mn TMR conference, Paris, France, April 1997.
2. The synthesis, purification and characterisation of ruthenium (II) Hppt mononuclear complexes and their deuteriated analogues, Irish Chemistry colloquium, Dublin City University, June 1997.
3. Photophysics of a dual emitting Ru(II) polypyridyl mixed ligand complex, EPA Summer School Noordwijk, The netherlands, June 1998.
4. Locating excited states in novel Ru(II) dinuclear complexes, Irish Chemistry colloquium, Kevin St.college, Dublin Institute of Technology, June 1999.

Presentations

1. The best of Irish research open day, Burligton Hotel, Dublin, November 1998.
2. Science Day, Waterford Institute of Technology, Waterford, Feburary 1998.

Publications

1. Evidence for the presence of dual emission in a ruthenium (II) polypyridyl mixed ligand complex, T. Keyes, C. O'Connor and J.G. Vos, Chem. Comm., 1998, 889.
2. Synthesis, characterisation and photophysics of Ru(II) complexes containing 3-(pyrazin-2-yl)-1,2,4-triazole, T. keyes, C. O'Connor and J.G. Vos, awaiting acceptance.
3. ^{99}Ru-NMR spectroscopy of Ru(II) organometallic complexes and mixtures of tris-polypyridyl complexes: A powerful analytical tool, S. Gaemers, J. van Slageren, C. O'Connor, J.G. Vos and C.J. Elsevier, awaiting acceptance.

4. Isolation of the stereoisomers of Ru(II) polypyridyl complexes by HPLC, F.Gasparrini, D. Misiti, C.M. O'Connor, J.G. Vos and C. Villani, awaiting acceptance.

5. Synthesis, characterisation and photophysics of Ru(II) complexes containing 3-(pyrazin-2-yl)-5-(pyridin-2-yl)-1,2,4-triazole, H. Hughes, C. O'Connor and J.G. Vos, future publication.

Evidence for the presence of dual emission in a ruthenium(II) polypyridyl mixed ligand complex

Tia E. Keyes, Christine O'Connor and Johannes G. Vos*†

Inorganic Chemistry Research Centre, School of Chemical Sciences, Dublin City University, Dublin 9, Ireland

The complex $[Ru(bpy)_2(pztr)]^+$ 1 [bpy = 2,2′-bipyridyl, Hpztr = 3-(pyrazin-2-yl)-1,2,4-triazole] exhibits two emission maxima in fluid solution [ethanol–methanol (4 : 1)] over the temperature range 120–260 K; from fluorometric studies two well resolved emission maxima are observed at 590 and 700 nm, accompanied by two different lifetimes; the observations suggest the presence of two emitting states in this compound, one bpy and one pyrazine based.

The photophysical properties of ruthenium(II) polypyridyl complexes make them attractive building blocks for supramolecular assemblies and as a result several thousands of homo- and hetero-leptic compounds have been reported in the literature.[1] It is generally accepted that emission in ruthenium polypyridyl complexes originates from a triplet metal-to-ligand charge-transfer (^{3}MLCT) state.[1] In the case of a mixed ligand complex this excited state can in principle be located on any of the ligands. Many detailed studies have therefore been carried out to determine the location of the emitting state in such compounds. From theoretical considerations one would predict that emission will occur from the lowest triplet state only[2] and indeed this is observed in almost all cases. In rigid media a number of dual emissions have been documented.[3] However, in solution such reports are rare,[4] and to our knowledge no clear-cut cases have been reported in solution for ruthenium polypyridyl type compounds.

In this contribution, we wish to present direct evidence for dual emission in solution over a wide temperature range for the mononuclear mixed ligand ruthenium(II) polypyridyl complex $[Ru(bpy)_2(pztr)][PF_6]_2$ **1** [bpy = 2,2′-bipyridyl, Hpztr = 3-(pyrazin-2-yl)-1,2,4-triazole].

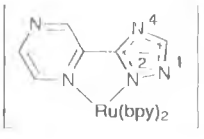

The compound under investigation was synthesised as described previously.[5] The N^2 and N^4 isomers were separated by semi-preparative HPLC and characterized by ^{1}H NMR spectroscopy, analytical diode array HPLC, and elemental analysis. These techniques confirm that the purity of **1** is >99%. In this study only the N^2 isomer, shown above, was investigated.

Earlier work on these compounds has shown that isomerisation, photoinduced or otherwise, of the deprotonated N^2 and N^4 isomers does not occur,[5c,d] while pK_a values obtained for the ground state and excited state for the N^2 isomer are between 3.5 and 4 and as a result, protonation of **1** under the experimental conditions discussed here is unlikely.[5a]

One can therefore be confident that in the experiments carried out in this contribution only one species will be present. It is furthermore important to note that pK_a values, electrochemical experiments and resonance Raman data have shown that bpy and pyrazine based excited states are similar in energy. In **1** the bpy state is lower in energy, while in the complex containing a protonated triazole the emitting state is pyrazine based.[5b,d] Finally, emission and absorption maxima of **1** in its protonated and deprotonated states are very similar.[5a]

Selected temperature dependent luminescence spectra for **1** [ethanol–methanol (4 : 1), containing 1% diethylamine or ammonia to assure deprotonation of the triazole ring] are shown in Fig. 1. At 90 K, the spectrum obtained [Fig. 1(*a*)] is typical for compounds of this type with a single emission being observed at 617 nm. After laser excitation at 355 nm the luminescence decays according to a single exponential with a lifetime of 3200 ns (all lifetimes ±10%). On increasing the temperature to 145 K, [Fig. 1(*b*)] the emission spectrum of **1** is resolved into two distinct bands; one, as expected, at 710 nm and an additional feature at 590 nm. The luminescent signal obtained at this temperature monitored at 650 nm cannot be fitted as a single exponential. Normal curve fitting procedures yield lifetimes of 2400 and 800 ns with ratios of 60 and 40%, respectively. Measurements monitored out at 700 and 590 nm yield single exponential decays and identify the long lifetime as belonging to the 700 nm signal. At higher temperatures the contribution from the higher energy component decreases. The temperature dependence of the emission decay for the two signals is therefore different. Excitation spectra obtained at both emission maxima are sufficiently similar to suggest that both emissions are based on MLCT emissions. The excitation spectrum of the 590 nm emission shows an absorption maximum at 440 nm, while for the 700 nm band a maximum is observed at 465 nm.

In cases where a dual emission is observed, the contribution from impurities is always a concern. However, we do not believe that the data above can be attributed to the presence of an impurity. First of all, the lifetimes and intensities observed for the two emission components (see above) suggest that the concentration of an impurity would have to be high and this is not observed. Also, the same results were obtained for various samples of **1**. Finally, when the triazole is protonated a normal single exponential behavior is obtained over the entire temperature range [77 K (2200 ns), 175 K (800 ns) and room temperature (230 ns)].

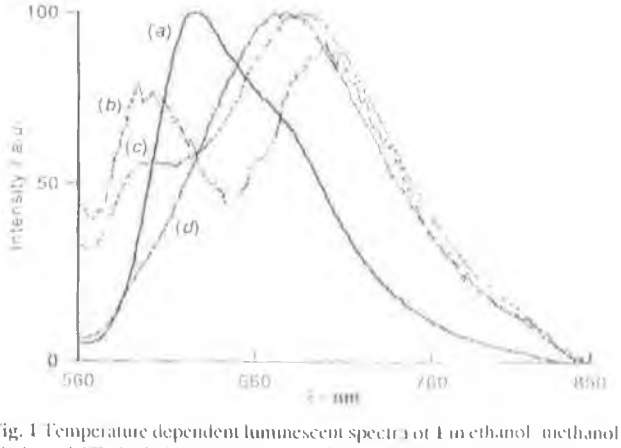

Fig. 1 Temperature dependent luminescent spectra of **1** in ethanol–methanol (4 : 1) and 1% diethylamine, at (*a*) 90, (*b*) 145, (*c*) 220 and (*d*) 298 K

On the basis of these considerations we are confident that the results obtained are best explained by the presence in the title compound of two weakly coupled emitting states. As pointed out above, earlier work has shown that bpy and pyrazine based MLCT states are similar in energy. For example, the energy separation between these two emitting states of 2400 cm^{-1} which at 145 K is consistent with the electrochemistry of this complex which shows a potential difference of 0.33 eV between the first two bpy and pyrazine based reductive steps of **1**. We therefore propose, based on our earlier results,[5] that the highest energy emitting state observed between 120 and 260 K, is pyrazine based. After excitation to the ^{1}MLCT level, efficient intersystem crossing to the lowest, strongly coupled bpy based triplet state is observed. Up to 260 K it is the lowest energy manifold of the bpy triplet that is populated. Population of the pyrazine based triplet state can in this model only occur by thermal means. The lower energy components of this manifold are weakly coupled to a pyrazine state, and population of the pyrazine state occurs thermally between *ca.* 120 and 260 K. Above this temperature the upper, fourth ^{3}MLCT of the bpy triplet manifold is thermally populated,[6] such population is observed in the temperature dependent luminescent lifetimes of related[5c] complexes, where population of this state was observed to occur from around 240 K. This upper state, which contains more singlet character, is not coupled to the pyrazine, and therefore a single emission primarily based on the fourth ^{3}MLCT is observed. Further investigations are at present in progress to further develop this picture.

The authors thank the EC Training and Mobility Programme (Contract CT96-0076), the EC Joule programme, Forbairt and the Electricity Supply Board for financial assistance. Johnson Matthey are thanked for a generous loan of $RuCl_3 \cdot xH_2O$.

Notes and References

† E-mail: vosh@ccmail.dcu.ie

1 A. Juris, V. Balzani, F. Barigelletti, S. Campagna, P. Belser and A. von Zelewsky, *Coord. Chem. Rev.*, 1988, **84**, 85; V. Balzani, A. Juris, M. Venturi, S. Campagna and S. Serroni, *Chem. Rev.*, 1996, **96**, 759.
2 M. Kasha, *Discuss. Faraday Soc.*, 1950, **9**, 14.
3 R. L. Blakley and M. K. DeArmond, *J. Am. Chem. Soc.*, 1987, **109**, 4895; A. P. Wilde, K. A. King and R. J. Watts, *J. Phys. Chem.*, 1991, **95**, 629; E. Taffarel, S. Chirayil, W. Y. Kim, R. P. Thummel and R. H. Schmehl, *Inorg. Chem.*, 1996, **35**, 2127.
4 R. J. Watts, *Inorg. Chem.*, 1981, **20**, 2302; L. Wallace, D. C. Jackman, D. P. Rillema and J. W. Merkert, *Inorg. Chem.*, 1995, **34**, 5210.
5 (*a*) R. Hage, J. G. Haasnoot, H. A. Nieuwenhuis, J. Reedijk, R. Wang and J. G. Vos, *J. Chem. Soc., Dalton Trans.*, 1991, 3271; (*b*) H. A. Nieuwenhuis, J. G. Haasnoot, R. Hage, J. Reedijk, T. L. Snoeck, D. J. Stufkens and J. G. Vos, *Inorg. Chem.*, 1991, **30**, 48; (*c*) R. Wang, J. G. Vos, R. H. Schmehl and R. Hage, *J. Am. Chem. Soc.*, 1992, **114**, 1964; (*d*) H. Hughes, Thesis, Dublin City University, 1993.
6 J. V. Casper and T. J. Meyer, *Inorg. Chem.*, 1983, **22**, 2444; E. M. Kober and T. J. Meyer, *Inorg. Chem.*, 1984, **23**, 3877.

Received in Cambridge, UK, 3rd February 1998; 8/00921J

APPENDIX II

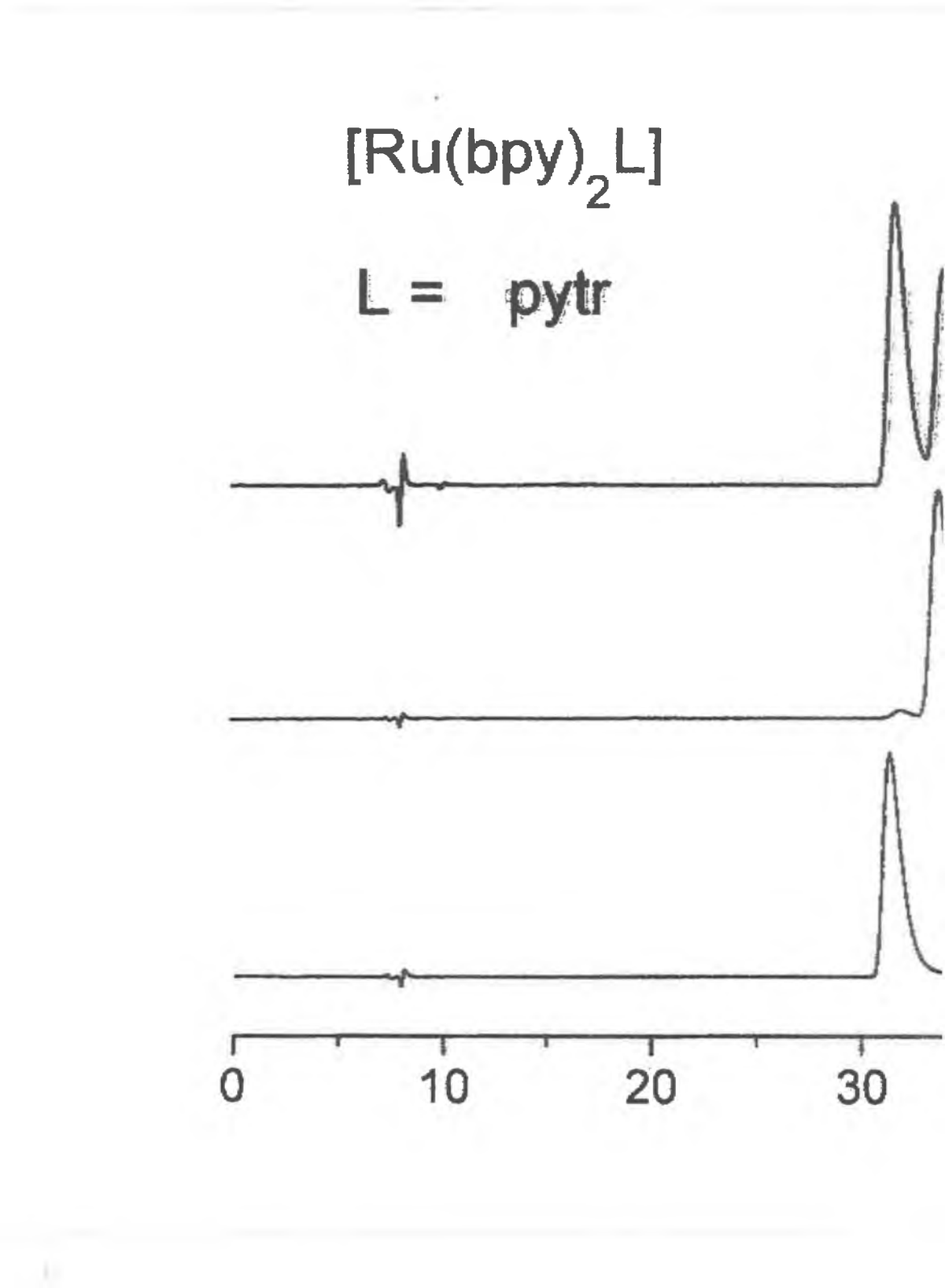
[Ru(bpy)2L]
L = pytr
0
10
20
30

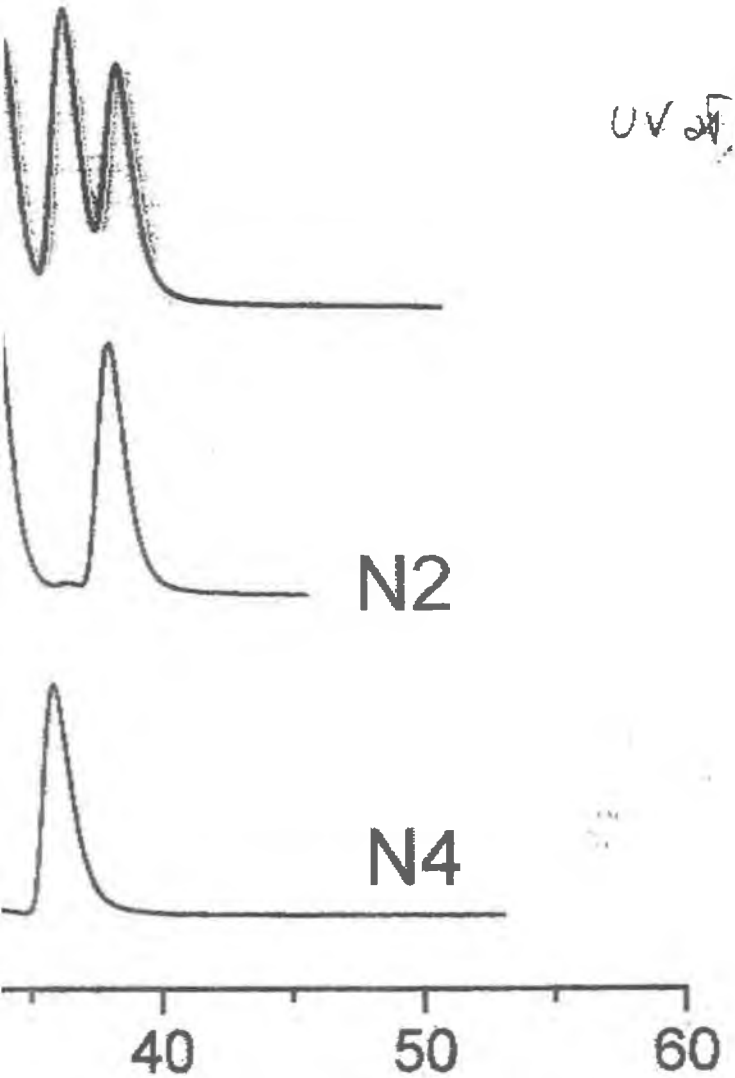
UV at 267nm
N2
N4
40
50
60

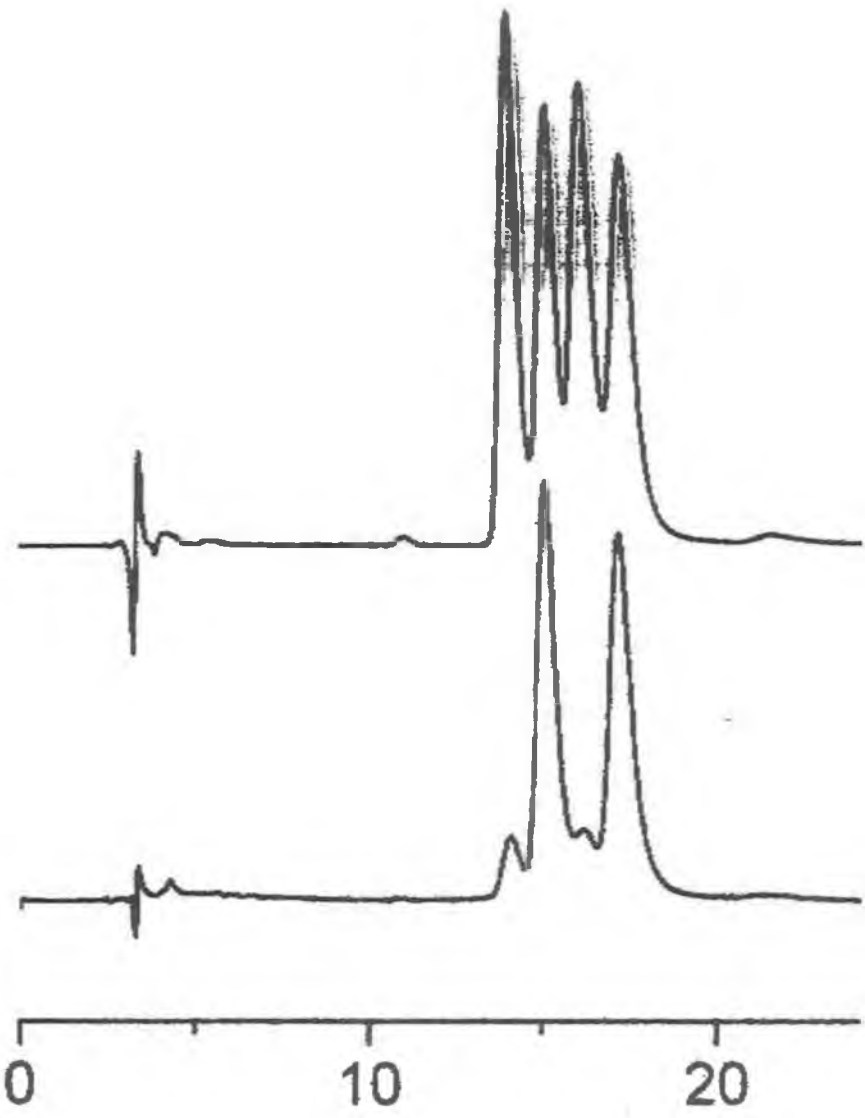
0
10
20

$[Ru(bpy)_2L]$

L = pztr

UV at 267 nm

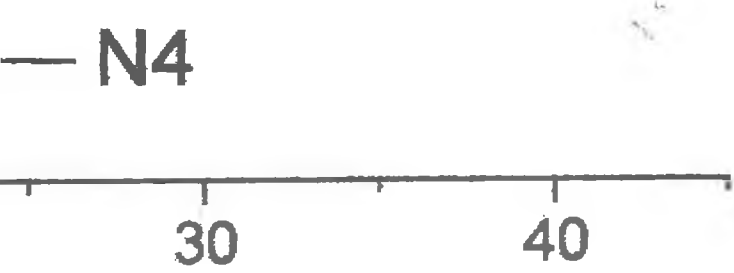

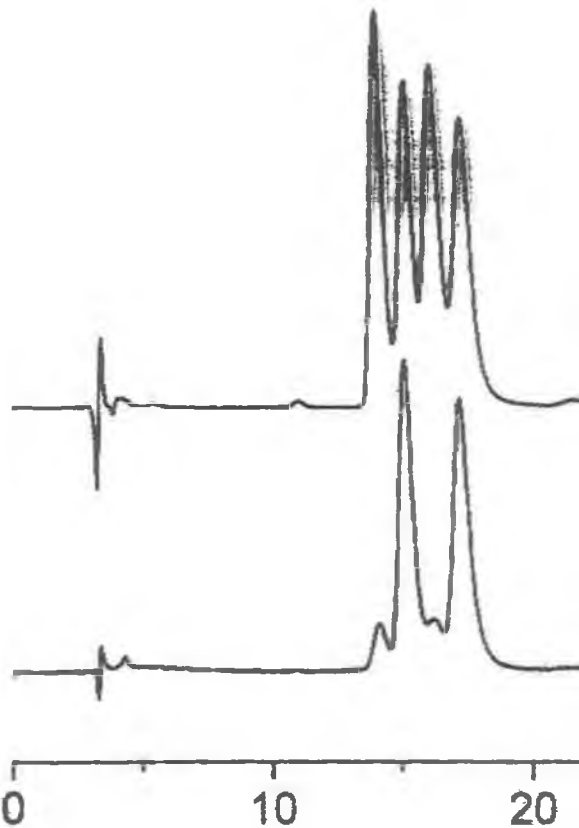
0
10
20

$[Ru(bpy)_2L]$

L = pztr

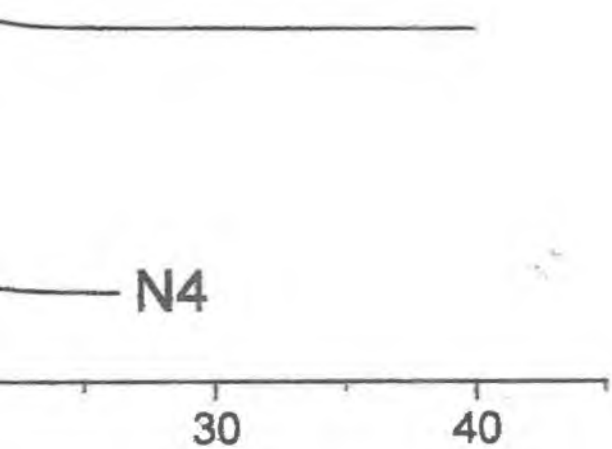

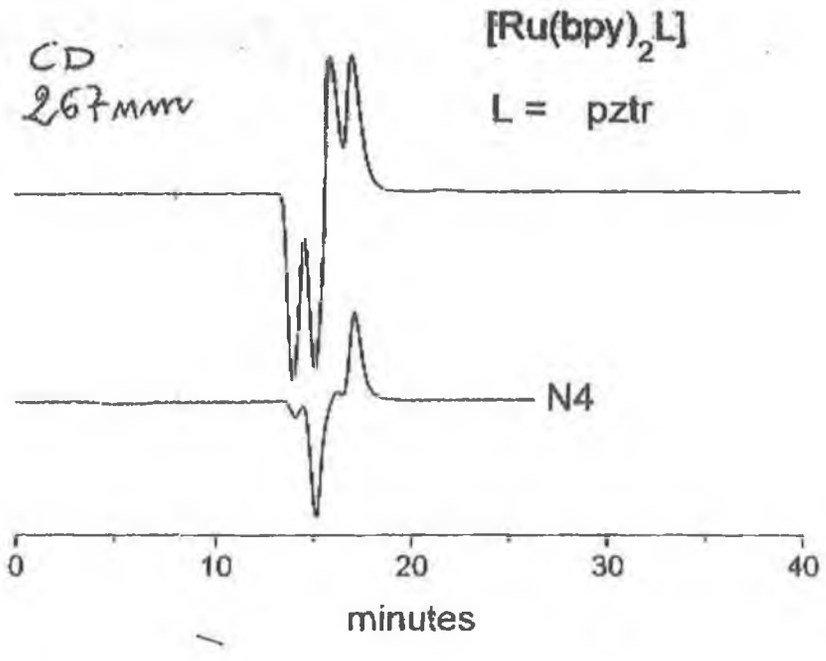
CD
267nm
[Ru(bpy)2L]
L = pztr
N4
0
10
20
30
40
minutes

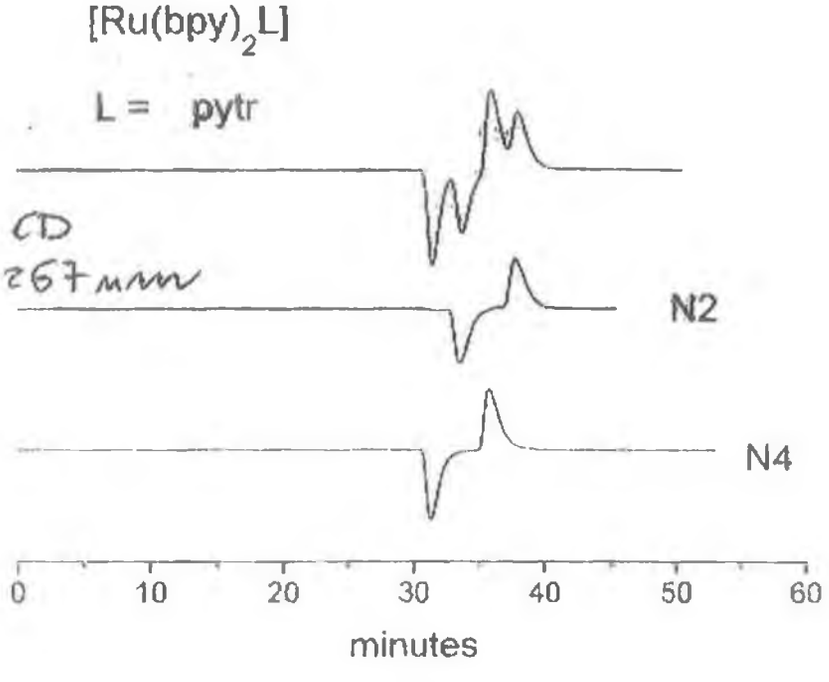
[Ru(bpy)2L]
L = pytr
CD
267nm
N2
N4
0
10
20
30
40
50
60
minutes

APPENDIX III

4817
N
N
N
N
N
[Ru]
5100
4900

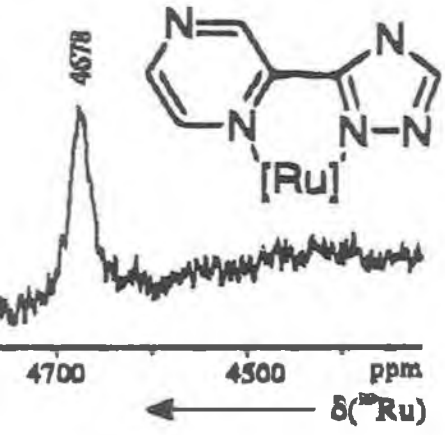
4678
N
N
N
N–N
[Ru]
4700
4500
ppm
δ(99Ru)

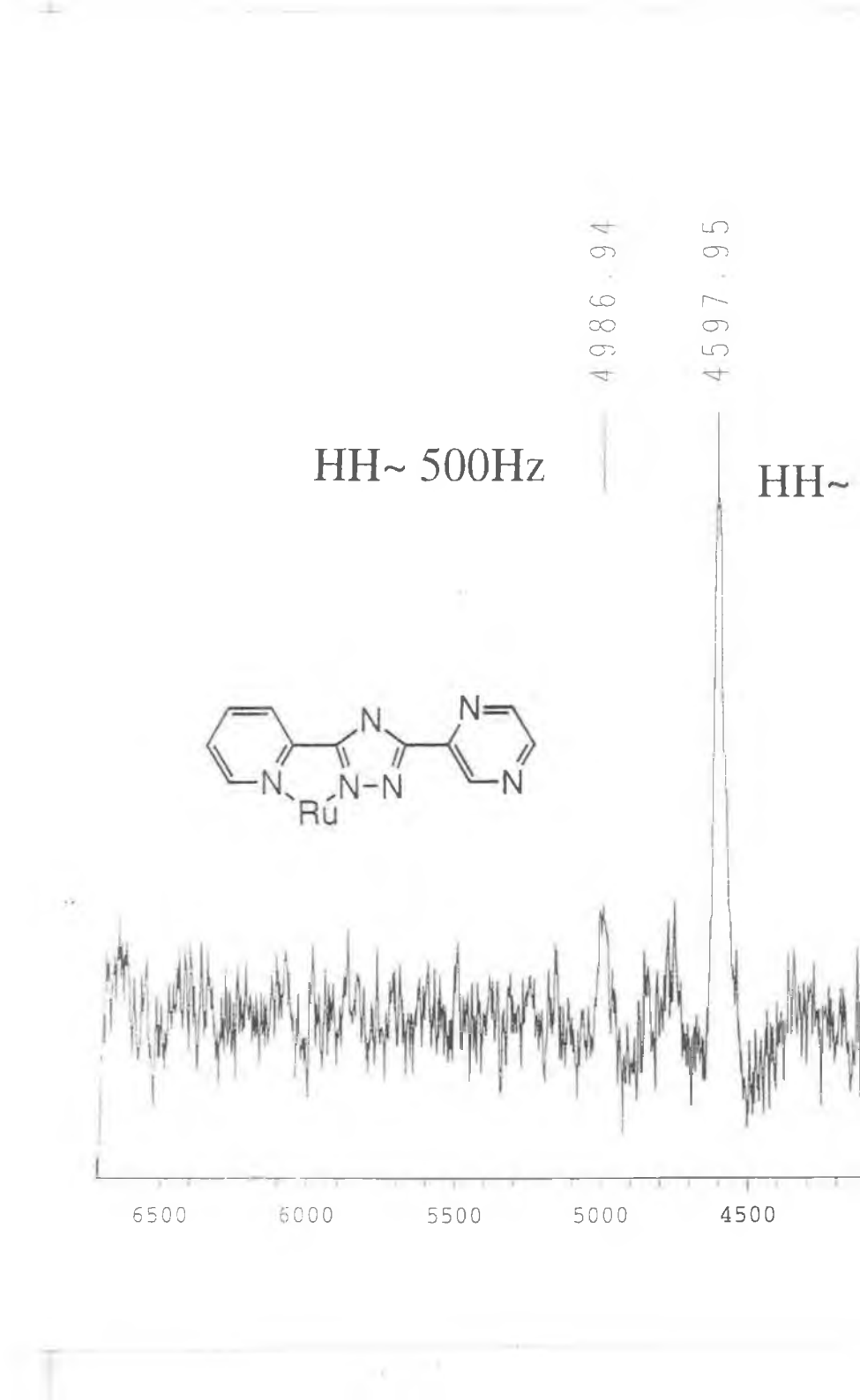
4986.94
4597.95
HH~ 500Hz
HH~
N
N
N
N
N
Ru
6500
6000
5500
5000
4500

99Ru in CH3CN T= 40°C

32 pnt. LpBc

530Hz

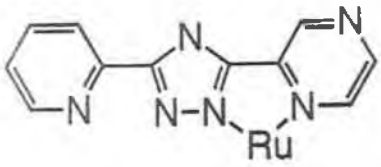

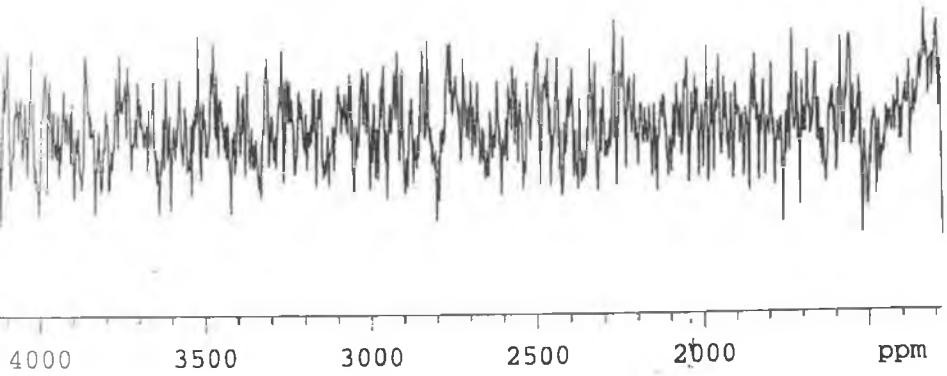

APPENDIX IV

Table I. Summary of Data Collection, Structure Solution and Refinement Details

	1, $[(bipy)_2Ru(pyrtrz)]^+[H]^+_{0.5}[PF_6]_{1.5}\bullet 0.37H_2O$
(a) **Crystal Data**	
empirical formula	$C_{26}H_{21.24}N_9RuO_{0.37}P_{1.5}F_9$
fw	784.2
color, habit	red, plate
crystal size, mm	0.08 x 0.28 x 0.45
cryst syst	Orthorhombic
a, Å	17.4944(13)
b, Å	17.5143(15)
c, Å	19.5605(20)
α, °	90
β, °	90
γ, °	90
V, Å^3	5993.4(9)
space group	B2cb
Z	8
molecular symmetry	/
F(000)	3126
d_{calc}, g cm^{-3}	1.731
μ, mm^{-1}	0.697
(b) **Data acquisition**[a]	
temp, °C	21
unit-cell reflcns (2θ-range°)	
max. 2θ (°) for reflcns	27.1
hkl range of reflcns	25 (21 - 35)
variation in 3 standard reflcns	< 1 %
reflcns measured	3430
unique reflcns	3170
R_{int}	0.052
reflcns with $I > 2\sigma(I)$, 2	2185
absorption correction type	*DIFABS*
min. max. abs. corr.	0.47, 1.00
(c) **Structure Solution and Refinement**[b]	
solution method	Direct methods
H-atom treatment	riding (SHELXL93 defaults)
no. of variables in LS	524, [73 restraints, PF_6^- disorder]
k in $w = 1/(\sigma^2Fo + kFo^2)$	0.0008 (NRCVAX) 0.0274 (SHELXL-93)
R, R_w, *gof*	0.035, 0.056, [0.073, 0.062]
density range in final Δ-map, e Å^{-3}	+0.29, -0.37(5).
final shift/error ratio	0.002
sec. extnct. correction	none

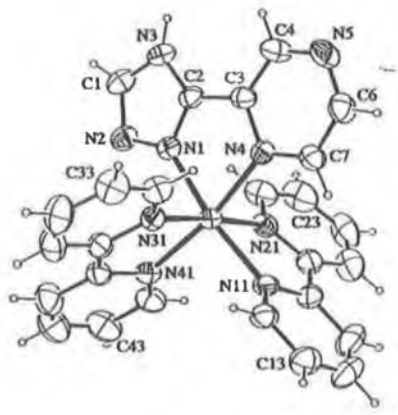

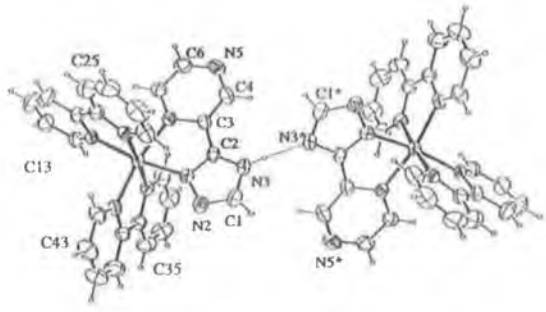

[a] Data collection on an Enraf Nonius CAD4 diffractometer with graphite monochromatised Mo-Kα radiation (λ 0.7093 Å). [b] All calculations were done on a Pentium 100 computer with the NRCVAX system of programs (E.J. Gabe, Y. Le Page, J-P. Charland, F.L. Lee and P.S. White, *J. Appl. Cryst.* (1989), **22**, 384-389) and refined using the SHELXL 93 program (G. Sheldrick, University of Goettingen, Program for the refinement of crystal structures).

9689dimu.plt

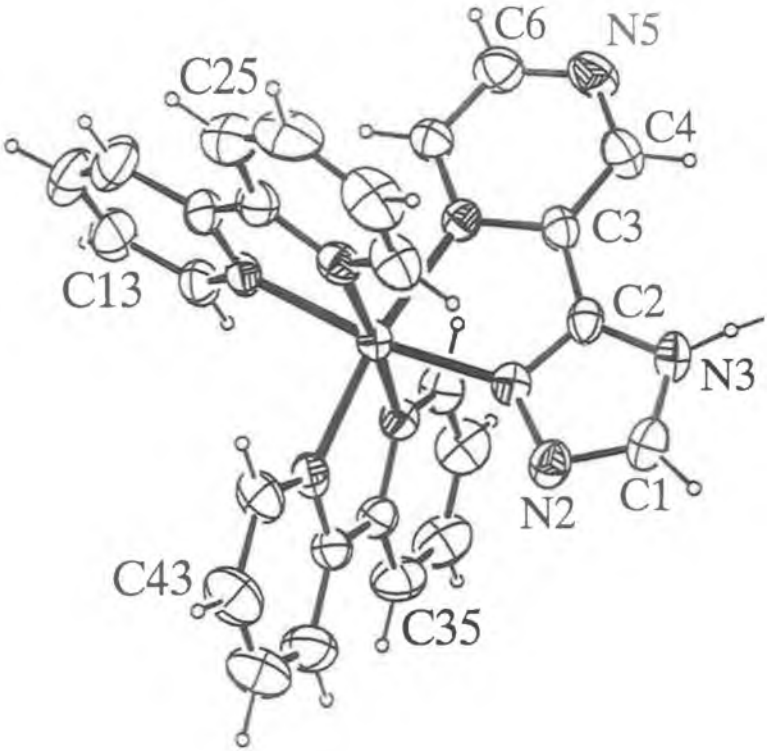

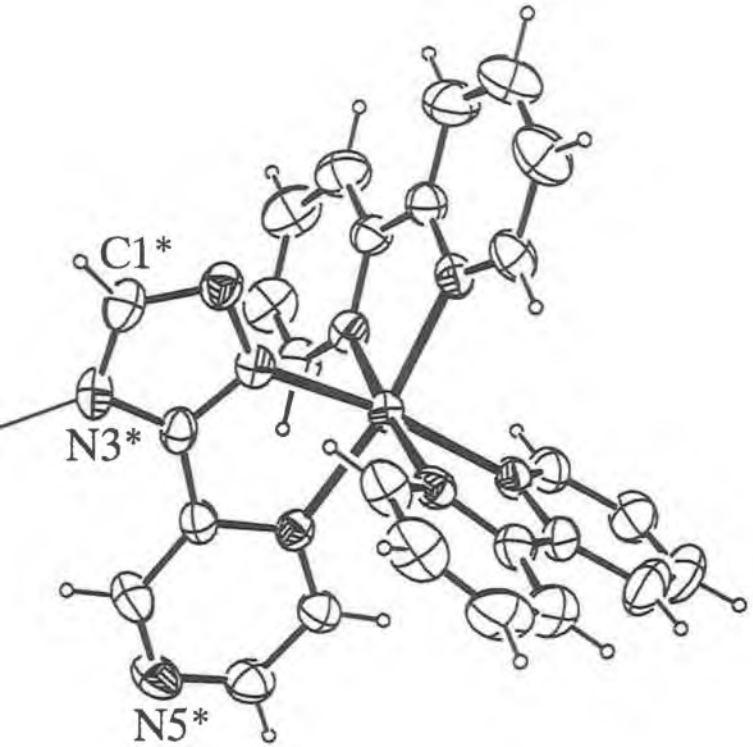
C1*
N3*
N5*

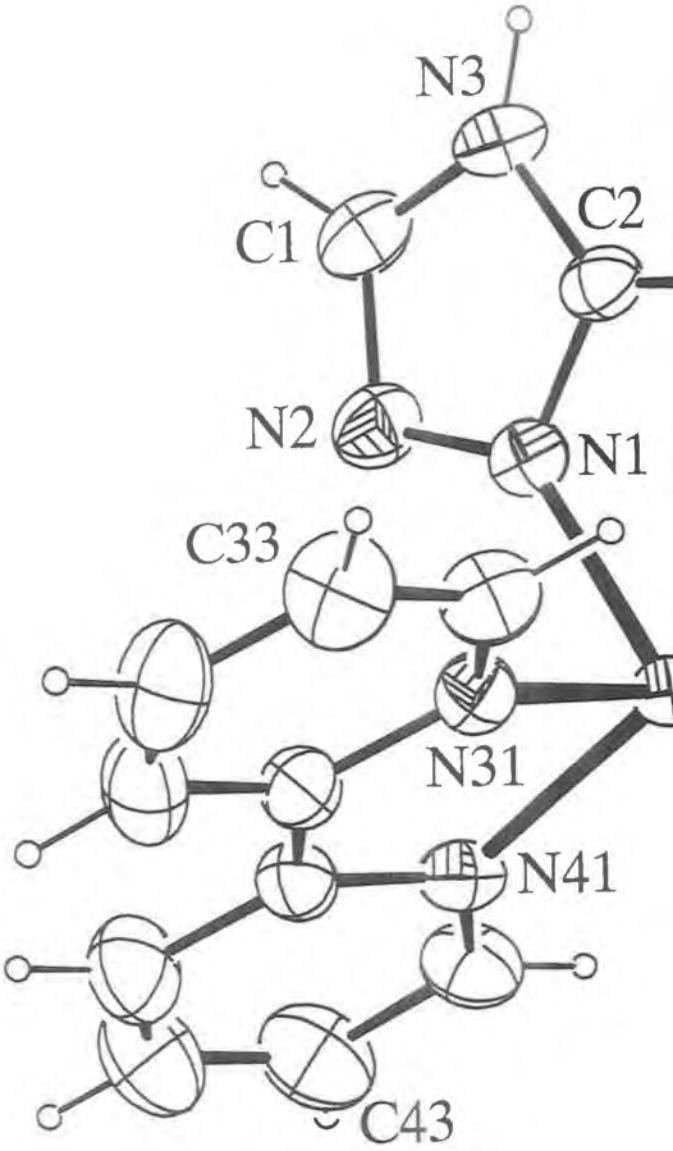
N3
C1
C2
N2
N1
C33
N31
N41
C43

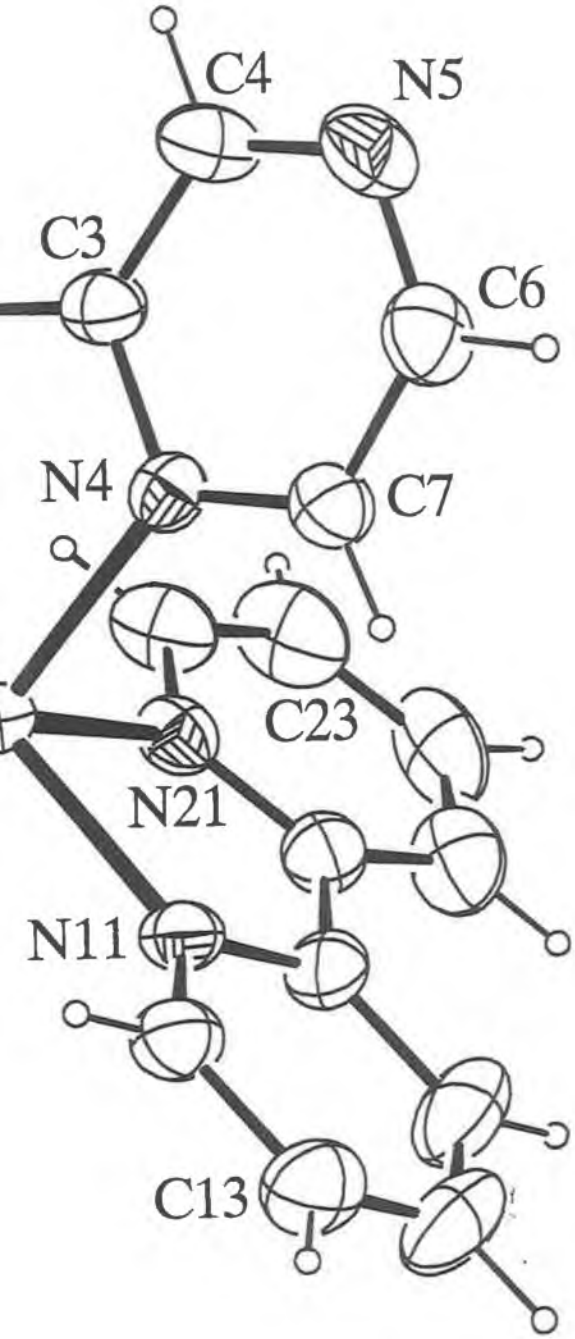
C4
N5
C3
C6
N4
C7
C23
N21
N11
C13

Table 2. Atomic coordinates (x 10^4) and equivalent isotropic displacement parameters (Å x 10^3) for 1. U(eq) is defined as one third of the trace of the orthogonalized Uij tensor.

Atom	x	y	z	U(eq)
Ru(1)	4750(1)	7983(1)	8019(1)	46(1)
N(1)	4388(3)	8389(3)	8932(2)	50(1)
N(2)	3992(3)	8107(3)	9479(2)	61(1)
N(3)	4244(3)	9334(3)	9666(2)	61(1)
N(4)	5069(2)	9120(2)	7961(2)	48(1)
N(11)	5061(3)	7727(2)	7027(2)	55(1)
N(21)	3764(3)	8255(2)	7503(3)	54(1)
N(31)	5721(3)	7630(2)	8509(2)	51(1)
N(41)	4461(3)	6873(2)	8268(2)	54(1)
C(1)	3929(4)	8694(4)	9907(3)	67(2)
C(2)	4527(3)	9125(3)	9055(3)	51(2)
C(3)	4905(4)	9552(3)	8523(3)	53(2)
C(4)	5117(4)	10316(3)	8528(4)	73(2)
N(5)	5464(4)	10655(3)	8026(4)	81(2)
C(6)	5616(4)	10218(4)	7493(4)	71(2)
C(7)	5420(4)	9464(3)	7443(3)	61(2)
C(12)	5719(4)	7453(3)	6815(3)	65(2)
C(13)	5876(5)	7310(4)	6132(4)	83(2)
C(14)	5337(6)	7451(5)	5667(3)	92(3)
C(15)	4631(7)	7753(4)	5866(3)	92(3)
C(16)	4503(4)	7896(3)	6552(3)	64(2)
C(22)	3137(4)	8531(4)	7795(4)	77(2)
C(23)	2513(5)	8772(5)	7419(5)	98(3)
C(24)	2573(7)	8743(5)	6715(6)	101(3)
C(25)	3198(5)	8448(5)	6411(4)	85(2)
C(26)	3790(4)	8209(4)	6818(3)	65(2)
C(32)	6366(3)	8024(4)	8608(3)	66(2)
C(33)	6969(4)	7777(5)	8995(4)	82(2)
C(34)	6918(5)	7097(5)	9308(4)	90(2)
C(35)	6270(5)	6658(4)	9224(3)	83(2)
C(36)	5677(3)	6934(3)	8827(3)	56(1)
C(42)	3812(4)	6523(3)	8092(4)	73(2)
C(43)	3605(5)	5823(4)	8382(5)	98(3)
C(44)	4076(6)	5495(5)	8845(5)	106(3)
C(45)	4764(7)	5846(3)	9021(3)	89(2)
C(46)	4949(4)	6536(3)	8708(3)	58(2)

Table 3. Selected bond lengths [Å] and angles [°] for 1.

Ru(1)-N(1)	2.023(4)	Ru(1)-N(31)	2.047(5)
Ru(1)-N(21)	2.054(5)	Ru(1)-N(11)	2.065(5)
Ru(1)-N(41)	2.067(4)	Ru(1)-N(4)	2.071(4)
N(1)-C(2)	1.334(7)	N(1)-N(2)	1.368(6)
N(2)-C(1)	1.331(7)	N(3)-C(1)	1.335(7)
N(3)-C(2)	1.346(6)	N(4)-C(7)	1.330(7)
N(4)-C(3)	1.365(6)	N(11)-C(12)	1.314(7)
N(11)-C(16)	1.380(7)	N(21)-C(22)	1.329(8)
N(21)-C(26)	1.343(7)	N(31)-C(32)	1.336(7)
N(31)-C(36)	1.371(7)	N(41)-C(42)	1.334(7)
N(41)-C(46)	1.348(7)	C(2)-C(3)	1.440(7)
C(3)-C(4)	1.388(7)	C(4)-N(5)	1.299(8)
N(5)-C(6)	1.321(8)	C(6)-C(7)	1.368(8)
C(12)-C(13)	1.386(8)	C(13)-C(14)	1.334(10)
C(14)-C(15)	1.398(12)	C(15)-C(16)	1.385(8)
C(16)-C(26)	1.458(9)	C(22)-C(23)	1.381(10)
C(23)-C(24)	1.383(14)	C(24)-C(25)	1.347(13)
C(25)-C(26)	1.371(10)	C(32)-C(33)	1.369(9)
C(33)-C(34)	1.342(9)	C(34)-C(35)	1.379(10)
C(35)-C(36)	1.383(9)	C(36)-C(46)	1.471(8)
C(42)-C(43)	1.398(9)	C(43)-C(44)	1.352(11)
C(44)-C(45)	1.395(14)	C(45)-C(46)	1.394(8)

N(1)-Ru(1)-N(31)	87.3(2)	N(1)-Ru(1)-N(21)	95.1(2)
N(31)-Ru(1)-N(21)	175.7(2)	N(1)-Ru(1)-N(11)	171.2(2)
N(31)-Ru(1)-N(11)	98.9(2)	N(21)-Ru(1)-N(11)	79.0(2)
N(1)-Ru(1)-N(41)	92.6(2)	N(31)-Ru(1)-N(41)	79.0(2)
N(21)-Ru(1)-N(41)	97.4(2)	N(11)-Ru(1)-N(41)	94.7(2)
N(1)-Ru(1)-N(4)	78.2(2)	N(31)-Ru(1)-N(4)	95.3(2)
N(21)-Ru(1)-N(4)	88.6(2)	N(11)-Ru(1)-N(4)	94.9(2)
N(41)-Ru(1)-N(4)	169.5(2)	C(2)-N(1)-N(2)	107.5(4)
C(2)-N(1)-Ru(1)	116.2(4)	N(2)-N(1)-Ru(1)	136.2(4)
C(1)-N(2)-N(1)	104.8(5)	C(1)-N(3)-C(2)	103.7(5)
C(7)-N(4)-C(3)	117.4(5)	C(7)-N(4)-Ru(1)	127.0(4)
C(3)-N(4)-Ru(1)	115.6(3)	C(12)-N(11)-C(16)	119.1(5)
C(12)-N(11)-Ru(1)	127.4(4)	C(16)-N(11)-Ru(1)	113.5(4)
C(22)-N(21)-C(26)	118.6(6)	C(22)-N(21)-Ru(1)	124.5(5)
C(26)-N(21)-Ru(1)	116.7(5)	C(32)-N(31)-C(36)	116.2(5)
C(32)-N(31)-Ru(1)	127.7(4)	C(36)-N(31)-Ru(1)	115.7(4)
C(42)-N(41)-C(46)	120.1(5)	C(42)-N(41)-Ru(1)	125.4(4)
C(46)-N(41)-Ru(1)	114.0(4)	N(2)-C(1)-N(3)	113.2(5)
N(1)-C(2)-N(3)	110.8(5)	N(1)-C(2)-C(3)	117.0(5)
N(3)-C(2)-C(3)	132.1(5)	N(4)-C(3)-C(4)	118.9(5)
N(4)-C(3)-C(2)	113.0(5)	C(4)-C(3)-C(2)	128.1(5)
N(5)-C(4)-C(3)	124.1(6)	C(4)-N(5)-C(6)	115.2(5)
N(5)-C(6)-C(7)	124.4(6)	N(4)-C(7)-C(6)	120.0(6)
N(11)-C(12)-C(13)	122.9(7)	C(14)-C(13)-C(12)	119.0(7)
C(13)-C(14)-C(15)	120.3(7)	C(16)-C(15)-C(14)	118.7(8)
N(11)-C(16)-C(15)	120.0(7)	N(11)-C(16)-C(26)	116.5(5)
C(15)-C(16)-C(26)	123.5(7)	N(21)-C(22)-C(23)	122.3(8)
C(22)-C(23)-C(24)	117.4(9)	C(25)-C(24)-C(23)	120.9(9)
C(24)-C(25)-C(26)	118.4(8)	N(21)-C(26)-C(25)	122.4(7)
N(21)-C(26)-C(16)	114.0(6)	C(25)-C(26)-C(16)	123.7(7)
N(31)-C(32)-C(33)	124.5(6)	C(34)-C(33)-C(32)	118.8(8)
C(33)-C(34)-C(35)	119.7(7)	C(34)-C(35)-C(36)	119.3(7)
N(31)-C(36)-C(35)	121.5(6)	N(31)-C(36)-C(46)	113.5(5)
C(35)-C(36)-C(46)	125.0(6)	N(41)-C(42)-C(43)	121.3(7)
C(44)-C(43)-C(42)	119.1(8)	C(43)-C(44)-C(45)	120.3(8)
C(46)-C(45) C(44)	118.2(8)	N(41)-C(46)-C(45)	120.9(7)
N(41)-C(46)-C(36)	116.3(5)	C(45)-C(46)-C(36)	122.8(7)

Table 5. Anisotropic displacement parameters ($Å^2$ x 10^3) for 1.

	U11	U22	U33	U23	U13	U12
Ru(1)	46(1)	45(1)	46(1)	-6(1)	0(1)	-1(1)
N(1)	46(3)	54(3)	50(3)	-3(2)	-1(2)	2(2)
N(2)	59(3)	70(3)	53(3)	-7(3)	8(3)	-7(3)
N(3)	64(3)	66(3)	52(3)	-19(2)	-2(3)	-4(3)
N(4)	44(2)	54(2)	46(2)	-1(2)	-4(2)	-3(2)
N(11)	66(3)	46(2)	51(3)	-10(2)	8(3)	-2(2)
N(21)	50(3)	47(2)	66(3)	0(2)	-6(3)	-4(2)
N(31)	47(3)	56(3)	51(3)	-1(2)	1(2)	5(2)
N(41)	56(3)	50(3)	57(3)	-11(2)	6(2)	-4(2)
C(1)	63(4)	85(5)	52(4)	-12(3)	8(3)	-1(4)
C(2)	48(4)	57(3)	47(3)	-10(2)	-9(2)	8(3)
C(3)	53(6)	50(3)	56(3)	-9(2)	-8(3)	2(3)
C(4)	82(5)	52(3)	85(5)	-15(3)	0(4)	-9(3)
N(5)	97(4)	51(3)	96(4)	6(3)	-3(4)	-19(3)
C(6)	70(5)	68(4)	75(4)	10(4)	6(4)	-14(4)
C(7)	66(4)	54(3)	63(4)	1(3)	4(4)	-6(3)
C(12)	75(5)	58(3)	62(4)	-8(3)	14(3)	-2(4)
C(13)	91(6)	82(5)	77(5)	-7(4)	26(5)	-10(4)
C(14)	104(7)	124(6)	49(4)	-11(5)	19(4)	-20(6)
C(15)	107(9)	117(6)	52(4)	-5(3)	-16(5)	-25(6)
C(16)	84(6)	57(3)	52(3)	-6(3)	-11(3)	-17(3)
C(22)	56(5)	69(4)	107(6)	-13(4)	-14(4)	9(4)
C(23)	62(6)	90(6)	143(9)	-6(6)	-27(6)	20(5)
C(24)	84(7)	87(6)	132(9)	30(6)	-60(7)	0(6)
C(25)	73(6)	91(6)	91(5)	11(5)	-27(5)	-9(5)
C(26)	73(5)	56(4)	64(4)	-3(3)	-15(4)	-7(3)
C(32)	51(4)	76(4)	72(4)	-7(4)	-5(3)	-11(4)
C(33)	46(4)	106(6)	95(5)	2(4)	-11(4)	1(4)
C(34)	62(5)	121(6)	85(5)	20(5)	-18(4)	17(5)
C(35)	81(6)	84(5)	83(5)	21(4)	-6(4)	21(5)
C(36)	62(4)	55(3)	52(3)	1(3)	11(3)	2(3)
C(42)	64(4)	61(4)	92(5)	-10(4)	-10(4)	-17(3)
C(43)	85(6)	76(5)	134(7)	-3(5)	0(6)	-22(5)
C(44)	117(8)	71(5)	130(8)	20(5)	8(6)	-26(5)
C(45)	98(5)	77(4)	91(4)	19(3)	1(8)	-18(8)
C(46)	66(6)	51(3)	56(3)	0(3)	9(3)	5(3)

Table 6. Hydrogen coordinates (x 10^4) and isotropic displacement parameters (Å x 10^3) for 1.

	x	y	z	U(eq)
H(3)	4261(3)	9776(3)	9857(2)	73
H(1)	3690(4)	8661(4)	10331(3)	80
H(4)	5003(4)	10602(3)	8915(4)	88
H(6)	5874(4)	10438(4)	7126(4)	85
H(7)	5533(4)	9192(3)	7047(3)	73
H(12)	6096(4)	7349(3)	7137(3)	78
H(13)	6349(5)	7119(4)	6001(4)	100
H(14)	5431(6)	7348(5)	5208(3)	111
H(15)	4255(7)	7857(4)	5543(3)	111
H(22)	3117(4)	8564(4)	8270(4)	93
H(23)	2071(5)	8946(5)	7631(5)	118
H(24)	2177(7)	8931(5)	6446(6)	121
H(25)	3227(5)	8406(5)	5938(4)	102
H(32)	6407(3)	8500(4)	8400(3)	79
H(33)	7406(4)	8075(5)	9040(4)	99
H(34)	7318(5)	6923(5)	9580(4)	108
H(35)	6233(5)	6182(4)	9431(3)	99
H(42)	3493(4)	6749(3)	7771(4)	87
H(43)	3150(5)	5587(4)	8258(5)	118
H(44)	3940(6)	5034(5)	9046(5)	127
H(45)	5091(7)	5624(3)	9340(3)	107

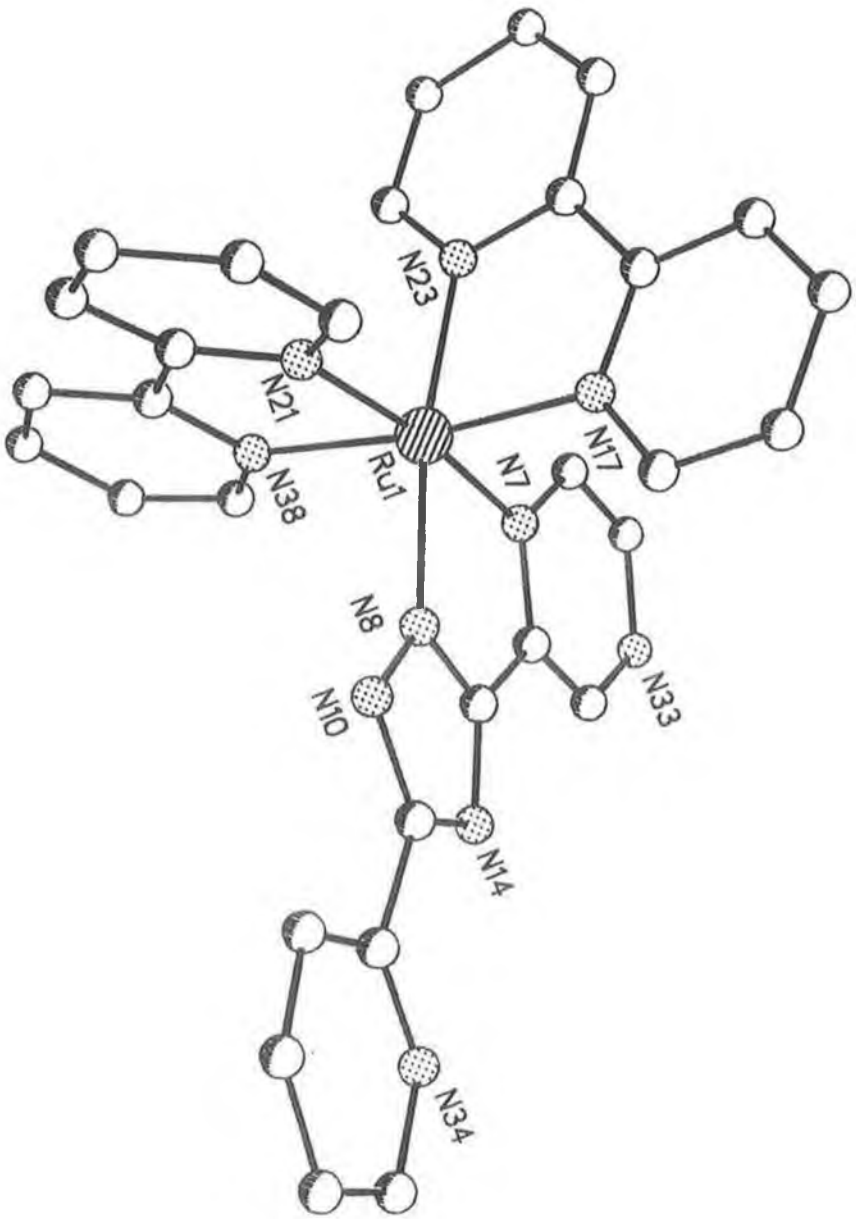
N23
N21
N38
Ru1
N17
N7
N8
N10
N33
N14
N34